

DTIC FILE COPY

NPS-62-89-016

(2)

# NAVAL POSTGRADUATE SCHOOL

## Monterey, California

DTIC  
ELECTE  
FEB 23 1989  
S D D &



AD-A204 360

# THESIS

AN INVESTIGATION OF NEAR FIELDS FOR HF  
SHIPBOARD ANTENNAS - SURFACE PATCH AND  
WIRE GRID MODELING USING THE  
NUMERICAL ELECTROMAGNETICS CODE

by

Elliniadis, Panagiotis

December 1988

Thesis Advisor:  
Co-Advisor:

Richard W. Adler  
James K. Breakall

Approved for public release; distribution is unlimited

Prepared for:  
Naval Ocean Systems Center  
San Diego, CA 92152

89 2 22 045

NAVPGSCOLINST 5600.5C  
15 December 1988

NAVAL POSTGRADUATE SCHOOL  
Monterey, California 93943-5000


Rear Admiral R.C. Austin  
Superintendent

H. Shull  
Provost

This thesis is prepared in conjunction with research sponsored in part by the Naval Ocean Systems Center and funded by the Naval Postgraduate School.

Reproduction of all or part of this report is authorized.

Released by:

  
\_\_\_\_\_  
GORDON E. SCHACHER  
Dean of Science and Engineering

UNCLASSIFIED

SECURITY CLASSIFICATION OF THIS PAGE

REPORT DOCUMENTATION PAGE				Form Approved OMB No. 0704-0188	
1a REPORT SECURITY CLASSIFICATION <b>UNCLASSIFIED</b>			1b RESTRICTIVE MARKINGS		
2a SECURITY CLASSIFICATION AUTHORITY			3 DISTRIBUTION / AVAILABILITY OF REPORT Approved for public release; distribution is unlimited		
2b DECLASSIFICATION / DOWNGRADING SCHEDULE					
4 PERFORMING ORGANIZATION REPORT NUMBER(S) <b>NPS-62-89-016</b>			5 MONITORING ORGANIZATION REPORT NUMBER(S)		
6a. NAME OF PERFORMING ORGANIZATION <b>Naval Postgraduate School</b>		6b OFFICE SYMBOL (If applicable) <b>62</b>	7a NAME OF MONITORING ORGANIZATION <b>Naval Postgraduate School</b>		
6c. ADDRESS (City, State, and ZIP Code) <b>Monterey, California 93943-5000</b>			7b ADDRESS (City, State, and ZIP Code) <b>Monterey, California 93943-5000</b>		
8a. NAME OF FUNDING / SPONSORING ORGANIZATION <b>Naval Ocean Systems Center</b>		8b OFFICE SYMBOL (If applicable)	9 PROCUREMENT INSTRUMENT IDENTIFICATION NUMBER <b>O&amp;MN, Direct Funding</b>		
8c. ADDRESS (City, State, and ZIP Code) <b>271 Catalina Boulevard San Diego, California 92152</b>			10 SOURCE OF FUNDING NUMBERS		
			PROGRAM ELEMENT NO	PROJECT NO	TASK NO
					WORK UNIT ACCESSION NO
11 TITLE (Include Security Classification) <b>AN INVESTIGATION OF NEAR FIELDS FOR HF SHIPBOARD ANTENNAS - SURFACE PATCH AND WIRE GRID MODELING USING THE NUMERICAL ELECTROMAGNETICS CODE</b>					
12 PERSONAL AUTHOR(S) <b>ELLINIADIS, Panagiotis</b>					
13a TYPE OF REPORT <b>Master's Thesis</b>		13b TIME COVERED FROM _____ TO _____		14 DATE OF REPORT (Year, Month, Day) <b>1988 December</b>	
				15 PAGE COUNT <b>217</b>	
16 SUPPLEMENTARY NOTATION The views expressed in this thesis are those of the author and do not reflect the official policy or position of the Department of Defense or the U.S. Government.					
17 COSATI CODES			18 SUBJECT TERMS (Continue on reverse if necessary and identify by block number)		
FIELD	GROUP	SUB-GROUP	Near fields; NEC (Numerical Electromagnetics Code); Antenna; Monopole; Wire grid; Surface patch, Admittance		
19 ABSTRACT (Continue on reverse if necessary and identify by block number)					
<p>The Numerical Electromagnetics Code (NEC) was used to evaluate the admittance, average power gain, and the electric near and far field of a monopole antenna mounted on a cubical box over a perfectly conducting ground plane. Two models of the box, employing surface patches and wire grids, were evaluated. The monopole was positioned at the center, the edge, and at a corner of the box's top surface. Admittance and average power gain of the antenna were calculated. NEC results were examined and compared with experimental data and with results from "PATCH", another independent electromagnetic modeling code. The near electric field was calculated for both models. Computer graphics techniques were presented for plotting NEC near field results using DISSPLA (Display Integrated Software System and Plotting Language), a commercial graphics package. Contour and 3-D</p>					
20 DISTRIBUTION / AVAILABILITY OF ABSTRACT <input checked="" type="checkbox"/> UNCLASSIFIED/UNLIMITED <input type="checkbox"/> SAME AS RPT <input type="checkbox"/> DTIC USERS			21 ABSTRACT SECURITY CLASSIFICATION <b>UNCLASSIFIED</b>		
22a NAME OF RESPONSIBLE INDIVIDUAL <b>ADLER, Richard W.</b>			22b TELEPHONE (Include Area Code) <b>408-646-2352</b>		22c OFFICE SYMBOL <b>62Ab</b>

DD Form 1473, JUN 86

Previous editions are obsolete

SECURITY CLASSIFICATION OF THIS PAGE

S/N 0102-LF-014-6603

i

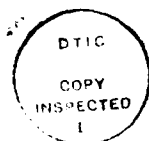
UNCLASSIFIED

UNCLASSIFIED

SECURITY CLASSIFICATION OF THIS PAGE

19. continued

amplitude, and phase plots of the near electric fields were presented. Radiation patterns were calculated to relate far field and near field behavior of the antenna. Surface patch and wire grid models are compared and conclusions were presented.

[illegible]

Approved for public release; distribution is unlimited

AN INVESTIGATION OF NEAR FIELDS FOR HF SHIPBOARD  
ANTENNAS - SURFACE PATCH AND WIRE GRID  
MODELING USING THE NUMERICAL  
ELECTROMAGNETICS CODE

by

Panagiotis Elliniadis  
Lieutenant, Hellenic Navy  
B.S.E.E., Naval Academy of Greece, 1979

Submitted in partial fulfillment of the  
requirements for the degree of

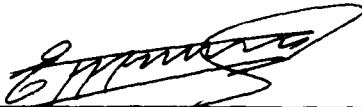
MASTER OF SCIENCE IN ELECTRICAL ENGINEERING

from the


NAVAL POSTGRADUATE SCHOOL

December 1988

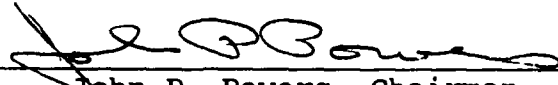
Author:


  
Panagiotis Elliniadis

Approved by:

  
Richard W. Adler, Thesis Advisor

  
James K. Breakall, Co-Advisor

  
John P. Powers, Chairman,  
Department of Electrical and  
Computer Engineering

  
Gordon E. Schacher,  
Dean of Science and Engineering

## ABSTRACT

The Numerical Electromagnetics Code (NEC) was used to evaluate the admittance, average power gain, and the electric near and far field of a monopole antenna mounted on a cubical box over a perfectly conducting ground plane. Two models of the box, employing surface patches and wire grids, were evaluated. The monopole was positioned at the center, the edge, and at a corner of the box's top surface. Admittance and average power gain of the antenna were calculated. NEC results were examined and compared with experimental data and with results from "PATCH", another independent electromagnetic modeling code. The near electric field was calculated for both models. Computer graphics techniques were presented for plotting NEC near field results using DISSPLA (Display Integrated Software System and Plotting Language), a commercial graphics package. Contour and 3-D amplitude, and phase plots of the near electric fields were presented. Radiation patterns were calculated to relate far field and near field behavior of the antenna. Surface patch and wire grid models are compared and conclusions were presented.

## TABLE OF CONTENTS

I.	INTRODUCTION.....	1
A.	GENERAL BACKGROUND.....	1
B.	REASONS FOR THIS STUDY.....	2
	1. Hazards of Electromagnetic Radiation (RADHAZ).....	2
	2. Electromagnetic Interference (EMI).....	3
C.	SCOPE OF THE STUDY.....	6
D.	THEORETICAL BACKGROUND.....	7
	1. Near Field Theory.....	7
	2. Numerical Electromagnetics Code (NEC) - Method of Moments.....	10
II.	SURFACE PATCH MODELING.....	12
A.	GUIDELINES FOR MODELING USING NEC.....	12
B.	LIMITATIONS AND OPTIMIZATION CRITERIA.....	13
C.	PREVIOUS STUDIES.....	14
D.	MODEL OF 6 CM MONOPOLE ANTENNA MOUNTED ON A CUBICAL CONDUCTING BOX--ADMITTANCE AND AVERAGE GAIN INVESTIGATION.....	15
	1. Monopole at Center.....	17
	2. Monopole at Edge.....	44
	3. Monopole at Corner.....	57
E.	NEAR ELECTRIC FIELD.....	63
	1. Near Electric Field in 2-Dimensions for the 6 cm Monopole Antenna on the Cubical Conducting Box.....	64
F.	NEAR ELECTRIC FIELD MAGNITUDE AND PHASE CONTOUR PLOTS.....	77

1.	Half Wave Dipole in Free Space vs 6 cm Monopole Over Ground Plane.....	78
2.	Monopole at Center of Patch Box vs Monopole Over Ground Plane.....	94
3.	Monopole at Edge of Patch Box vs Monopole at Center.....	104
4.	Monopole at Corner of Patch Box vs Monopole at Center.....	112
G.	RADIATION PATTERNS.....	120
1.	Monopole at Center.....	120
2.	Monopole at Edge.....	120
3.	Monopole at Corner.....	120
III.	WIRE GRID MODELING FOR NEAR ELECTRIC FIELD PREDICTIONS.....	129
A.	GUIDELINES FOR WIRE GRID MODELING USING NEC....	129
B.	WIRE GRID BOX MODEL FOR NEAR ELECTRIC FIELD INVESTIGATION.....	129
1.	Monopole at Center of Wire Grid Box vs Monopole at Center of Surface Patch Box...	134
2.	Monopole at Edge of Wire Grid Box vs Monopole at Edge of Surface Patch Box ....	142
3.	Monopole at Corner of Wire Grid Box vs Monopole at Corner of Surface Patch Box...	150
IV.	CONCLUSIONS AND RECOMMENDATIONS.....	158
APPENDIX A	NEC INPUT DATA FILES.....	161
APPENDIX B	FORTRAN PROGRAMS AND NEC INPUT DATA FILES...	169
APPENDIX C	NEC INPUT DATA FILES.....	191



LIST OF REFERENCES.....	196
BIBLIOGRAPHY.....	197
INITIAL DISTRIBUTION LIST.....	198

## LIST OF TABLES

1. MAJOR LOSSES DUE TO EMI OR EMI "FIXES".....	5
2. MEASURED DATA FOR A 6CM MONOPOLE ON A CUBICAL BOX....	21
3. NEC STATISTICS FOR MONOPOLE AT CENTER OF PATCH BOX AS THE NUMBER OF PATCHES ON TOP INCREASES (NPS MAINFRAME COMPUTER - IBM SYSTEM 370).....	22
4. CALCULATED DATA MONOPOLE AT CENTER OF SURFACE PATCH BOX (5 X 5 PATCHES ON THE TOP SURFACE - BASE SEGMENT FEED).....	23
5. CALCULATED DATA MONOPOLE AT CENTER OF SURFACE PATCH BOX (7 X 7 PATCHES ON THE TOP SURFACE - BASE SEGMENT FEED).....	24
6. CALCULATED DATA MONOPOLE AT CENTER OF SURFACE PATCH BOX (9 X 9 PATCHES ON THE TOP SURFACE - BASE SEGMENT FEED).....	25
7. CALCULATED DATA MONOPOLE AT CENTER OF SURFACE PATCH BOX (11 X 11 PATCHES ON THE TOP SURFACE - BASE SEGMENT FEED).....	26
8. CALCULATED DATA MONOPOLE AT CENTER OF SURFACE PATCH BOX (5 X 5 PATCHES ON THE TOP SURFACE - BASE SEGMENT FEED) (DOUBLE PRECISION CALCULATION).....	27
9. CALCULATED DATA MONOPOLE AT CENTER OF SURFACE PATCH BOX (7 X 7 PATCHES ON THE TOP SURFACE - BASE SEGMENT FEED) (DOUBLE PRECISION CALCULATION).....	28
10. CALCULATED DATA MONOPOLE AT EDGE OF SURFACE PATCH BOX (3.33CM FROM CENTER) (9 X 9 PATCHES ON THE TOP SURFACE - BASE SEGMENT FEED).....	47
11. CALCULATED DATA MONOPOLE AT EDGE OF SURFACE PATCH BOX (3.63CM FROM CENTER) (11 X 11 PATCHES ON THE TOP SURFACE - BASE SEGMENT FEED).....	48
12. CALCULATED DATA MONOPOLE AT EDGE OF SURFACE PATCH BOX (3.63 CM FROM CENTER) (11 X 11 PATCHES ON THE TOP SURFACE - BASE SEGMENT FEED) (DOUBLE PRECISION CALCULATION).....	49
13. CALCULATED DATA MONOPOLE AT CORNER OF SURFACE PATCH BOX (5.14CM ON THE DIAGONAL FROM CENTER) (11 X 11 PATCHES ON THE TOP SURFACE - BASE SEGMENT FEED).....	58
14. RESULTS FROM NEC OUTPUTS.....	82

## LIST OF FIGURES

1a. Fields of a Radiating Antenna.....	8
1b. Energy Flow Near a Dipole Antenna.....	9
2. Rectangular Surface Covered by Multiple Patches...	13
3. Geometry of Monopole Attached to the Conducting Box Over a Ground Plane.....	16
4. Monopole at Center of Patch Box (5x5 Patches on Top) NEC Admittance vs Measurements.....	29
5. Monopole at Center of Patch Box (5x5 Patches on Top) NEC Admittance vs Measurements and "PATCH" Code.....	30
6. Monopole at Center of Patch Box (7x7 Patches on Top) NEC Admittance vs Measurements.....	31
7. Monopole at Center of Patch Box (7x7 Patches on Top) NEC Admittance vs Measurements and "PATCH" Code.....	32
8. Monopole at Center of Patch Box (9x9 Patches on Top) NEC Admittance vs Measurements.....	33
9. Monopole at Center of Patch Box (9x9 Patches on Top) NEC Admittance vs Measurements and "PATCH" Code.....	34
10. Monopole at Center of Patch Box (11x11 Patches on Top) NEC Admittance vs Measurements.....	35
11. Monopole at Center of Patch Box (11x11 Patches on Top) NEC Admittance vs Measurements and "PATCH" Code.....	36
12. Monopole at Center of Patch Box. "PATCH" Code Admittance vs Measurements.....	37
13. Monopole at Center of Patch Box (5x5 Patches on Top). NEC Admittance vs "PATCH" Code.....	38
14. Monopole at Center of Patch Box (7x7 Patches on Top). NEC Admittance vs "PATCH" Code.....	39
15. Monopole at Center of Patch Box (9x9 Patches on Top). NEC Admittance vs "PATCH" Code.....	40

16.	Monopole at Center of Patch Box (11x11 Patches on Top). NEC Admittance vs "PATCH" Code.....	41
17.	Monopole at Center of Patch Box. NEC Conductance vs Patch Density.....	42
18.	Monopole at Center of Patch Box. NEC Susceptance vs Patch Density.....	43
19.	Monopole at Edge of Patch Box (9x9 Patches on Top). NEC Admittance vs Measurements.....	50
20.	Monopole at Edge of Patch Box (9x9 Patches on Top). NEC Admittance vs Measurements and "PATCH" Code..	51
21.	Monopole at Edge of Patch Box (11x11 Patches on Top). NEC Admittance vs Measurements.....	52
22.	Monopole at Edge of Patch Box (11x11 Patches on Top). NEC Admittance vs Measurements and "PATCH" Code.....	53
23.	Monopole at Edge of Patch Box. "PATCH" Code Admittance vs Measurements.....	54
24.	Monopole at Edge of Patch Box (9x9 Patches on Top). NEC Admittance vs "PATCH" Code.....	55
25.	Monopole at Edge of Patch Box (11x11 Patches on Top). NEC Admittance vs "PATCH" Code.....	56
26.	Monopole at Corner of Patch Box (11x11 Patches on Top). NEC Admittance vs Measurements.....	59
27.	Monopole at Corner of Patch box (11x11 Patches on Top). NEC Admittance vs Measurements and "PATCH" Code.....	60
28.	Monopole at Corner of Patch Box. "PATCH" Code Admittance vs Measurements.....	61
29.	Monopole at Corner of Patch Box (11x11 Patches on Top). NEC Admittance vs "PATCH" Code.....	62
30.	A Linear Current Radiator.....	65
31.	Monopole at Center of Patch Box (7x7 Patches on Top). Near Electric Field on X-Axis.....	68
32.	Monopole at Center of Patch Box. Near Electric Field on Z-Axis.....	69

33.	Monopole at Edge of Patch Box. Near Electric Field on X-Axis.....	70
34.	Monopole at Edge of Patch Box. Near Electric Field on Y-Axis.....	71
35.	Monopole at Edge of Patch Box. Near Electric Field on Z-Axis.....	72
36.	Monopole at Corner of Patch Box. Near Electric Field on X-Axis.....	73
37.	Monopole at Corner of Patch Box. Near Electric Field on Y-Axis.....	74
38.	Monopole at Corner of Patch Box. Near Electric Field on Z-Axis.....	75
39.	Near Electric Field of a Current Element.....	76
40.	Total E-Field Contours, Dipole $\lambda/2$ on Z-Axis in Free Space.....	83
40a.	Total E-Field Contours, Dipole $\lambda/2$ in Free Space (0.5 $\lambda$ Away From the Wire).....	84
40b.	Total E-Field Contours, Dipole $\lambda/2$ in Free Space (0.8 $\lambda$ Away From the Wire).....	85
41.	X-Component, E-Field Phase Contours, Dipole $\lambda/2$ in Free Space.....	86
42.	Z-Component, E-Field Phase Contours, Dipole $\lambda/2$ in Free Space.....	87
43.	Total E-Field Contours, Monopole 6 cm Over Perfect Ground.....	88
43a.	Total E-Field Contours, Monopole 6 cm Over Perfect Ground (1 $\lambda$ Away From the Wire).....	89
43b.	Total E-Field Contours, Monopole 6 cm Over Perfect Ground (2 $\lambda$ Away From the Wire).....	90
43c.	Total E-Field Contours, Monopole 6 cm Over Perfect Ground (8 $\lambda$ Away From the Wire).....	91
44.	X-Component, E-Field Phase Contours, Monopole 6 cm Over Perfect Ground.....	92
45.	Z-Component, E-Field Phase Contours, Monopole 6 cm Over Perfect Ground.....	93

46. Total E-Field Contours, Monopole at Patch Box Center.....	97
47. X-Component, E-Field Contours, Monopole at Patch Box Center.....	98
48. X-Component, E-Field Phase Contours, Monopole at Patch Box Center.....	99
49. Z-Component, E-Field Contours, Monopole at Patch Box Center.....	100
50. Z-Component, E-Field Phase Contours, Monopole at Patch box Center.....	101
51. Total E-Field 3-D Plot, View Toward Monopole (Monopole at Patch Box Center).....	102
52. Total E-Field 3-D Plot, Viewed From Monopole (Monopole at Patch Box Center).....	103
53. Total E-Field Contours, Monopole at Patch Box Edge.....	105
54. X-Component, E-Field Contours, Monopole at Patch Box Edge.....	106
55. X-Component, E-Field Phase Contours, Monopole at Patch Box Edge.....	107
56. Z-Component, E-Field Contours, Monopole at Patch Box Edge.....	108
57. Z-Component, E-Field Phase Contours, Monopole at Patch Box Edge.....	109
58. Total E-Field 3-D Plot, View Toward Monopole (Monopole at Patch Box Edge).....	110
59. Total E-Field 3-D Plot, Viewed from Monopole (Monopole at Patch Box Edge).....	111
60. Total E-Field Contours, Monopole at Patch Box Corner.....	113
61. X-Component, E-Field Contours, Monopole at Patch Box Corner.....	114
62. X-Component, E-Field Phase Contours, Monopole at Patch Box Corner.....	115

63. Z-Component, E-Field Contours, Monopole at Patch Box Corner.....	116
64. Z-Component, E-Field Phase Contours, Monopole at Patch Box Corner.....	117
65. Total E-Field 3-D Plot, View Toward Monopole (Monopole at Patch Box Corner).....	118
66. Total E-Field 3-D Plot, Viewed from Monopole (Monopole at Patch Box Corner).....	119
67. Vertical Pattern, Monopole at Patch Box Center....	121
68. Horizontal Pattern, Monopole at Patch Box Center..	122
69. Vertical Pattern (X-Axis Cut), Monopole at Patch Box Edge.....	123
70. Vertical Pattern (Y-Axis Cut), Monopole at Patch Box Edge.....	124
71. Horizontal Pattern, Monopole at Patch Box Edge....	125
72. Vertical Pattern (X-Axis Cut), Monopole at Patch Box Corner.....	126
73. Vertical Pattern (45° Cut), Monopole at Patch Box Corner).....	127
74. Horizontal Pattern, Monopole at Patch Box Corner..	128
75. Monopole at Center of Wire Grid Box.....	131
76. Monopole at Edge of Wire Grid Box.....	132
77. Monopole at Corner of Wire Grid Box.....	133
78. Total E-Field Contours, Monopole at Wire Grid Box Center.....	135
79. X-Component, E-Field Contours, Monopole at Wire Grid Box Center.....	136
80. X-Component, E-Field Phase Contours, Monopole at Wire Grid Box Center.....	137
81. Z-Component, E-Field Contours, Monopole at Wire Grid Box Center.....	138
82. Z-Component, E-Field Phase Contours, Monopole at Wire Grid Box Center.....	139

83. Total E-Field 3-D Plot, View Toward Monopole (Monopole at Wire Grid Box Center).....	140
84. Total E-Field 3-D Plot, Viewed from Monopole (Monopole at Wire Grid Box Center).....	141
85. Total E-Field Contours, Monopole at Wire Grid Box Edge.....	143
86. X-Component, E-Field Contours, Monopole at Wire Grid Box Edge.....	144
87. X-Component, E-Field Phase Contours, Monopole at Wire Grid Box Edge.....	145
88. Z-Component, E-Field Contours, Monopole at Wire Grid Box Edge.....	146
89. Z-Component, E-Field Phase Contours, Monopole at Wire Grid Box Edge.....	147
90. Total E-Field 3-D Plot, View Toward Monopole (Monopole at Wire Grid Box Edge).....	148
91. Total E-Field 3-D Plot, Viewed From Monopole (Monopole at Wire Grid Box Edge).....	149
92. Total E-Field Contours, Monopole at Wire Grid Box Corner.....	151
93. X-Component, E-Field Contours, Monopole at Wire Grid Box Corner.....	152
94. X-Component, E-Field Phase Contours, Monopole at Wire Grid Box Corner.....	153
95. Z-Component, E-Field Contours, Monopole at Wire Grid Box Corner.....	154
96. Z-Component, E-Field Phase Contours, Monopole at Wire Grid Box Corner.....	155
97. Total E-Field 3-D Plot, View Toward Monopole (Monopole at Wire Grid Box Corner).....	156
98. Total E-Field 3-D Plot, Viewed from Monopole (Monopole at Wire Grid Box Corner).....	157



## ACKNOWLEDGEMENT

I would like to express my gratitude to Dr. Richard W. Adler and Dr. James K. Breakall for their guidance, expertise, patience and assistance throughout this work.

My sincere appreciation goes to the Hellenic Navy for giving me the opportunity to earn my Master's degree.

This thesis is dedicated to my wife Roula and to my children Dimitris and Christina for their support and understanding during these years of study at the Naval Postgraduate School.

## I. INTRODUCTION

### A. GENERAL BACKGROUND

The arrangement of HF antennas aboard ships requires the consideration of many factors. Among these are: input impedance, gain, blockage angles, patterns, weight, firing arcs of weapons, and transmission line length restrictions. Additional factors that greatly influence naval operations are RF radiation hazards (RADHAZ) and electromagnetic interference (EMI).

Shipboard operations are carried out within fixed (small) distances from HF transmitting antennas, so the Navy has a unique and long-standing operational problem--the radiation from these antennas can be hazardous to personnel, ordnance, fuel, and electronic equipment because of the intensity of the fields close to the radiating elements (near fields). The goal of the antenna designer is to select a location for the antenna that permits it to perform with a minimum of restrictions placed on personnel activity, electronic communication equipment, fuels and ordnance.

In the selection of a site for an antenna, it becomes evident that all of the desired requirements cannot be met, therefore, trade-offs have to be made based on a priority system determined by the ship's primary mission. For instance, on a combatant ship, placing antennas relative to gun mounts, missile launchers, and magazines are of major

importance. On an auxiliary, however, the underway replenishment gear might receive the greatest attention.

For the above reasons, the Navy has recognized the need and focused its interest on the investigation of the near fields of antennas for a number of years.

Near field structure is very complex, and previous theoretical analysis is practical for only very simple antennas in uncomplicated geometrical settings. With the advent of high-speed computers, approximate solution techniques such as the Method of Moments became practical. This technique is suitable for the calculation of electromagnetic fields anywhere, including in close proximity to the radiating element. The degree of accuracy of the solution is a function of the number of computations required to obtain that solution (computer-time).

The Method of Moments technique is the theoretical basis for the Numerical Electromagnetics Code (NEC), which is a code for the simulation and analysis of the electromagnetic response of antennas and other metal structures [Ref. 1]. NEC is the computer simulation tool that was used in this investigation of near fields.

## B. REASONS FOR THIS STUDY

### 1. Hazards of Electromagnetic Radiation (RADHAZ)

Since near fields of Navy HF antennas are primarily responsible for radiation hazards (RADHAZ), the accuracy of near field predictions must be adequate to ensure that

personnel and equipment can continue to function safely in modern shipboard environments. There are three types of radiation hazards:

- a. Hazards of Electromagnetic Radiation to Personnel (HERP).
- b. Hazards of Electromagnetic Radiation to Ordnance (HERO).
- c. Hazards of Electromagnetic Radiation to Fuels (HERF).

These hazards and their general near field criteria are discussed in detail in Reference 2.

## 2. Electromagnetic Interference (EMI)

Near fields of shipboard antennas can also be the cause of radio frequency interference. On board ships RF interference problems can be quite complex. In land installations, there are several preventive measures for reducing interference, such as isolation of communication related equipment and separation of transmitting and receiving antennas to avoid near field interaction. On a ship, it is almost impossible to do this. The design is constrained by the nature of the ship and care has to be taken in operating radiating equipment in order to minimize interferences.

Because shipboard transmitting and receiving antennas are close together and the ship's superstructure provides a very large nonlinear surface to interact with communications signals (near field interaction), intermodulation problems

are likely because of currents induced by nonlinear devices in the near field region of an antenna.

Intermodulation sources are nonlinear items present in the immediate surroundings of the receive or transmit antennas. Metallic life lines are major sources of interference; expansion joints and mooring or anchor chains used to secure the ship at the pier are found to introduce significant nonlinearities. Other nonlinear items include ladders, guard rails, antenna guying wires, and booms. [Ref. 3]

These environmental nonlinear sources can be classified as two major categories, (1) nonlinear resistive "junctions" created by metallic mating surfaces, and (2) ferromagnetic materials. Ferromagnetic materials, such as steel, generate interfering frequencies when driven by strong fundamental currents caused by the near fields of an antenna.

Table 1 from Reference 4 is a listing of a number of significant losses in lives, fleet assets, and dollars due to RADHAZ and due to Electromagnetic Interference (EMI).

TABLE 1 [Ref. 4]  
MAJOR LOSSES DUE TO EMI OR EMI "FIXES"

**During Time of Military Active Environment:**

-- 32 aircraft/134 crew lost, \$172M damage, EMI triggered A/C rocket detonation on USS Forrestal flight deck - Late 60's.

-- Most of the topside destroyed, crew injuries, \$100+M damage, anti-radiation missile detected friendly cruiser - Late 60's.

-- All equipment lost, crew fatalities, \$10+M damage, anti-radiation missile detected USMC radar - Early 70's.

-- Frigate lost, crew fatalities, \$200+M replacement, HMS Sheffield secured ASMD radar to use SATCOM to avoid EMI-1984.

**During Peacetime Environment - Late 70's thru 1986:**

-- Planes Crashed: NATO aircraft (A/C) overseas - A/C lost, crew fatalities, \$10+M replacement. USN aircraft in California - A/C lost, crew fatalities, \$10+M replacement.

-- FFG ASW helo while hovering over FFG, ship radiation caused blade servo fault, helo damage, crew injuries, \$750K damage.

**Ship Missiles Lost and Near Miss Hits of USN Ships:**

-- Cruiser destroyed missile to avoid another cruiser, 1 missile and 1 target drone lost, \$10+M.

**Ship Damage Due to EMI:**

-- Terrier launcher rail fire, target drone lost, \$100K+ replacement.

-- Craft dropped from foilborne operation due to ship control system EMI - Bow damaged, crew injuries unknown, \$10+M.

-- Fires in propulsion room due to EMI "fixes" installed to prevent total shutdown of plant in presence of RF, minor damage, no injuries, crew repaired.

**Equipment Damage Due to EM Environment:**

-- ECM equipment burned out by radiator on neighbor ship, equipment lost, \$1M+ replacement.

**Sailors RF Burned:**

Common occurrence for crew. Increases noted from 1982-1985:

- |                        |                      |
|------------------------|----------------------|
| -- Personnel RADHAZ    | - ten-fold increase  |
| -- Personnel RF burns  | - six-fold increase  |
| -- Hazards to ordnance | - five-fold increase |

### C. SCOPE OF THE STUDY

The Numerical Electromagnetics Code (NEC) is used to evaluate the effects of the shipboard topside environment on the admittance and the electric-near field structure of a 6 cm monopole antenna mounted on a cubical box.

A ship's superstructure has been approximated by two theoretical scaled models of cube-shaped boxes of 0.1 m sides ( $\lambda/3$  at a frequency of 1 GHz) over a perfectly conducting ground plane. For the first model, the surface patch modeling technique is used and for the second, the wire grid modeling technique.

The antenna is  $\lambda/5$  at a frequency of 1 GHz and is mounted at the center, edge, and corner of the top surface. NEC results for admittance are obtained for these three positions.

For the surface patch model, the results are compared to measured experimental data from References 5 and 6. For the same model, NEC results are compared with "PATCH" code results. "PATCH" is another independent code recently developed using a much different theoretical and numerical algorithm implementation [Ref. 7]. The computational accuracy of NEC is then examined and discussed. For the wire grid model, the admittance characteristic results from Reference 8 are compared with the experimental data mentioned above. Comparison between surface patch and wire grid numerical modeling techniques are made.

NEC is then used for calculation of near electric fields for surface patch and wire grid models. Fortran programs were constructed for plotting NEC results of near electric fields in conjunction with DISSPLA (Display Integrated Software System and Plotting Language), [Ref. 9], which is a commercial proprietary plotting package.

Contour plots and 3-D plots of near electric field are presented. The phase variation of the near electric field is examined and plotted also. The effect of the shipboard topside environment on the electric near field of the monopole antenna is discussed.

For the surface patch model radiation patterns were calculated in order to relate the far field and near field behavior of the antenna.

#### D. THEORETICAL BACKGROUND

##### 1. Near Field Theory

The fields around an antenna may be divided into two regions, one near the antenna called the near field or Fresnel zone and one at a large distance called the far-field or Fraunhofer zone. Figure 1a indicates these two regions.



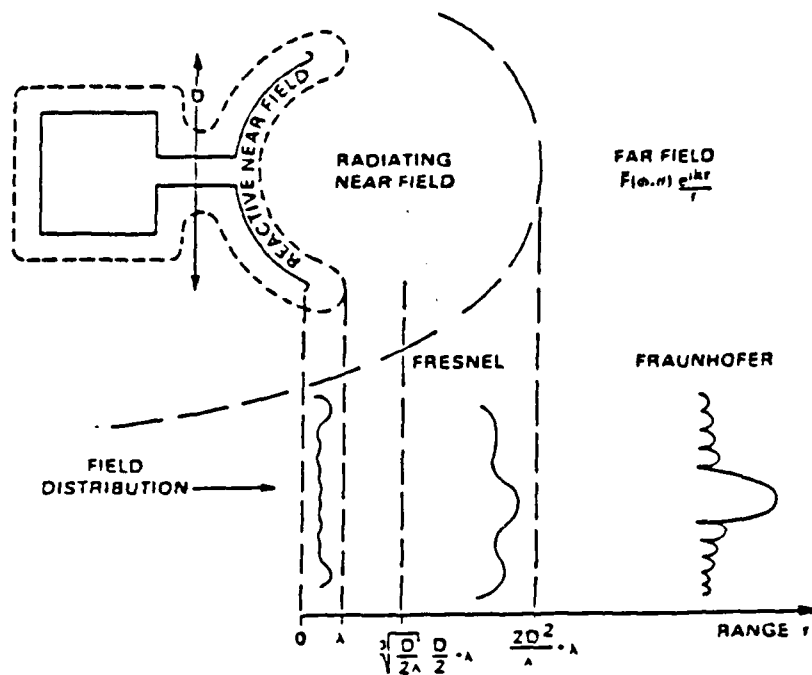


Figure 1a. Fields of a Radiating Antenna [Ref. 8]

The boundary between the far field and near field is the distance  $r = 2D^2/\lambda$ , where  $D$  is the maximum length of the antenna in meters and  $\lambda$  is the wavelength in meters. The distance from the surface of the antenna to this boundary is called the near field region, while beyond this boundary the region is called far field. The near field region is divided into two subregions -- the reactive and radiating near field. The reactive near field is extended to  $\lambda/2\pi$  from the antenna's surface, while in practice a distance of  $\lambda$  represents this boundary. The phase of the magnetic and electric field is almost quadrature in regions within a wavelength of the antenna (reactive near field). Beyond the distance of a wavelength, the electric and magnetic fields

are propagating in phase (radiating near field) until the far field is reached. In the far field, the shape of the field pattern is independent of the distance, while in the near field the shape depends on it.

Consider a dipole antenna which is enclosed in an imaginary sphere. Figure 1b shows the energy flow near the dipole.

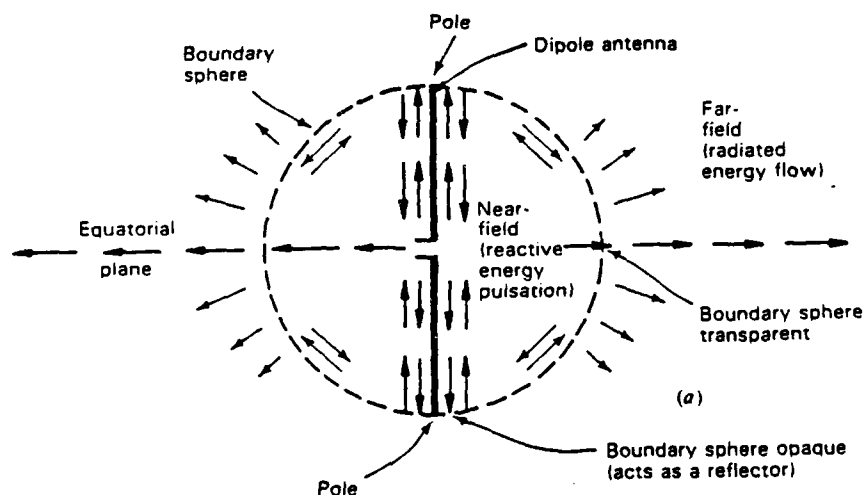


Figure 1b. Energy Flow Near a Dipole Antenna [Ref. 8]

The waves are reflected near the poles while in the equator are diffusing perpendicular to the dipole. Consequently, energy is oscillating near the antenna while part of it flows outward in the region of the equator. The oscillating energy represents reactive power, while the outward flow represents radiated power. The near field is related to charge and current density while the far field is related only to current.

## 2. Numerical Electromagnetics Code (NEC) - Method of Moments

NEC is a computer code which analyzes the electromagnetic response of antennas. The program uses an electric field integral equation (EFIE) and a magnetic field integral equation (MFIE) to do this analysis. The EFIE and MFIE integral equations are solved in NEC, for current distribution using the method of moments approach. This approach reduces the integral equation to a system of linear algebraic equations in the form of a matrix, where the unknowns are coefficients in an expansion of the current. The matrix equations can be solved for the current in a high-speed computer. There are two limitations to the moment method: (1) the amount of computer storage necessary for the elements of the impedance matrix and (2) the time required to calculate those elements and solve the system of equations. When the current distribution is computed, all effects of the antenna structure can be determined. [Ref. 1]

During this investigation, two modeling approaches are used, surface patch modeling and wire grid modeling. In surface patch modeling a two-dimensional field equation and appropriate surface boundary conditions are applied to solve for two orthogonal components of current on small patches representing the actual surface. Either an electric field integral equation (EFIE) or a magnetic field integral equation (MFIE) may be used theoretically. NEC employs the MFIE method while the code mentioned previously, "PATCH",

uses an EFIE method. The wire grid modeling approach approximates the antennas and the surfaces on the ship with thin wires using the EFIE method. Surfaces are represented as wire grids in which the grid cells are much smaller than the wavelength. Either modeling approach can provide data upon which engineering judgments can be made. The investigations of the two modeling approaches in the past shows that wire gridding provides slightly more accurate data in comparison to surface patch modeling. This is another point of investigation of this thesis. However, surface patch modeling can apparently offer some amount of savings in computer time cost. [Ref. 2]

## II. SURFACE PATCH MODELING

### A. GUIDELINES FOR MODELING USING NEC

A conducting surface is modeled by means of multiple, small flat surface patches, corresponding to segments used to model wires. The patches are chosen to completely cover the surface to be modeled. The parameters defining the surface patch are the cartesian coordinates of the patch center, the components of the outward-directed, unit normal vector and the patch area. The program computes the surface current on each patch along the orthogonal unit vectors which are tangent to the surface. Four patch shape options exist: arbitrary shape, rectangular, triangular, and quadrilateral. For the rectangular, triangular, and quadrilateral patches, the outward normal vector  $\hat{n}$  is specified by ordering of corners 1, 2, and 3 using the right-hand rule. The vectors  $\hat{t}_1$  are parallel to the side from corner 1 to corner 2, and  $\hat{t}_2 = \hat{n} \times \hat{t}_1$ . The coordinates of corners 1, 2, and 3 have to be specified in the program. Figure 2 shows how the multiple patches are defined for a rectangular surface. Rectangular patches were used for the modeling purposes of this thesis.

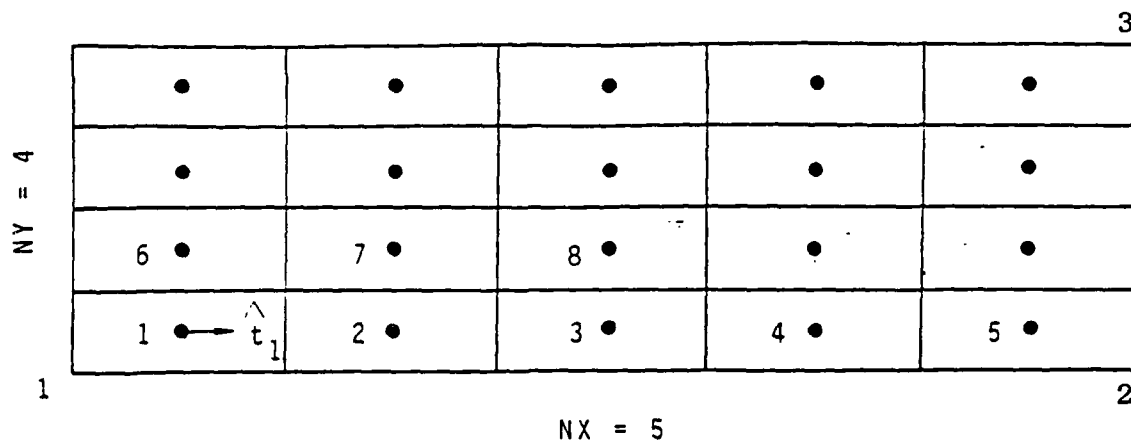


Figure 2. Rectangular Surface Covered by Multiple Patches  
[Ref. 1]

When a wire is connected to a surface, the wire must end at the center of a patch with identical coordinates used for the wire end and the patch center. The program then divides the patch into four equal patches about the wire end. Only a single wire may connect to a given patch and a segment may have a patch connection on only one of its ends. A wire may never connect to a patch formed by subdividing another patch for a previous connection. The use of surface patches is restricted to modeling voluminous bodies. Very long narrow patches should be avoided when subdividing the surface. [Ref. 1]

#### B. LIMITATIONS AND OPTIMIZATION CRITERIA

The accuracy of the results depends on the patch size measured in wavelengths. A minimum of about 25 patches should be used per square wavelength of surface area, with the maximum size for an individual patch less than or equal to 0.04 square wavelengths.

In NPGNEC (an NPS customized version of NEC-3) which was used for simulation purposes in this thesis, the number of patches plus the number of segments must be less than 300. When the total number is greater than 300 and less than 1,000, the NPG1000 version of NEC-3 must be used; this is done for the wire grid modeling in the second part of this thesis. Since the program does not integrate over patches except at a wire connection (active patch), the patch shape does not affect the results. The parameters affecting the results are the location of the patch centroid, the patch area, and the outward unit normal vector.

The optimum model for complex structures which the first part of the thesis investigated can be estimated by varying the segment and patch density, observing the results and the convergence of the solution. In the case of an edge-mounted antenna, the accuracy of the results are expected to depend upon the size of the patches near the edge. Smaller patches are suggested at edge areas since the current magnitude may vary rapidly in this region.

### C. PREVIOUS STUDIES

In References 5 and 6, experimental and computational investigations were performed to determine the admittance characteristics of a monopole antenna mounted on a cubical conducting box of 0.1 m sides ( $\lambda/3$  at frequency 1 GHz) over a ground plane. The antenna, a 6 cm monopole ( $\lambda/5$  at frequency 1 GHz), was tested for three different mounting positions on

the top surface. Experimental admittance data for the 6 cm monopole antenna were plotted vs. frequency [Ref. 5]. Numerically calculated data using the "PATCH" computer code were also tabulated [Ref. 5]. "PATCH" is a frequency domain electromagnetic analysis code based on a method of moments solution to the Electric Field Integral Equation (EFIE) [Ref. 7]. In this code objects are modeled by planar triangular patches which easily conform to surfaces and boundaries of general shape and allow variable patch densities over the surface of the object.

D. MODEL OF 6 CM MONOPOLE ANTENNA MOUNTED ON A CUBICAL CONDUCTING BOX--ADMITTANCE AND AVERAGE GAIN INVESTIGATION

Monopole antennas mounted on arbitrary shaped objects have received much attention because they represent practical situations where antennas are mounted on aircraft, ships, vehicles, and buildings. The antennas are not always centrally mounted and are often located near edges and corners.

Super-structures of Navy ships can be modeled as conducting boxes which form a "ship-like" structure. Navy shipboard topside antennas are often monopoles and are attached to the top of these boxes, in different locations.

The numerical model of a cubical five-sided box of 0.1 m per side was constructed using NEC (the bottom was not included as a surface since the box was placed on a perfectly conducting ground plane). A 6 cm monopole antenna was placed



at the center, at the edge (3.63 cm from center) and at a corner (5.14 cm on a diagonal from center), as shown in Figure 3. This model configuration was selected since experimental data was available for it for comparison from Reference 5.

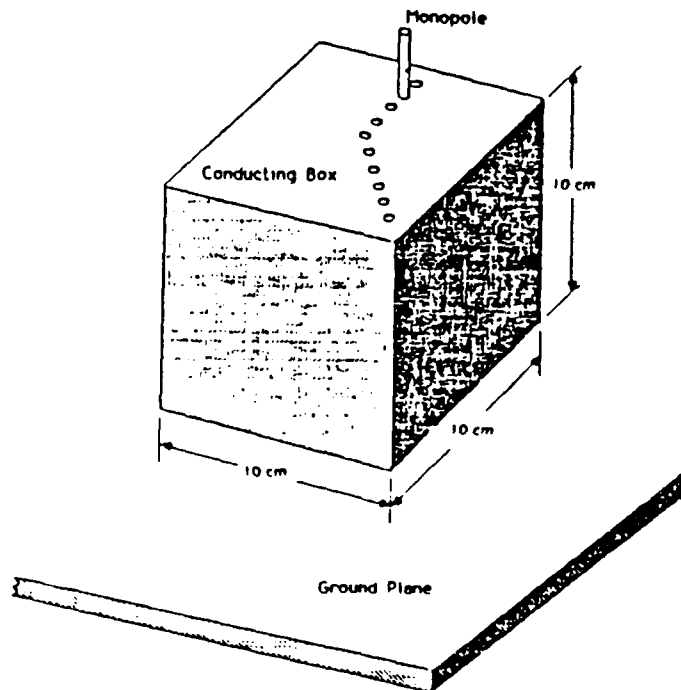


Figure 3. Geometry of Monopole Attached to the Conducting Box Over a Ground Plane

The first part of the investigation checked the input impedance and average gain of the model using NEC-3 (NPGNEC). Comparisons of calculated values for input impedance and average gain were made to experimental values from Reference 5 in order to validate the computer model before proceeding with an investigation of near fields.

This modeling exercise compared driving point admittance from NEC as patch density is varied, to both experimental

values and PATCH code results from Reference 5. The number of patches on the top of the box was varied in search of an optimum value of surface samples, which would later be used for near field calculations. The top was subdivided to retain symmetry, as much as possible, and to closely match positions of the antenna on the experimental model. The monopole was positioned at the center, at an edge (3.63 cm from the center) and at a corner (5.14 cm on a diagonal from the center), very close to the experimental model positions.

Nine frequencies from 1 to 1.4 GHz were selected. NEC input data files for the three different locations of the monopole are presented in Appendix A.

The Numerical Green's Function option (NGF) was used to exploit partial symmetry, reducing solution time. The nonsymmetric part, the 6 cm monopole antenna, was added to the NGF file of the box for impedance and average gain calculations.

#### 1. Monopole at the Center

The monopole was divided into five segments and placed at center of the top surface. The top surface was divided into 25 (5x5), 49 (7x7), 81 (9x9), and 121 (11x11) patches. The impedance (in OHMS) and admittance (in mmHOS) are listed in Tables 4, 5, 6, and 7 for the nine frequencies. Experimental data from Reference 5 are shown in Table 2. NEC statistics for the four top surface configurations are in Table 3. The number of patches used for each case, the patch

area, and the variation of run time are shown. Double precision NEC (DNPGNEC) was used for the 5x5 and 7x7 patch case to investigate the possibility of better accuracy than single precision NEC. The results are in Tables 8 and 9.

To gain insight into the accuracy of the results, the average power gain was calculated. Correct average power gain does not necessarily insure accurate results. Therefore, input impedance was also checked. The average power gain provides a good check of the solution accuracy if it is close to two for radiating systems located over perfectly conducting ground which is our case, or close to one for free space conditions. Average power gain within 10% of theoretical is adequate for engineering purposes. For all cases, the calculated average power gain is between 1.96 (minimum) to 2.02 (maximum) which is in good agreement with theory.

NEC results and measurements, for the monopole at the center, while the patch density varies on the top surface (Case 1: 5x5, Case 2: 7x7, Case 3: 9x9, and Case 4: 11x11), are presented in Figures 4, 6, 8, and 10. In Figures 5, 7, 9, and 11, the PATCH code results have been superimposed on those of NEC and the measurements for comparison. The PATCH code is compared to experimental results in Figure 12.

Single precision (NPGNEC) calculations vs double precision (DNPGNEC) results (Tables 4, 6, 8, and 9) for conductance and susceptance vary only in the second and

third decimal places. This difference is negligible and cannot be observed in a plot. For all cases, the antenna was fed at the base segment.

**CASE 1: 5x5 patches on top surface (Figures 4 and 5)**

The correlation between measurements and NEC calculations for admittance in Figure 4, was generally quite poor. Apparently, the solution has not converged. There is good correlation for susceptance between 1.2 and 1.4 GHz. PATCH results of Figure 5 correlate well with measurements in comparison to NEC.

**CASE 2: 7x7 patches on top surface (Figures 6 and 7)**

NEC values of admittance correlate well with measurements (Figure 6), but the run time observed in Table 3 is almost double compared to Case 1. The solution has apparently converged. The increased accuracy is probably due to the top of the surface patch box having been more finely divided into smaller patches which provides finer details of surface currents. Observing Figure 7, we see that NEC has somewhat better correlation with measurements than PATCH does.

**CASE 3: 9x9 patches on top surface (Figures 8 and 9)**

There is good correlation of NEC results with measurements in Figure 8, especially in conductance, but not quite as good as in Case 2.

NEC performs better than PATCH for both conductance and susceptance. As the number of patches increases (81

patches on the top surface vs 49 for Case 2 and 25 for Case 1), the run time is doubled and tripled correspondingly.

**CASE 4:** 11x11 patches on the top surface (Figures 10 and 11)

The correlation of NEC results is good especially in conductance (Figure 10) and is better than PATCH (Figure 11). Run time is doubled compared to Case 3, as can be observed from Table 3.

**GENERAL RESULTS:** The solution seems to converge at Case 2 with  $7 \times 7 = 49$  patches on the top surface, patch area  $0.00020 \text{ m}^2$  ( $0.0022$  square wavelengths at  $1 \text{ GHz}$ ) and  $0.00005 \text{ m}^2$  ( $0.00055$  square wavelengths at  $1 \text{ GHz}$ ) for each of the four central "subpatches" where NEC subdivides a normal size patch at the connection point to the monopole. NEC gives excellent results compared to measurements for Cases 2, 3, and 4 and has better performance than PATCH for these three cases. PATCH results are better than NEC results for Case 1 ( $5 \times 5 = 25$  patches on the top). For easier comparison between the two codes, NEC vs. PATCH admittance values for the Cases 1, 2, 3 and 4 are plotted separately in Figures 13, 14, 15, and 16. In Figures 17 and 18, NEC's conductance and susceptance vs measurements as the top surface patch density increases ( $5 \times 5$ ,  $7 \times 7$ ,  $9 \times 9$ , and  $11 \times 11$  patches) are available for comparison. Consequently, the optimum model appears to be Case 2 ( $7 \times 7 = 49$  patches on the top), the one that is selected for the near field investigation for surface patch numerical model.

TABLE 2  
MEASURED DATA FOR A 6CM MONOPOLE ON A CUBICAL BOX

FREQUENCY (GHZ)	6CM MONOPOLE POSITION		
	ADMITTANCE (mMHOS)		
	AT CENTER	AT EDGE 3.5cm FROM CENTER	AT CORNER 5.15cm FROM CENTER
1.00	5.0 + j20.0	7.0 + j17.0	8.0 + j12.0
1.05	14.0 + j28.0	13.0 + j19.5	12.0 + j13.0
1.1	37.0 + j24.0	24.0 + j17.0	18.0 + j10.0
1.15	41.0 - j 8.0	32.0 + j 3.0	21.0 + j 4.0
1.2	26.0 - j16.0	26.0 - j 7.5	20.0 - j 2.0
1.225	19.0 - j15.0	22.0 - j10.0	17.0 - j 4.5
1.3	11.0 - j10.0	12.0 - j 9.0	12.0 - j 5.0
1.4	7.0 - j 6.0	7.0 - j 6.0	8.0 - j 3.0

TABLE 3  
 NEC STATISTICS FOR MONOPOLE AT CENTER OF PATCH BOX  
 AS THE NUMBER OF PATCHES ON TOP INCREASES  
 (NPS MAINFRAME COMPUTER - IBM SYSTEM 370)

CASE	NUMBER OF PATCHES	PATCH AREA (m <sup>2</sup> )	RUN TIME (sec) SINGLE PRECISION NEC
1	surface on sides 18 x 4 = 72	0.00056	13.937
	surface on top 5 x 5 = 25	0.00040	
	monopole attach- ment patch 4	0.00010	6.747
	TOTAL #PATCHES 101		
2	surface on sides 18 x 4 = 72	0.00056	25.883
	surface on top 7 x 7 = 49	0.00020	
	monopole attach- ment patch 4	0.00005	8.940
	TOTAL #PATCHES 125		
3	surface on sides 18 x 4 = 72	0.00056	54.170
	surface on top 9 x 9 = 81	0.00012	
	monopole attach- ment patch 4	0.00003	13.107
	TOTAL #PATCHES 157		
4	surface on sides 18 x 4 = 72	0.00056	107.00
	surface on top 11 x 11 = 121	0.00008	
	monopole attach- ment patch 4	0.00002	17.767
	TOTAL #PATCHES 197		

TABLE 4  
CALCULATED DATA  
MONOPOLE AT CENTER OF SURFACE PATCH BOX  
(5 X 5 PATCHES ON THE TOP SURFACE - BASE SEGMENT FEED)

FREQUENCY (GHZ)	AVERAGE POWER GAIN	IMPEDANCE (OHMS) ADMITTANCE (MMHOS)
1.00	2.02	10.82 - j20.21 20.58 + j38.45
1.05	2.02	14.38 - j 5.51 60.64 + j23.24
1.10	2.01	18.86 + j 8.57 43.94 - j19.97
1.15	2.01	24.29 + j21.89 22.72 - j20.47
1.175	2.01	27.34 + j28.20 17.72 - j18.28
1.2	2.01	30.60 + j34.25 14.50 - j16.24
1.225	2.01	34.03 + j39.99 12.34 - j14.50
1.3	2.01	44.86 + j55.32 8.84 - j10.90
1.4	2.02	58.47 + j71.83 6.81 - j 8.37



TABLE 5  
CALCULATED DATA  
MONOPOLE AT CENTER OF SURFACE PATCH BOX  
(7 X 7 PATCHES ON THE TOP SURFACE - BASE SEGMENT FEED)

FREQUENCY (GHZ)	AVERAGE POWER GAIN	IMPEDANCE (OHMS) ADMITTANCE (mMHOS)
1.00	1.99	10.99 - j37.53 7.19 + j24.54
1.05	1.99	14.60 - j21.82 21.18 + j31.65
1.10	1.99	19.14 - j 6.81 46.36 + j16.50
1.15	1.99	24.64 + j 7.36 37.26 - j11.12
1.175	1.99	27.74 + j14.08 28.66 - j14.55
1.2	1.99	31.04 + j20.50 22.43 - j14.81
1.225	1.99	34.52 + j26.62 18.17 - j14.01
1.3	1.99	45.53 + j42.98 11.61 - j10.97
1.4	1.99	59.41 + j60.67 8.24 - j 8.41

TABLE 6  
CALCULATED DATA  
MONOPOLE AT CENTER OF SURFACE PATCH BOX  
(9 X 9 PATCHES ON THE TOP SURFACE - BASE SEGMENT FEED)

FREQUENCY (GHZ)	AVERAGE POWER GAIN	IMPEDANCE (OHMS) ADMITTANCE (MMHOS)
1.00	1.98	11.11 - j48.08 4.56 + j19.74
1.05	1.98	14.75 - j31.73 12.05 + j25.92
1.10	1.97	19.33 - j16.14 30.48 + j25.45
1.15	1.97	24.88 - j 1.42 40.06 + j 2.29
1.175	1.97	28.00 + j 5.54 34.36 - j 6.80
1.2	1.97	31.34 + j12.22 27.70 - j10.80
1.225	1.97	34.84 + j18.57 22.35 - j11.91
1.3	1.98	45.96 + j35.57 13.60 - j10.53
1.4	1.98	59.99 + j54.01 9.20 - j 8.29

TABLE 7  
CALCULATED DATA  
MONOPOLE AT CENTER OF SURFACE PATCH BOX  
(11 X 11 PATCHES ON THE TOP SURFACE - BASE SEGMENT FEED)

FREQUENCY (GHZ)	AVERAGE POWER GAIN	IMPEDANCE (OHMS) ADMITTANCE (MMHOS)
1.00	1.97	11.19 - j50.03 4.26 + j19.04
1.05	1.96	14.85 - j33.49 11.06 + j24.95
1.10	1.96	19.46 - j17.73 28.08 + j25.58
1.15	1.96	25.05 - j 2.86 39.41 + j 4.49
1.175	1.96	28.20 + j 4.19 34.69 - j 5.16
1.2	1.96	31.55 + j10.94 28.29 - j 9.80
1.225	1.96	35.04 + j17.36 22.90 - j11.33
1.3	1.97	46.27 + j34.56 13.87 - j10.36
1.4	1.97	60.42 + j53.21 9.32 - j 8.20

TABLE 8  
CALCULATED DATA  
MONOPOLE AT CENTER OF SURFACE PATCH BOX  
(5 X 5 PATCHES ON THE TOP SURFACE - BASE SEGMENT FEED)  
(DOUBLE PRECISION CALCULATION)

FREQUENCY (GHZ)	AVERAGE POWER GAIN	IMPEDANCE (OHMS) ADMITTANCE (MMHOS)
1.00	2.02	10.82 - j20.20 20.60 + j38.46
1.05	2.01	14.38 - j 5.49 60.67 + j23.19
1.10	2.01	18.86 + j 8.58 43.91 - j19.99
1.15	2.01	24.29 + j21.90 22.70 - j20.47
1.175	2.01	27.35 + j28.22 17.71 - j18.27
1.2	2.01	30.61 + j34.26 14.50 - j16.23
1.225	2.01	34.53 + j40.00 12.34 - j14.50
1.3	2.01	44.87 + j55.33 8.84 - j10.90
1.4	2.02	58.47 + j71.84 6.81 - j 8.37

TABLE 9  
 CALCULATED DATA  
 MONOPOLE AT CENTER OF SURFACE PATCH BOX  
 (7 X 7 PATCHES ON THE TOP SURFACE - BASE SEGMENT FEED)  
 (DOUBLE PRECISION CALCULATION)

FREQUENCY (GHZ)	AVERAGE POWER GAIN	IMPEDANCE (OHMS) ADMITTANCE (MMHOS)
1.00	1.99	10.99 - j37.52 7.19 + j24.54
1.05	1.99	14.60 - j21.81 21.20 + j31.66
1.10	1.99	19.14 - j 6.79 46.39 + j16.47
1.15	1.99	24.65 + j 7.37 37.23 - j11.14
1.175	1.99	27.75 + j14.09 28.65 - j14.55
1.2	1.99	31.05 + j20.51 22.42 - j14.81
1.225	1.99	34.52 + j26.63 18.16 - j14.00
1.3	1.99	45.53 + j42.99 11.61 - j10.96
1.4	1.99	59.42 + j60.67 8.24 - j 8.41

# MONOPOLE AT CENTER OF PATCH BOX

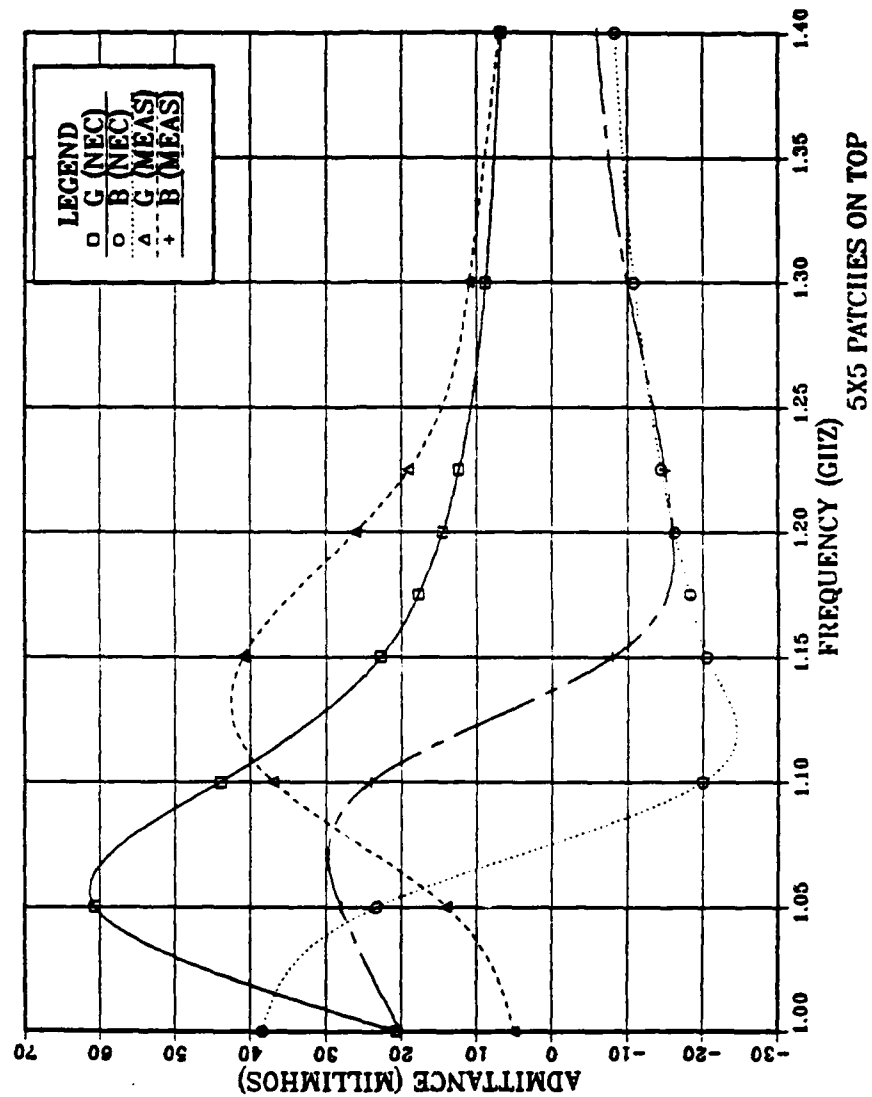


Figure 4. Monopole at Center of Patch Box  
(5x5 Patches on Top)  
NEC Admittance vs Measurements

# MONOPOLE AT CENTER OF PATCH BOX

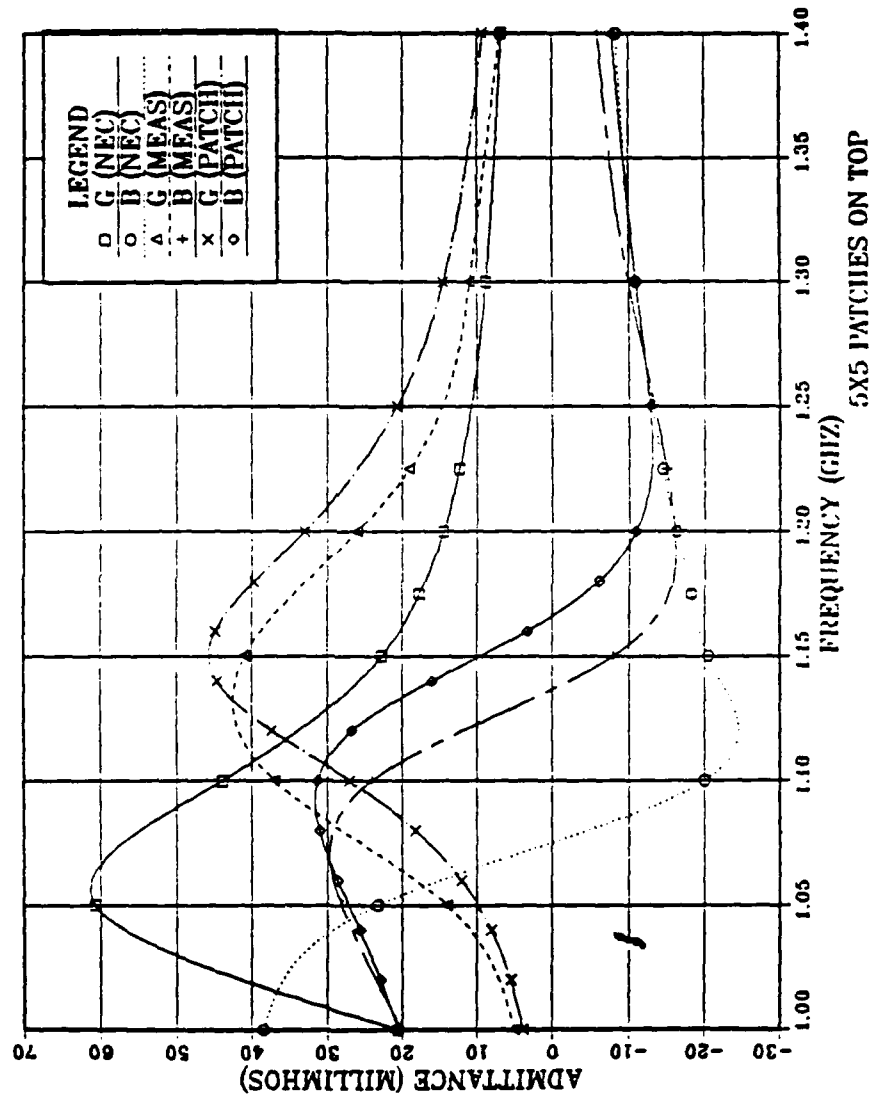


Figure 5. Monopole at Center of Patch Box  
(5x5 Patches on Top)  
NEC Admittance vs Measurements and "PATCH" Code

# MONOPOLE AT CENTER OF PATCH BOX

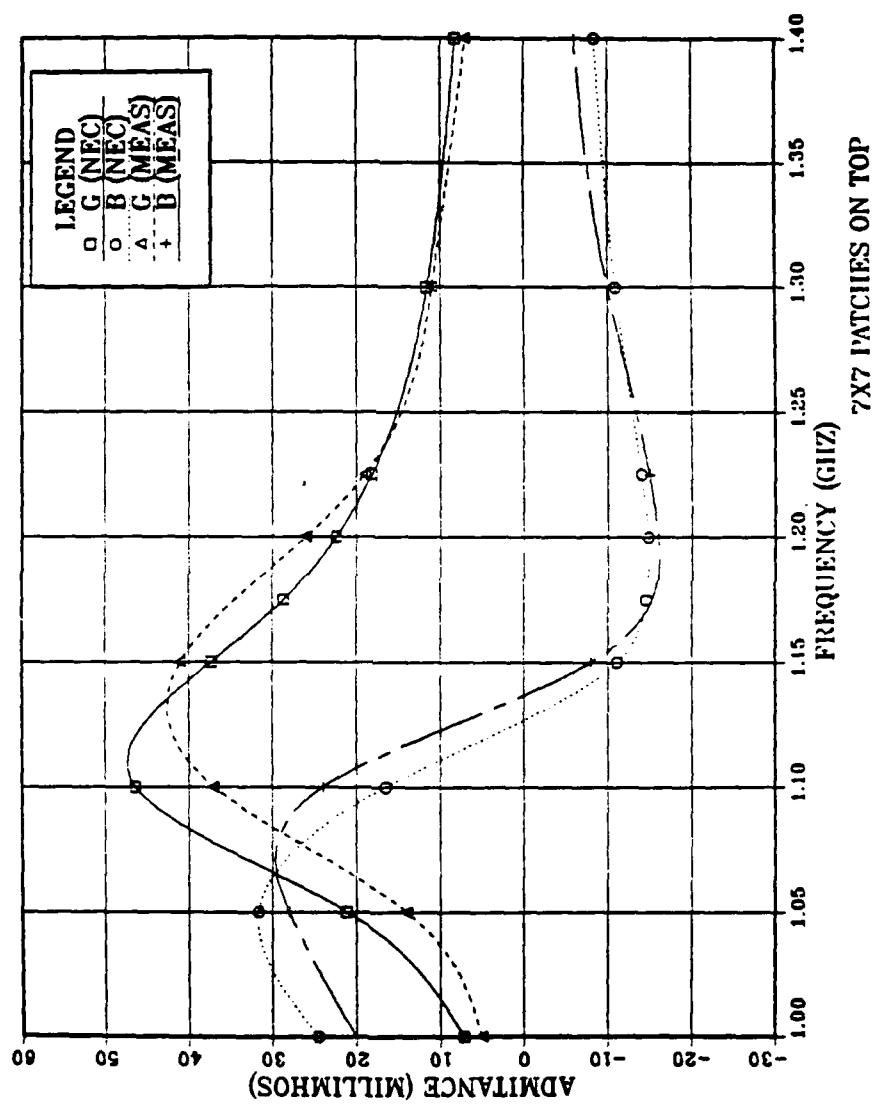


Figure 6. Monopole at Center of Patch Box  
(7x7 Patches on Top)  
NEC Admittance vs Measurements



# MONOPOLE AT CENTER OF PATCH BOX

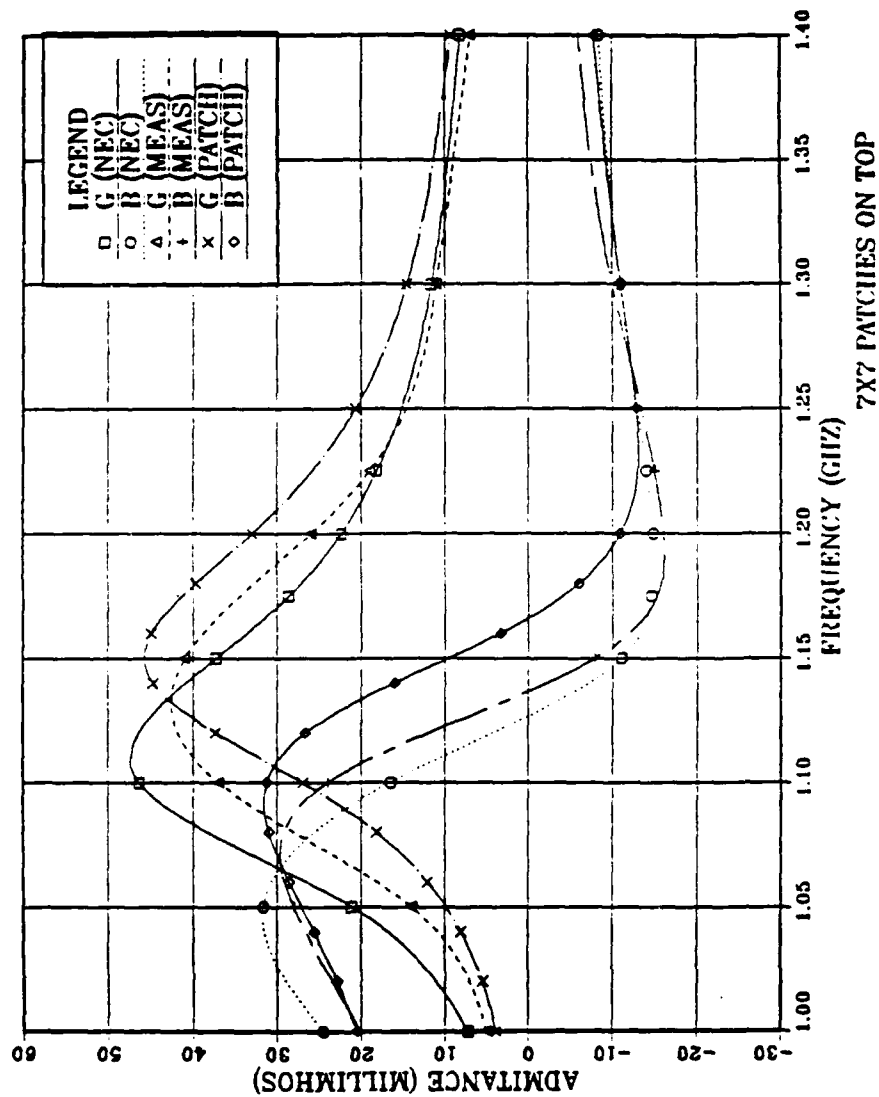


Figure 7. Monopole at Center of Patch Box  
(7x7 Patches on Top)  
NEC Admittance vs Measurements and "PATCH" Code

# MONOPOLE AT CENTER OF PATCH BOX

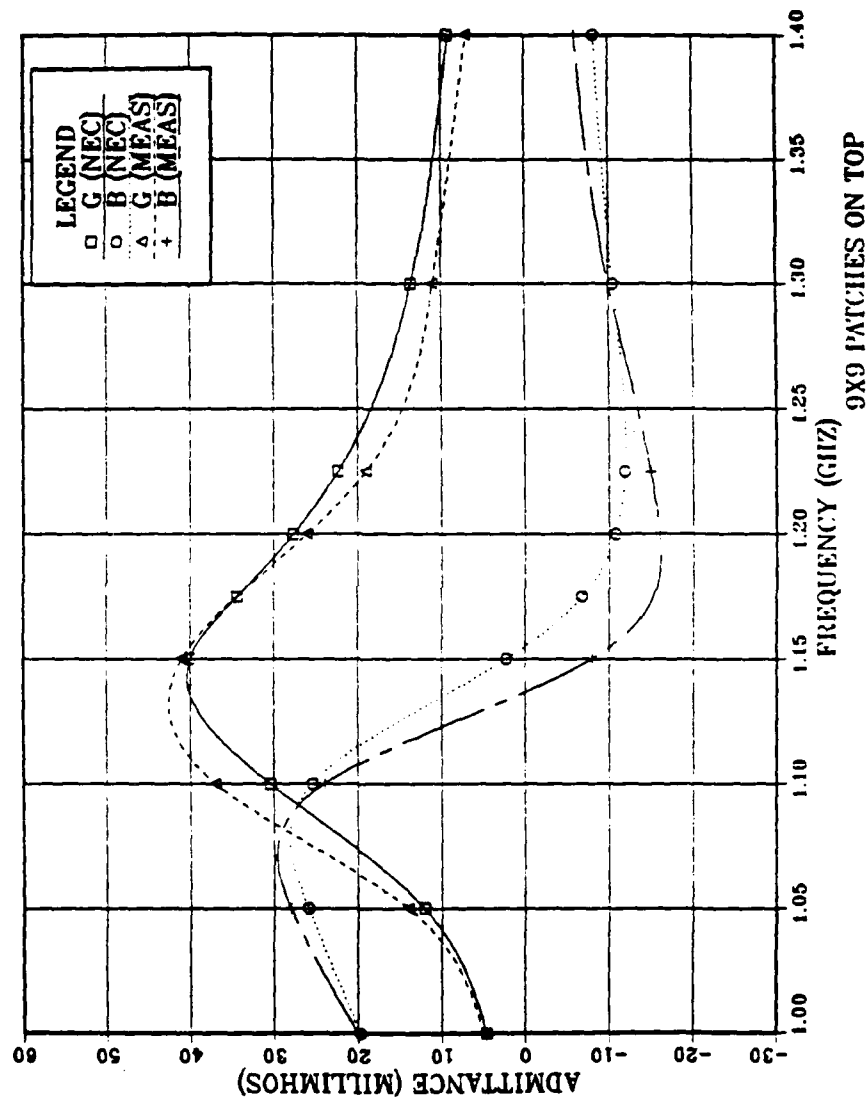


Figure 8. Monopole at Center of Patch Box  
(9x9 Patches on Top)  
NEC Admittance vs Measurements

# MONOPOLE AT CENTER OF PATCH BOX

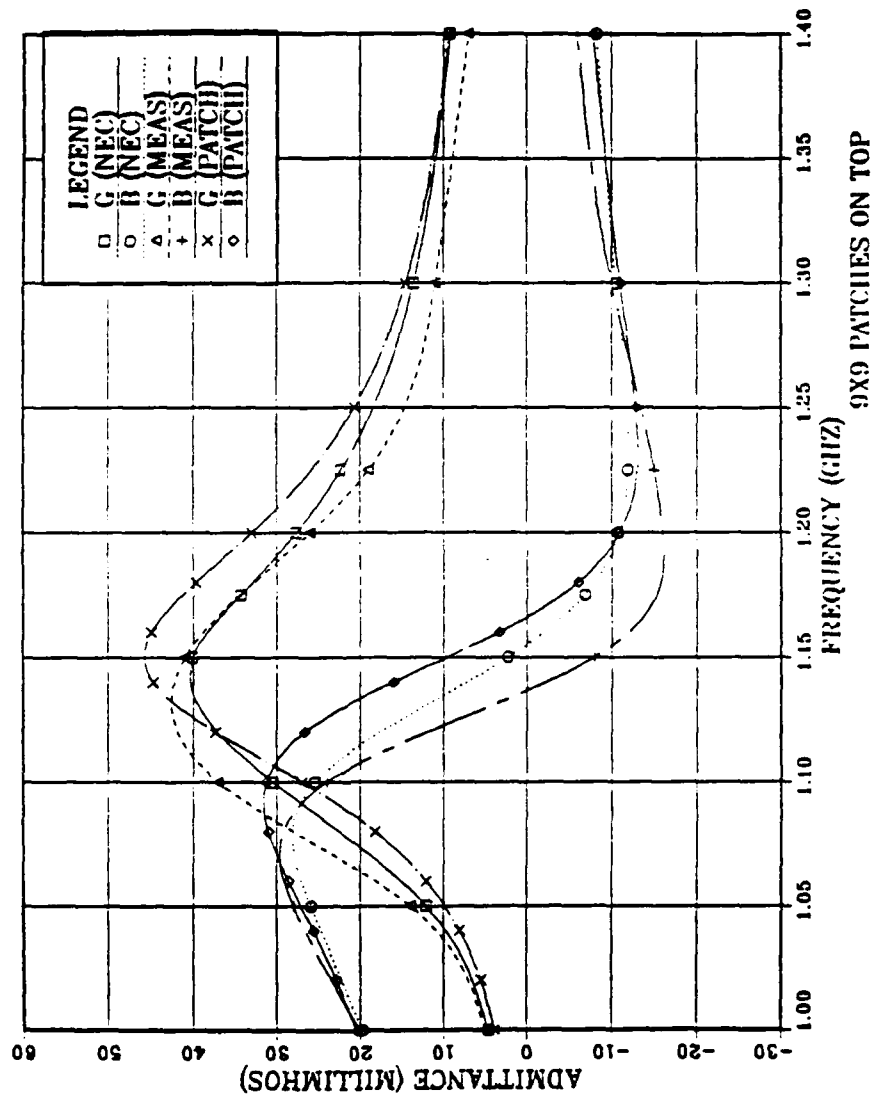


Figure 9. Monopole at Center of Patch Box  
(9x9 Patches on Top)  
NEC Admittance vs Measurements and "PATCH" Code

# MONOPOLE AT CENTER OF PATCH BOX

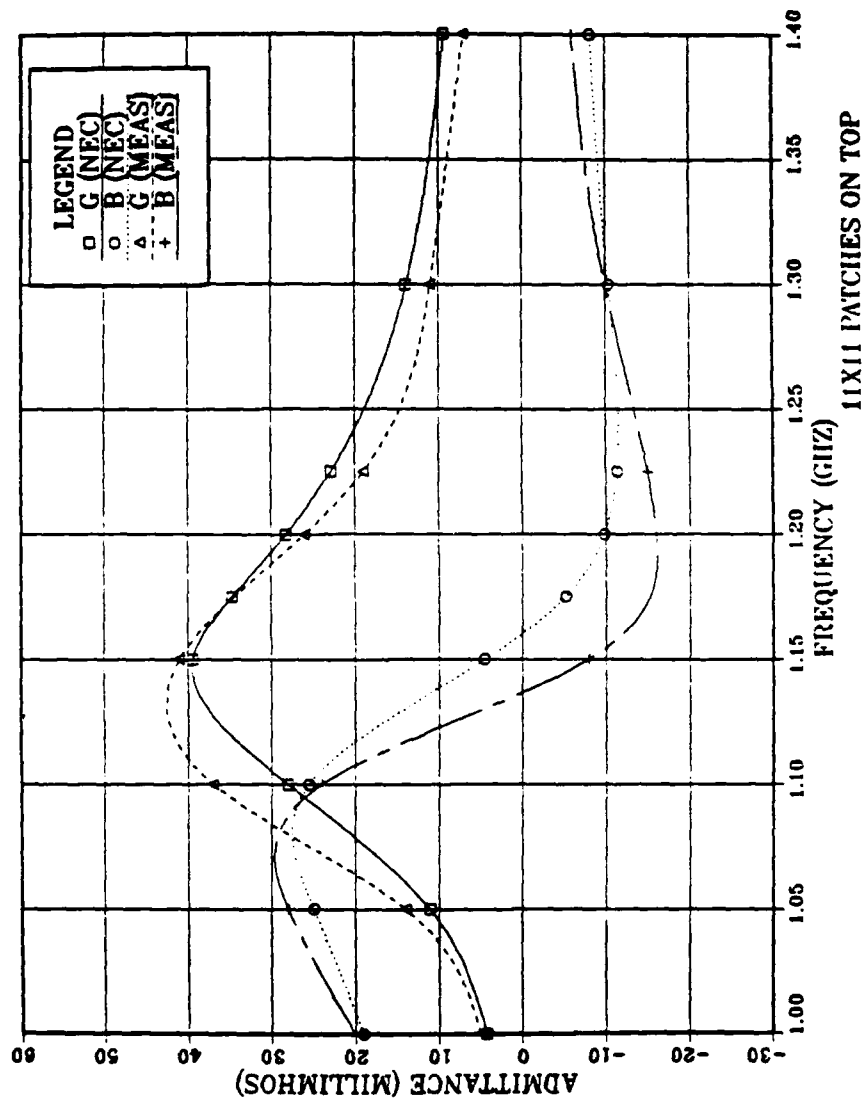


Figure 10. Monopole at Center of Patch Box  
(11x11 Patches on Top)  
NEC Admittance vs Measurements

# MONOPOLE AT CENTER OF PATCH BOX

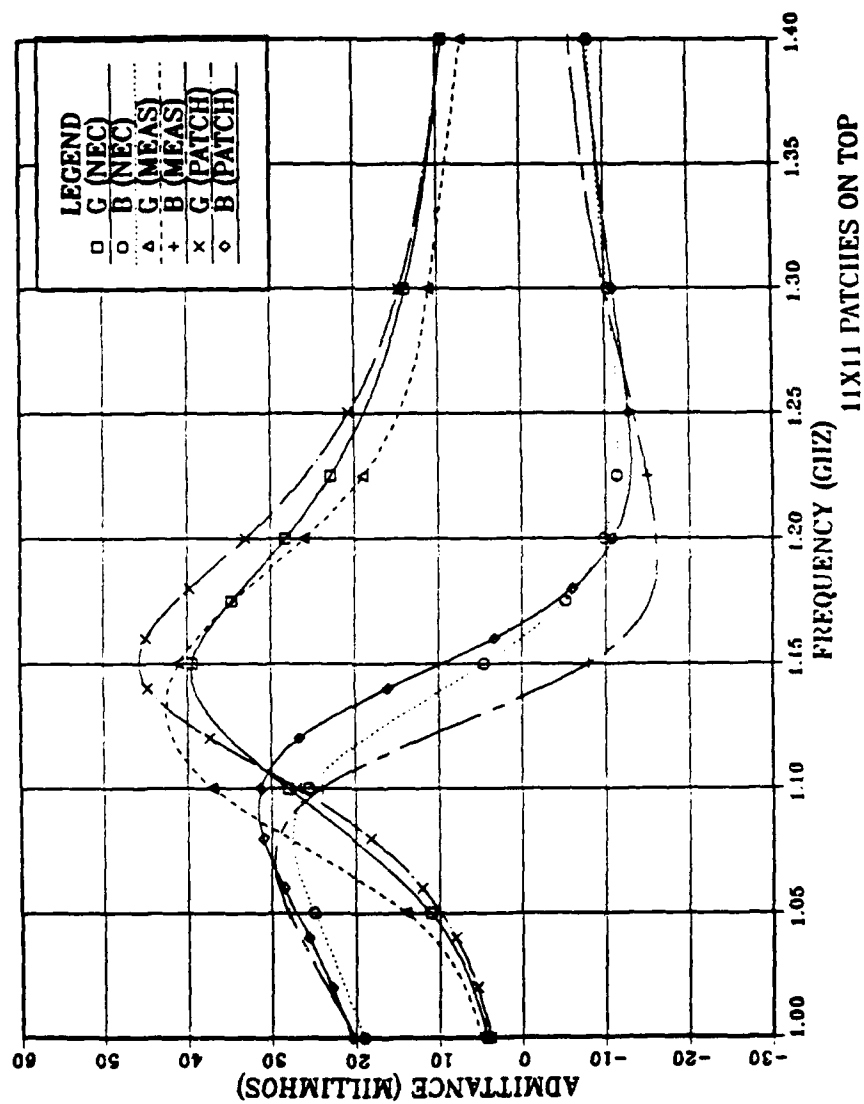


Figure 11. Monopole at Center of Patch Box  
(11x11 Patches on Top)  
NEC Admittance vs Measurements and "PATCH" Code

# MONOPOLE AT CENTER OF PATCH BOX

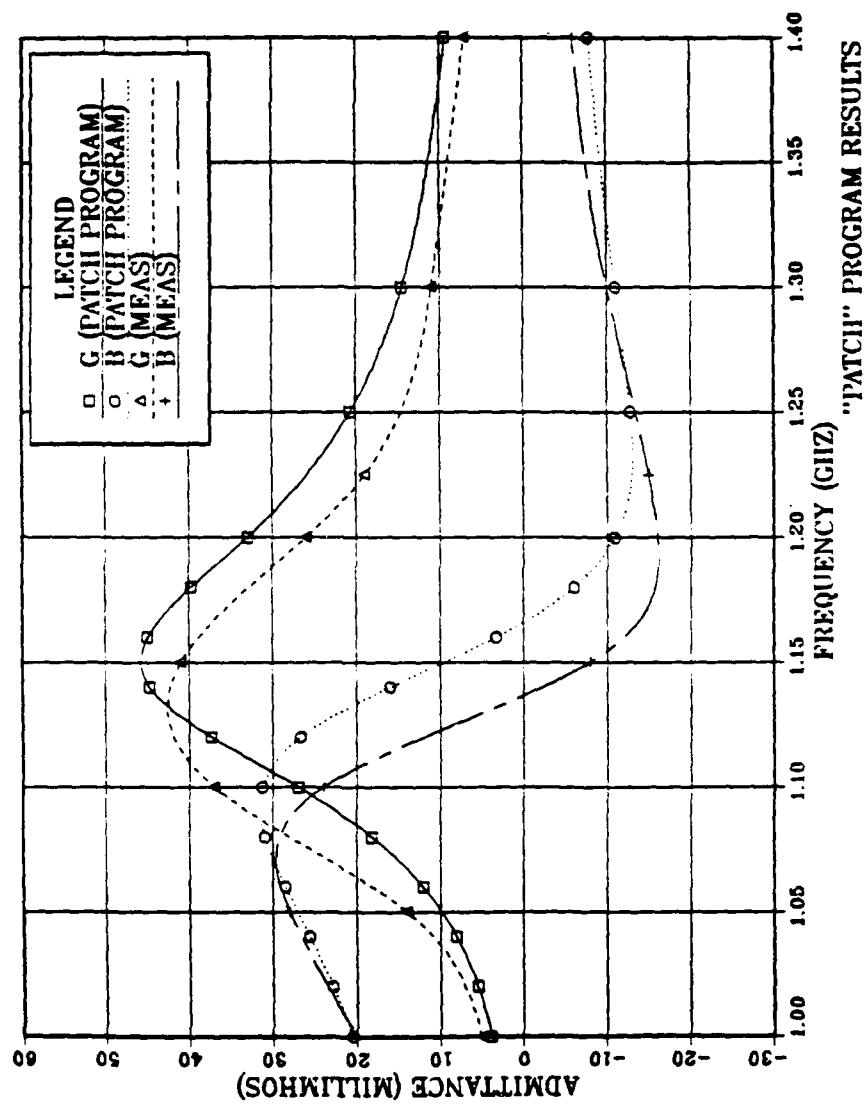


Figure 12. Monopole at Center of Patch Box  
"PATCH" Code Admittance vs Measurements

# MONOPOLE AT CENTER OF PATCH BOX

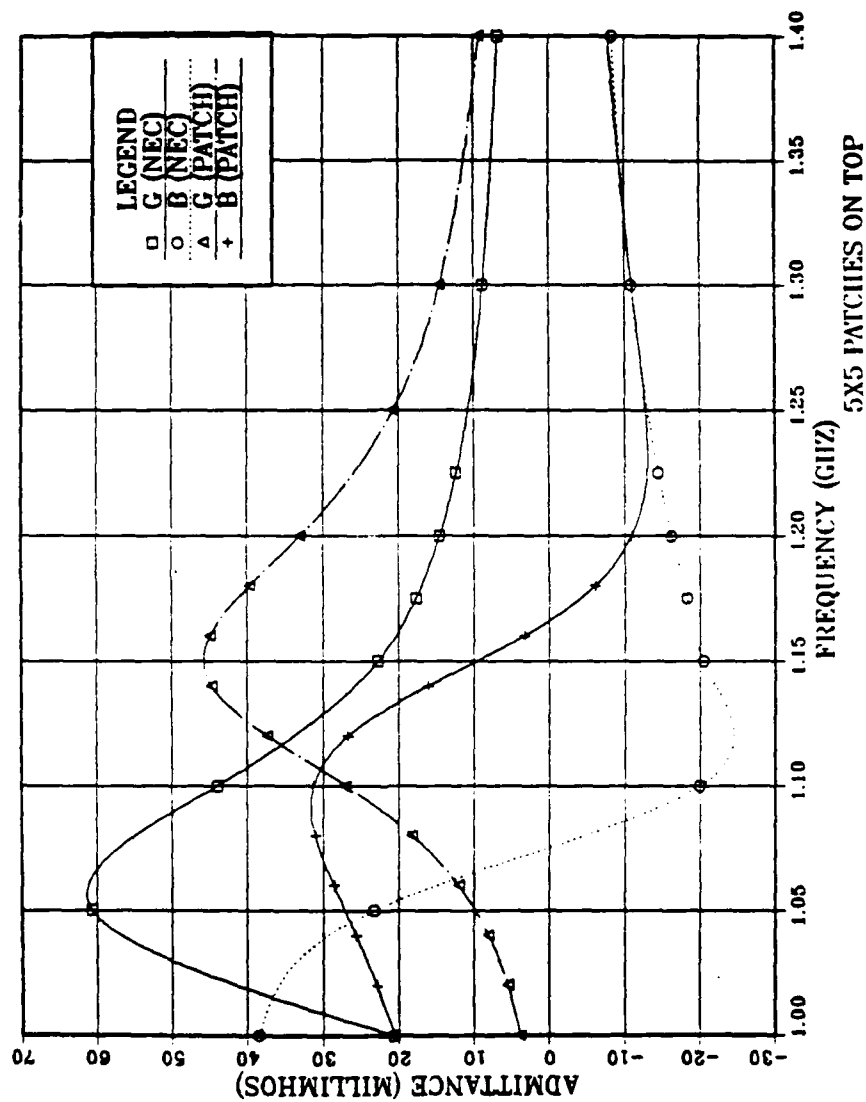


Figure 13. Monopole at Center of Patch Box  
(5x5 Patches on Top)  
NEC Admittance vs "PATCH" Code

# MONOPOLE AT CENTER OF PATCH BOX

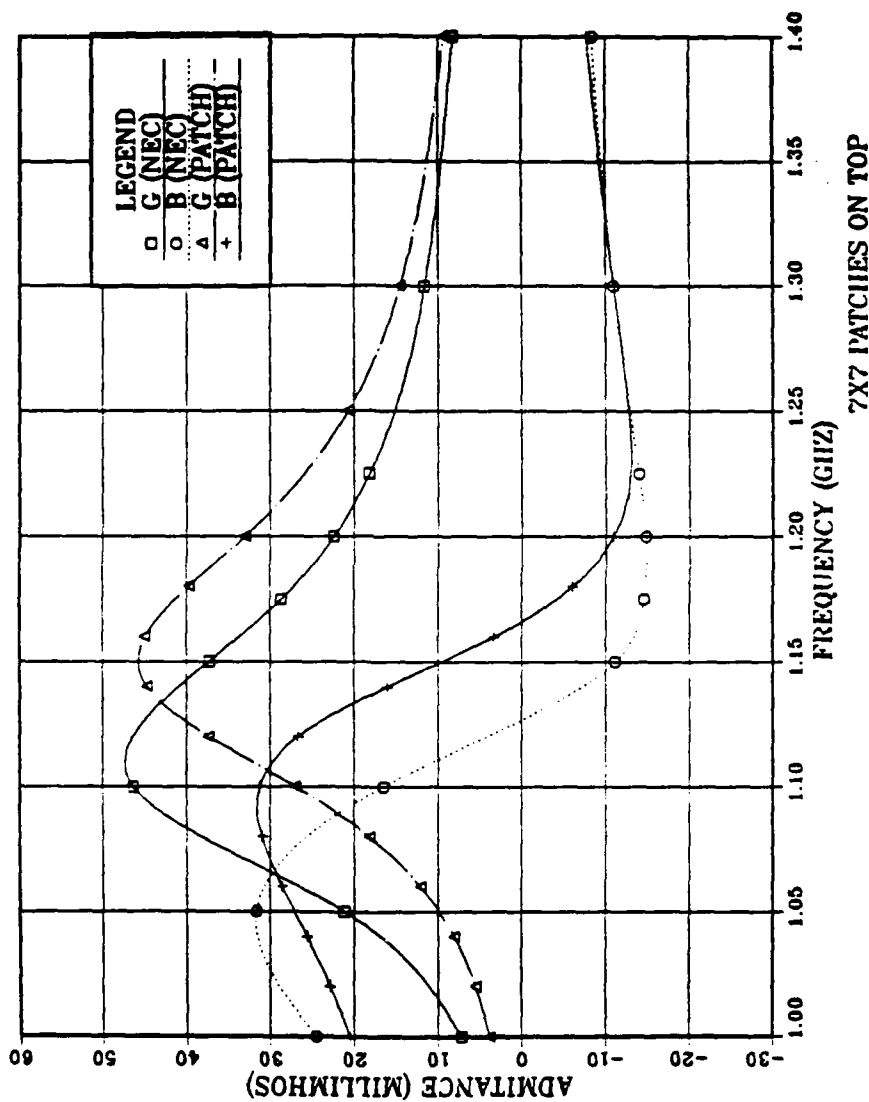


Figure 14. Monopole at Center of Patch Box  
(7x7 Patches on Top)  
NEC Admittance vs "PATCH" Code



# MONOPOLE AT CENTER OF PATCH BOX

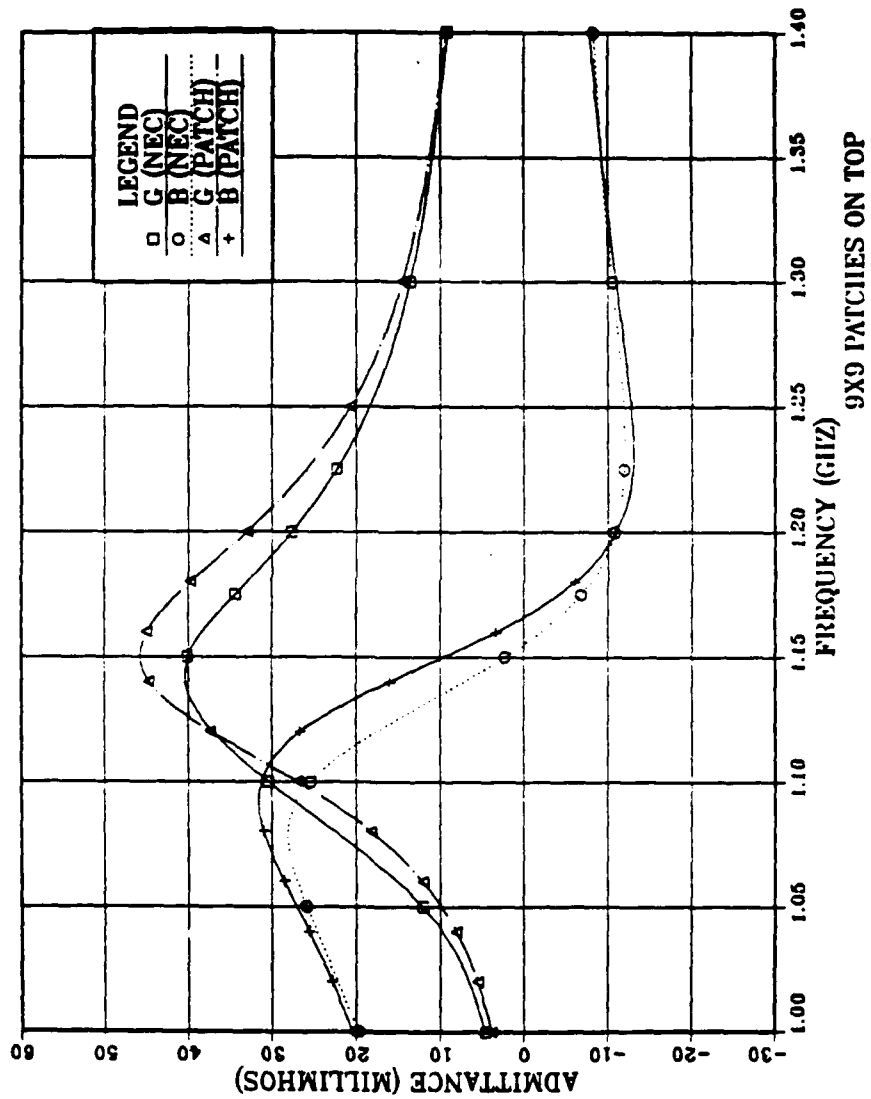


Figure 15. Monopole at Center of Patch Box  
(9x9 Patches on Top)  
NEC Admittance vs "PATCH" Code

# MONOPOLE AT CENTER OF PATCH BOX

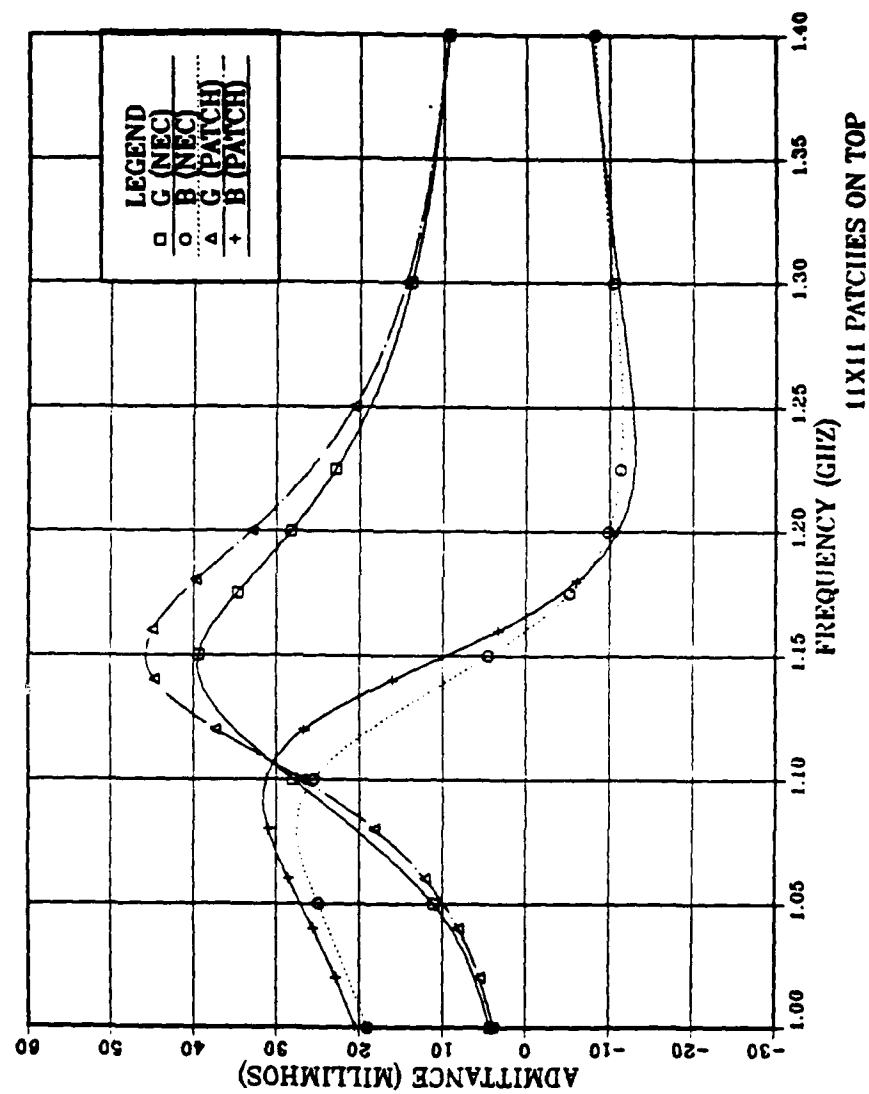


Figure 16. Monopole at Center of Patch Box  
(11x11 Patches on Top)  
NEC Admittance vs "PATCH" Code

# MONOPOLE AT CENTER OF PATCH BOX

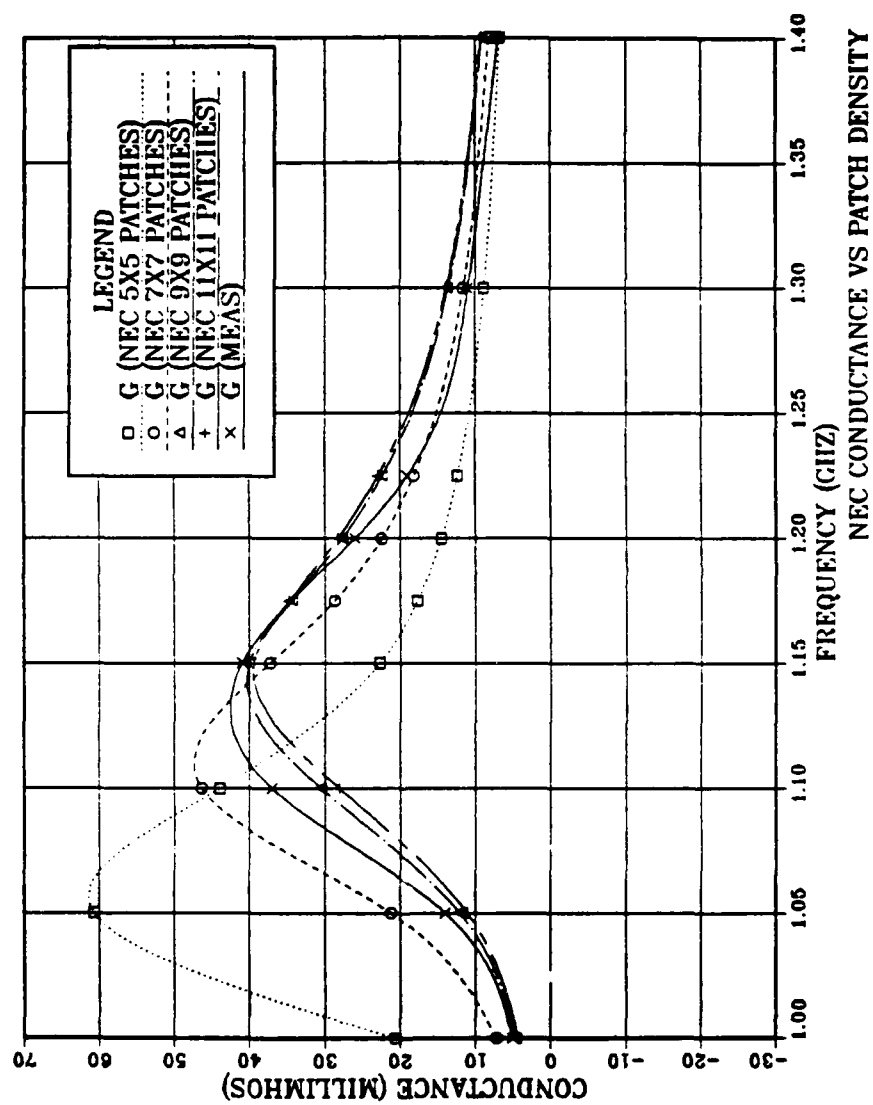


Figure 17. Monopole at Center of Patch Box  
NEC Conductance vs Patch Density

# MONOPOLE AT CENTER OF PATCH BOX

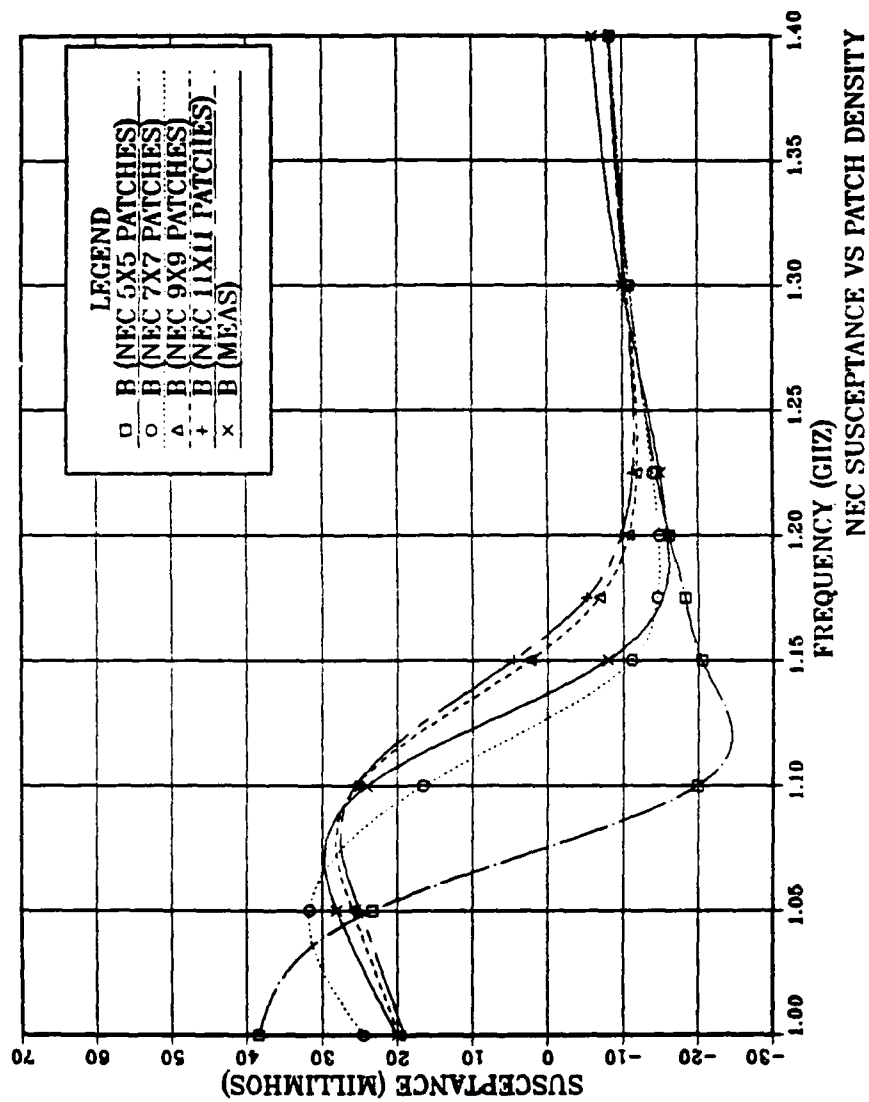


Figure 18. Monopole at Center of Patch Box  
NEC Susceptance vs Patch Density

## 2. Monopole at Edge

The 6 cm monopole was divided into five segments and placed at an edge (Fig. 3). The measured data [Ref. 5] are for a monopole attached to an edge at a distance 3.5 cm from the center. Two computer model configurations of the top surface were selected in an attempt to match the geometry of the experimental model: 81 (9x9) patches which corresponds to a monopole position of 3.33 cm from the center and 121 (11x11) patches which corresponds to 3.63 cm. The difference in distance for the position of the monopole in the NEC model compared to the actual physical geometry, is 0.17 cm less and 0.13 cm more, correspondingly.

For each configuration, the frequency was varied from 1 to 1.4 GHz in nine computer runs. The impedance (in OHMS), admittance (in MMHOS) and calculated values of the average gain are shown in Tables 10 and 11. DNPGNEC was used for the case of 9x9 patches on top, in order to investigate the possibility of higher accuracy than single precision NEC; the results are shown in Table 12. From Tables 10, 11, and 12, the calculated average gain varies from 1.89 (minimum) to 1.92 (maximum), which is in good agreement with the theoretical value of 2.0.

Results of NEC predictions vs. measurements for the monopole at the edge, with top surface patch density varying (Case 1: 9x9, Case 2: 11x11), are presented in Figures 19 and 21. Figures 20 and 22, show PATCH code results of Reference

5 superimposed with NEC calculations and include measurement plots for comparison. PATCH code and experimental results are presented in Figure 23. Experimental data for the monopole located at the edge are shown in Table 2. The total number of patches and the patch area are listed in Table 3. To compare performance between NEC and PATCH for each case, see Figures 24 and 25.

Comparing NPGNEC vs. DNPNEC results (Tables 11 and 12), we observe that the values of conductance and susceptance differ only in the second and third decimal place. This difference is negligible and cannot be observed in plots of NPGNEC vs DNPNEC results. For all cases, the antenna was fed at the base segment.

**CASE 1: 9x9 patches on the top surface (Figures 19 and 20)**

The agreement is very good for conductance (G) and susceptance (B), when NEC results are correlated with measurements (Figure 19).

In Figure 20, a conductance comparison between the performance of NEC and PATCH vs. measurements shows performance to be almost the same between frequencies of 1 to 1.15 GHz.

**CASE 2: 11x11 patches on the top surface (Figures 21 and 22)**

For this configuration, the position of the monopole in the NEC model is closer to the experimental position (3.63 cm vs 3.5 cm) than in the 9x9 patch case. NEC conductance appears to follow the same general trend as measurements.

PATCH's conductance values are 17% closer to measurements than NEC. NEC and PATCH have almost identical performance for susceptance and both have the same resonant frequency of 1.20 GHz vs 1.16 GHz for the measurement.

#### GENERAL RESULTS:

In both cases, NEC results are reasonably close to experimental data. For clarity, results for NEC and PATCH for Case 1 are plotted in Figure 24 and those for Case 2 are plotted in Figure 25.

NEC performs better than PATCH in Case 1 and vice versa for Case 2. The solution seems to converge at Case 1 (9x9 patches on top). However, the model of Case 2 is selected for the near field calculations because the position of the monopole is closer to the experimental model position.

TABLE 10  
CALCULATED DATA  
MONOPOLE AT EDGE OF SURFACE PATCH BOX (3.33CM FROM CENTER)  
(9 X 9 PATCHES ON THE TOP SURFACE - BASE SEGMENT FEED)

FREQUENCY (GHZ)	AVERAGE POWER GAIN	IMPEDANCE (OHMS) ADMITTANCE (MMHOS)
1.00	1.90	21.62 - j52.92 6.62 + j16.19
1.05	1.90	24.44 - j38.36 11.81 + j18.54
1.10	1.91	27.79 - j24.12 20.52 + j17.81
1.15	1.91	31.89 - j10.25 28.42 + j 9.13
1.175	1.91	34.26 - j 3.49 28.88 + j 2.94
1.2	1.91	36.85 + j 3.08 26.95 - j 2.26
1.225	1.91	39.64 + j 9.49 23.86 - j 5.71
1.3	1.92	49.09 + j27.47 15.51 - j 8.68
1.4	1.92	63.24 + j48.51 9.95 - j 7.63



TABLE 11  
CALCULATED DATA  
MONOPOLE AT EDGE OF SURFACE PATCH BOX (3.63CM FROM CENTER)  
(11 X 11 PATCHES ON THE TOP SURFACE - BASE SEGMENT FEED)

FREQUENCY (GHZ)	AVERAGE POWER GAIN	IMPEDANCE (OHMS) ADMITTANCE (MMHOS)
1.00	1.89	23.67 - j57.39 6.14 + j14.89
1.05	1.89	26.31 - j42.92 10.38 + j16.93
1.10	1.89	29.41 - j28.69 17.42 + j16.99
1.15	1.90	33.24 - j14.74 25.14 + j11.15
1.175	1.90	35.47 - j 7.92 26.85 + j 5.99
1.2	1.90	37.92 - j 1.24 26.34 + j 0.86
1.225	1.90	40.59 + j 5.27 24.22 - j 3.15
1.3	1.90	49.75 + j23.72 16.38 - j 7.80
1.4	1.91	63.89 + j45.58 10.37 - j 7.39

TABLE 12  
CALCULATED DATA  
MONOPOLE AT EDGE OF SURFACE PATCH BOX (3.63CM FROM CENTER)  
(11 X 11 PATCHES ON THE TOP SURFACE - BASE SEGMENT FEED)  
(DOUBLE PRECISION CALCULATION)

FREQUENCY (GHZ)	AVERAGE POWER GAIN	IMPEDANCE (OHMS) ADMITTANCE (MMHOS)
1.00	1.89	23.68 - j57.38 6.14 + j14.89
1.05	1.89	26.31 - j42.91 10.39 + j16.93
1.10	1.89	29.42 - j28.67 17.43 + j16.99
1.15	1.90	33.24 - j14.73 25.14 + j11.14
1.175	1.90	35.48 - j 7.90 26.85 + j 5.98
1.2	1.90	37.93 - j 1.23 26.34 + j 0.85
1.225	1.90	40.60 + j 5.29 24.22 - j 3.15
1.3	1.90	49.76 + j23.73 16.37 - j 7.80
1.4	1.91	63.90 + j45.58 10.37 - j 7.39

# MONOPOLE AT EDGE OF PATCH BOX

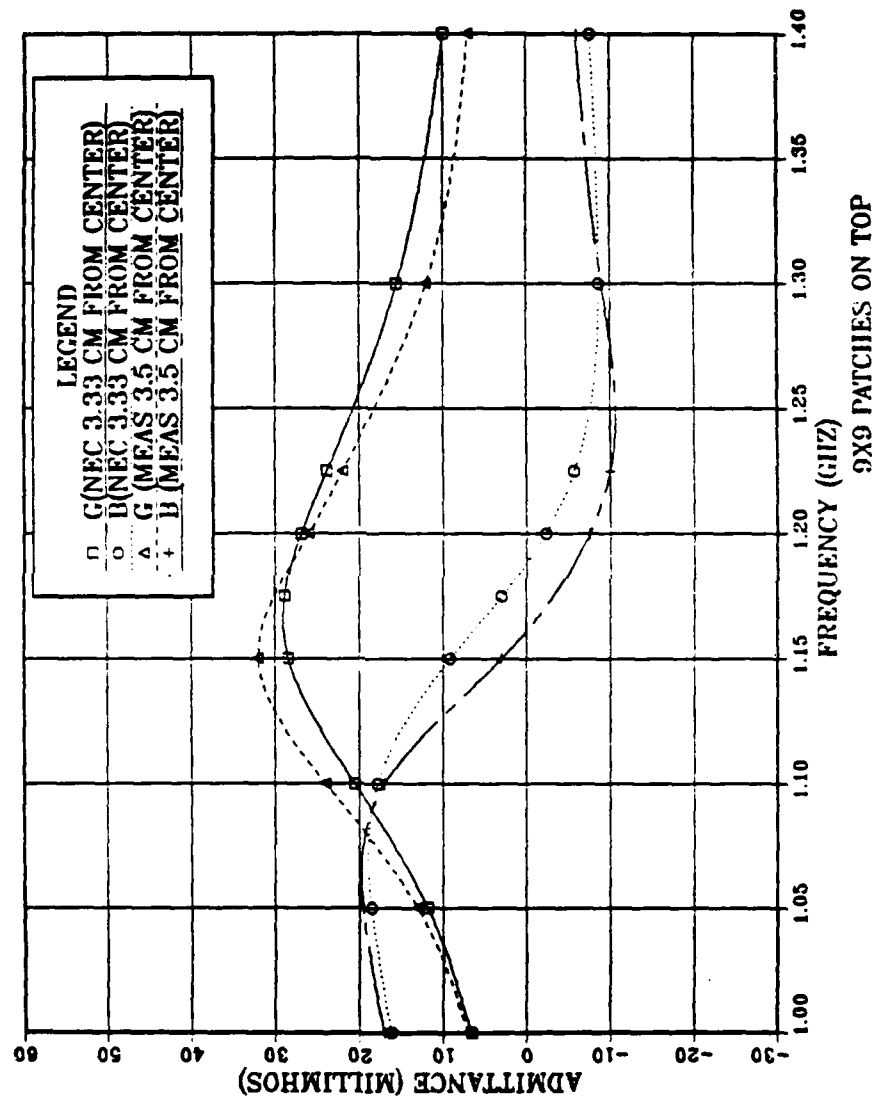


Figure 19. Monopole at Edge of Patch Box  
(9x9 Patches on Top)  
NEC Admittance vs Measurements

# MONOPOLE AT EDGE OF PATCH BOX

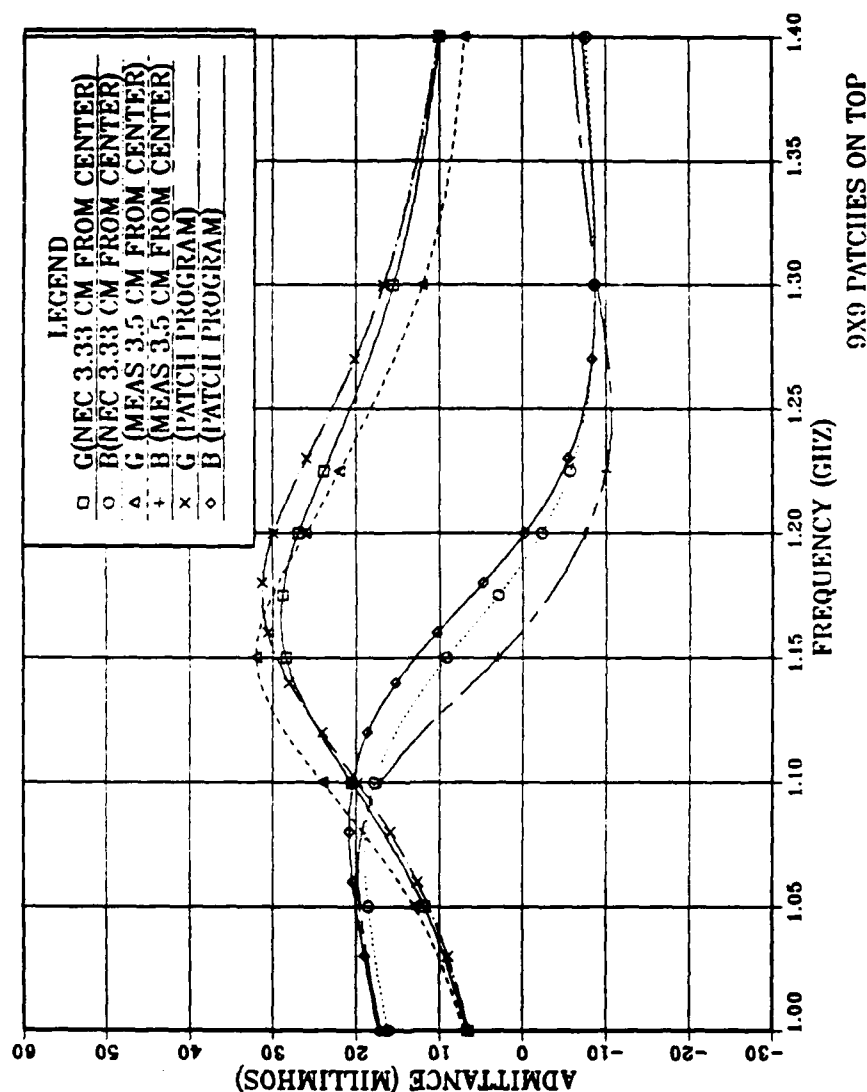


Figure 20. Monopole at Edge of Patch Box  
(9x9 Patches on Top)  
NEC Admittance vs Measurements and "PATCH" Code

# MONOPOLE AT EDGE OF PATCH BOX

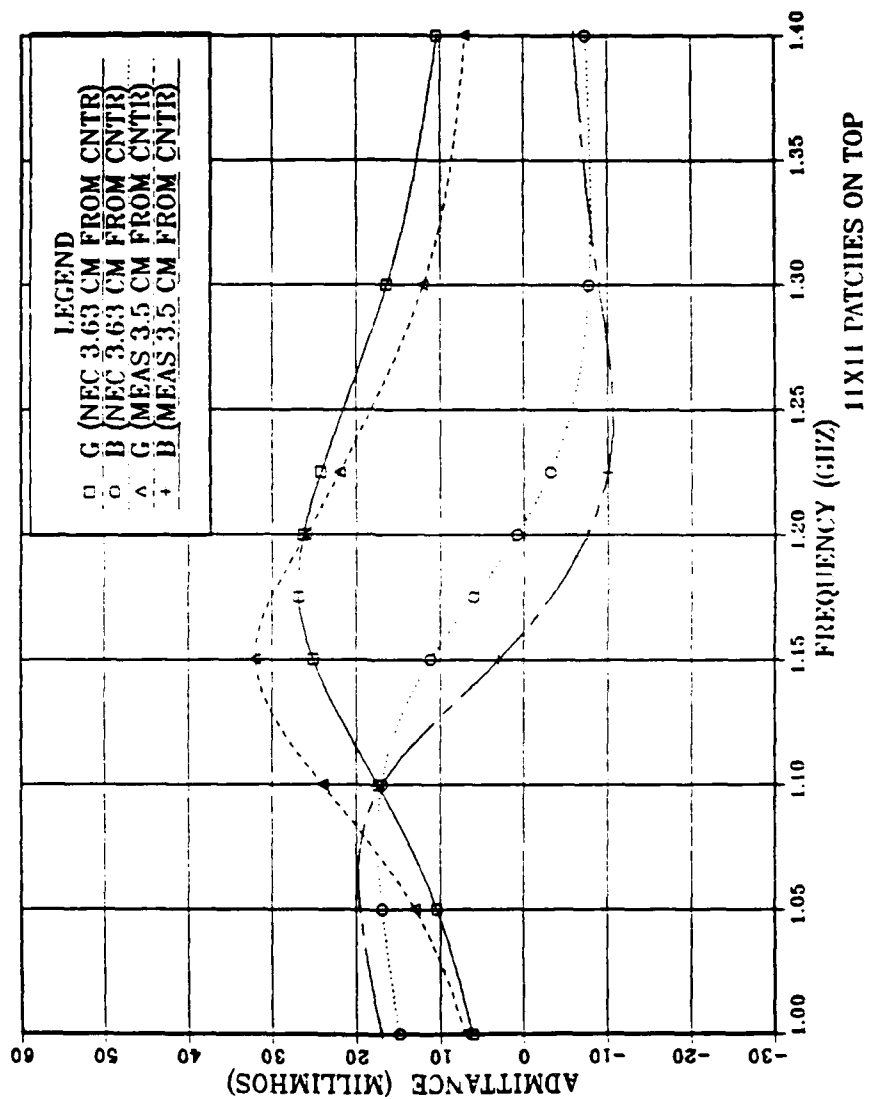


Figure 21. Monopole at Edge of Patch Box  
(11x11 Patches on Top)  
NEC Admittance vs Measurements

# MONOPOLE AT EDGE OF PATCH BOX

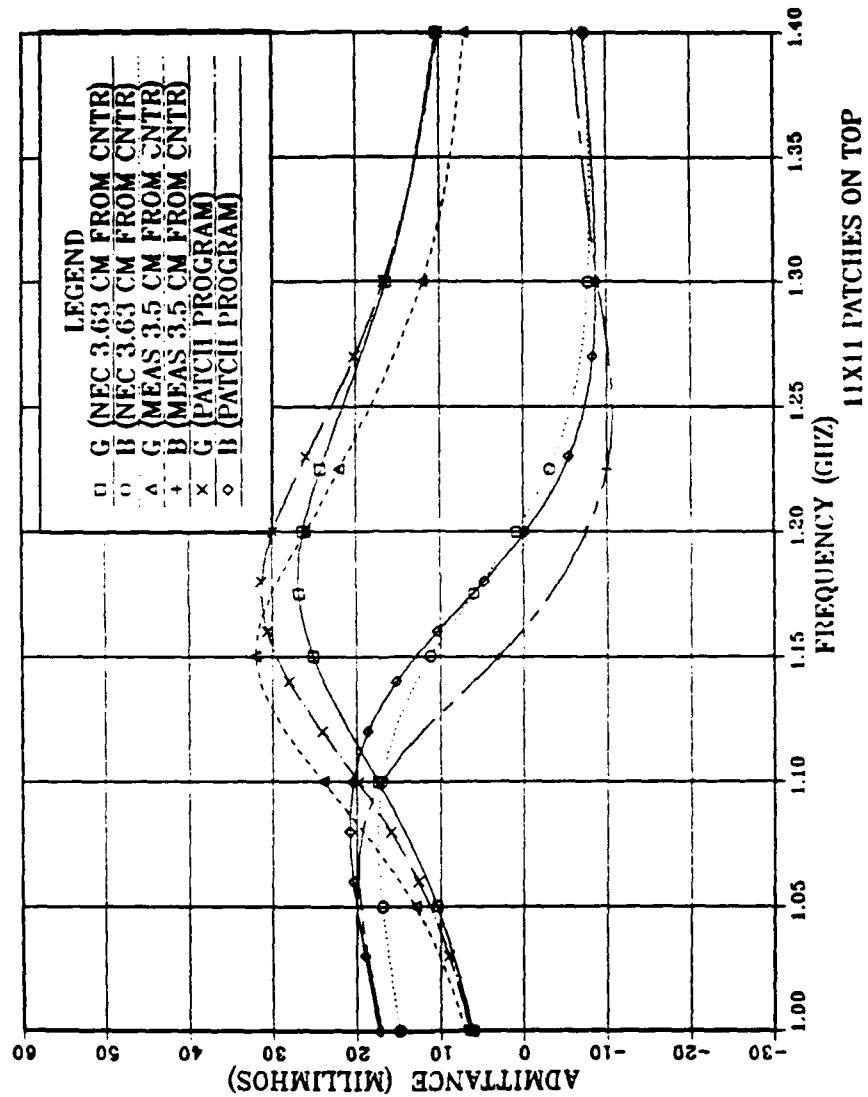


Figure 22. Monopole at Edge of Patch Box  
(11x11 Patches on Top)  
NEC Admittance vs Measurements and "PATCH" Code

# MONOPOLE AT EDGE OF PATCH BOX

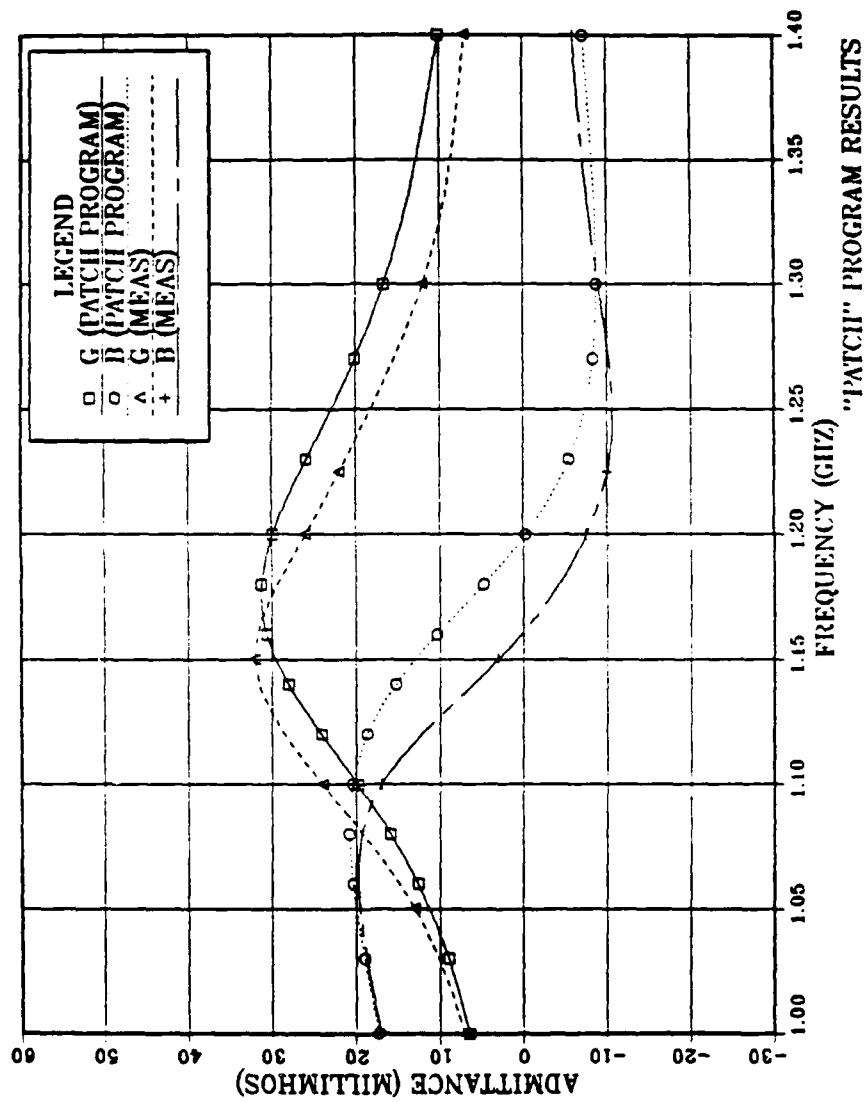


Figure 23. Monopole at Edge of Patch Box  
"PATCH" Code Admittance vs Measurements

# MONOPOLE AT EDGE OF PATCH BOX

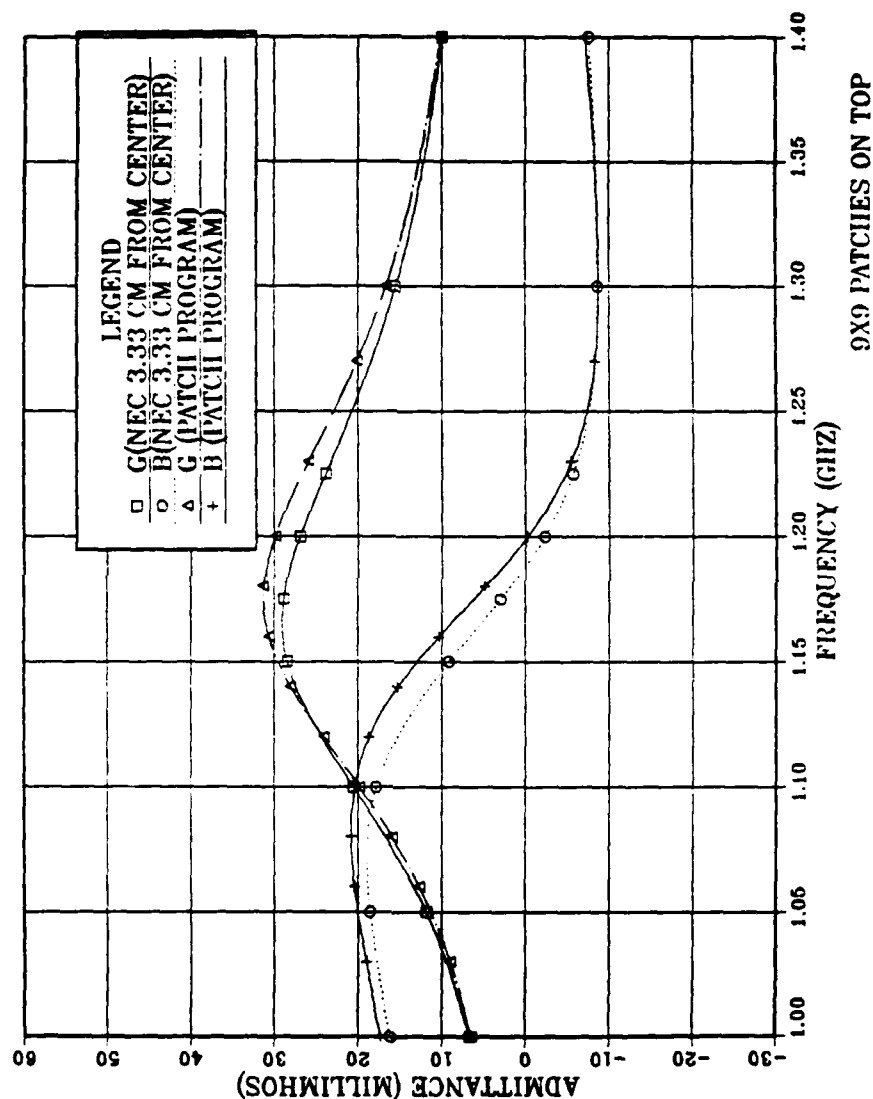


Figure 24. Monopole at Edge of Patch Box  
(9x9 Patches on Top)  
NEC Admittance vs "PATCH" Code



# MONOPOLE AT EDGE OF PATCH BOX

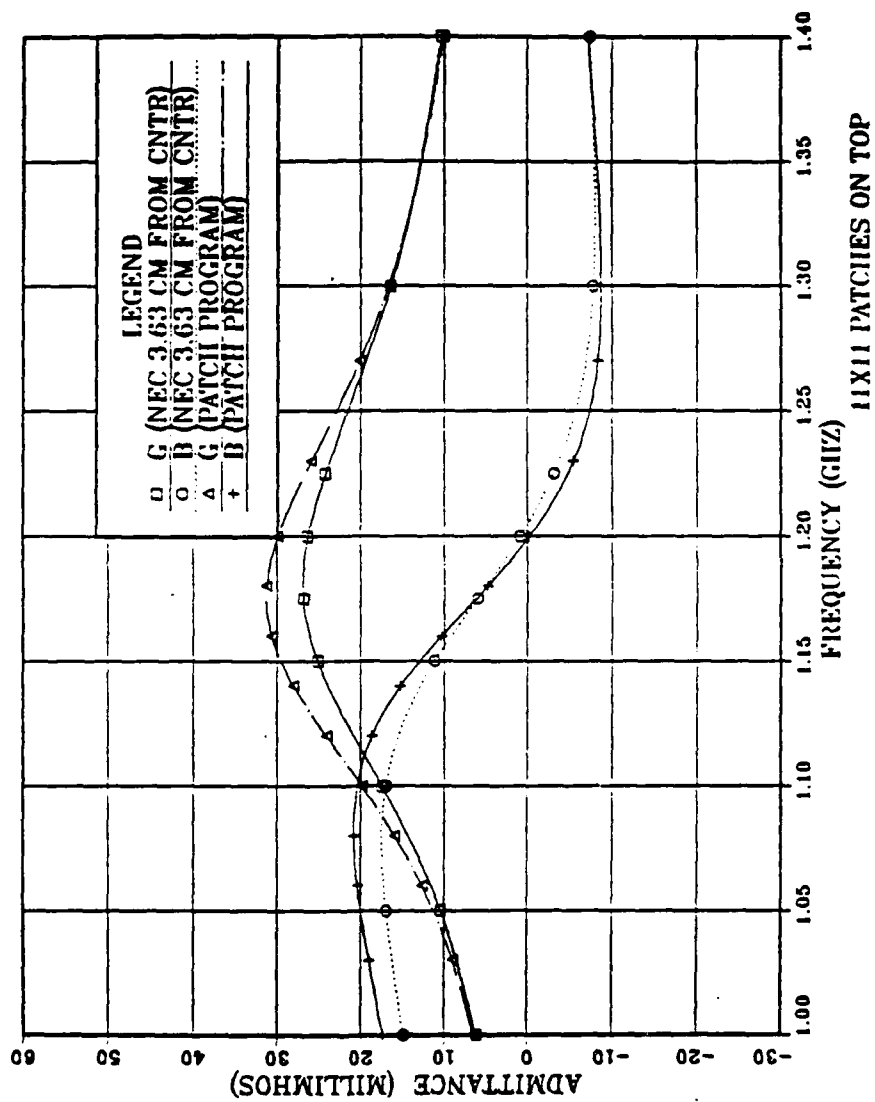


Figure 25. Monopole at Edge of Patch Box  
(11x11 Patches on Top)  
NEC Admittance vs "PATCH" Code

### 3. Monopole at Corner

The 6 cm monopole in the NEC model was placed at the corner, 5.14 cm on the diagonal from the center and fed at the base. The position of the monopole for the experimental model is 5.15 cm. The top surface was divided into 121 (11x11) patches. The calculated values for the impedance, admittance and average power gain are shown in Table 13. Experimental data are presented in Table 2 and the total number of patches as well as the patch area in Table 3. Average power gain is between 1.80 (minimum) and 1.83 (maximum) and is within the 10% tolerance of the theoretical value.

NEC results of admittance vs. measurements are presented in Figure 26. PATCH code results from the calculated data of Reference 5 have been superimposed on NEC's data, for comparison, in Figure 27. PATCH code results are compared to experimental results Figure 28. NEC vs. PATCH is compared in Figure 29.

NEC is in excellent agreement with measurements in both conductance and susceptance (Figure 26). PATCH seems to perform slightly better than NEC (Figure 27), however, conductance and susceptance in the range of 1.15 to 1.40 GHz are virtually identical for both codes.

TABLE 13  
CALCULATED DATA  
MONOPOLE AT CORNER OF SURFACE PATCH BOX  
(5.14CM ON THE DIAGONAL FROM CENTER)  
(11 X 11 PATCHES ON THE TOP SURFACE - BASE SEGMENT FEED)

FREQUENCY (GHZ)	AVERAGE POWER GAIN	IMPEDANCE (OHMS) ADMITTANCE (mMHOS)
1.00	1.80	36.48 - j56.15 8.13 + j12.52
1.05	1.81	35.53 - j42.85 11.60 + j12.90
1.10	1.82	40.93 - j29.24 16.17 + j11.55
1.15	1.82	44.23 - j15.43 20.16 + j 7.03
1.175	1.83	46.32 - j 8.53 20.88 + j 3.85
1.2	1.83	48.74 - j 1.71 20.49 + j 0.72
1.225	1.83	51.50 + j 4.99 19.24 - j 1.86
1.3	1.82	61.73 + j23.94 14.08 - j 5.46
1.4	1.81	78.84 + j45.42 9.52 - j 5.48

# MONOPOLE AT CORNER OF PATCH BOX

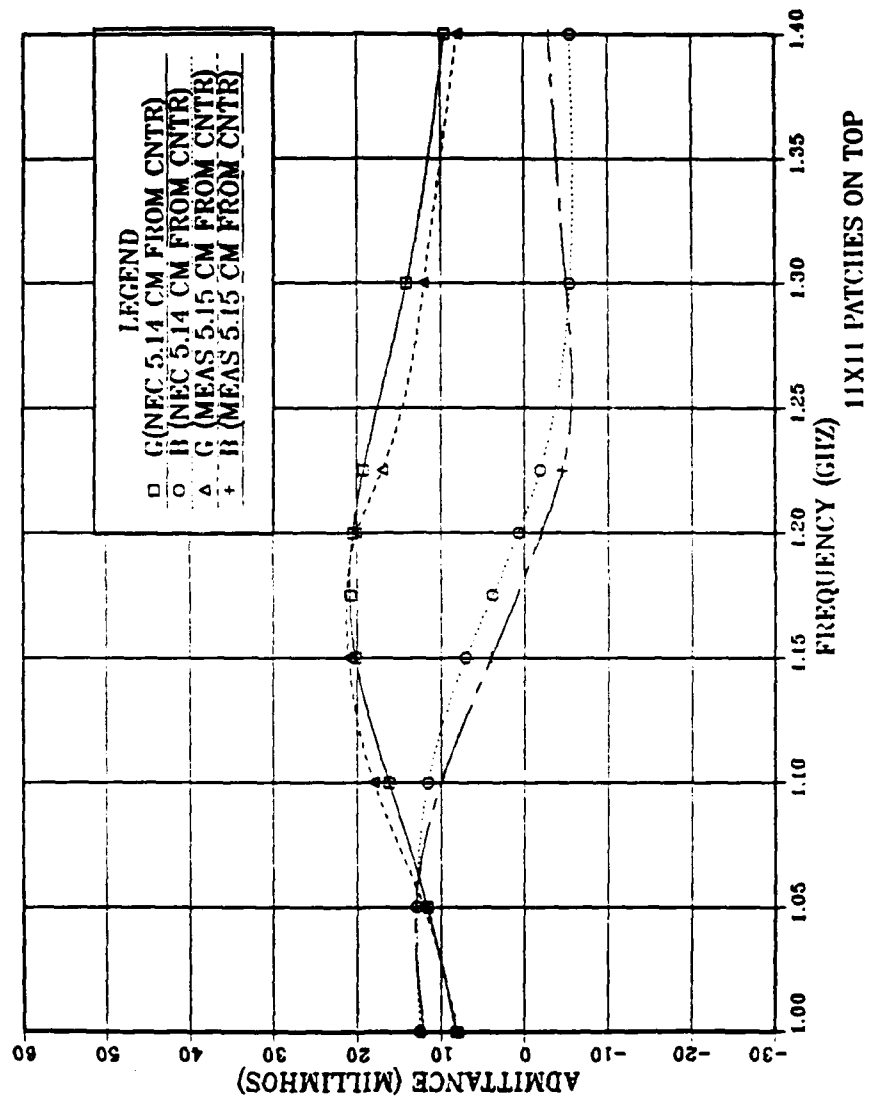


Figure 26. Monopole at Corner of Patch Box  
(11x11 Patches on Top)  
NEC Admittance vs Measurements

# MONOPOLE AT CORNER OF PATCH BOX

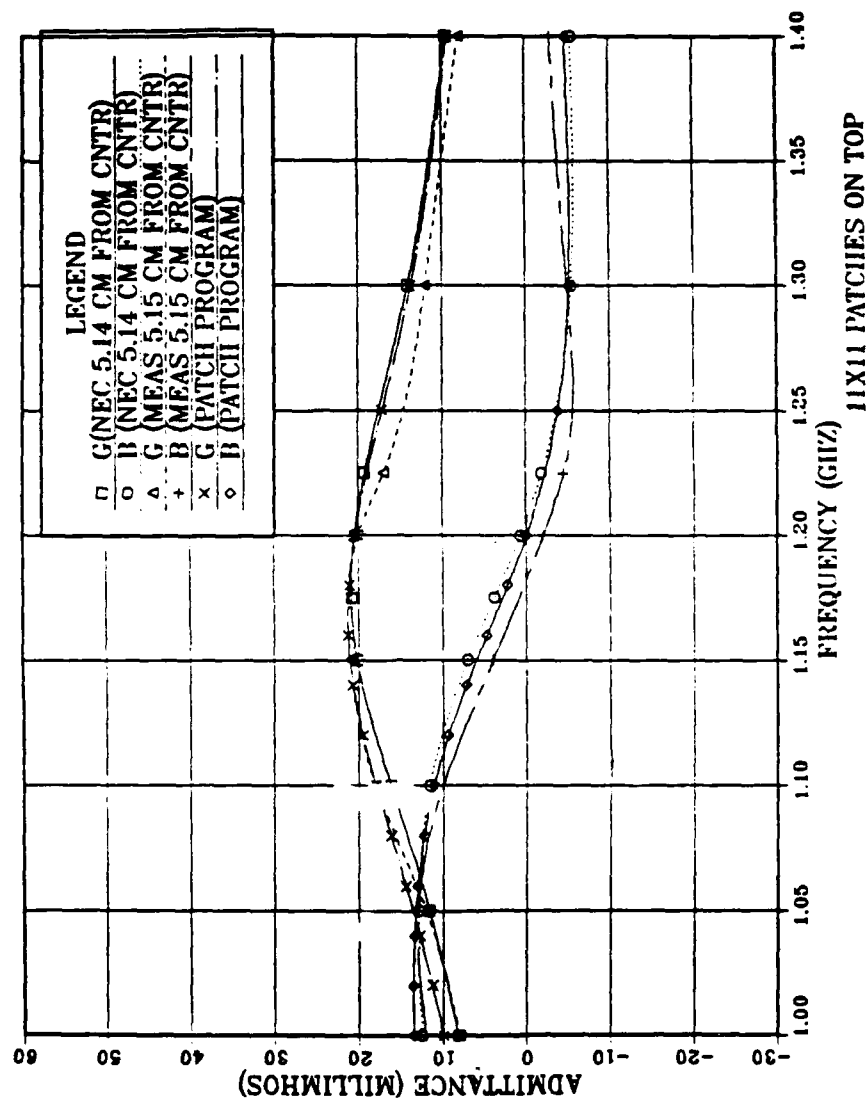


Figure 27. Monopole at Corner of Patch Box  
(11x11 Patches on Top)  
NEC Admittance vs Measurements and "PATCH" Code

# MONOPOLE AT CORNER OF PATCH BOX

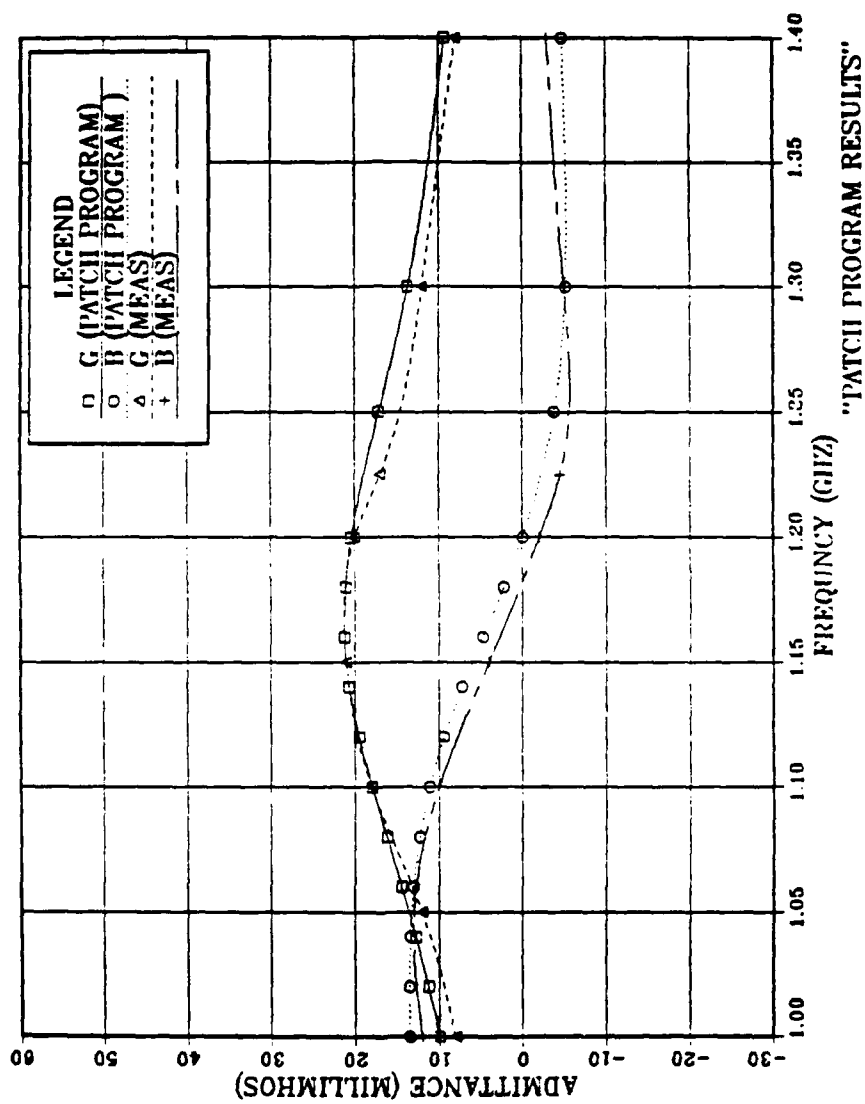


Figure 28. Monopole at Corner of Patch Box  
"PATCH" Code Admittance vs Measurements

# MONOPOLE AT CORNER OF PATCH BOX

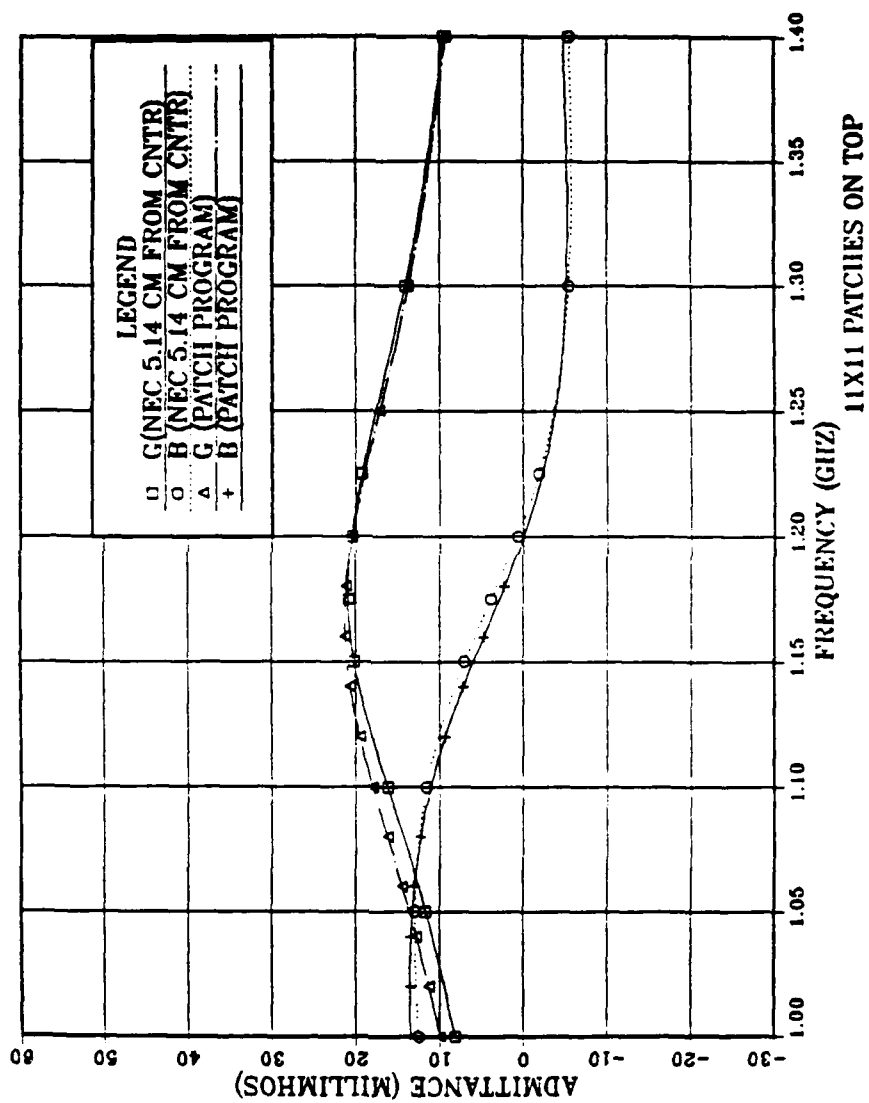


Figure 29. Monopole at Corner of Patch Box  
(11x11 Patches on Top)  
NEC Admittance vs "PATCH" Code

## E. NEAR ELECTRIC FIELD

Near fields are more difficult to calculate than far fields. When calculating radiation in close proximity to an antenna, the antenna no longer appears as an infinitesimal point (as is the assumption for far field), and the energy radiating from it comes from separated locations insofar as the strength of radiation from each sub-section of the radiator is concerned. This means that terms in the field expressions with powers of  $1/r^2$  ( $r$  is the distance from the origin of the antenna to the field point) are appreciable in magnitude compared to the  $1/r$  dependent terms which are dominant in the far field. The complex Poynting vector  $1/2 (\vec{E} \times \vec{H}^*)$  thus contain terms with higher powers of  $(1/r)$ , in addition to the radiation field term. The near field is thus very dependent on the charge density and the current while the far field is affected only by the current.

For near field calculations, NPGNEC computes the magnitude of the peak electric field ( $E_{\text{Total}}$ ) in (V/m), which is the vector sum of the three components  $E_x$ ,  $E_y$ , and  $E_z$  (the calculation of  $E_{\text{peak}}$  is a special feature that has been added to the NPGNEC version of NEC which is in use at NPS). NEC outputs the magnitude and phase of each component  $E_x$ ,  $E_y$ , and  $E_z$  separately.



1. Near Electric Field in 2-Dimensions For the 6 cm Monopole Antenna on the Cubical Conducting Box

Using the optimum models in NEC for the monopole at the center (7x7 patches), at the edge (11x11 patches) and the corner (11x11 patches), we proceed with the near field investigation. The NE card is used in conjunction with the PL card; both are described in detail in Reference 1. The input data files are presented in Appendix A for the near field calculations and for the three positions of the monopole on the patch box. For all cases, NEC was tasked to produce two hundred points in x, y, or z directions, with a spatial variation of 0.01 m. The starting point for the near field calculation is  $0.05\lambda$  away from the wire and box metal structure. The calculation of the near field is extended to a distance of at least  $6\lambda$  in the x, y, or z directions, respectively. In that manner, we ensure that the field points are far enough away from any metallic structure and at a distance where the near field variation can be observed in detail. The plots of the near field are presented in Figures 31 and 32 (Monopole at center -- variation in x and z), Figures 33, 34, and 35 (Monopole at edge -- variation in x, y, and z), and Figures 36, 37, and 38 (Monopole at corner-- variation in x, y, and z).

In order to compare NEC near fields for the monopole on the box with theoretical values, we consider a linear current element  $I=I_0e^{j\omega t}$  of length  $\Delta z$  oriented in the z direction and located at the origin as in Figure 30 [Ref.

10]. For convenience, assume  $I_0$  is the amplitude of the current. This antenna is a simple radiating structure but it will demonstrate basic properties of the near electric field for all small linear antennas.

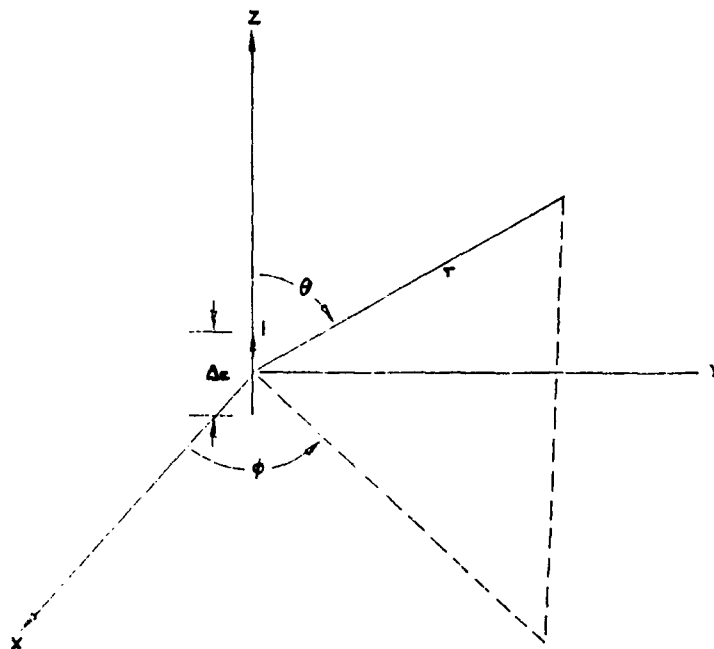


Figure 30. A Linear Current Radiator

The complete electric-field intensity of the antenna is:

$$\begin{aligned} \vec{E} = & \frac{-I_0 \Delta z}{2\pi} j \frac{\mu_0^{1/2}}{k_0 \epsilon_0^{1/2}} \cos \theta \left( \frac{jk_0}{r^2} + \frac{1}{r^3} \right) e^{-jk_0 r} \vec{i}_r \\ & \frac{-I_0 \Delta z}{4\pi} j \frac{\mu_0^{1/2}}{k_0 \epsilon_0^{1/2}} \sin \theta \left( \frac{-k_0^2}{r} + \frac{jk_0}{r^2} + \frac{1}{r^3} \right) e^{-jk_0 r} \vec{i}_\theta \quad (2.1) \end{aligned}$$

The only part of the field entering into the expression for the radiated power is that part consisting of the terms varying as  $r_0^{-1}$ , that is;

$$E_\theta = \frac{jk_0 I_0 \Delta z}{4\pi r} \sin \theta e^{-jk_0 r}$$

This is called the radiation field. The parts of the field varying as  $r^{-2}$  and  $r^{-3}$  are called the induction field. The induction field does not represent an outward flow of power, but instead depicts a storage of reactive energy in the vicinity of the radiating current element (Reference 10). Consequently, the terms that are functions of distance  $r$  of the E-Field in Eq 2.1 are:

$$-\frac{k_0^2}{r} + j\frac{k_0}{r^2} + \frac{1}{r^3}$$

All the other terms are phase terms or constants. Generally, the magnitude of electric field has an  $r$  dependence which can be expressed as:

$$|E(r)| = c \sqrt{\left(\frac{1}{r^3} - \frac{k_0^2}{r}\right)^2 + \left(\frac{k_0}{r^2}\right)^2} \quad (2.2)$$

For the monopole at the box center, the near electric field is presented in Figure 31. From this figure and NEC output, we observe for a distance close to zero,  $r = 0.0166$  m, the value of the field is  $|E(r)| = 45.9$  (V/m). Using this value in Eq. 2.2, we can find the constant factor  $C = 0.000222065$  (normalization factor). Using the calculated value of the constant  $C$  in Eq. 2.2 and varying the distance  $r$  from the linear current element, we calculate the corresponding  $|E(r)|$  for each distance; the  $r$ -dependence is plotted in Figure 39. Comparing Figure 31, for the near electric field of the monopole on the box center with the near field of the current element in Figure 39, both near electric fields follow the same trend which is: a maximum in close proximity to the antenna with a gradual reduction as the observation point moves away. A knee of the curve appears approximately at  $0.125$  m ( $0.41\lambda$  away from the antenna). The results for the monopole at the edge and corner are almost the same. The "spikes" observed in Figures 31, 33, and 34 are from the edge of the box.

MAGNITUDE VS DISTANCE freq=1ghz  
monopole at center of patch box 7x7 patches on top

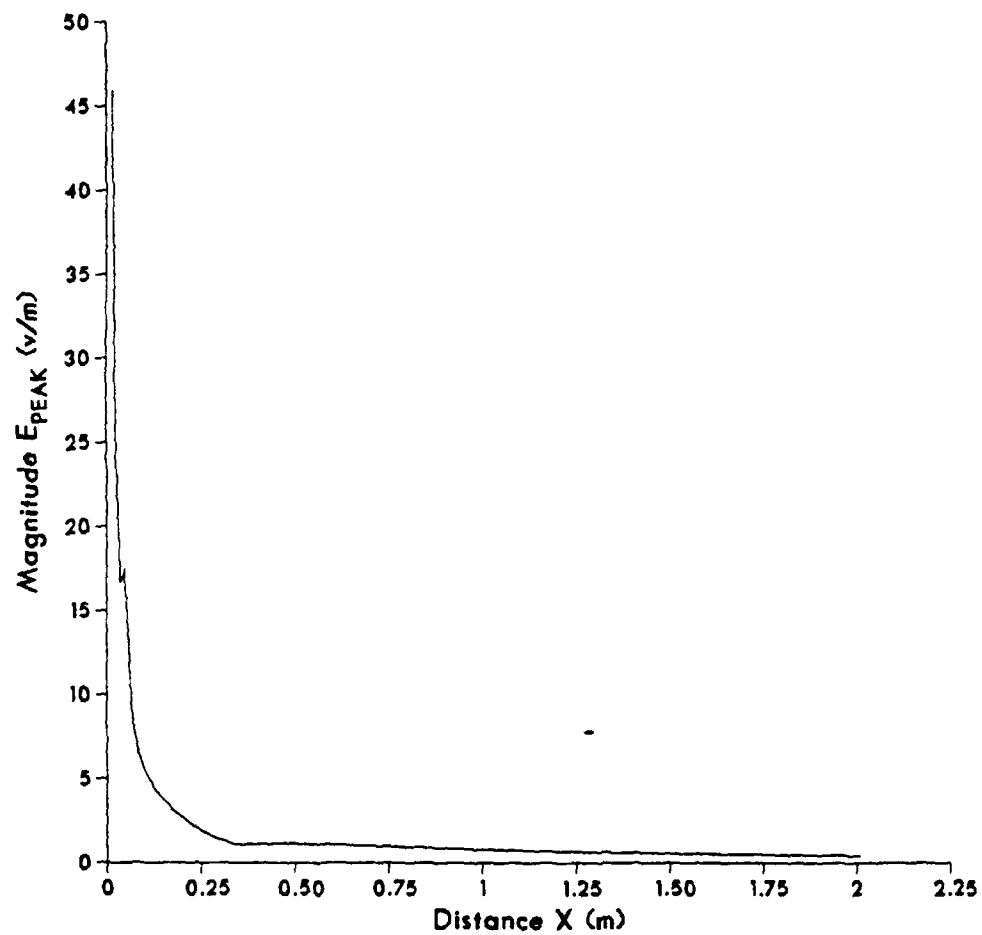


Figure 31. Monopole at Center of Patch Box  
(7x7 Patches on Top)  
Near Electric Field on X Axis

MAGNITUDE VS DISTANCE freq=1ghz  
monopole at center of patch box 7x7 patches on top

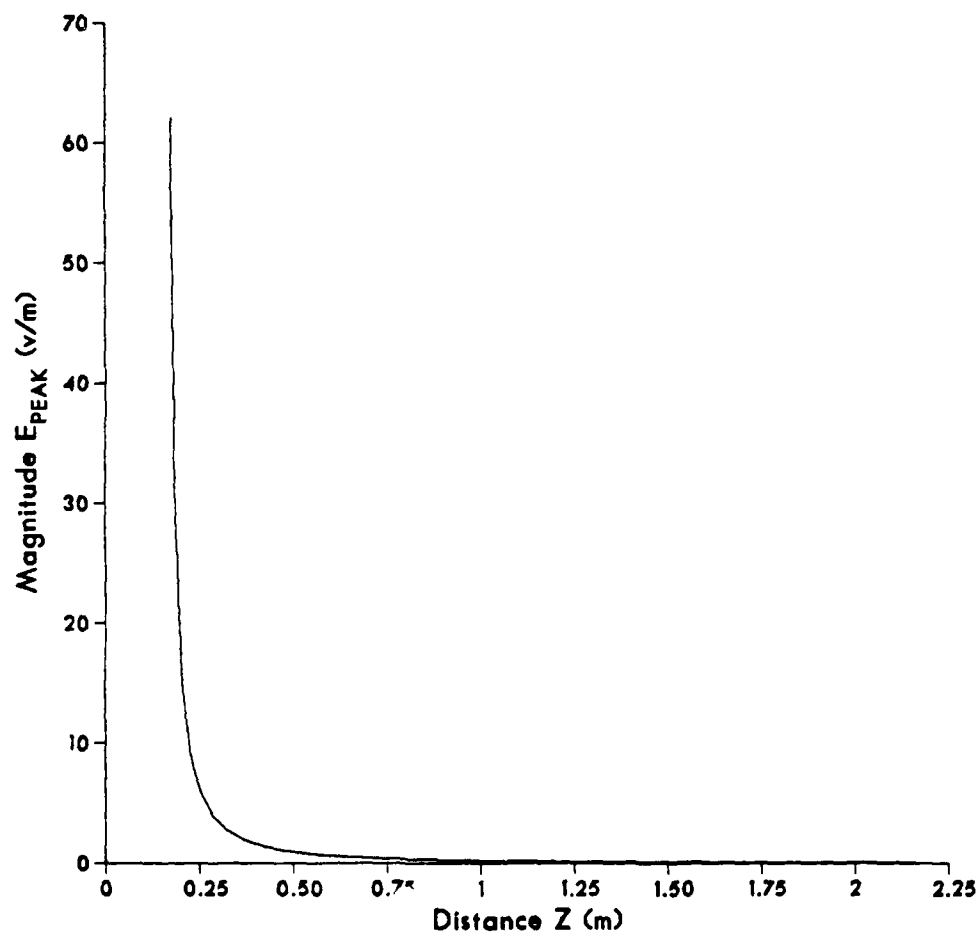


Figure 32. Monopole at Center of Patch Box  
Near Electric Field on Z Axis

MAGNITUDE VS DISTANCE freq 1ghz  
near e-field 6 cm monopole at edge 3.63 cm from center

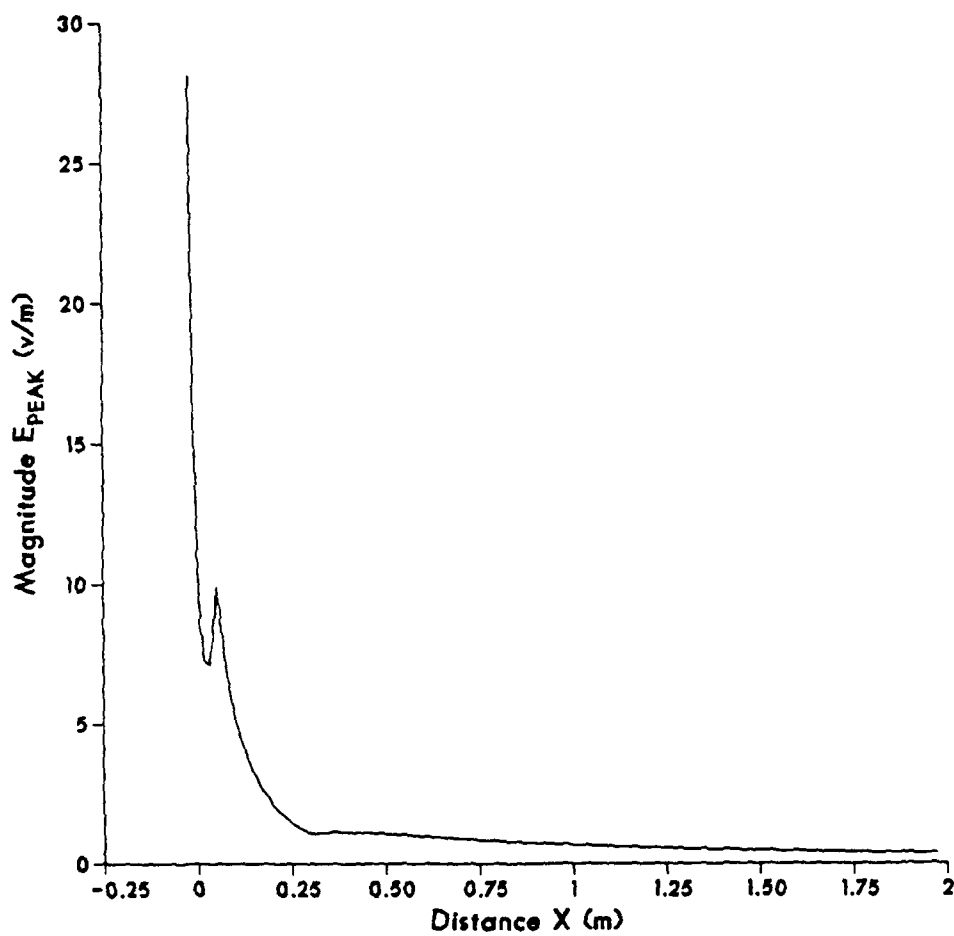


Figure 33. Monopole at Edge of Patch Box  
Near Electric on X Axis

MAGNITUDE VS DISTANCE freq 1 ghz  
near e-field 6 cm monopole at edge 3.63 cm from center

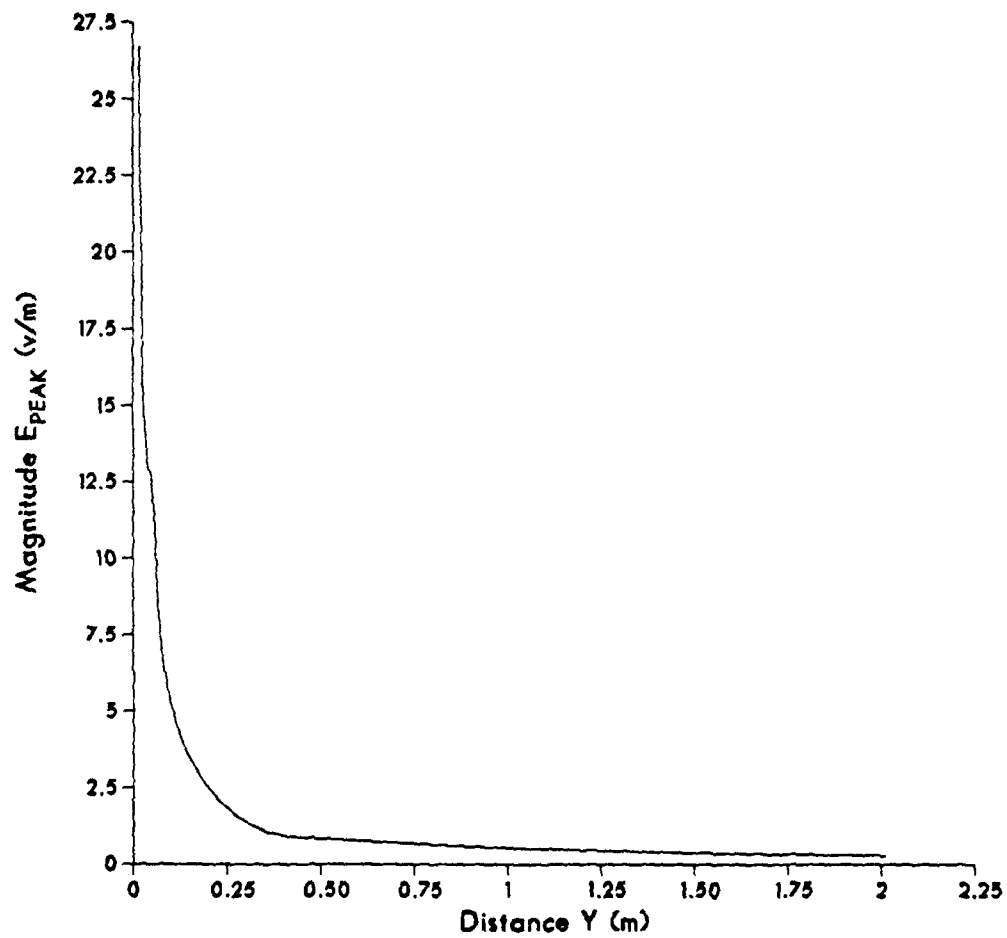


Figure 34. Monopole at Edge of Patch Box  
Near Electric Field on Y Axis



MAGNITUDE VS DISTANCE freq 1 ghz  
near e-field 6 cm monopole at edge 3.63 cm from center

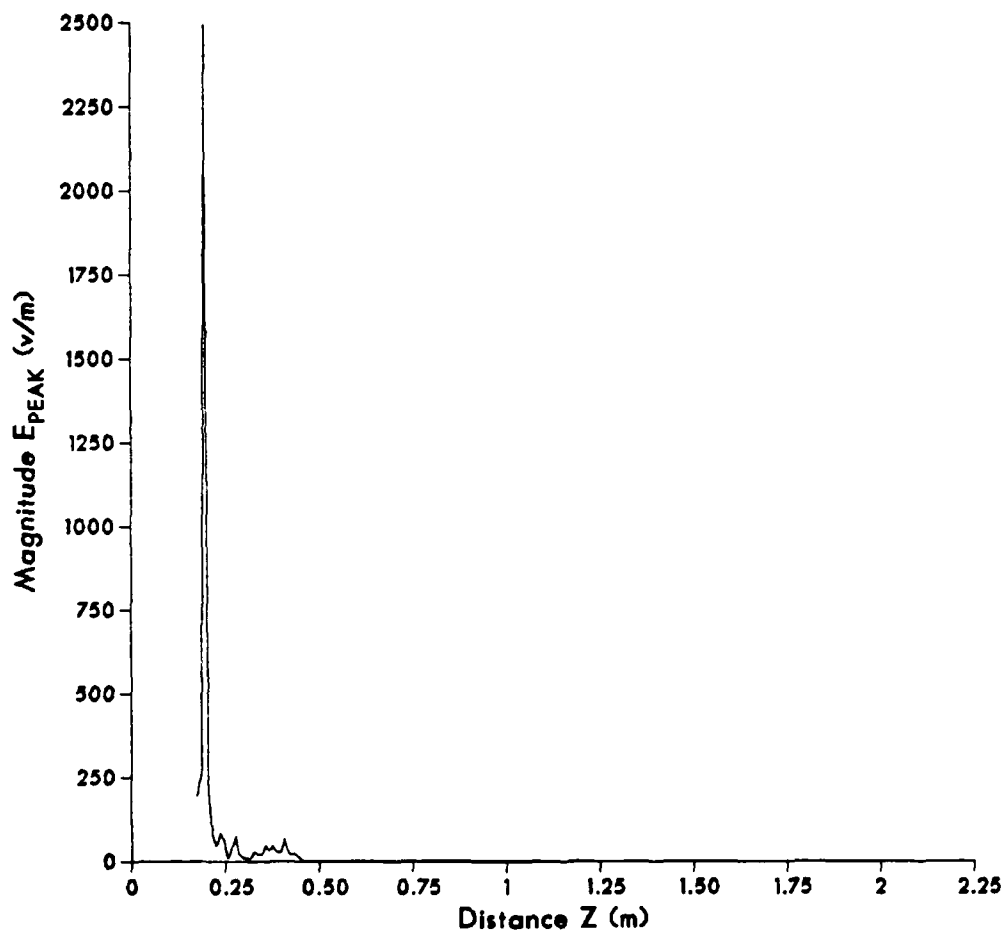


Figure 35. Monopole at Edge of Patch Box  
Near Electric Field on Z Axis

MAGNITUDE VS DISTANCE freq 1ghz  
near e-field 6 cm monopole at corner 5.14 cm on diagonal

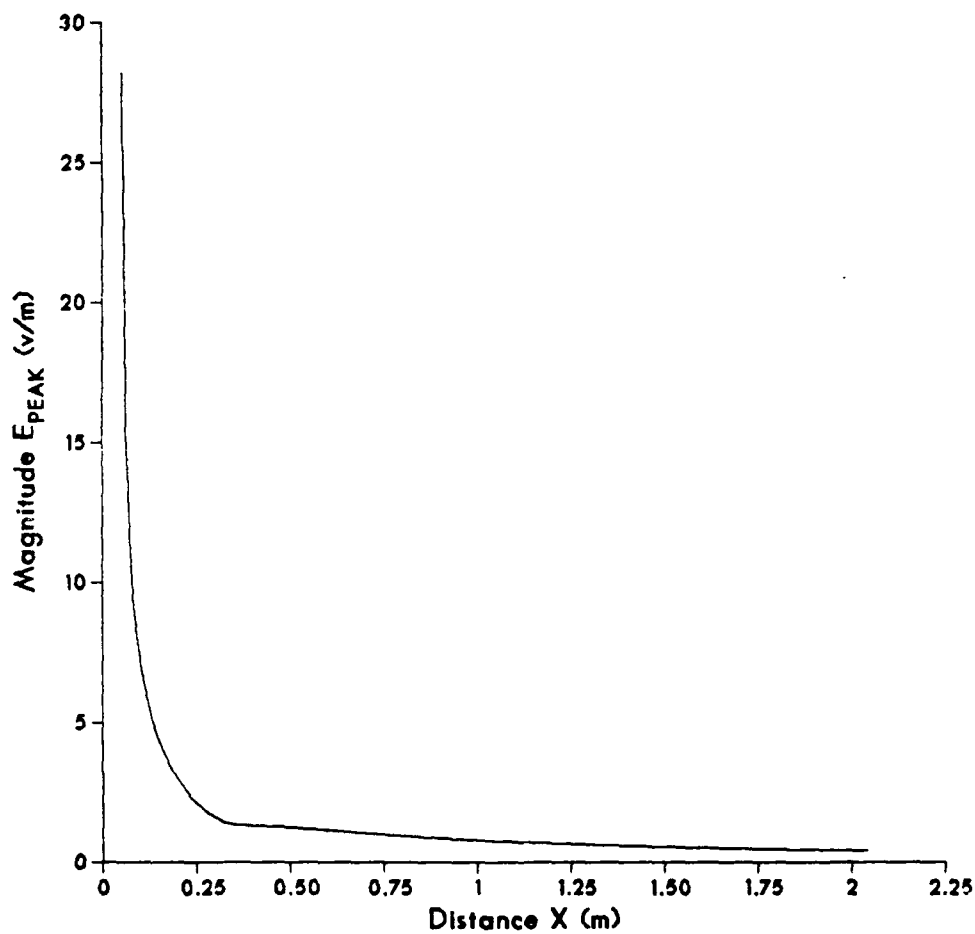


Figure 36. Monopole at Corner of Patch Box  
Near Electric Field on X Axis

MAGNITUDE VS DISTANCE freq 1ghz  
near e-field 6 cm monopole at corner 5.14 cm on diagonal

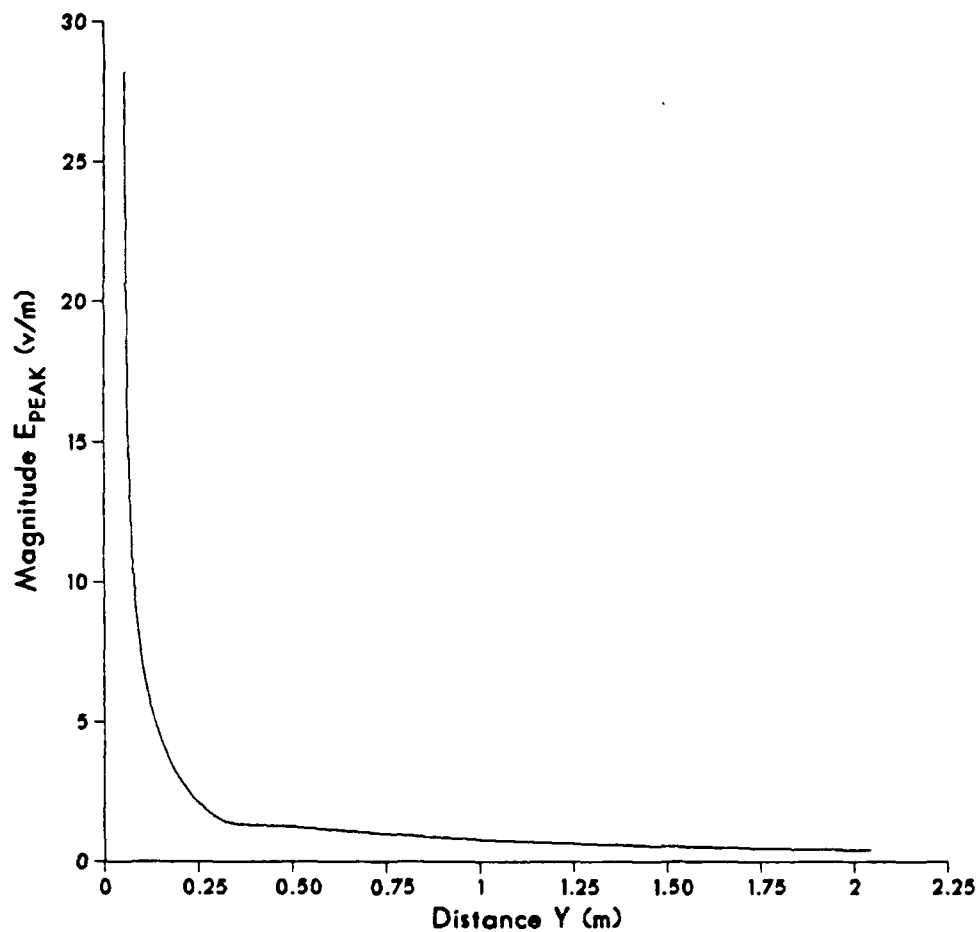


Figure 37. Monopole at Corner of Patch Box  
Near Electric Field on Y Axis

MAGNITUDE VS DISTANCE freq 1ghz  
near e-field 6 cm monopole at corner 5.14 cm on diagonal

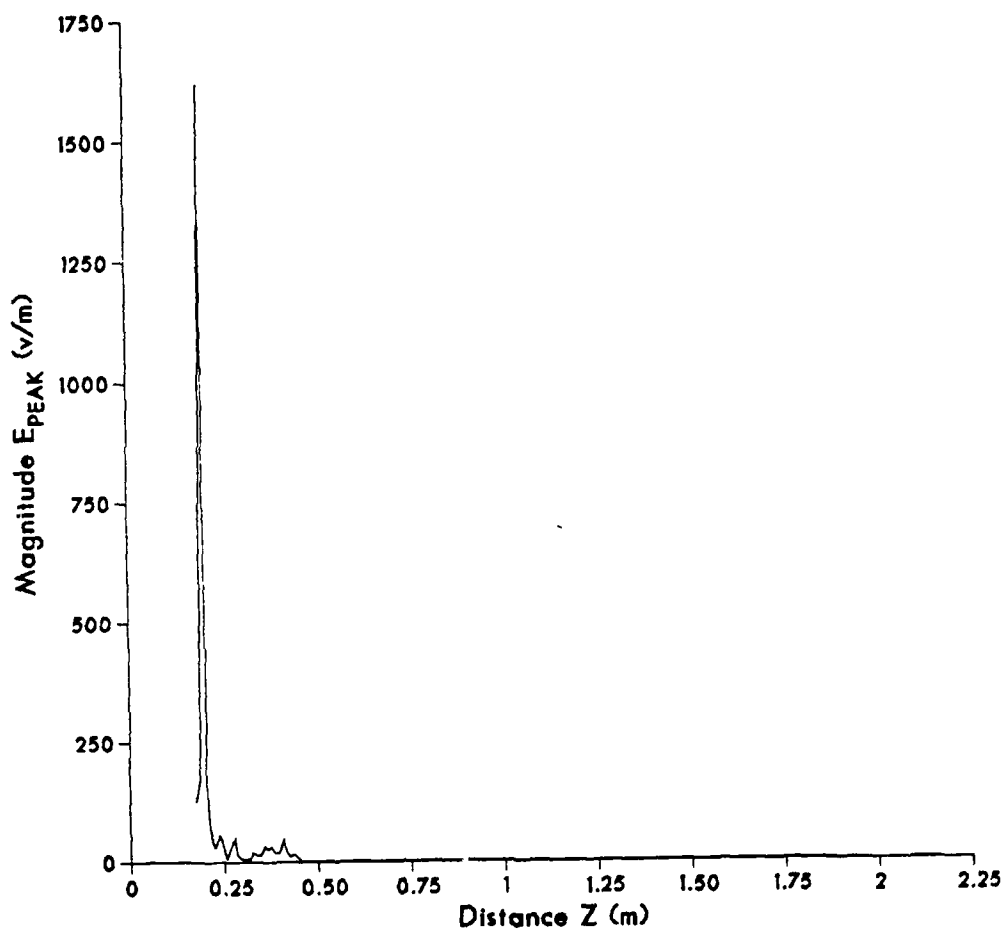


Figure 38. Monopole at Corner of Patch Box  
Near Electric Field on Z Axis

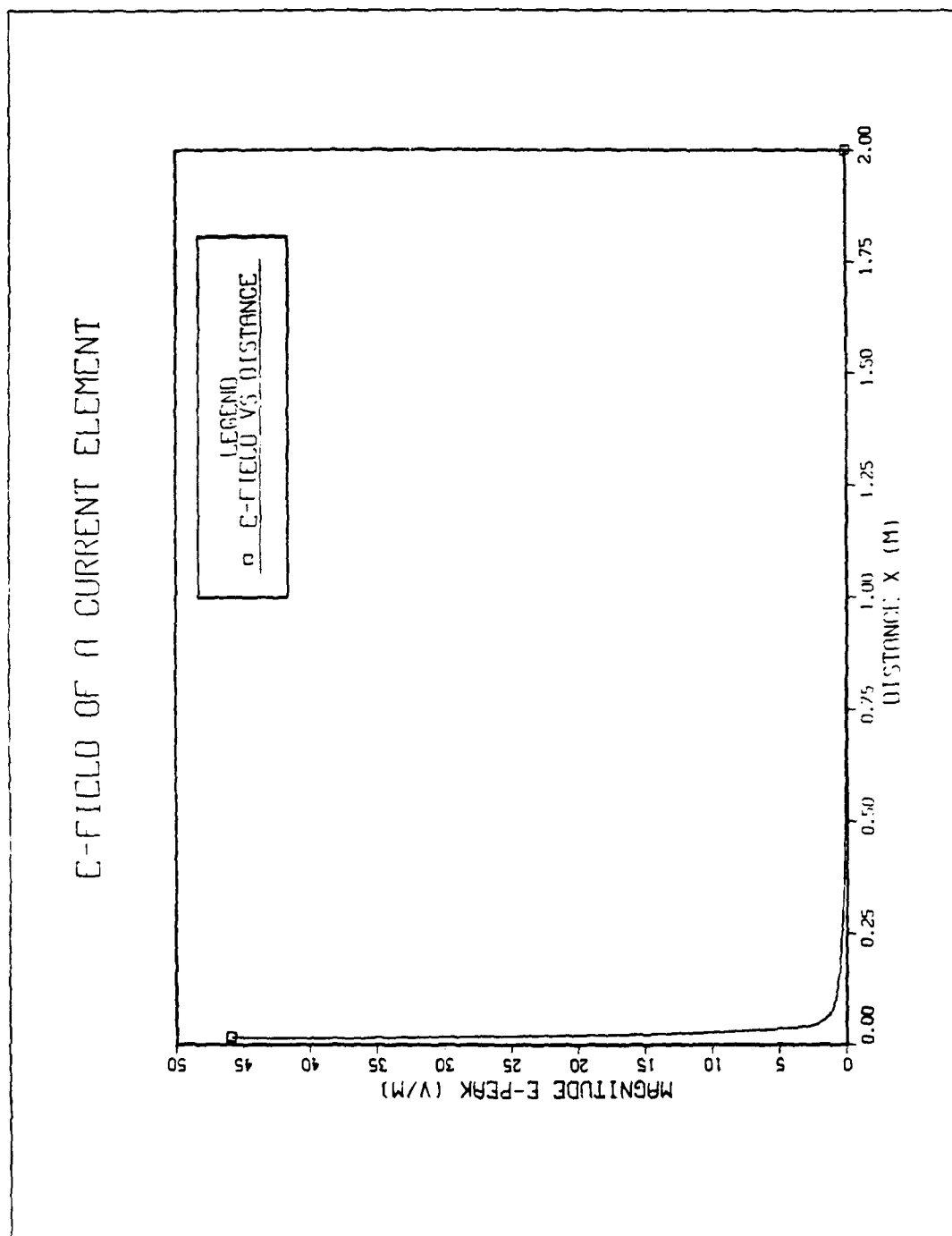


Figure 39. Near Electric Field of a Current Element

#### F. NEAR ELECTRIC FIELD MAGNITUDE AND PHASE CONTOUR PLOTS

Fortran programs were developed to plot the magnitude and phase of the near electric field using NEC output data. The programs use subroutines of the DISSPLA (Display Integrated Software System and Plotting Language) graphics software package [Ref. 9]. Appendix B lists the Fortran source codes and describes their function. PROGRAM I: Contour plot data sets of the magnitude  $E_{\text{peak}}$  as well as the magnitude of the individual components  $E_x$  and  $E_z$  of the electric field (a section of a plane in 3-dimensional space), composed of a 30 X 30 point window in space, are produced. PROGRAM II: This is similar to Program I but for the phase of x and z components of the electric field, for 100X100 points. PROGRAM III: Three-dimensional plot data sets of  $E_{\text{peak}}$  are produced. For these plots, a 3-D map of the electric field is shown on the top and the 2-D contours of the field are presented on the bottom. CONTOUR FORTRAN: This is a subroutine which is called by the above three programs and creates the plots. Positive value contours are presented by solid lines and negative contours by dashed lines. In these programs, NEC output for the near electric field is interfaced with the plotting facilities of DISSPLA.

For reference, two simple antennas with known results are examined: (1) a 0.15 m ( $\lambda/2$ ) dipole antenna in free space, and (2) a 0.06 m ( $\lambda/5$ ) monopole antenna over a perfect ground plane. NEC input data files which produce magnitude and

phase of near electric field for the two antennas are listed in Appendix B.

1. Half Wave Dipole In Free Space vs 6 cm Monopole Over Ground Plane

Near field plots for magnitude and phase for the two antennas are presented in Figures 40 through 45. The near electric field is displayed in a section of a plane in 3-dimensional space. For comparison purposes, the same view plane in the x and z directions are used for all such plots in this study. The origin of the view space plane is very close to the wire antenna and box surface (just  $0.05\lambda$  away) and extends to a distance of  $10\lambda$  in the x and z directions. For these two simple antennas, additional view planes were selected in order to observe how the E-field varies away from the antenna. For this case, the results for peak E-field for the dipole are presented in Figures 40(a) and 40(b) ( $0.5\lambda$  and  $0.8\lambda$  away) and for the monopole in Figures 43(a), 43(b), and 43(c) ( $1\lambda$ ,  $2\lambda$ , and  $8\lambda$  away). The electric near fields are referenced to one volt per meter for all plots.

It is well known that the  $\lambda/2$  dipole has the same behavior as a  $\lambda/4$  monopole (note that we test a  $\lambda/5$  monopole in this study).

Before comparing the dipole and monopole field plots, consider the following:

It is known that  $Z_M = \frac{Z_D}{2}$ . Assume resonance for the two antennas, then:

$$R_M = \frac{R_D}{2} \quad (2.3)$$

The gain of an antenna over an isotropic radiator can be expressed as:

$$G = \frac{S}{P_R/4\pi R^2} = \frac{E^2/\eta}{P_R/4\pi R^2}$$

where  $S$  = power density (watts/m<sup>2</sup>)

and  $P_R$  = power radiated (watts)

Then for the  $\lambda/2$  dipole:

$$G_D = \frac{E_D^2/\eta}{P_R/4\pi R^2} \quad (2.4)$$

and for the monopole:

$$G_M = \frac{E_M^2/\eta}{P_R/4\pi R^2} \quad (2.5)$$

It is well known that:

$$G_M = 2G_D \quad (2.6)$$

(In practice  $G_D = 2.15$  dBi and  $G_M = 5.15$  dBi)

Forming the ratio of Equations 2.4 and 2.5 and using Equation 2.6, we get:

$$\frac{G_D}{G_M} = \frac{E_D^2}{E_M^2} = \frac{1}{2} \quad \text{Thus} \quad \boxed{\frac{E_D}{E_M} = \frac{1}{\sqrt{2}}} \quad (2.7)$$

However  $P_D = I_D^2 R_D$

$$P_M = I_M^2 R_M$$

In order to compare the gains of the two antennas, we have to have:

$$P_D = P_M : \quad \boxed{I_D^2 R_D = I_M^2 R_M} \quad (2.8)$$



Using Equation 2.3 in Equation 2.8, we get

$$I_D^2 R_D = I_M^2 \frac{R_D}{2} . \quad \text{Thus} \quad I_D = \frac{I_M}{\sqrt{2}} \quad \text{and} \quad \boxed{\frac{I_D}{I_M} = \frac{1}{\sqrt{2}}}$$

From Equations 2.7 and 2.9, we conclude that:

$$\boxed{\frac{E_D}{E_M} = \frac{I_D}{I_M}}$$

Thus, the electric fields will be equal only if the currents are equal for the two antennas.

In Table 14, characteristics of the two antennas from the NEC output files are presented. From Figures 40 and 43, we conclude that the shape of near electric field is the same for the dipole and monopole antenna. The ratio of the input maximum current for the two antennas is:

$$20 \log_{10} \frac{0.9764 \times 10^{-2}}{0.2259 \times 10^{-1}} = -7.28 \text{ dB}$$

From Figures 40 and 43, we see that the 0 dB contours for the dipole are at a distance  $2\lambda$  away on the x-axis and for the monopole at a distance of  $3\lambda$  on the same axis. It appears that the field attenuates more rapidly with radial distance away from the dipole as compared to the monopole. For both antennas, the maximum value appears at a  $40^\circ$  angle from the x-axis. As the observation point moves away from the antenna along the x-axis, there is a difference of 4.6 dB between the electric field values on the contour plots of the two

antennas. Also, note that as the observation point moves away from the box surface along the z-axis, the difference appears to be 5.6 dB. Compared to the theoretical difference of 7.28 dB that we expect, there is a 2 dB offset which is a result of comparing a  $\lambda/5$  monopole instead of a  $\lambda/4$  one to the  $\lambda/2$  dipole.

The phase plots of the  $E_x$  and  $E_z$  components of the electric fields for the  $\lambda/2$  dipole and 0.06 m monopole in Figures 41, 42, 44, and 45 show that both antennas have a smooth spherical wavefront pattern.

TABLE 14  
RESULTS FROM NEC OUTPUTS

	DIPOLE $\lambda/2$ IN FREE SPACE (5-SEGMENTS)	6 CM MONOPOLE OVER PERFECT GROUND (5-SEGMENTS)	6CM MONOPOLE MOUNTED ON SURFACE PATCH BOX CENTER (5-SEGMENTS)
LENGTH (meters)	0.15m ( $\lambda/2$ )	0.06m ( $\lambda/5$ )	0.06m ( $\lambda/5$ )
WAVELENGTH (meters)	0.3m	0.3m	0.3m
EXCITATION (voltage source)	1 Volt	1 Volt	1 Volt
FEED POSITION (# OF SEGMENT)	3rd	1st	1st
MAXIMUM CURRENT (magnitude in amps)	$0.98 \times 10^{-2}$	$0.22 \times 10^{-1}$	$0.26 \times 10^{-1}$
IMPEDANCE (ohms)	$89.61 + j49.57$	$26 - j35.82$	$10.99 - j37.53$
INPUT POWER (watts)	$0.43 \times 10^{-2}$	$0.66 \times 10^{-2}$	$0.36 \times 10^{-2}$

CONTOUR E-FIELD (DB REFER TO 1V/M)  
 DIPOLE LENGTH  $\lambda/2$  ON Z AXIS  
 FREE SPACE-FREQ=1GHZ

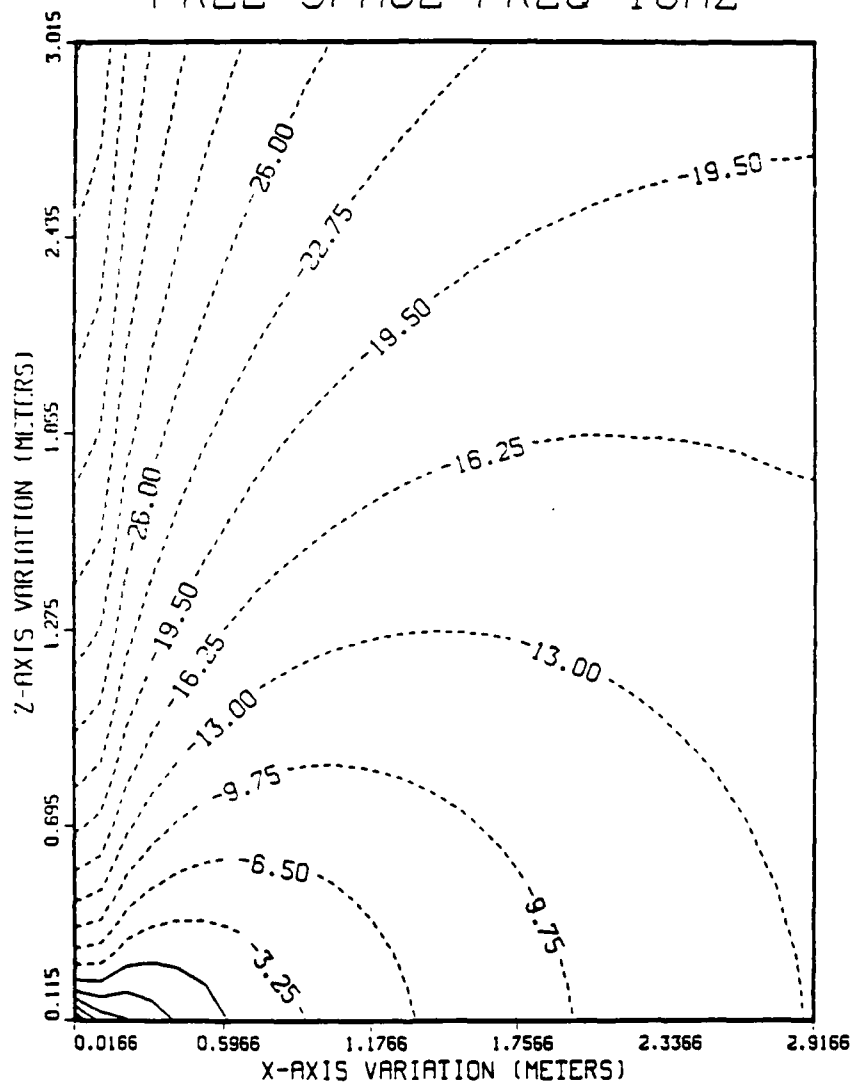


Figure 40. Total E-Field Contours  
 Dipole  $\lambda/2$  on Z Axis in Free Space

CONTOUR E-FIELD (DB REF TO 1V/M)  
 DIPOLE LENGTH  $\lambda/2$  ON Z-AXIS  
 FREE SPACE-FREQ=1GHZ

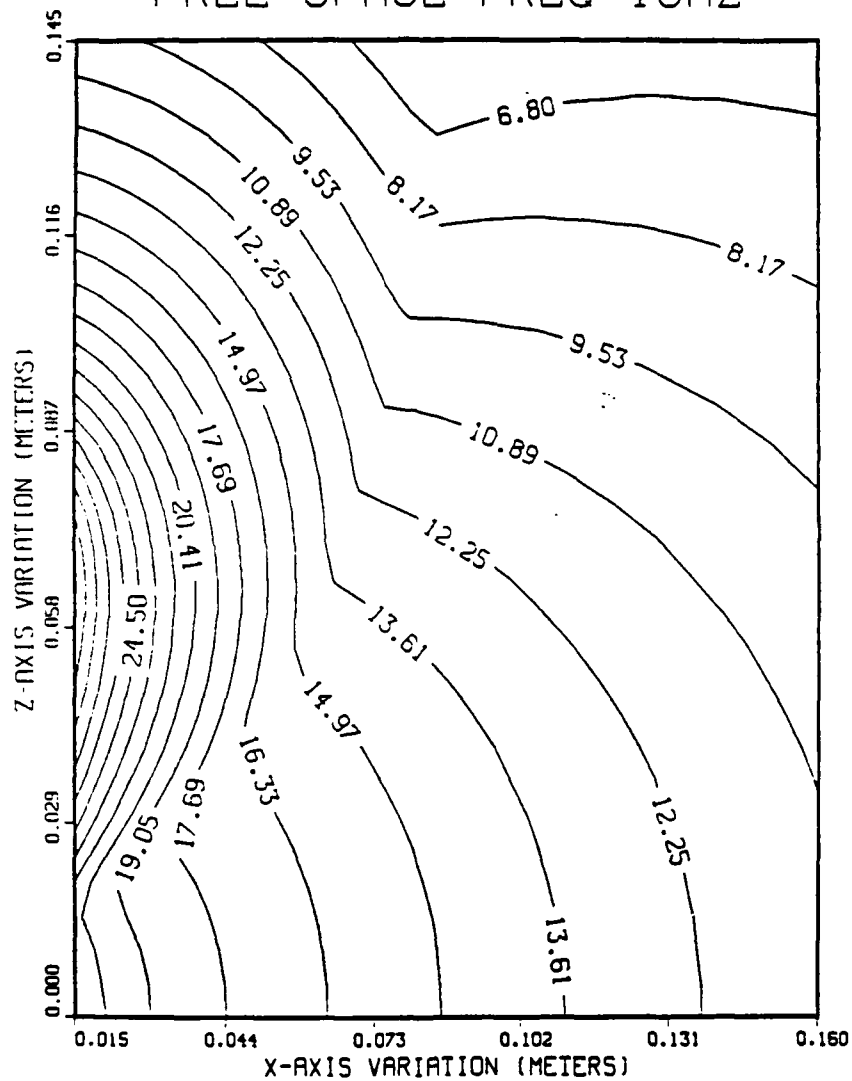


Figure 40(a). Total E-Field Contours  
 Dipole  $\lambda/2$  in Free Space ( $0.5 \lambda$  away from the wire)

CONTOUR E-FIELD (DB REF TO 1V/M)  
 DIPOLE LENGTH  $\lambda/2$  ON Z-AXIS  
 FREE SPACE-FREQ=1GHZ

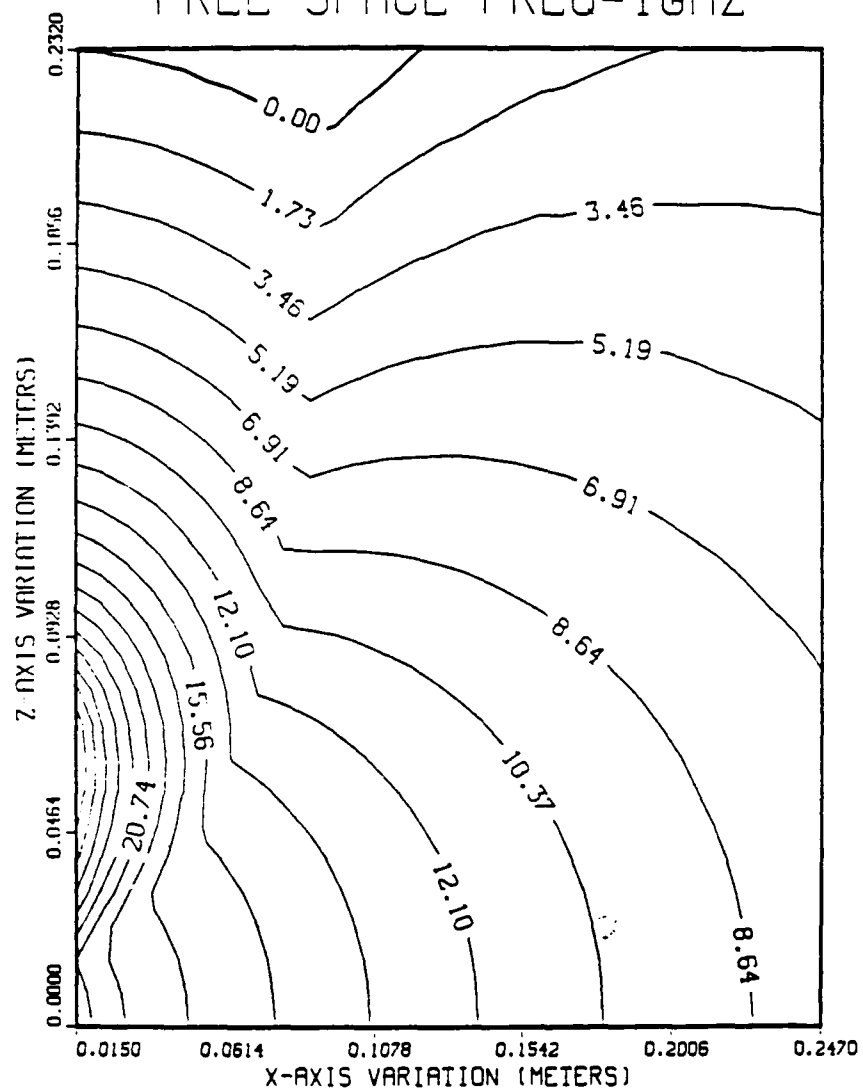


Figure 40(b). Total E-Field Contours  
 Dipole  $\lambda/2$  in Free Space ( $0.8 \lambda$  away from the wire)

PHASE OF X COMPONENT OF E-FIELD  
 DIPOLE  $\lambda/2$  ON Z AXIS  
 IN FREE SPACE-FREQ=1GHZ

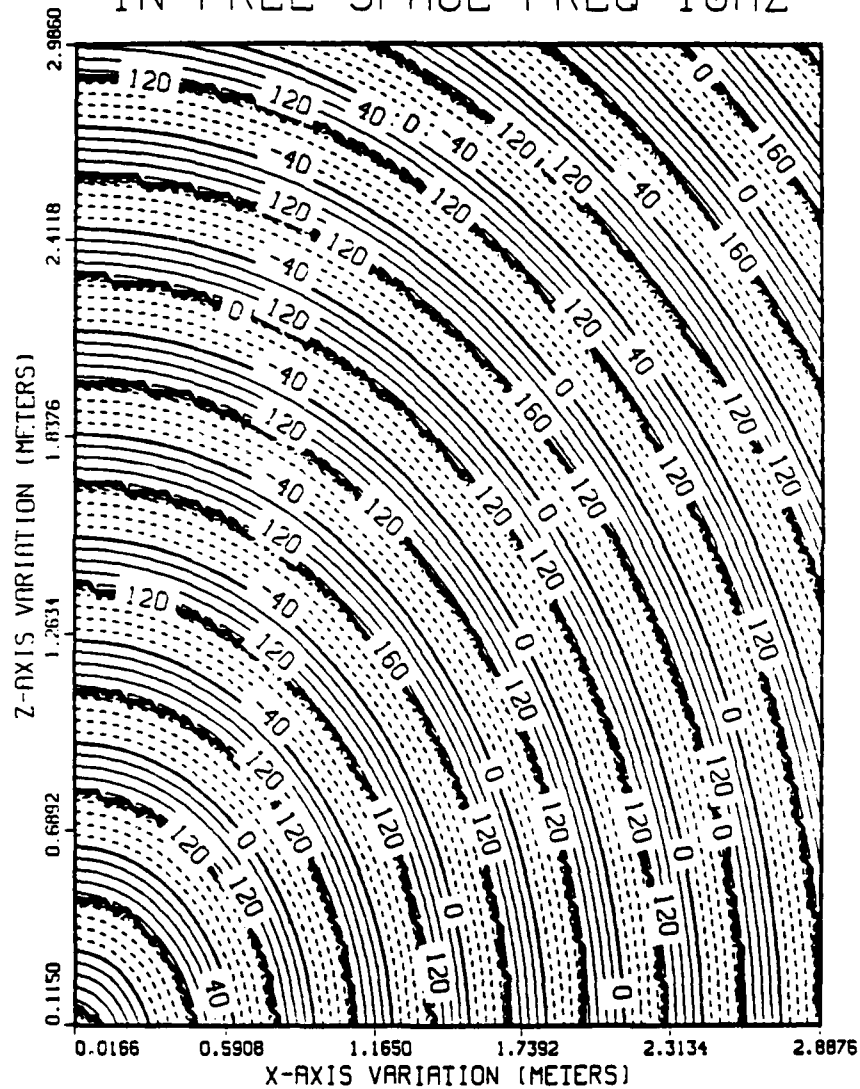


Figure 41. X-Component, E-Field Phase Contours  
 Dipole  $\lambda/2$  in Free Space

PHASE OF Z COMPONENT OF E-FIELD  
 DIPOLE  $\lambda/2$  ON Z AXIS  
 IN FREE SPACE-FREQ=1GHZ

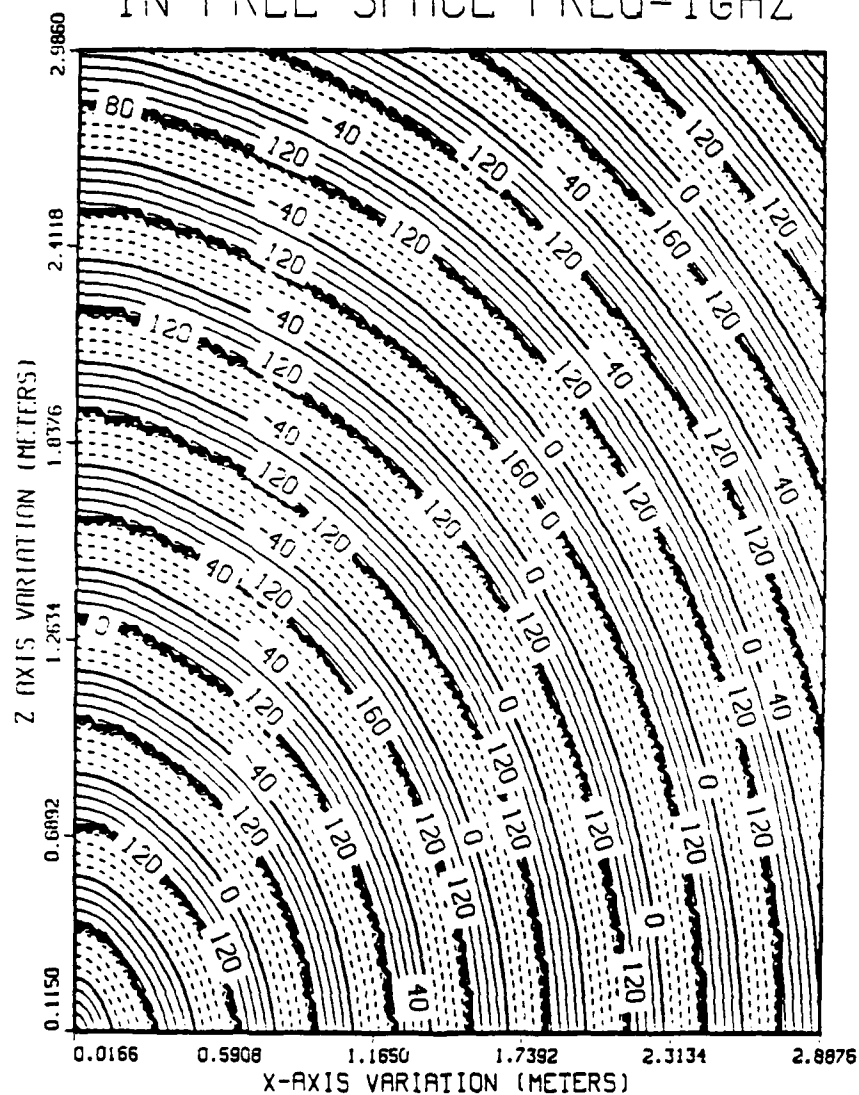


Figure 42. Z-Component, E-Field Phase Contours  
 Dipole  $\lambda/2$  in Free Space



CONTOUR E-FIELD (DB REFER TO 1V/M)  
 MONOPOLE 6 CM ON Z AXIS  
 OVER PERFECT GROUND-FREQ=1GHZ

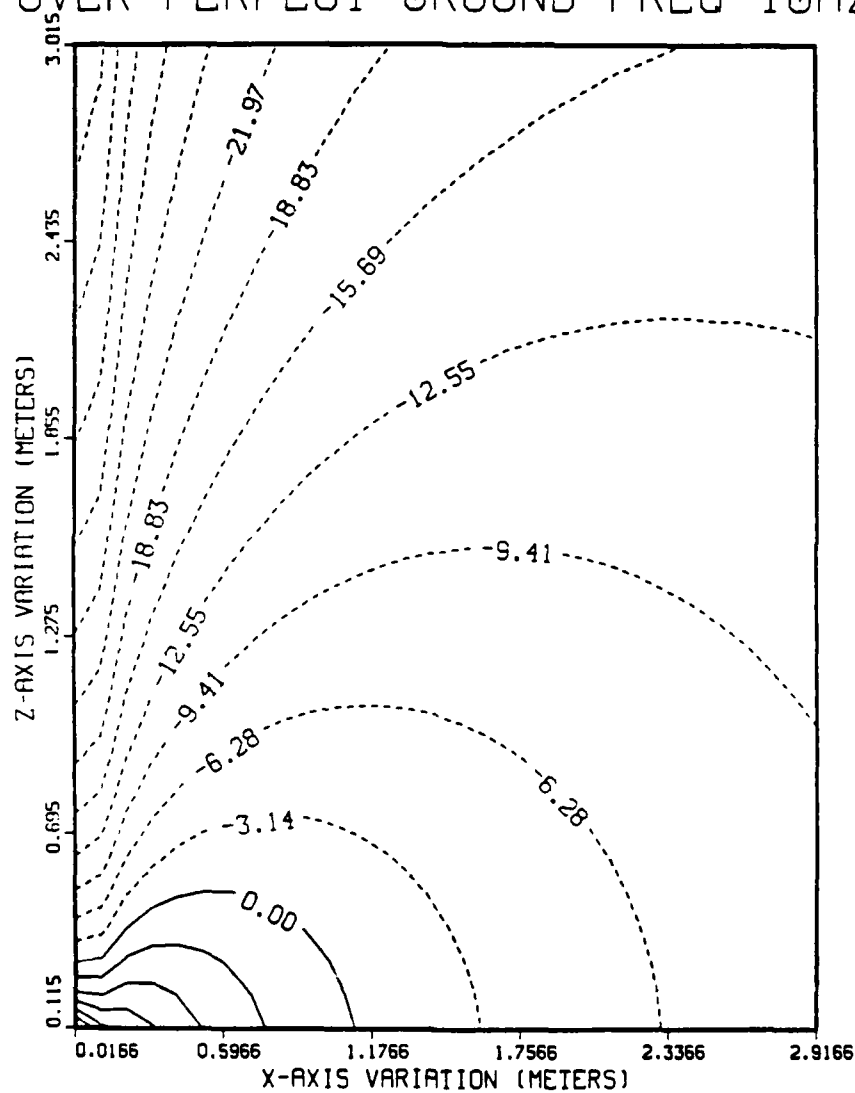


Figure 43. Total E-Field Contours  
 Monopole 6cm Over Perfect Ground

CONTOUR E-FIELD (DB REF TO 1V/M)  
 MONOPOLE 6 CM ON Z-AXIS  
 OVER PERFECT GROUND-FREQ=1GHZ

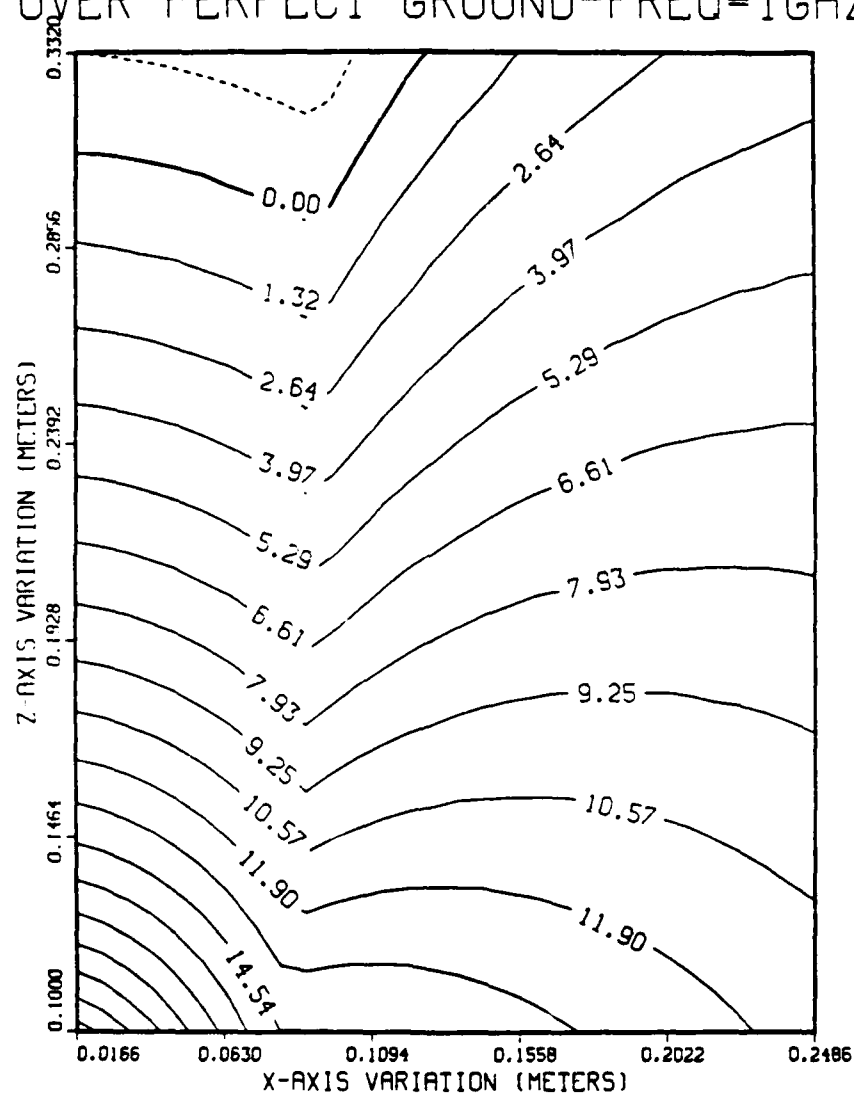


Figure 43(a). Total E-Field Contours  
 Monopole 6cm Over Perfect Ground ( $1\lambda$  away from the wire)

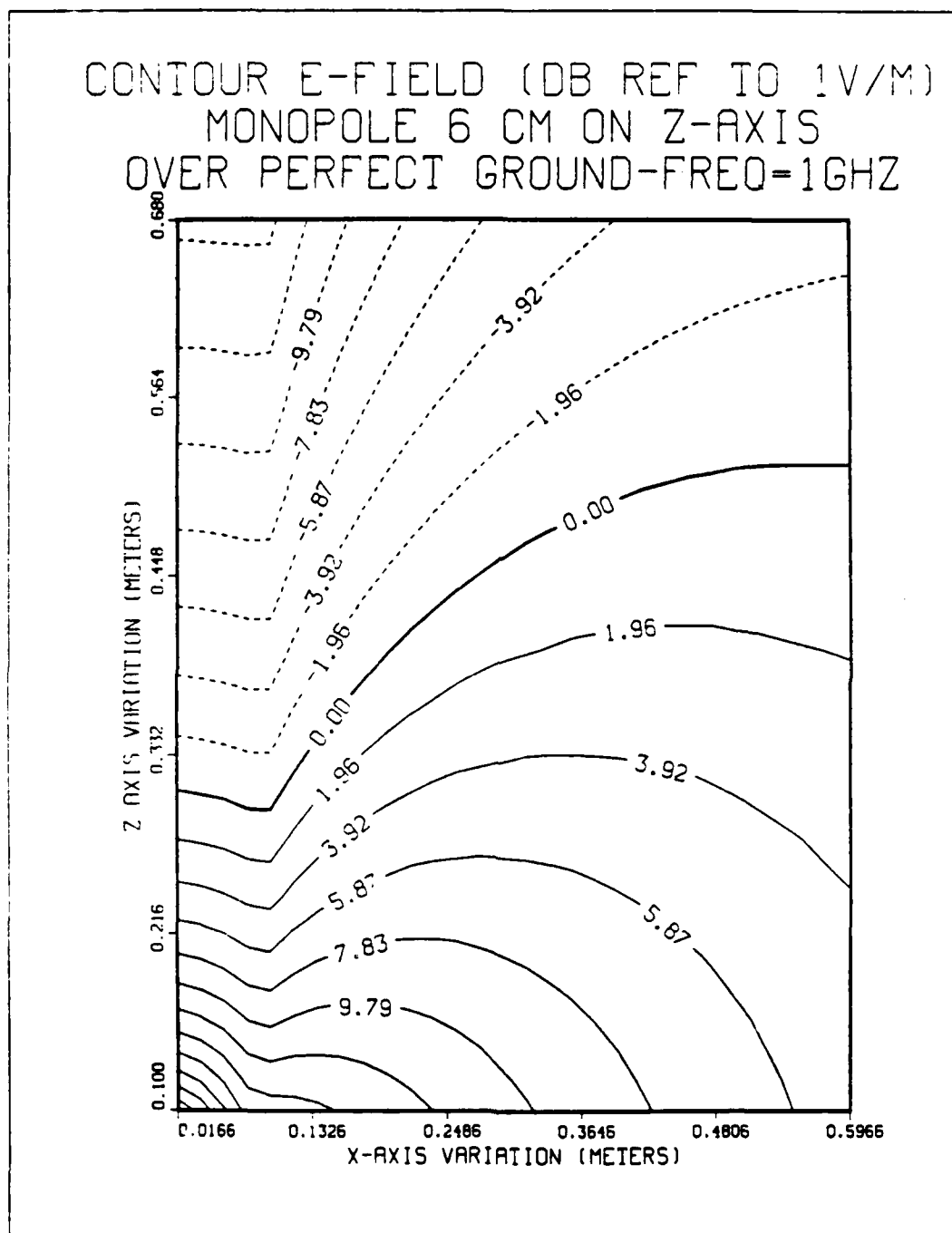


Figure 43(b). Total E-Field Contours  
 Monopole 6cm Over Perfect Ground ( $2\lambda$  away from the wire)

CONTOUR E-FIELD (DB REF TO 1V/M)  
 MONOPOLE 6 CM ON Z-AXIS  
 OVER PERFECT GROUND-FREQ=1GHZ

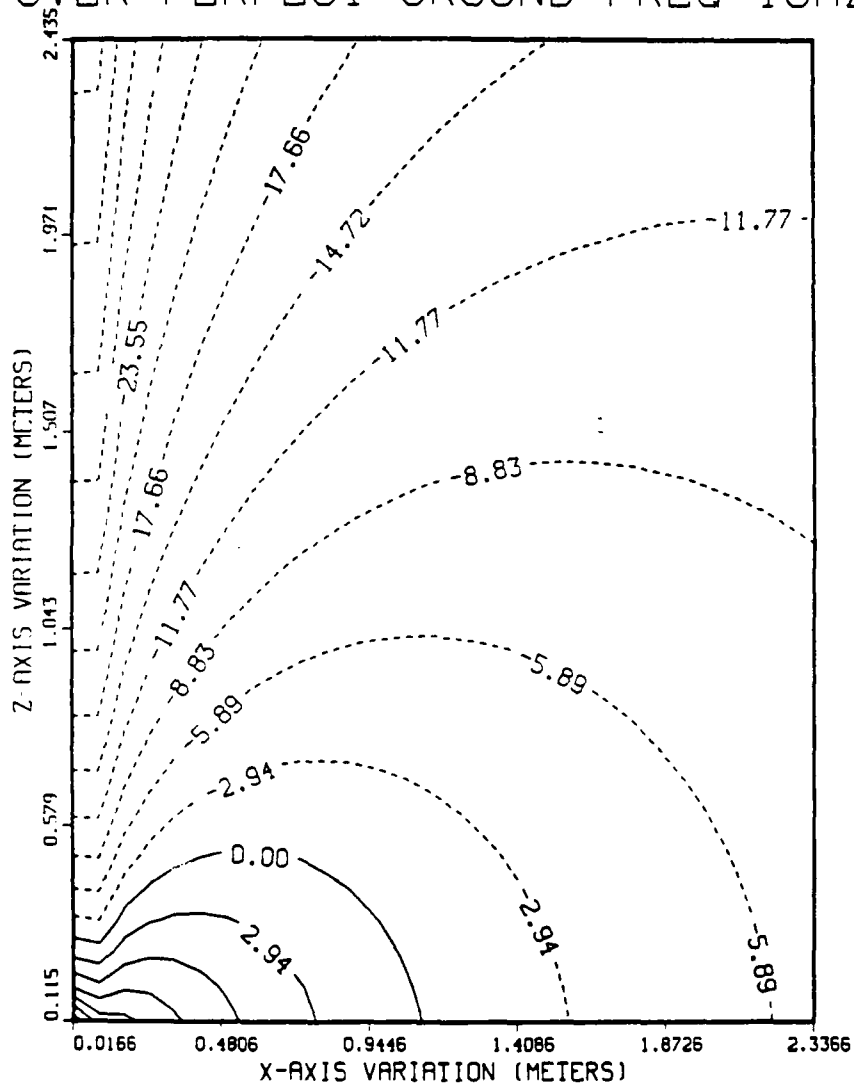


Figure 43(c). Total E-Field Contours  
 Monopole 6cm Over Perfect Ground ( $8\lambda$  away from the wire)

PHASE OF X COMPONENT OF E-FIELD  
 MONOPOLE 6CM ON Z AXIS  
 OVER PERFECT GROUND-FREQ=1GHZ

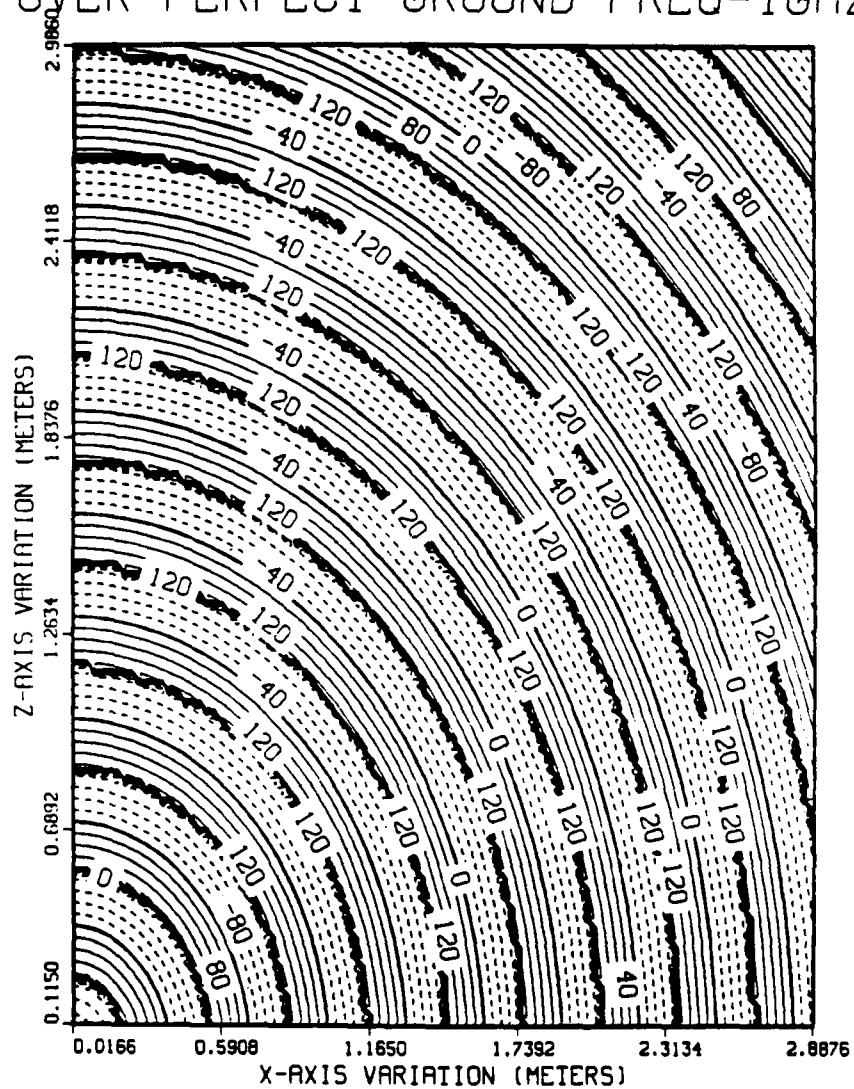


Figure 44. X-Component, E-Field Phase Contours  
 Monopole 6cm Over Perfect Ground

PHASE OF Z COMPONENT OF E-FIELD  
 MONOPOLE 6CM ON Z AXIS  
 OVER PERFECT GROUND-FREQ=1GHZ

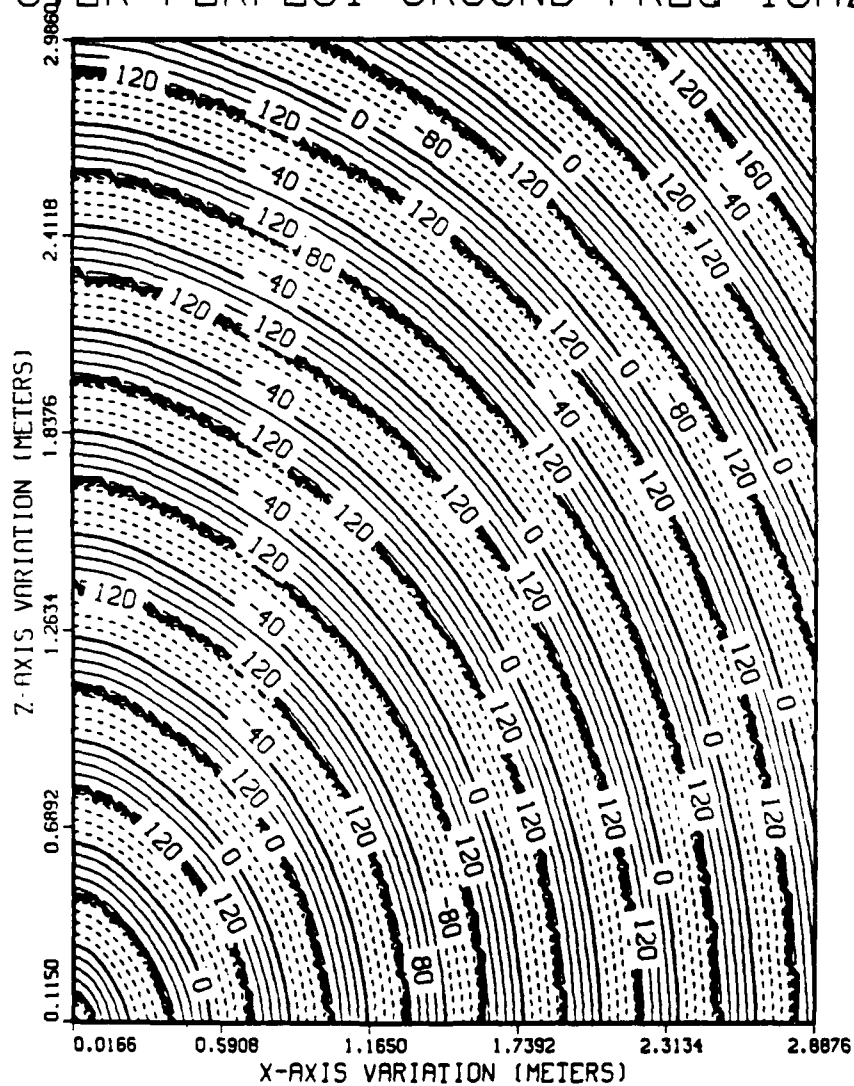


Figure 45. Z-Component, E-Field Phase Contours  
 Monopole 6cm Over Perfect Goound

## 2. Monopole at Center of Patch Box vs Monopole Over Ground Plane

Input data files for NEC solutions of the near electric field of the monopole on the box center are contained in Appendix B. In Figures 46 to 50, the magnitude of the total electric field and the magnitude and phase of the  $E_x$  and  $E_z$  components are shown. In Figure 46, the E-field zero dB contour is observed to be closer to the antenna (it is at  $2\lambda$  vs.  $3\lambda$ ) than for the monopole over a ground plane. Using the ratio of the maximum input currents alone, we calculate that the theoretical difference in the electric fields of the two antennas should be -1.08 dB. The contour plots of Figures 46 and 43 show that there is a difference of -3 dB along the box surface direction and a difference of +8 dB up the z-axis, perpendicular to the surface, compared to the isolated monopole reference case. These differences in near field densities are attributed to box radiation and diffraction. In this near field region we can observe beams and nulls forming. A maximum occurs at  $60^\circ$  up from the box surface vs.  $40^\circ$  for the monopole over the ground plane. The main lobe (Figure 46) starts to develop at a distance  $2\lambda$  (0.6 m) from the antenna, along the x-axis. Beyond this point, it generally has the same pattern independent of distance. Within the  $2\lambda$  distance, the pattern shape has not yet fully developed.

In Figures 47 and 49,  $E_x$  and  $E_z$  contour plots demonstrate the behavior of the magnitude (the  $E_y$  component is negligible and is not presented).

Recalling the  $E_{\text{peak}}$  field variations and noting that  $E_{\text{peak}}$  consists of  $E_z$  and  $E_x$  components, we can scan Figures 47 and 49 and see how these components contribute to the total field of Figure 46. Different variations with distance along the x- and z-axes and with take-off (elevation) angle are noted. The z-component is predominant, as it should be, for a z-directed monopole. Null effects are most apparent for  $E_z$  at moderate elevation angles and, as expected,  $E_x$  nulls at the zenith.

Figures 48 and 50 show the phase of the x and z components. The electric field phase has the same spherical wavefront pattern as the monopole over the ground plane (Figures 44 and 45), except for the region of the null, caused by the box. The disturbance in the electric field phase appears at the same  $27^\circ$  location in both phase plots (Figures 48 and 50). It is quite severe in the z component phase (Figure 50) and is barely observed in the x component phase (Figure 48).

In order to get better insight into the electric near field variations and where the maxima and minima occur, 3-dimensional plots are presented in Figures 51 and 52. These plots were produced from Fortran program III, described in Appendix B and use the same view plane as previous plots.



Each plot displays a surface whose elevation points represents field strength in the upper portion, and a normal 2-D contour plot "projection" in the lower portion. Two different view points were selected, one "looking away from" the monopole and one towards it. In each figure the vertex that corresponds to the pointed "spike-like" area of the surface is the origin where the antenna is mounted. The delay of the field as the observation point moves away from the monopole source is expected. The null "trough" is very striking in this type of presentation.

CONTOUR E-FIELD (DB REF TO 1V/M)  
 MONOPOLE 6 CM AT CENTER OF SPBOX  
 7X7 PATCHES ON TOP-FREQ=1GHZ

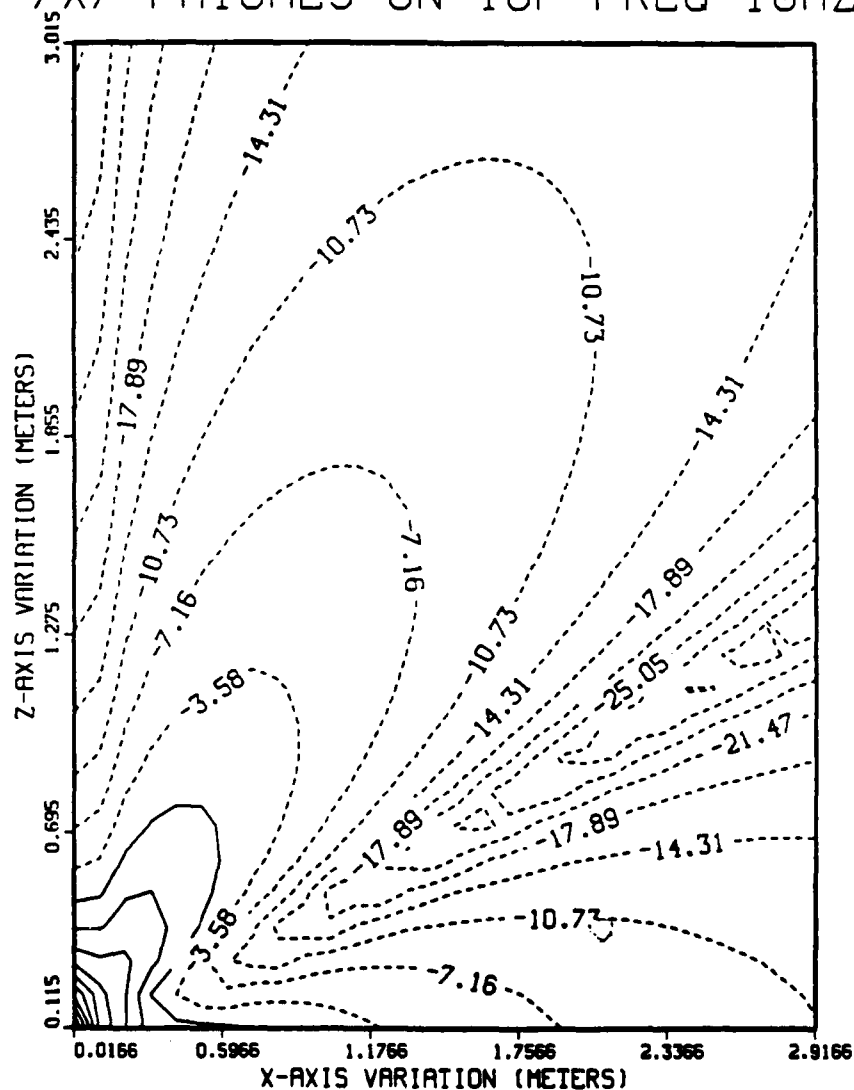


Figure 46. Total E-Field Contours  
 Monopole at Patch Box Center

MAGNITUDE (EX PEAK) OF E-FIELD  
 MONOPOLE 6CM AT CENTER OF SPBOX  
 7X7 PATCHES ON TOP-FREQ=1GHZ

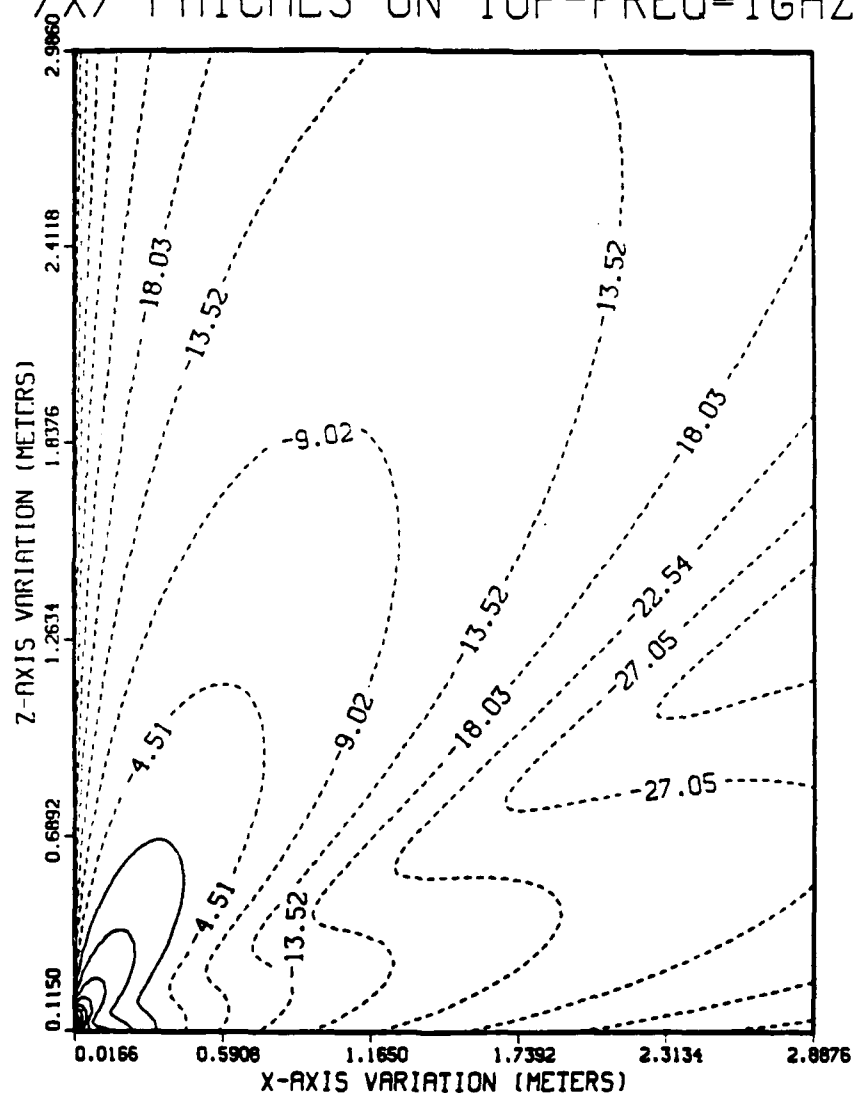


Figure 47. X-Component, E-Field Contours  
 Monopole at Patch Box Center

PHASE OF X COMPONENT OF E-FIELD  
MONOPOLE 6CM AT CENTER OF SPBOX  
7X7 PATCHES ON TOP-FREQ=1GHZ

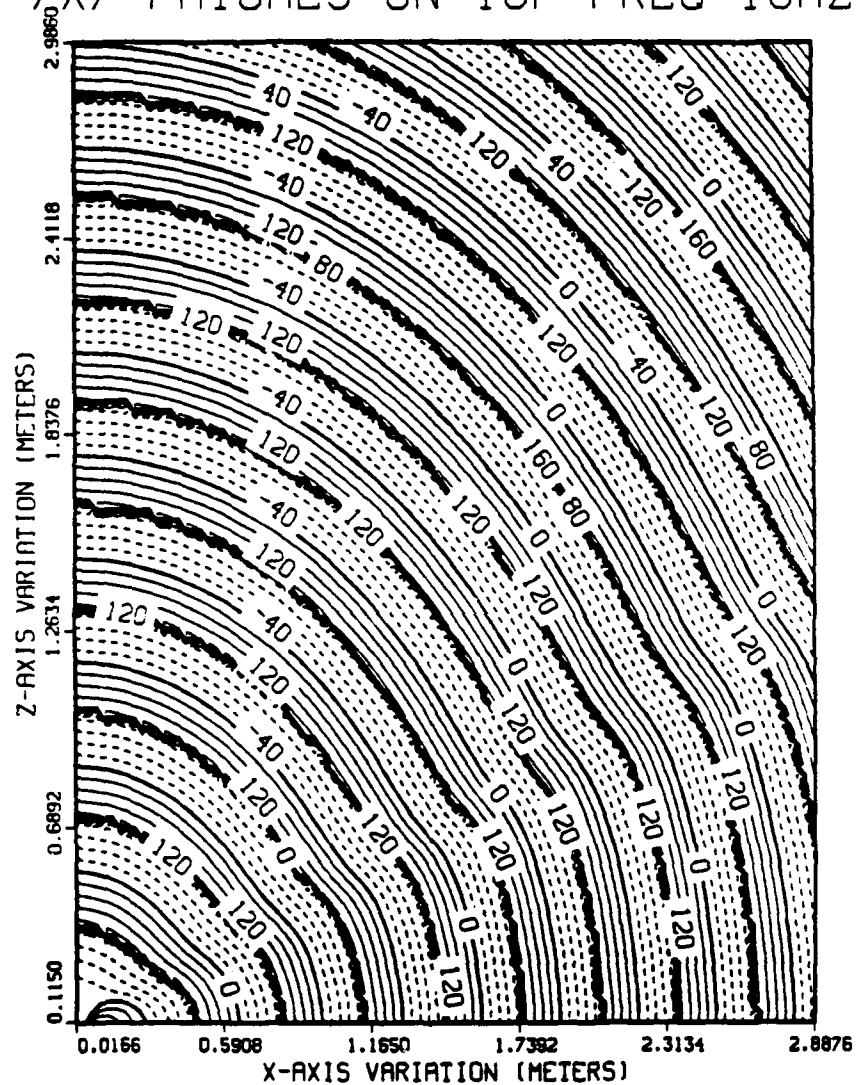


Figure 48. X-Component, E-Field Phase Contours  
Monopole at Patch Box Center

MAGNITUDE (EZ PEAK) OF E-FIELD  
 MONOPOLE 6CM AT CENTER OF SPBOX  
 7X7 PATCHES ON TOP-FREQ=1GHZ

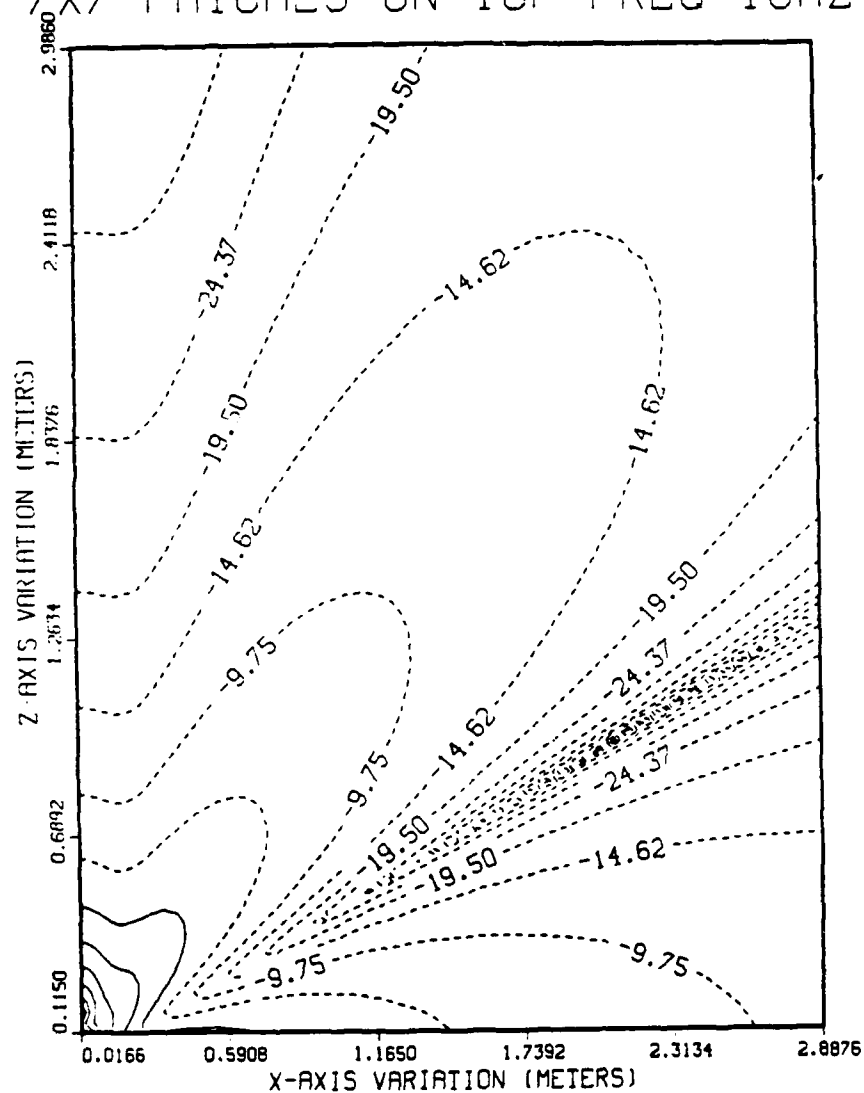


Figure 49. Z-Component, E-Field Contours  
 Monopole at Patch Box Center

PHASE OF Z COMPONENT OF E-FIELD  
 MONOPOLE 6CM AT CENTER OF SPBOX  
 7X7 PATCHES ON TOP-FREQ=1GHZ

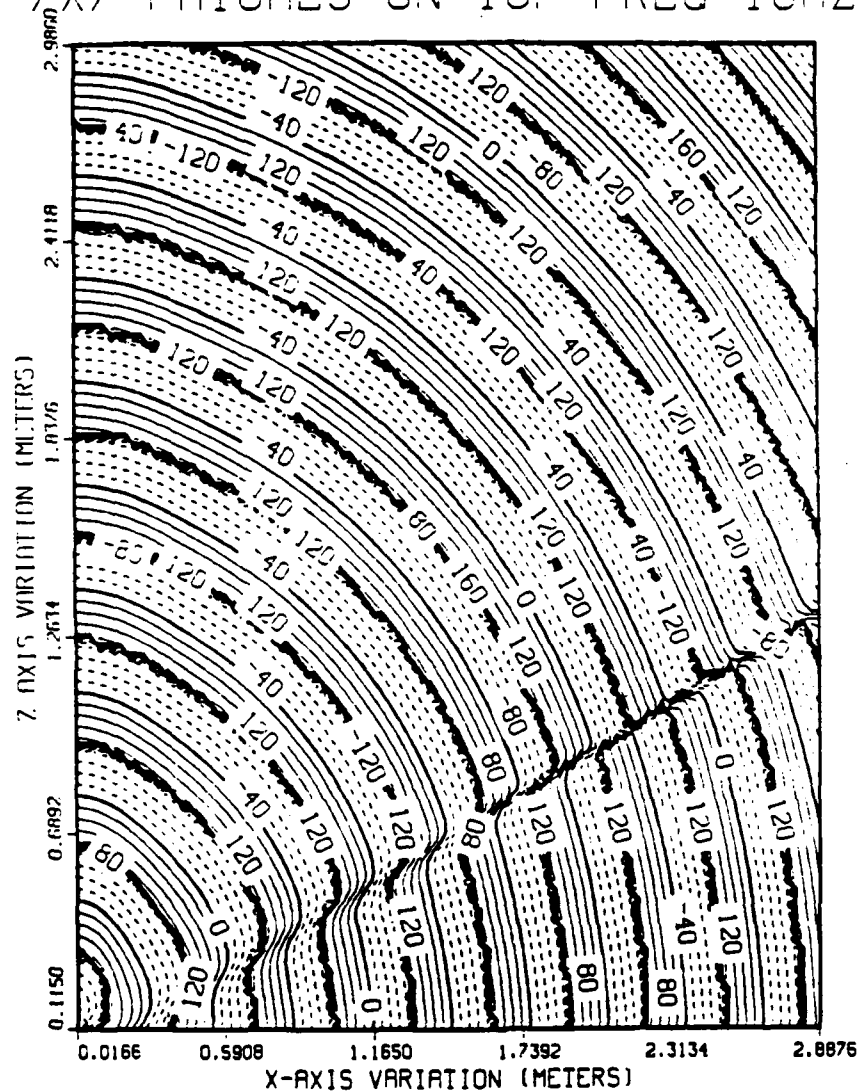
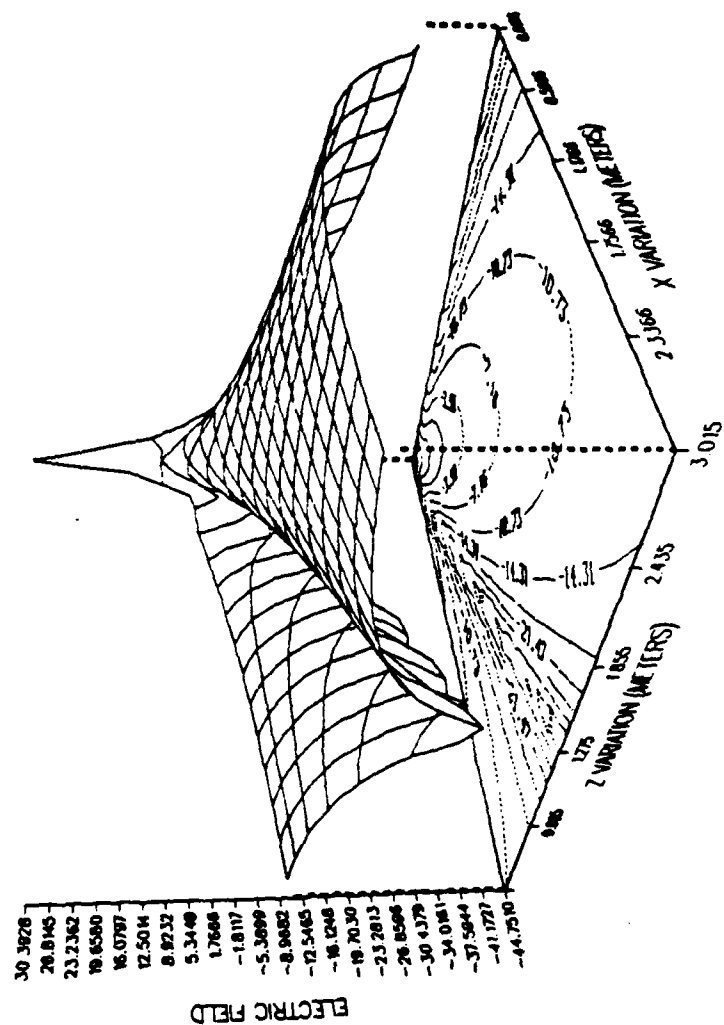


Figure 50. Z-Component, E-Field Phase Contours  
 Monopole at Patch Box Center

# 3-D ELECTRIC FIELD (DB REF TO 1V/M) MONOPOLE AT CENTER OF SPBOX (7X7 PATCHES)



3-D ELECTRIC FIELD (DB REF TO 1V/M)  
MONOPOLE AT CENTER OF SPBOX(7X7 PATCHES)

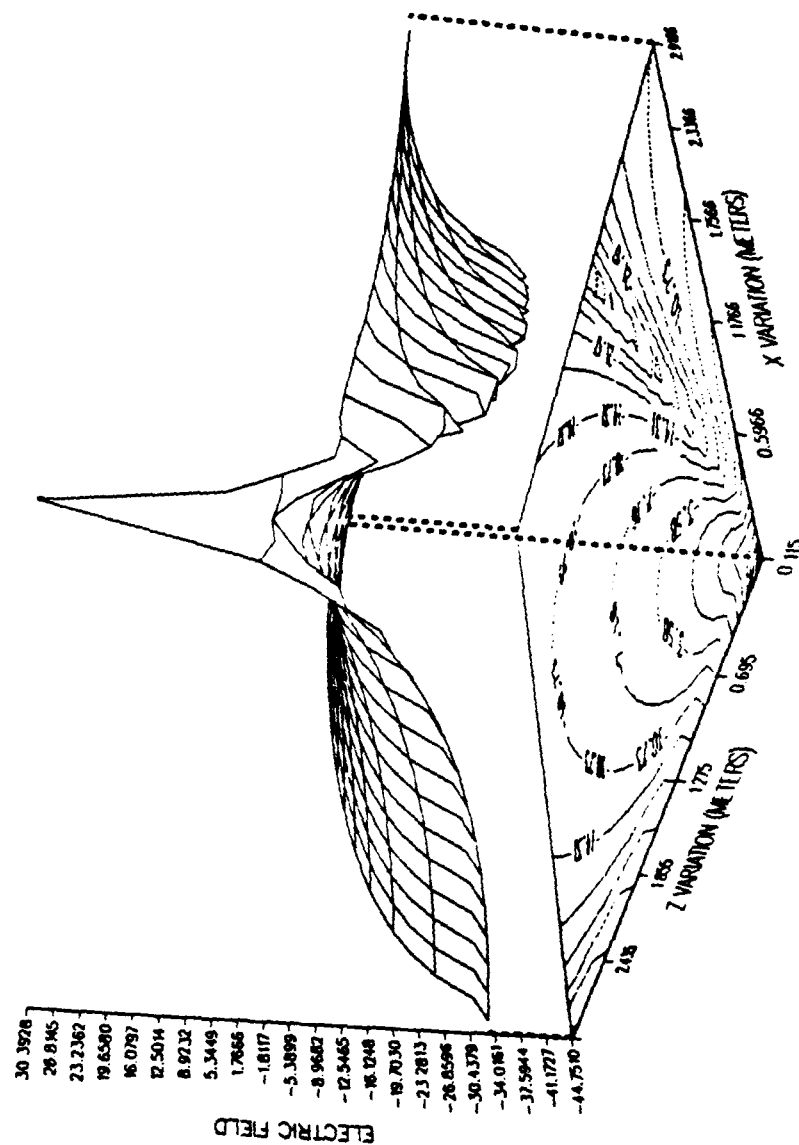


Figure 52. Total E-Field 3-D Plot. Viewed from Monopole  
(Monopole at Patch Box Center)



### 3. Monopole at Edge of Patch Box vs. Monopole at Center

Figures 53 to 59, for the edge-mounted monopole follow the same format and trend as the center-mounted case. The following comments will amplify differences from the center case and interesting features of the field distributions (NEC input data sets are in Appendix B).

The edge-mounted geometry provides a larger planar surface (box top) in front of the monopole view plane and results in the following differences with respect to the center-mount geometry:

- The z-axis peak field is somewhat greater at given distances from the box surface. This is traced to a larger  $E_x$  component.
- The elevation plane null is not as deep.
- The phase contours for the z component shown evidence of two close-in nulls, but very little "phase wrinkles" beyond the near zone.
- The contour plots depict a more uniform field overall, with a less severe null.

CONTOUR E-FIELD (DB REF TO 1V/M)  
 MONOPOLE 60CM AT EDGE (3.63 CM FROM CENTER) OF SPBOX  
 11X11 PATCHES ON TOP-FREQ=1GHZ

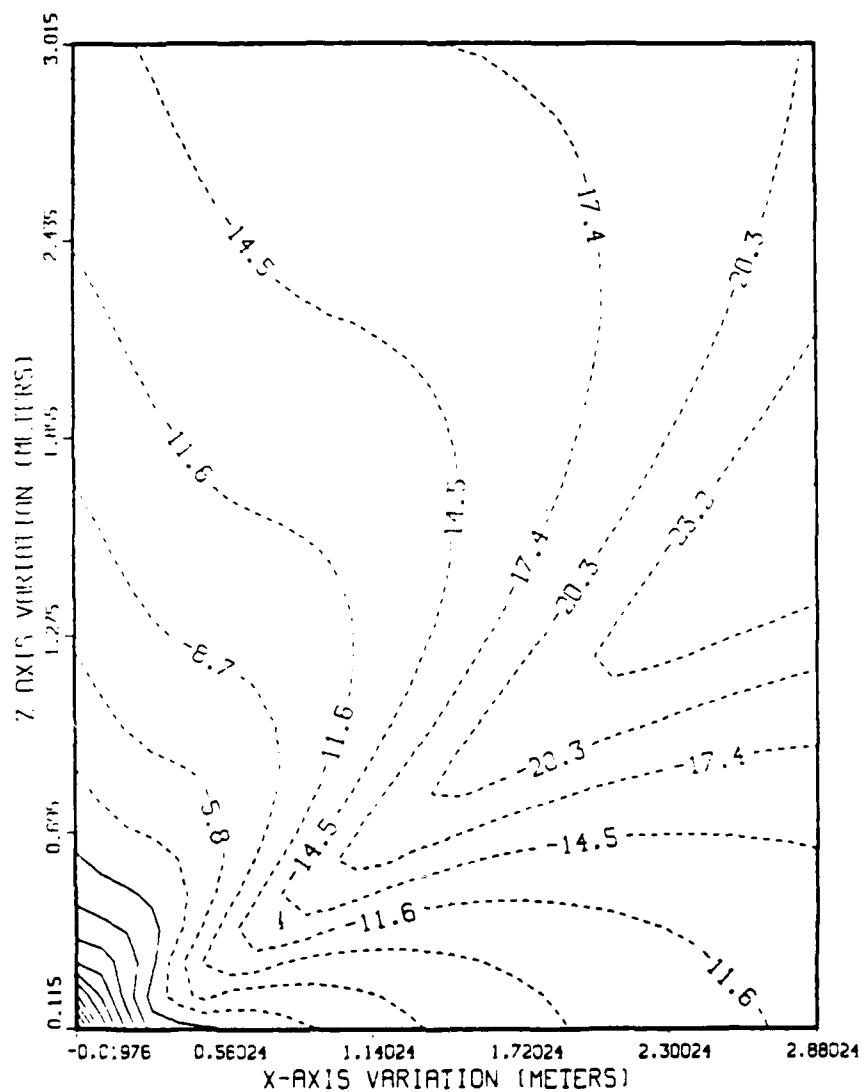


Figure 53. Total E-Field Contours  
 Monopole at Patch Box Edge

MAGNITUDE (EX PEAK) OF E-FIELD  
 MONOPOLE 6CM AT EDGE OF SPBOX  
 11X11 PATCHES ON TOP-FREQ=1GHZ

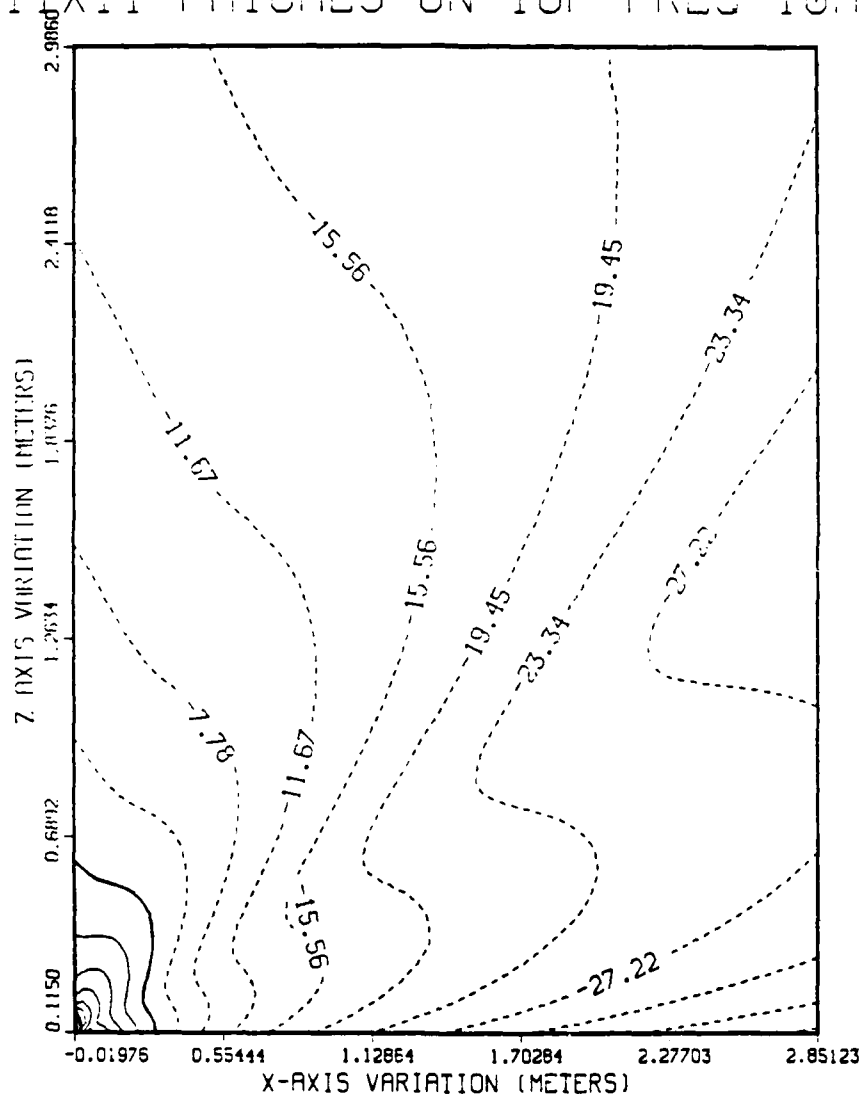


Figure 54. X-Component, E-Field Contours  
 Monopole at Patch Box Edge

PHASE OF X COMPONENT OF E-FIELD  
MONOPOLE 6CM AT EDGE OF SPBOX  
11X11 PATCHES ON TOP-FREQ=1GHz

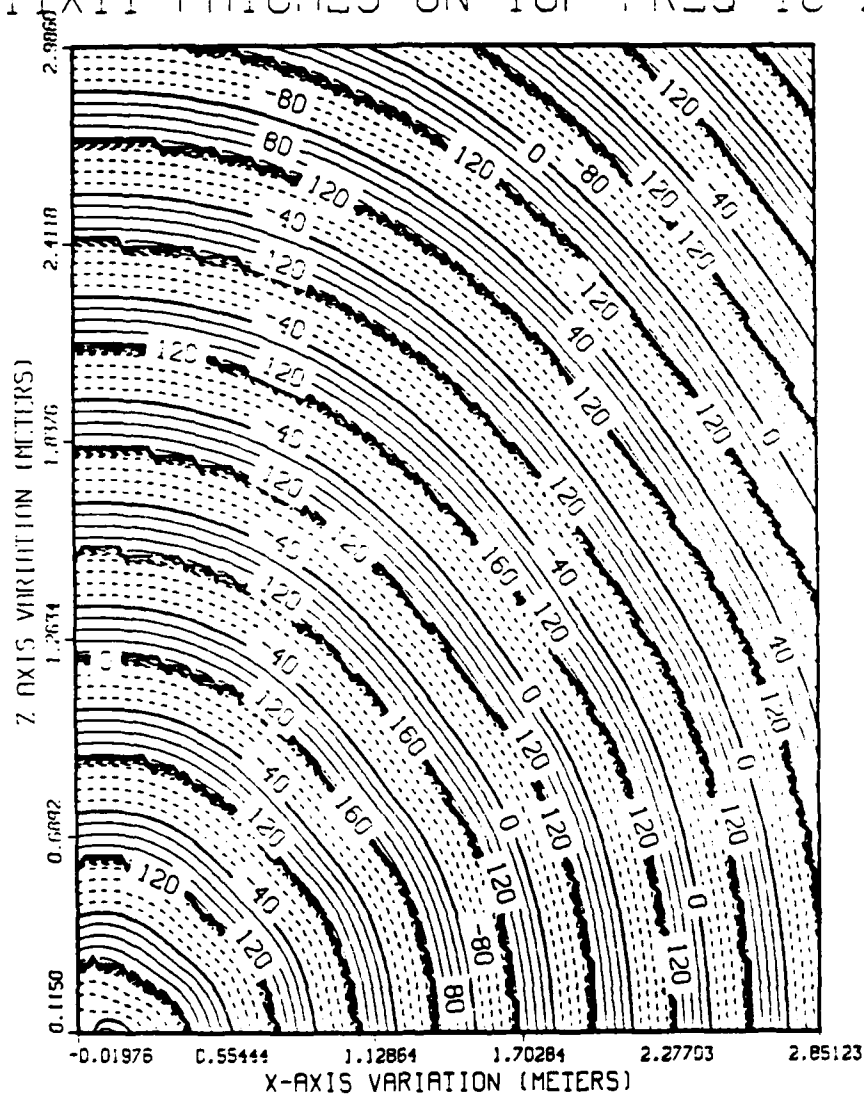


Figure 55. X-Component, E-Field Phase Contours  
Monopole at Patch Box Edge

MAGNITUDE (EZ PEAK) OF E-FIELD  
 MONOPOLE 6CM AT EDGE OF SPBOX  
 11X11 PATCHES ON TOP-FREQ=1GHZ

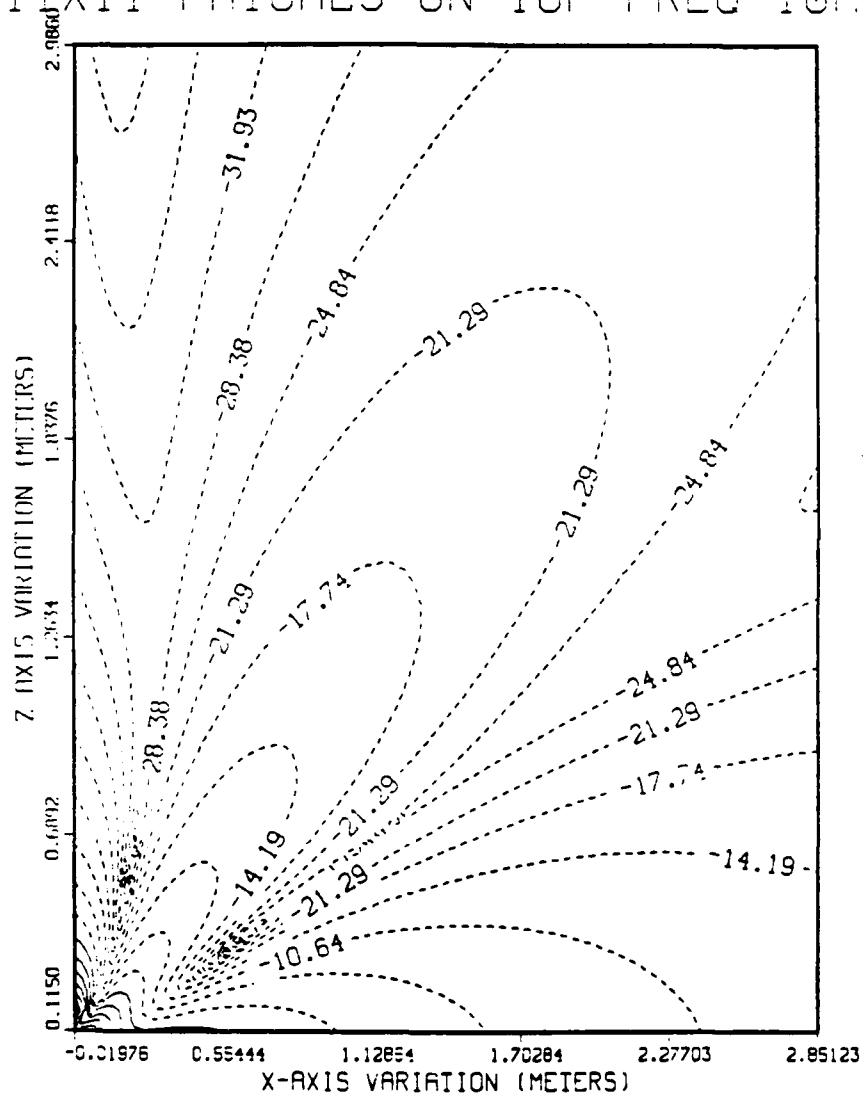


Figure 56. Z-Component, E-Field Contours  
 Monopole at Patch Box Edge

PHASE OF Z COMPONENT OF E-FIELD  
 MONOPOLE 6CM AT EDGE OF SPBOX  
 11X11 PATCHES ON TOP-FREQ=1GHZ

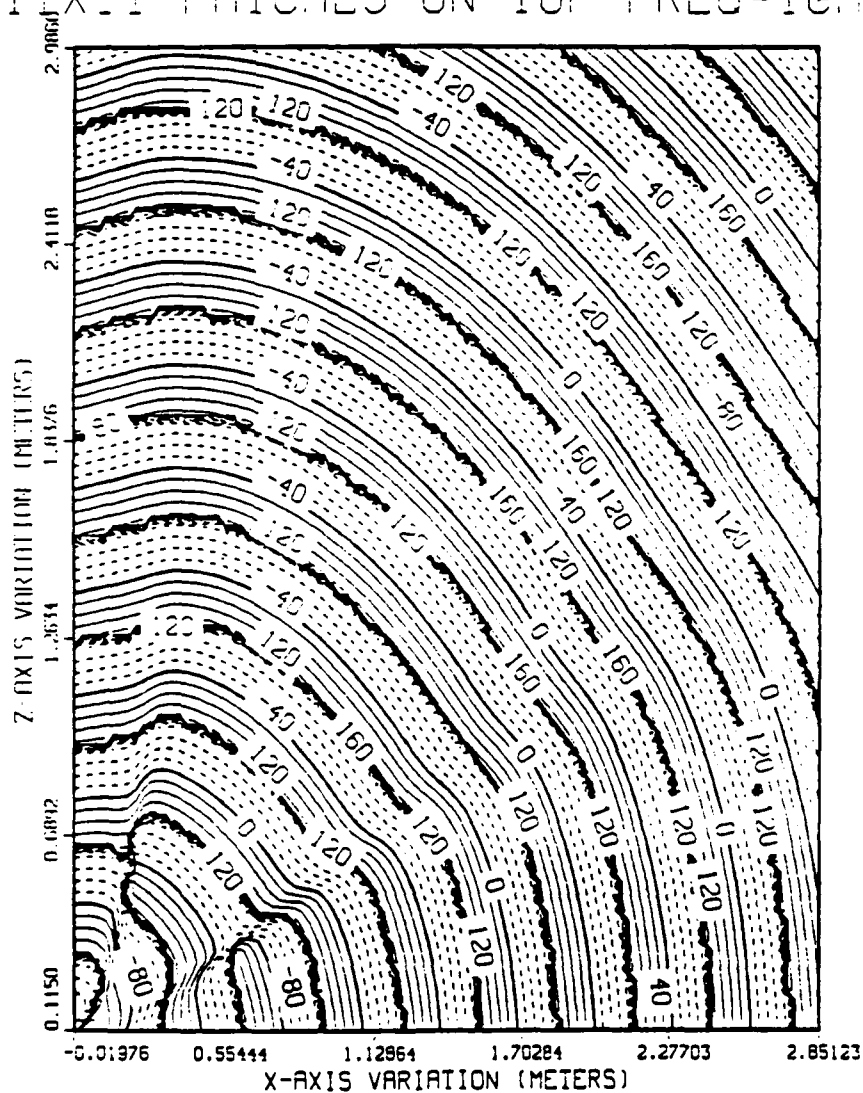


Figure 57. Z-Component, E-Field Phase Contours  
 Monopole at Patch Box Edge

3-D ELECTRIC FIELD (DB REF TO 1V/M)  
 MONOPOLE AT EDGE OF SPBOX (11X11 PATCHES)  
 (3.63 CM FROM CLINER)

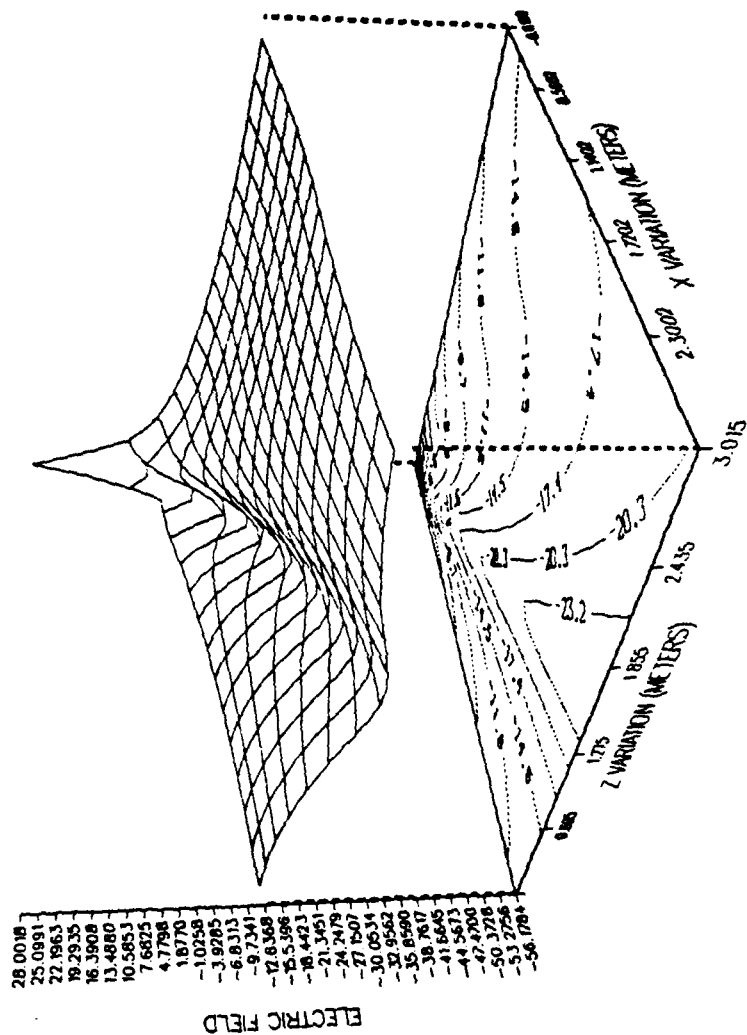


Figure 58. Total E-Field 3-D Plot, View Toward Monopole  
 (Monopole at Patch Box Edge)

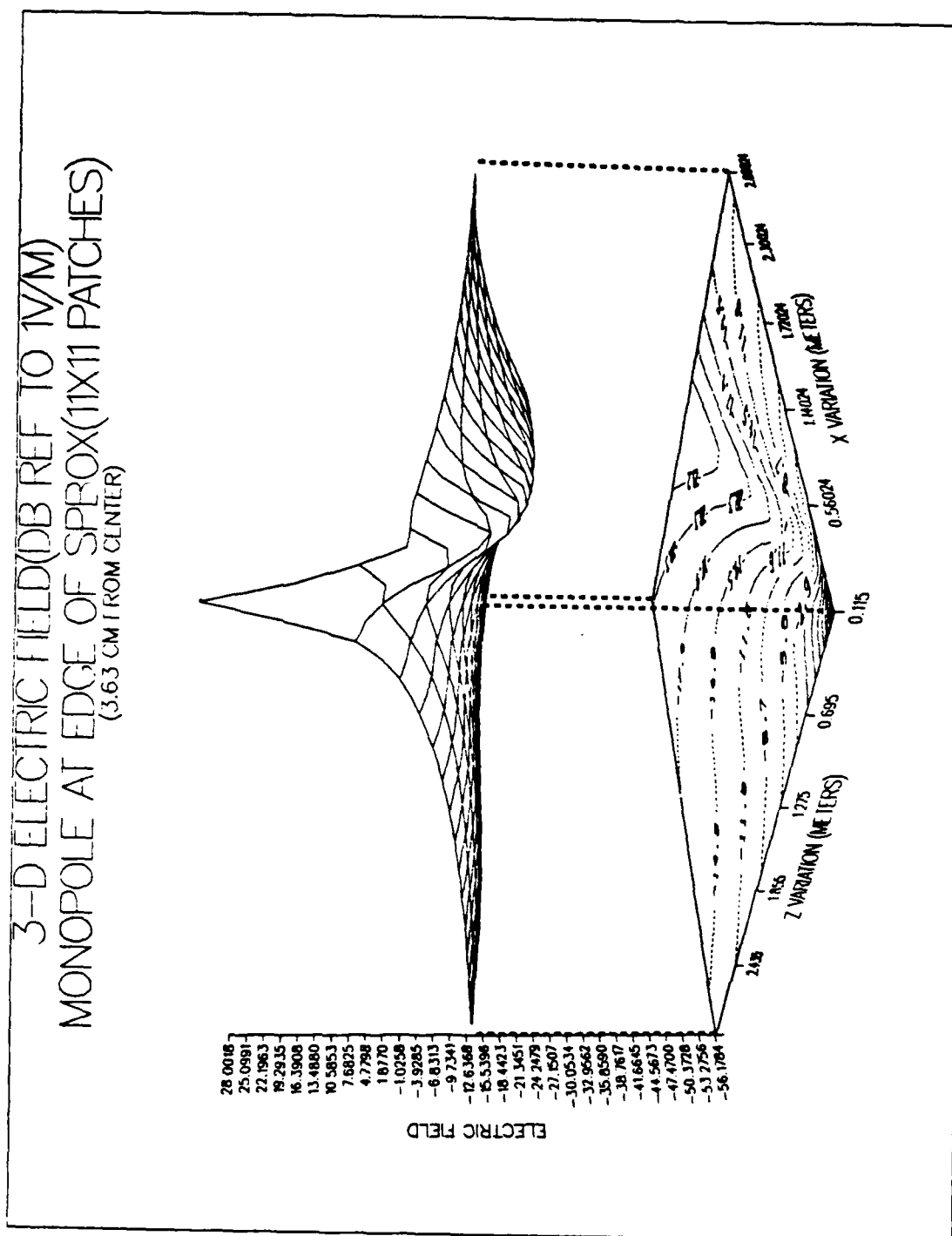


Figure 59. Total E-Field 3-D Plot, Viewed From Monopole  
(Monopole at Patch Box Edge)



#### 4. Monopole at Corner of Patch Box vs Monopole at Center

The corner-mounted monopole near field plots are in Figures 60 to 66. The NEC input data is in Appendix B. The fields for this case fall in between the center and edge-mounted field configurations. That is:

- The elevation plane null is between the other two configurations' nulls.
- Phase wrinkles show one null, as does the center-mounted case, but it is not as severe.
- Contour plots indicate a "flatter" field pattern with a fairly uniform distribution away from the monopole.

CONTOUR E-FIELD (DB REF TO 1V/M)  
 MONOPOLE 6CM AT CORNER(5.14CM ON DIAGONAL) OF SPECX  
 11X11 PATCHES ON TOP-FREQ-1GHZ

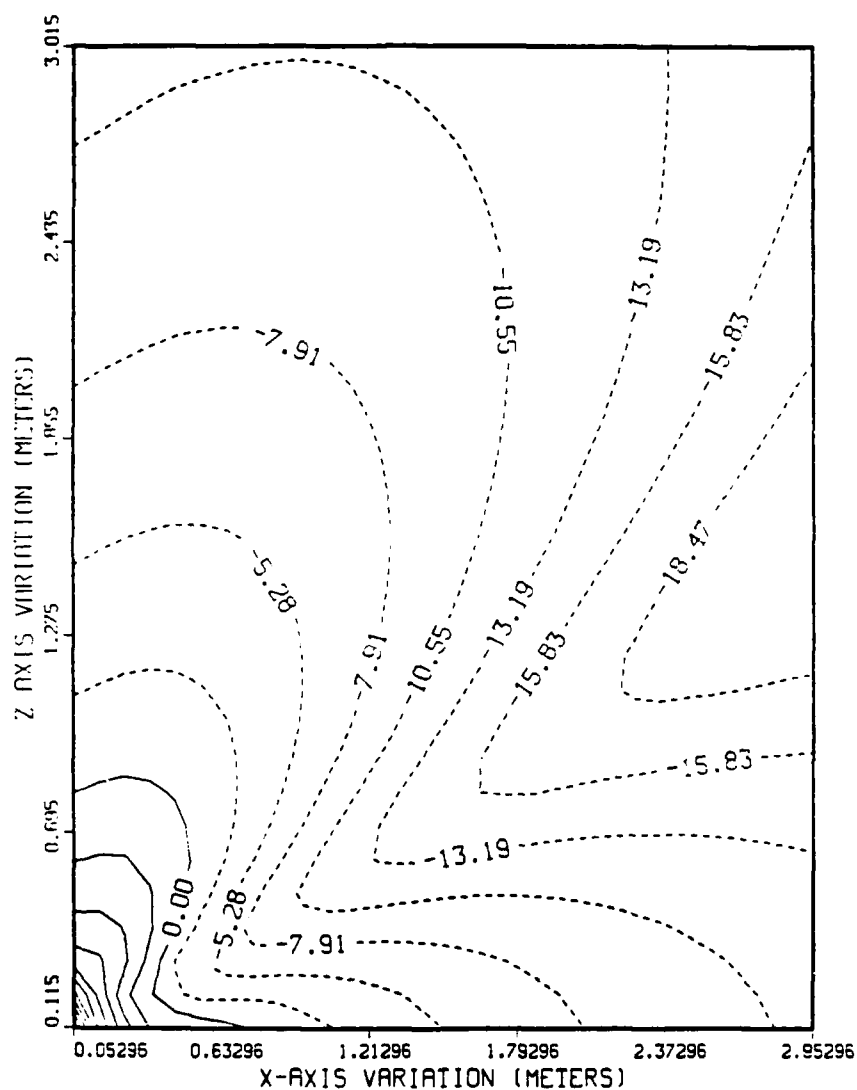


Figure 60. Total E-Field Contours  
 Monopole at Patch Box Corner

MAGNITUDE (EX PEAK) OF E-FIELD  
 MONOPOLE 6CM AT CORNER OF SPBOX  
 11X11 PATCHES ON TOP-FREQ=1GHZ

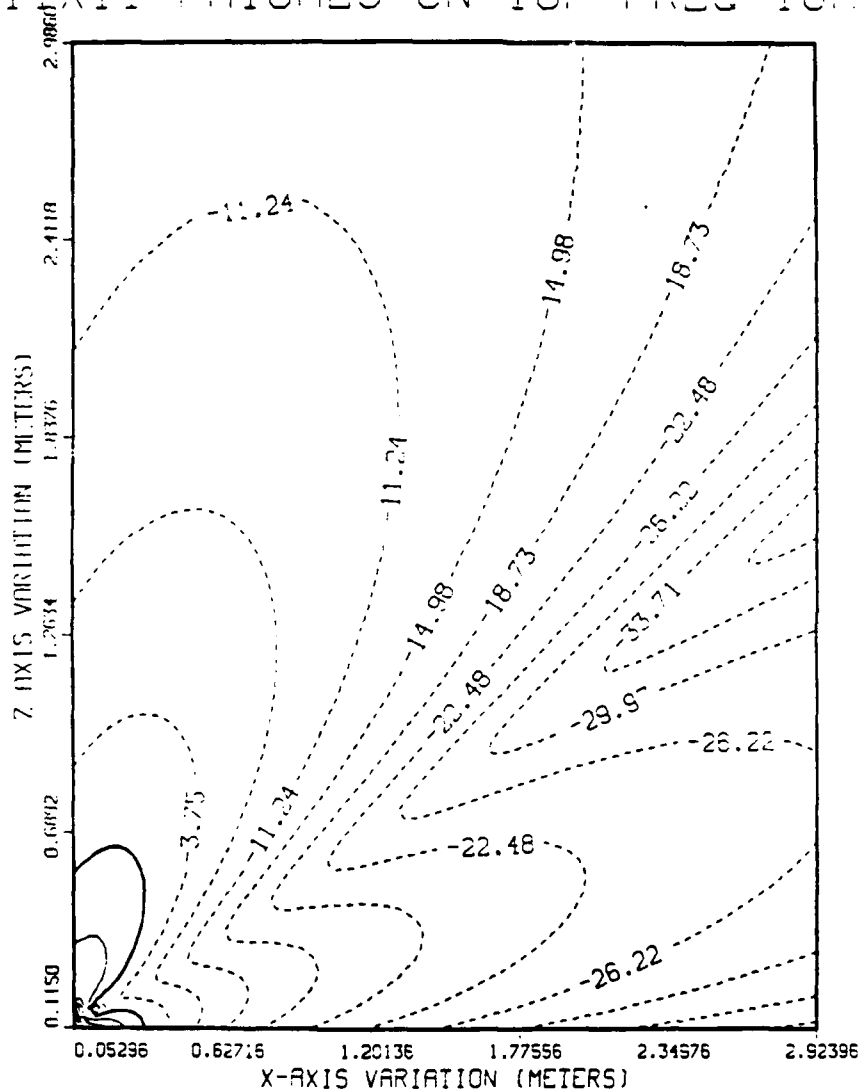


Figure 61. X-Component, E-Field Contours  
 Monopole at Patch Box Corner

PHASE OF X COMPONENT OF E-FIELD  
MONOPOLE 6CM AT CORNER OF SPBOX  
11X11 PATCHES ON TOP-FREQ=1GHZ

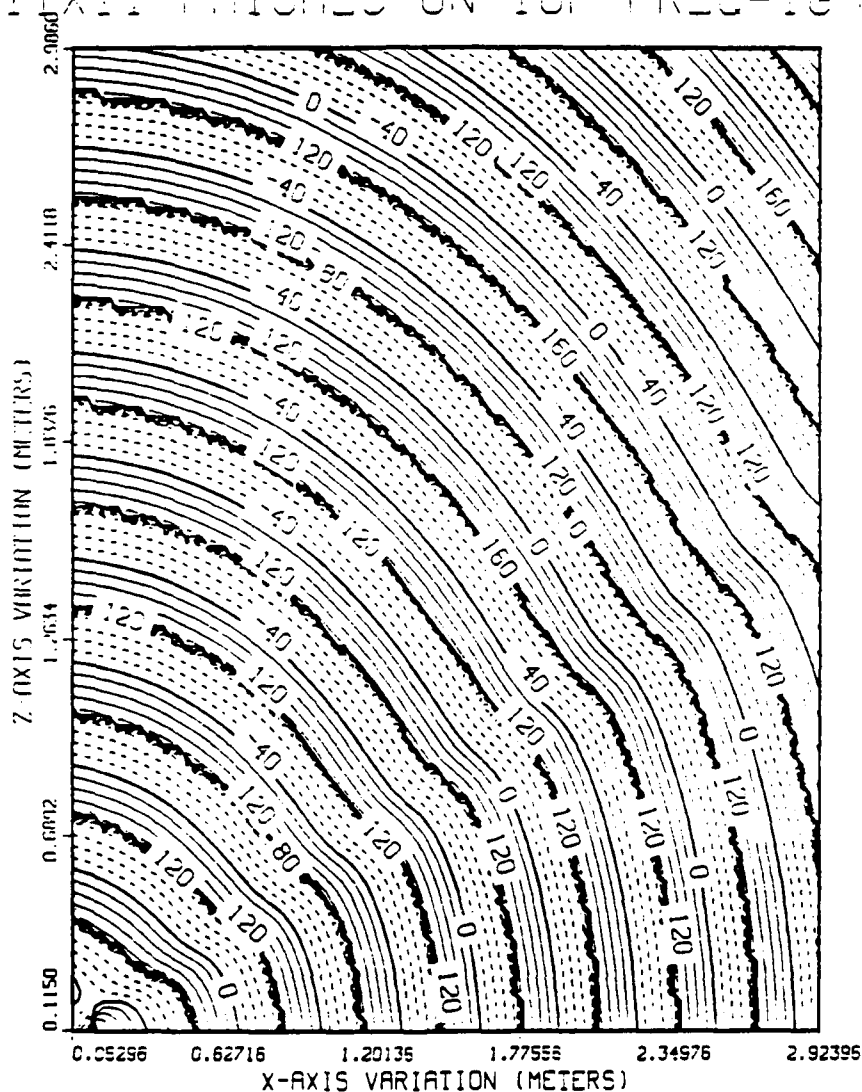


Figure 62. X-Component, E-Field Phase Contours  
Monopole at Patch Box Corner

MAGNITUDE (EZ PEAK) OF E-FIELD  
 MONOPOLE 6CM AT CORNER OF SPBOX  
 11X11 PATCHES ON TOP-FREQ=1GHZ

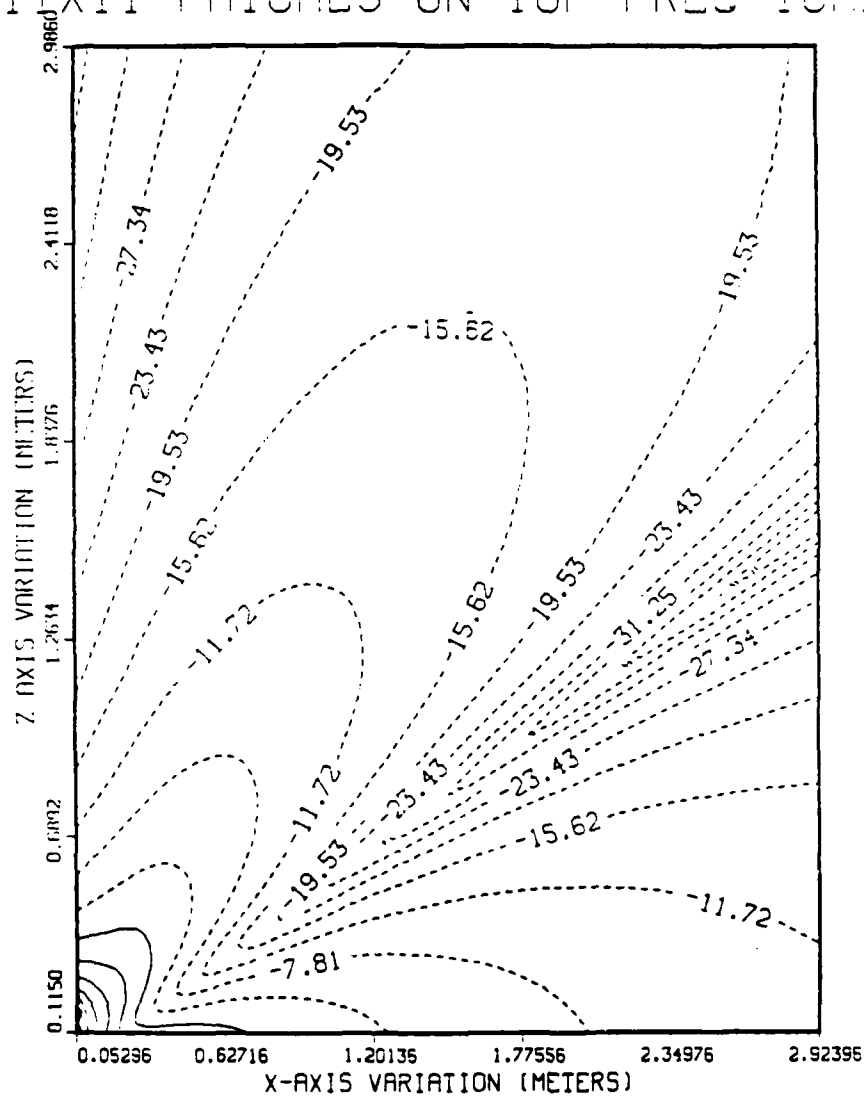


Figure 63. Z-Component, E-Field Contours  
 Monopole at Patch Box Corner

PHASE OF Z COMPONENT OF E-FIELD  
 MONOPOLE 6CM AT CORNER OF SPBOX  
 11X11 PATCHES ON TOP-FREQ=1GHZ

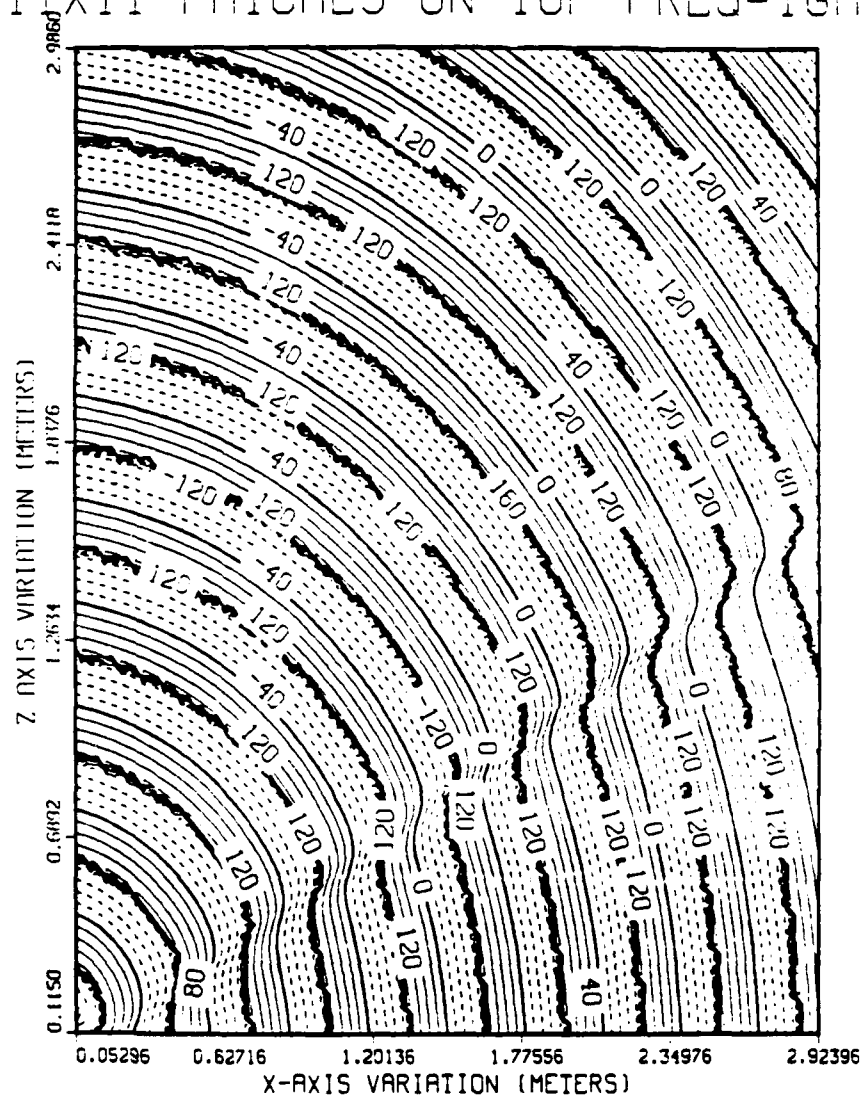


Figure 64. Z-Component, E-Field Phase Contours  
 Monopole at Patch Box Corner

3-D ELECTRIC FIELD (DB REF 10 1V/M)  
 MONOPOLE AT CORNER OF SP-BOX (11X11 PATCHES)  
 (5.14 CM ON THE DIAGONAL FROM CENTER)

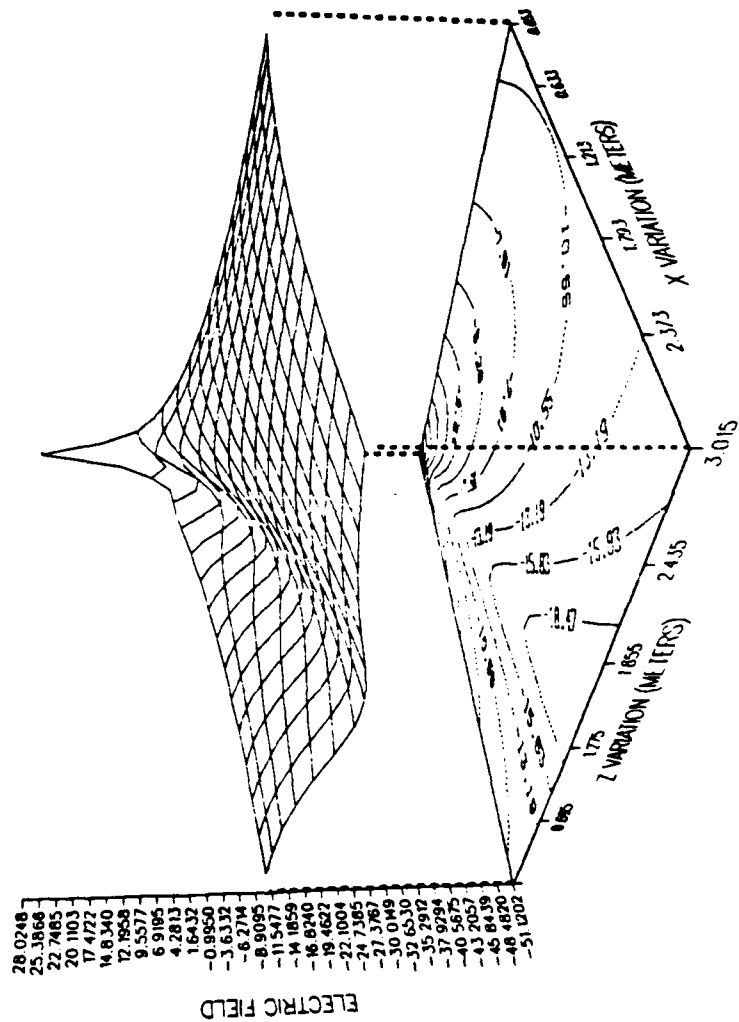


Figure 65. Total E-Field 3-D Plot, View Toward Monopole  
 (Monopole at Patch Box Corner)

# 3-D ELECTRIC FIELD (DB REL TO 1V/M) MONOPOLE AT CORNER OF SPBOX(1X11 PATCHES) (5.14 CM ON THE DIAGONAL FROM CENTER)

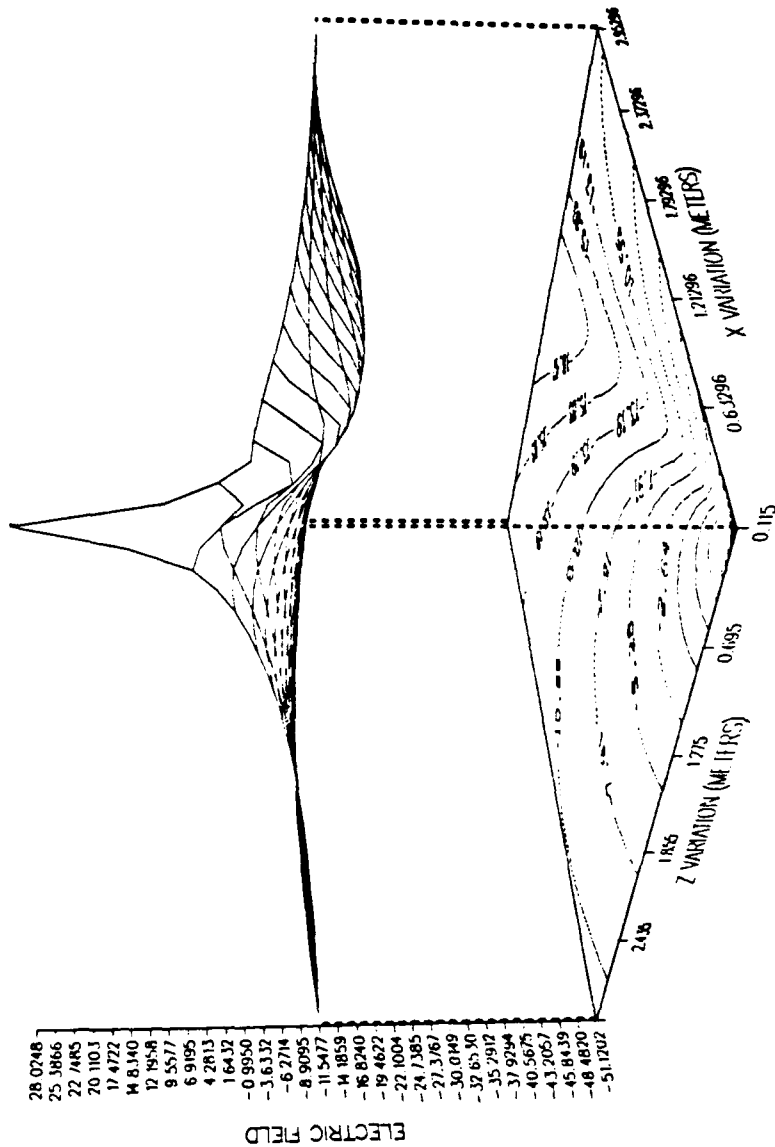


Figure 66. Total E-Field 3-D Plot, Viewed From Monopole  
 (Monopole at Patch Box Corner)



## G. RADIATION PATTERNS

Radiation patterns were calculated and are presented in Figures 67 and 68 (Monopole at center), 69 - 71, (Monopole at edge), and 72 - 74 (Monopole at corner).

### 1. Monopole at Center

In Figure 67, the vertical pattern shows that the maximum gain is very close to 5.15 dBi, the theoretical value for a monopole over an infinite perfectly conducting ground plane. The metallic surface of the box which re-radiates affects the pattern causing four lobes to appear instead of the usual two. In Figure 68, the horizontal pattern shows omnidirectional radiation from the box-monopole, which is fairly small electrically, and not expected to contribute much directionality in azimuth.

### 2. Monopole at Edge

The vertical pattern (x-axis cut) in Figure 69 shows an unsymmetrical pattern with the maximum lobe of 6.6 dBi skewed away from the monopole. The y-axis cut in Figure 70 shows an expected symmetric vertical plane pattern. The horizontal pattern of Figure 71 shows a skewed pattern, with the maximum field opposite to the monopole location.

### 3. Monopole at Corner

The results of vertical and horizontal patterns for a corner-mounted monopole (Figures 72 - 74) are similar to the ones for the edge-mounted case with unsymmetrical patterns occurring.

SPBOX 7X7 PATCHES ON THE TOP (MONOPOLE AT CENTER)  
VERTICAL PATTERN

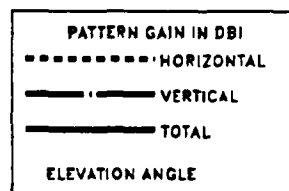
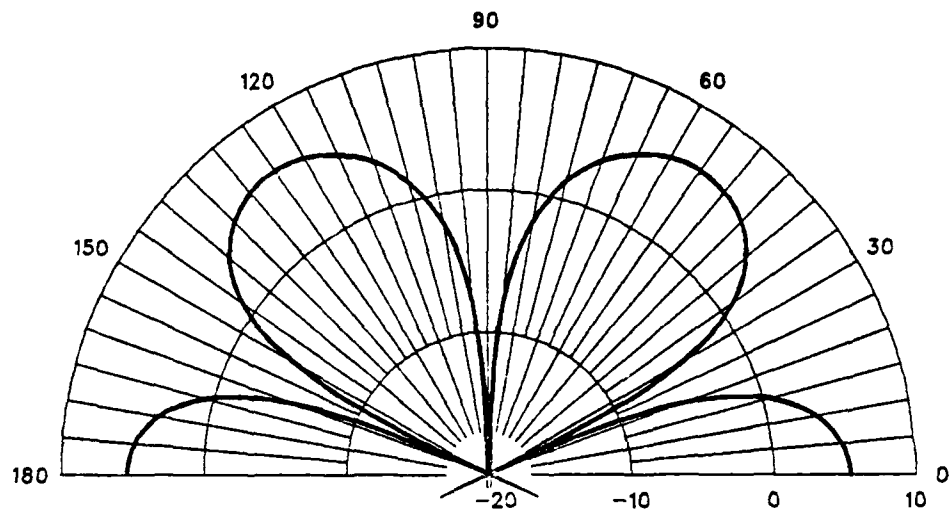


Figure 67. Vertical Pattern, Monopole at Patch Box Center

SPBOX 7X7 PATCHES ON THE TOP (MONOPOLE AT CENTER)  
HORIZONTAL PATTERN

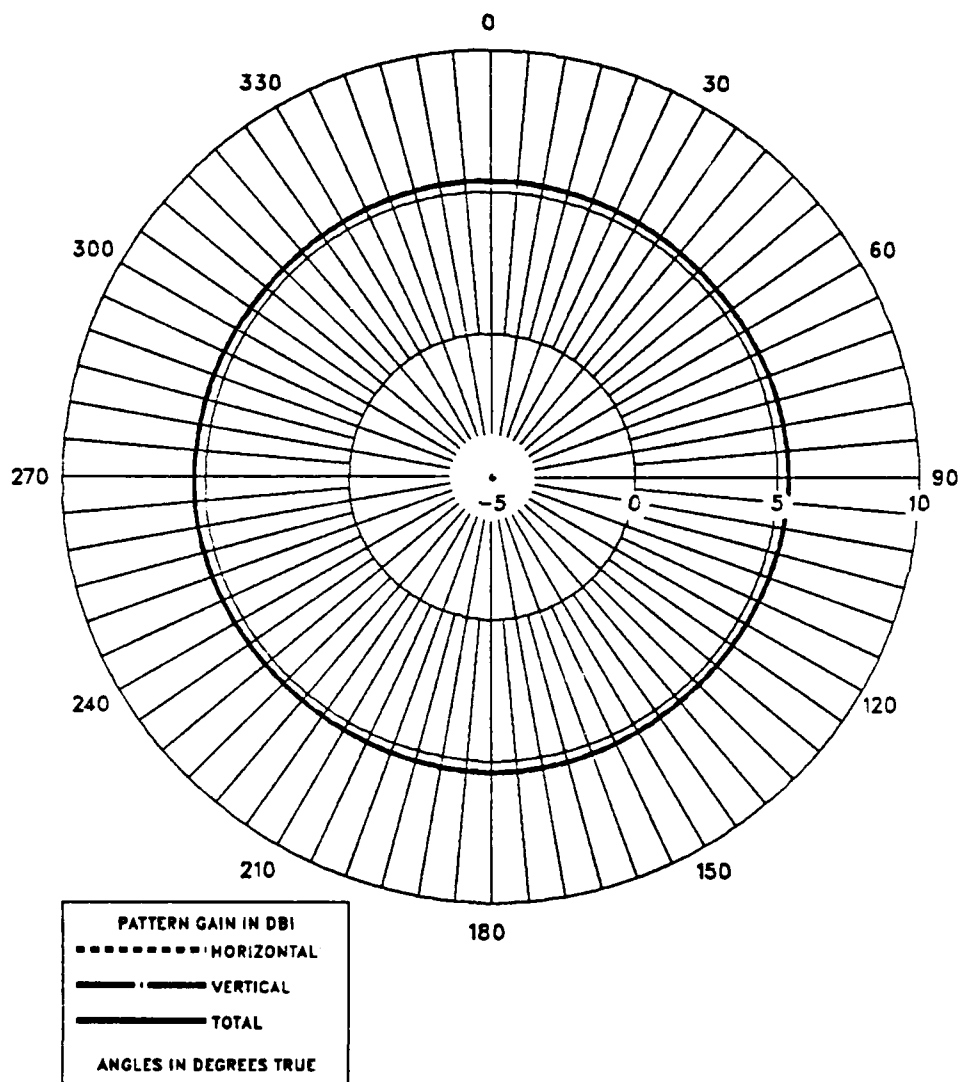


Figure 68. Horizontal Pattern, Monopole at Patch Box Center

SPBOX 11X11 PATCHES ON THE TOP (MONOPOLE AT EDGE 3.63 CM)  
VERTICAL PATTERN (X-AXIS CUT)

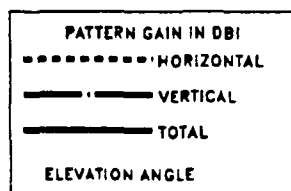
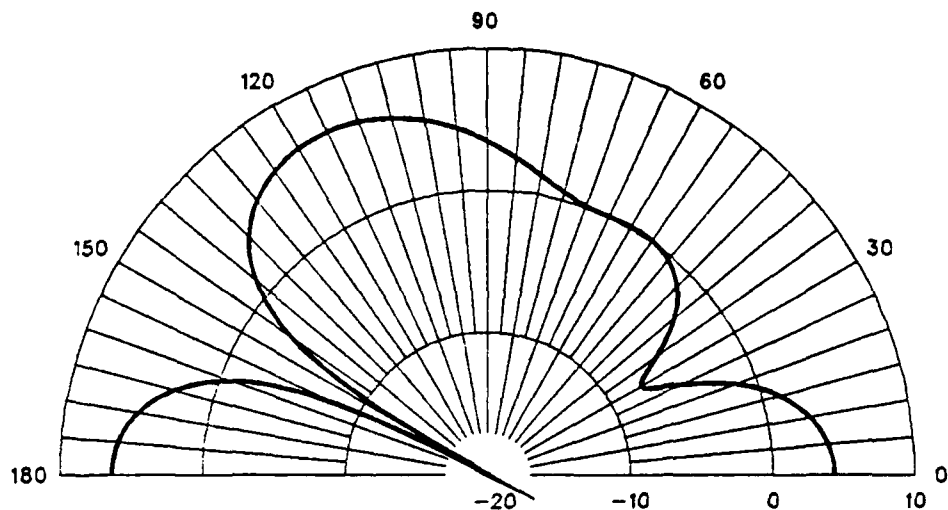


Figure 69. Vertical Pattern (X-Axis Cut)  
 Monopole at Patch Box Edge

SPBOX 11X11 PATCHES ON THE TOP (MONOPOLE AT EDGE 3.63 CM)  
VERTICAL PATTERN (Y-AXIS CUT)

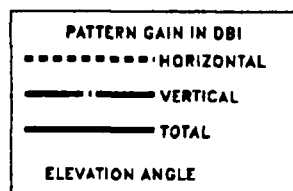
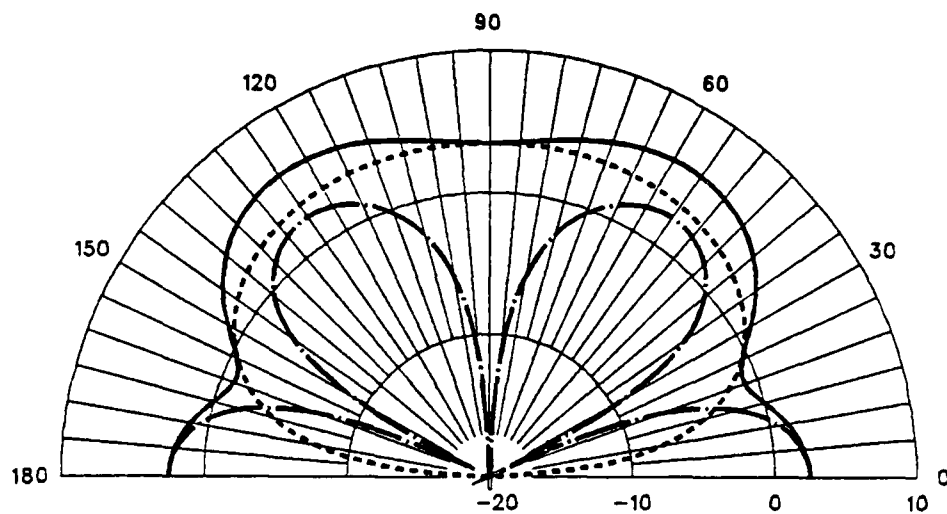


Figure 70. Vertical Pattern (Y-Axis Cut)  
 Monopole at Patch Box Edge

SPBOX 11X11 PATCHES ON THE TOP (MONOPOLE AT EDGE 3.63 CM)  
HORIZONTAL PATTERN

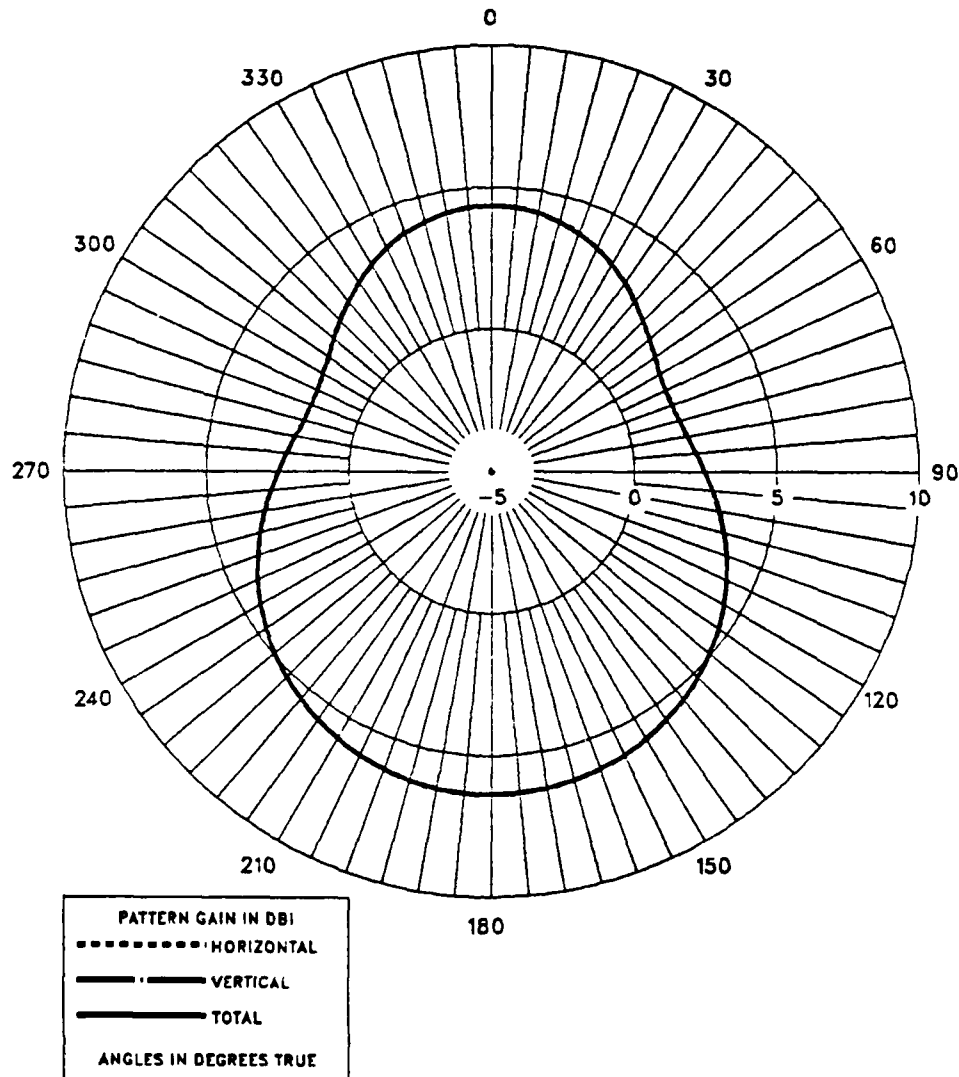


Figure 71. Horizontal Pattern  
Monopole at Patch Box Edge

SPBOX 11X11 PATCHES (MONOPOLE AT CORNER-5.14CM ON DIAGONAL)  
VERTICAL PATTERN (X-AXIS CUT)

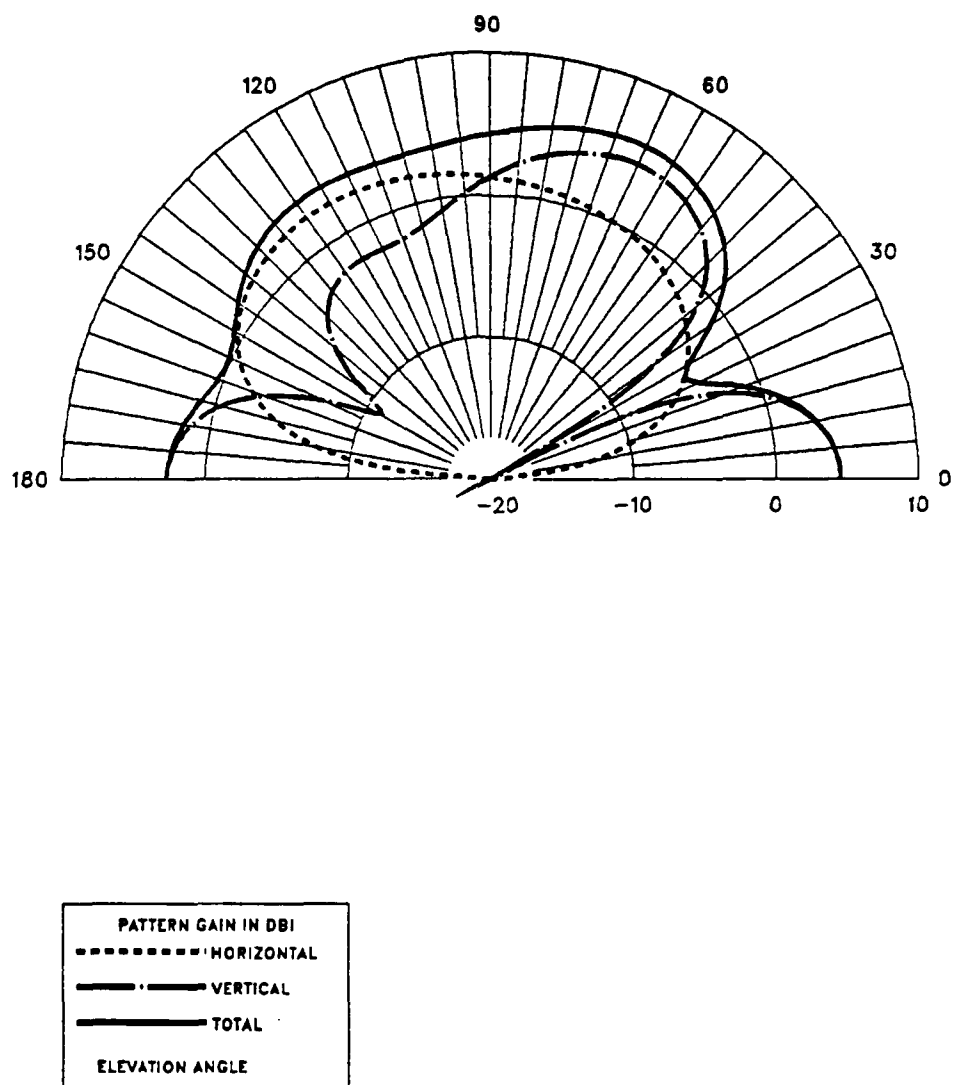


Figure 72. Vertical Pattern (X-Axis Cut)  
 Monopole at Patch Box Corner

SPBOX 11X11 PATCHES (MONOPOLE AT CORNER—5.14CM ON DIAGONAL)  
VERTICAL PATTERN (45 DEGREES CUT)

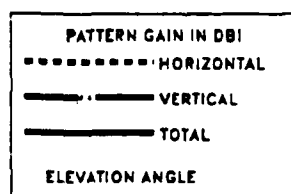
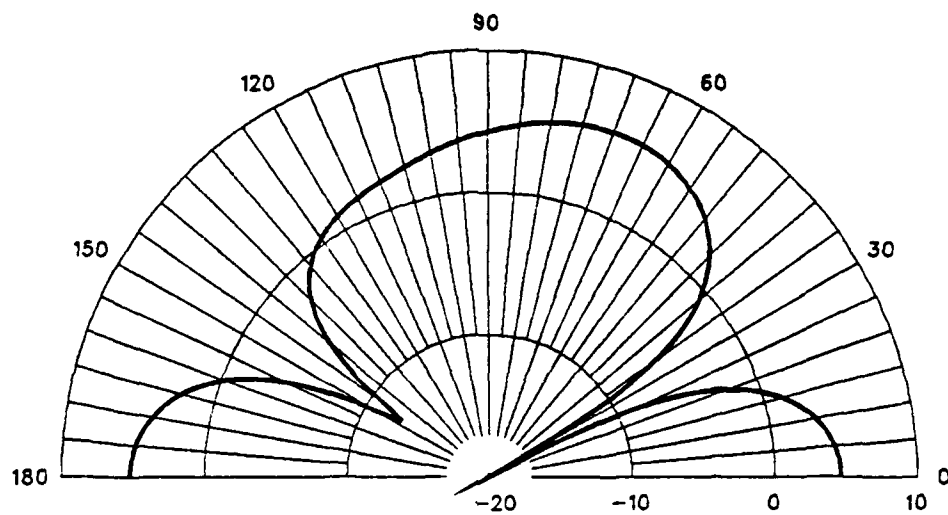


Figure 73. Vertical Pattern (45° Cut)  
 Monopole at Patch Box Corner



SPBOX 11X11 PATCHES (MONOPOLE AT CORNER-5.14CM ON DIAGONAL)  
HORIZONTAL PATTERN

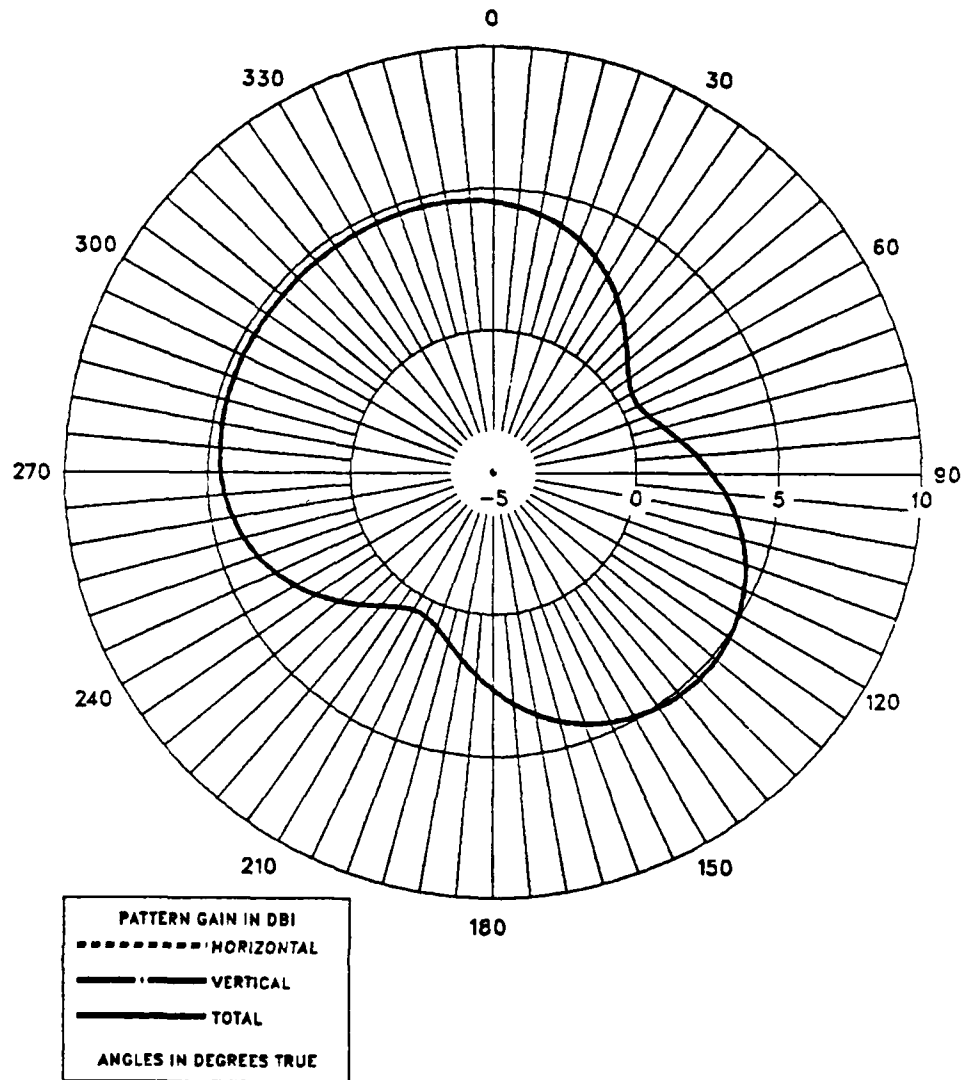


Figure 74. Horizontal Pattern  
Monopole at Patch Box Corner

### III. WIRE GRID MODELING FOR NEAR ELECTRIC FIELD PREDICTIONS

#### A. GUIDELINES FOR WIRE GRID MODELING USING NEC

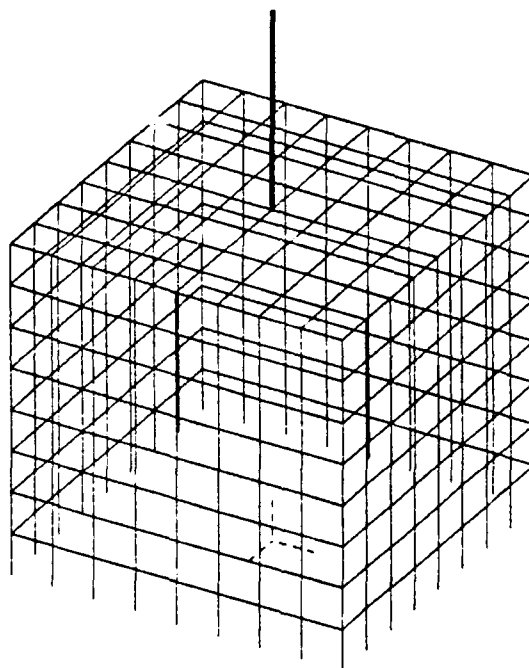
Solid surfaces can be modeled in NEC with a grid of wires, with the restriction that the grid cells are to be small in terms of a wavelength. Wire grid modeling guidelines are given in Reference 1.

#### B. WIRE-GRID BOX MODEL FOR NEAR ELECTRIC FIELD INVESTIGATION

For the wire grid modeling technique, the NPG1000 version of NEC allows up to 1000 wire segments. Typical run-times for wire grid models of the box-monopole are six times those of the surface patch models. The box of Figure 3 is modeled as a five-sided wire-grid box of 0.1 m ( $\lambda/3$  at 1 GHz) per side and cells of 0.0125 by 0.0125 meters. The 0.06 m monopole antenna was divided into 5 segments and placed on top of the wire grid box at the center, edge (3.75 cm from center), and corner (5.3 cm on the diagonal). The geometry of the wire grid box is shown in Figures 75 - 77. Appendix C contains NEC input data files for these geometries. The antenna was fed at the base segment for all cases. The wire grid geometry of Reference 8, was used for calculations of near electric field in the present study. This geometry produced good results for admittance and average gain compared with experimental data of Reference 5. The Fortran programs of Chapter II are also used for magnitude and phase

contour plots, and 3-D plots of near electric field for the wire grid box case with the same field point locations used in the surface patch model.

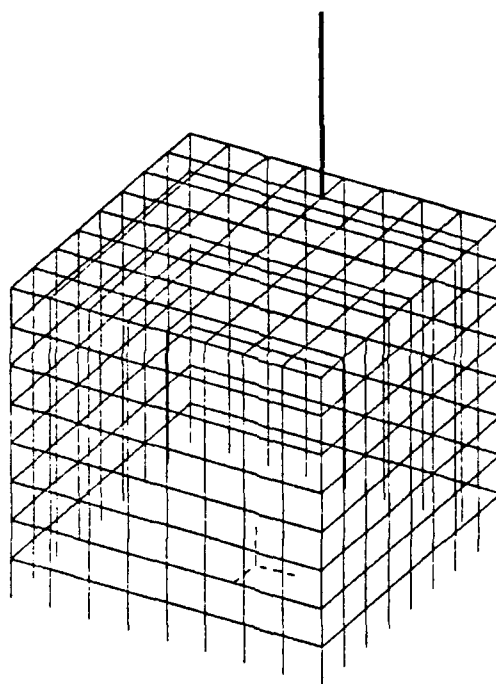
MONOPOLE 6 CM AT CENTER OF WIRE GRID BOX



THETA = 60.00 PHI = 30.00 ETA = 90.00

Figure 75. Monopole at Center of Wire Grid Box

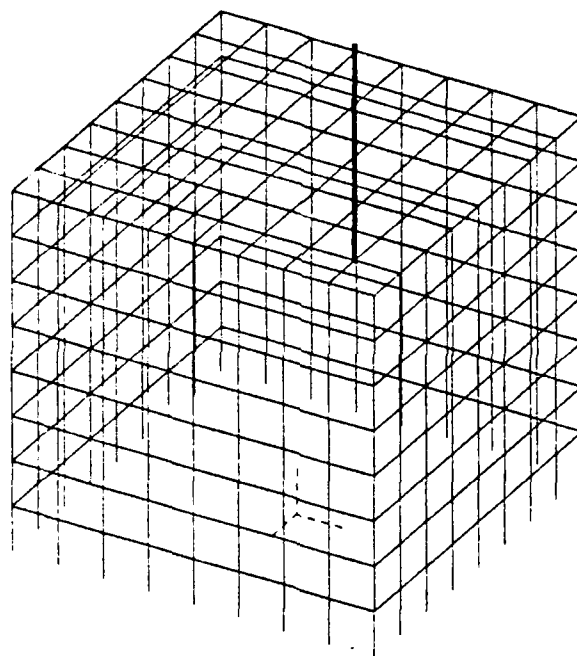
MONOPOLE AT EDGE (3.75 CM) OF WIRE GRID BOX



THETA = 60.00 PHI = 30.00 ETA = 90.00

Figure 76. Monopole at Edge of Wire Grid Box

MONOPOLE 6 CM AT CORNER (5.3 CM) OF WIRE GRID BOX



THETA = 60.00 PHI = 30.00 ETA = 90.00

Figure 77. Monopole at Corner of Wire Grid Box

1. Monopole at Center of Wire Grid Box vs. Monopole at Center of Surface Patch Box

The excellent agreement of near fields (Figures 78 to 84) for the wire grid box with center-mounted monopole to those of the surface patch/center monopole model (Figures 46 to 52) attests to the equivalence of the two numerical models. Differences are less than 1 dB, a value which is difficult to measure.

CONTOUR E-FIELD (DB REF TO 1V/M)  
 MONOPOLE 6CM AT CENTER OF WIRE GRID BOX  
 FREQ-1GHZ

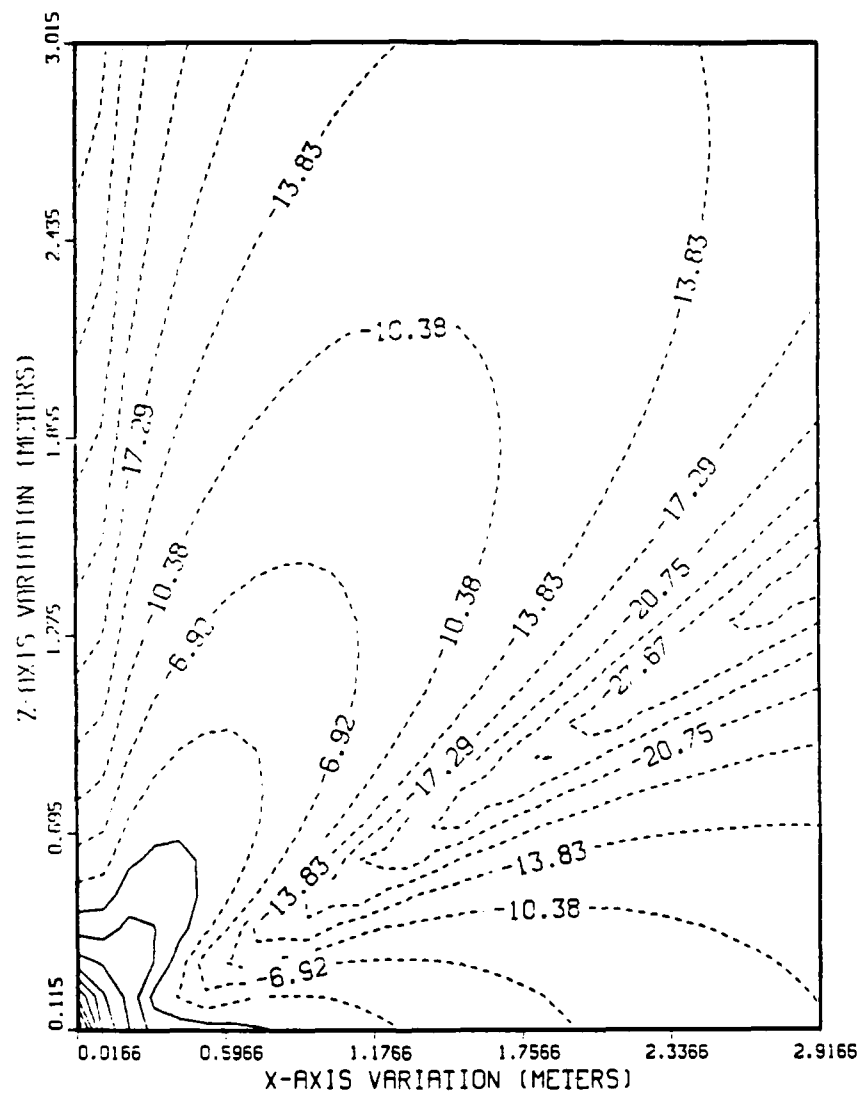


Figure 78. Total E-Field Contours  
 Monopole at Wire Grid Box Center



# MAGNITUDE (EX PEAK) OF E-FIELD MONOPOLE 6CM AT CENTER OF WIRE GRID BOX FREQ-1GHZ

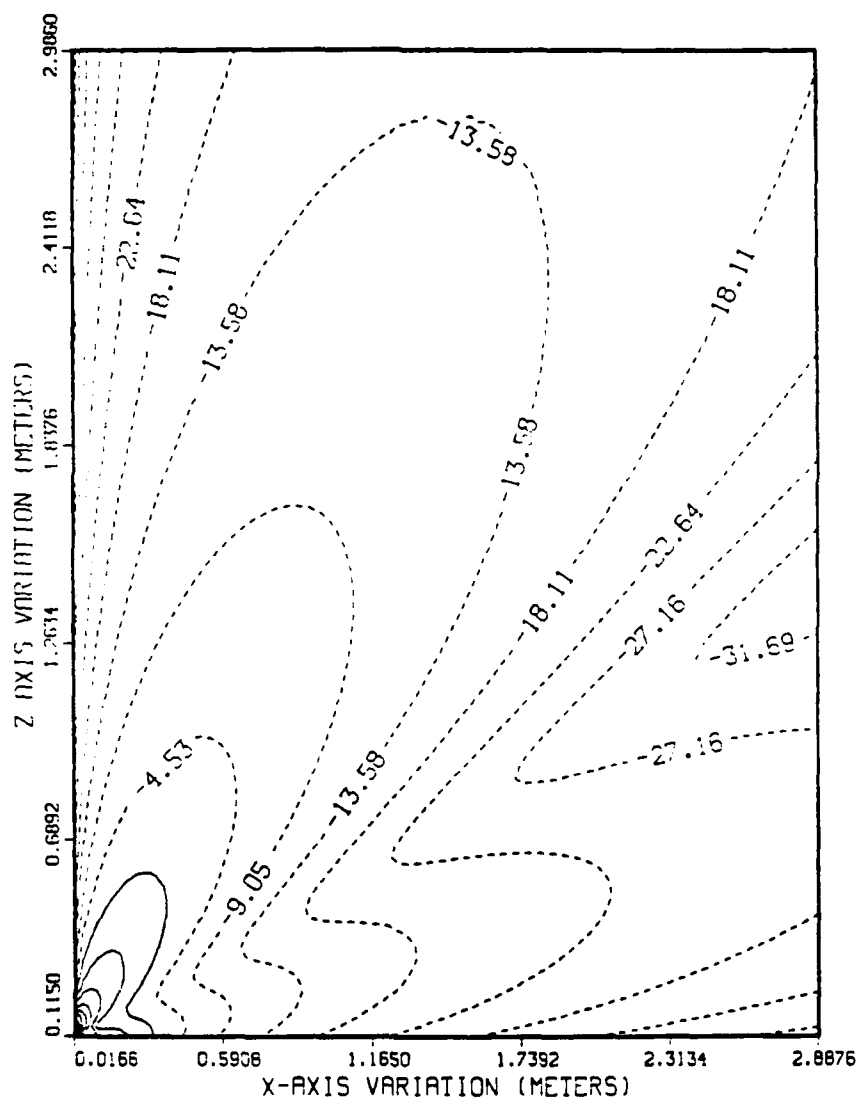


Figure 79. X-Component, E-Field Contours  
 Monopole at Wire Grid Box Center

# PHASE OF X COMPONENT OF E-FIELD MONOPOLE 6CM AT CENTER OF WIRE GRID BOX FREQ-1GHZ

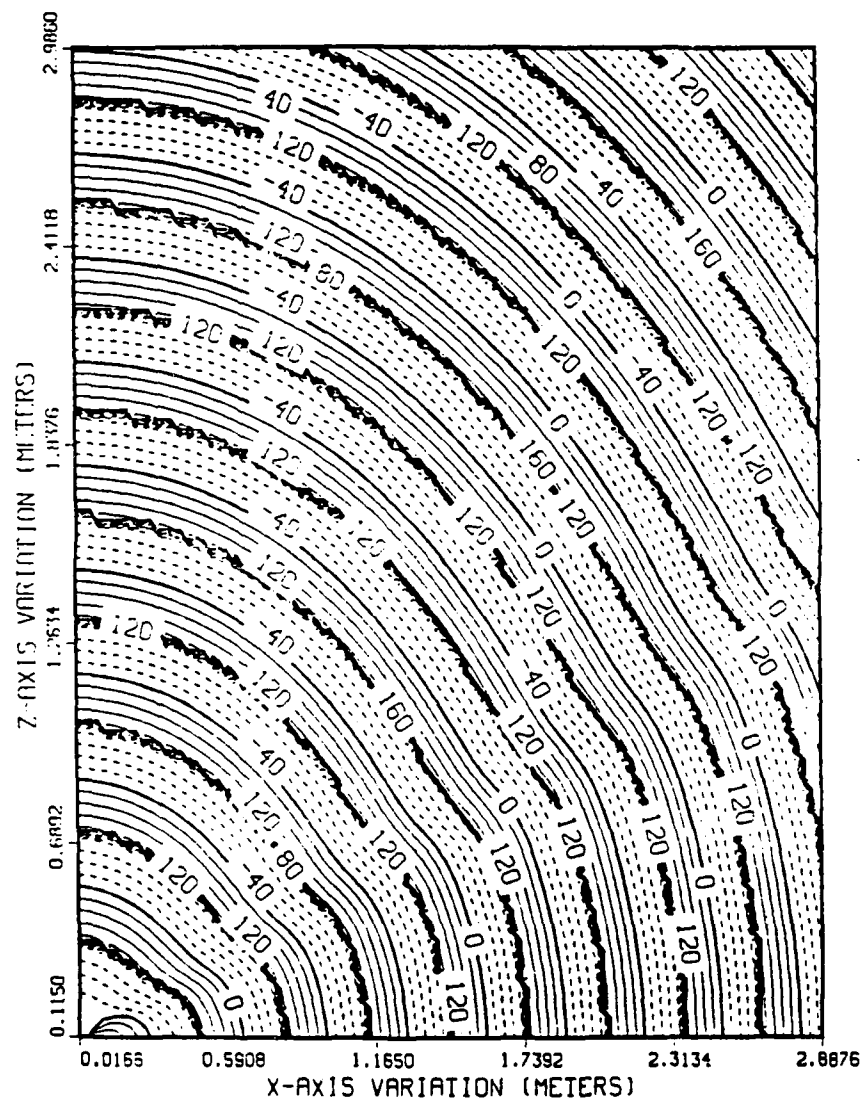


Figure 80. X-Component, E-Field Phase Contours  
 Monopole at Wire Grid Box Center

MAGNITUDE (EZ PEAK) OF E-FIELD  
 MONOPOLE 60CM AT CENTER OF WIRE GRID BOX  
 FREQ=1GHZ

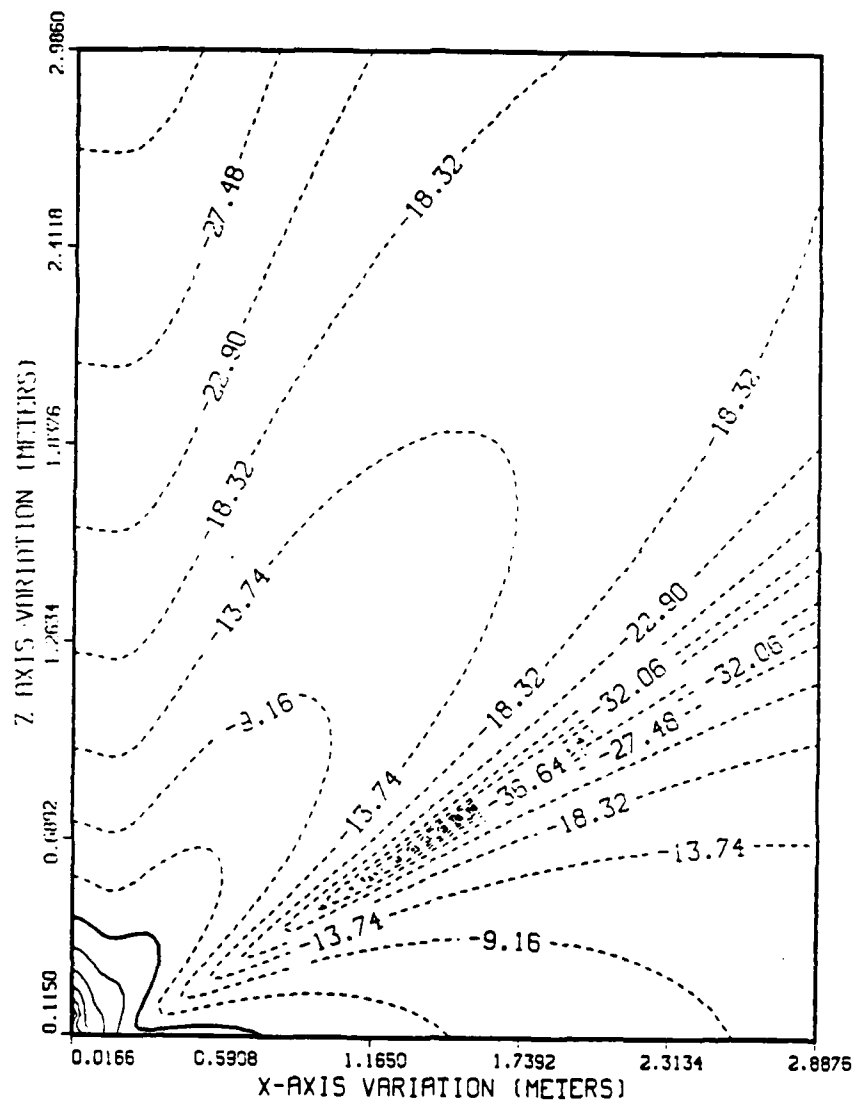


Figure 81. Z-Component, E-Field Contours  
 Monopole at Wire Grid Box Center

PHASE OF Z COMPONENT OF E-FIELD  
MONOPOLE 6CM AT CENTER OF WIRE GRID BOX  
FREQ-1GHZ

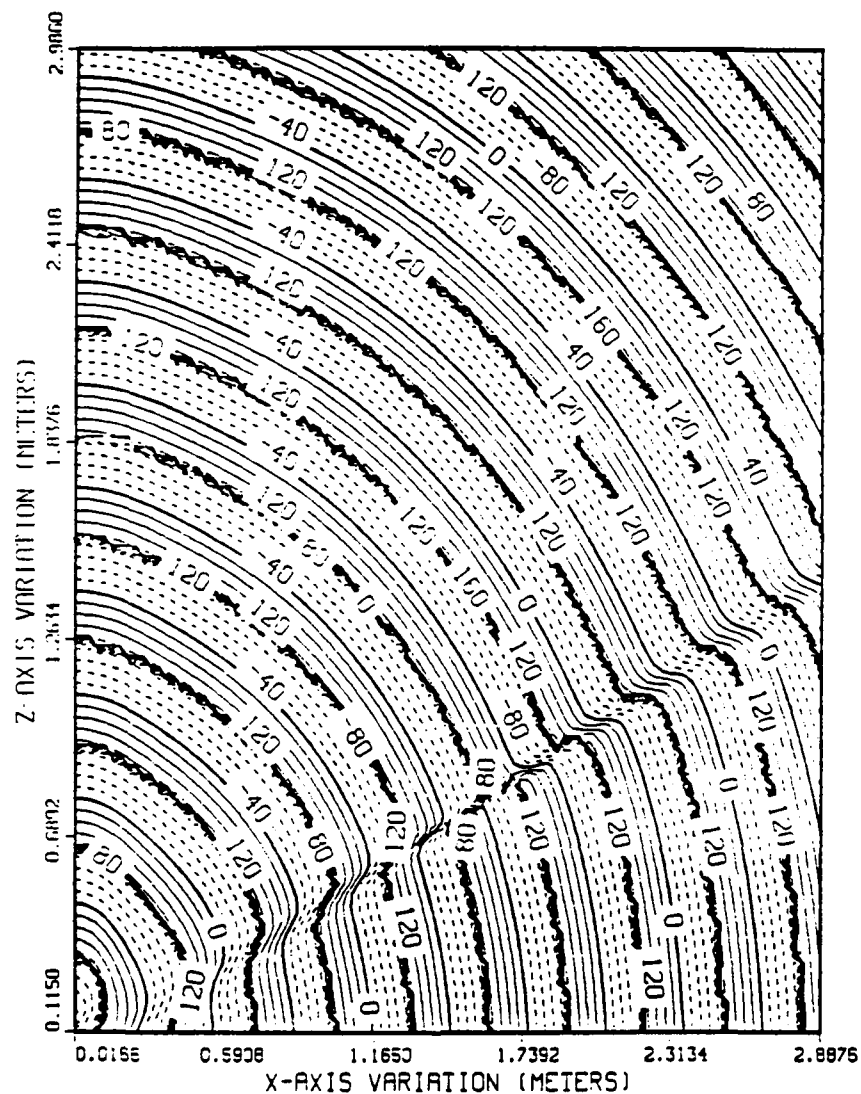


Figure 82. Z-Component, E-Field Phase Contours  
Monopole at Wire Grid Box Center

# 3-D ELECTRIC FIELD (DB REF TO 1V/M) MONOPOLE 6CM AT CENTER OF WIRE GRID BOX

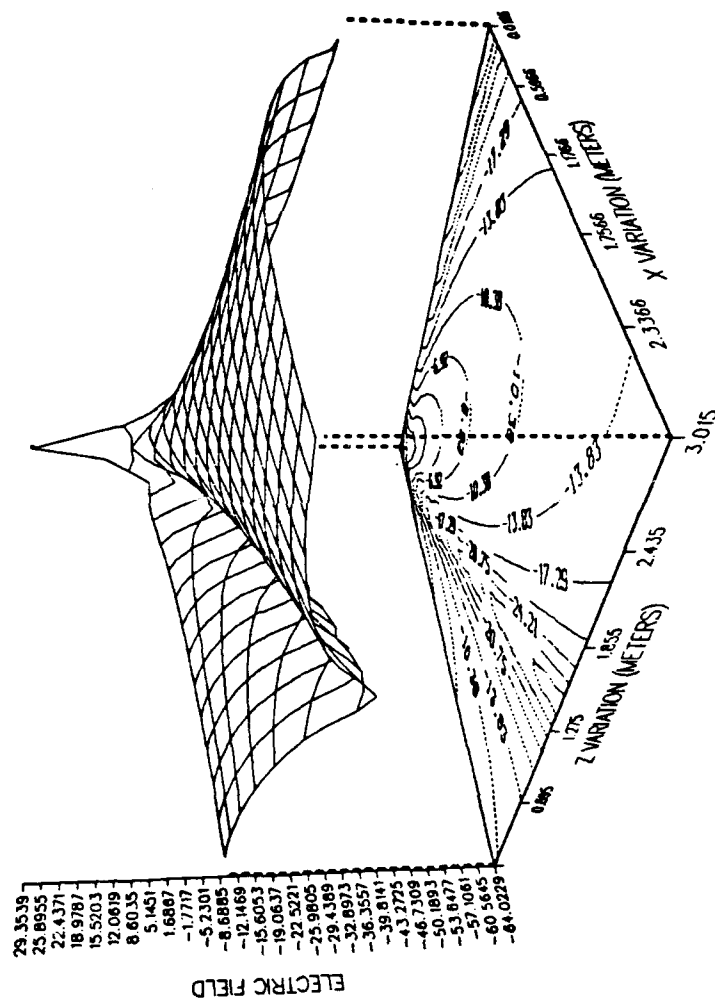


Figure 83. Total E-Field 3-D Plot, View Toward Monopole  
 (Monopole at Wire Grid Box Center)

# 3-D ELECTRIC FIELD (DB REF TO 1V/M) MONOPOLE 6CM AT CENTER OF WIRE GRID BOX

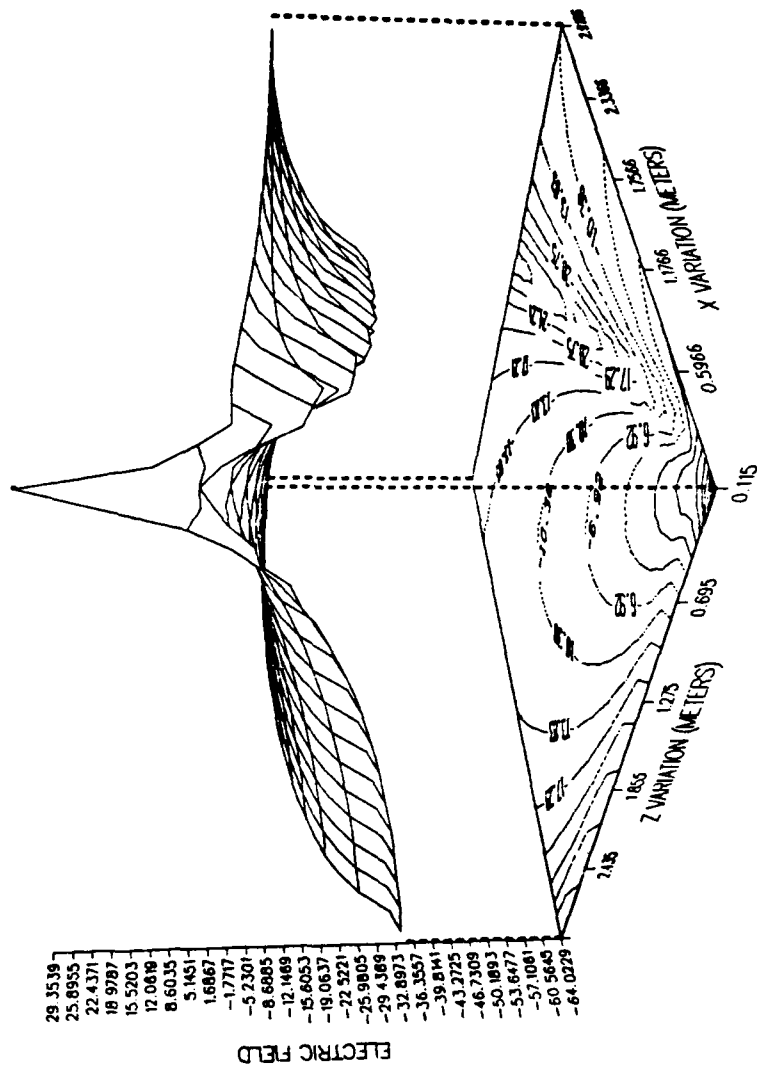


Figure 84. Total E-Field 3-D Plot, Viewed From Monopole  
 (Monopole at Wire Grid Box Center)

2. Monopole at Edge of Wire Grid Box vs. Monopole at Edge of Surface Patch Box

The edge-mounted monopole for the wire grid model compares well to the surface patch version. The differences are expected to be attributed to a more accurate rendition of edge effects for the grid model versus the patch model. Observable differences between Figures 85 to 91 and 53 to 59 relate to deeper nulls for the wire grid model.

CONTOUR E-FIELD (DB REF TO 1V/M)  
 MONOPOLE 6CM AT EDGE OF WIRE GRID BOX  
 FREQ-1GHZ-(3.75 CM FROM CENTER)

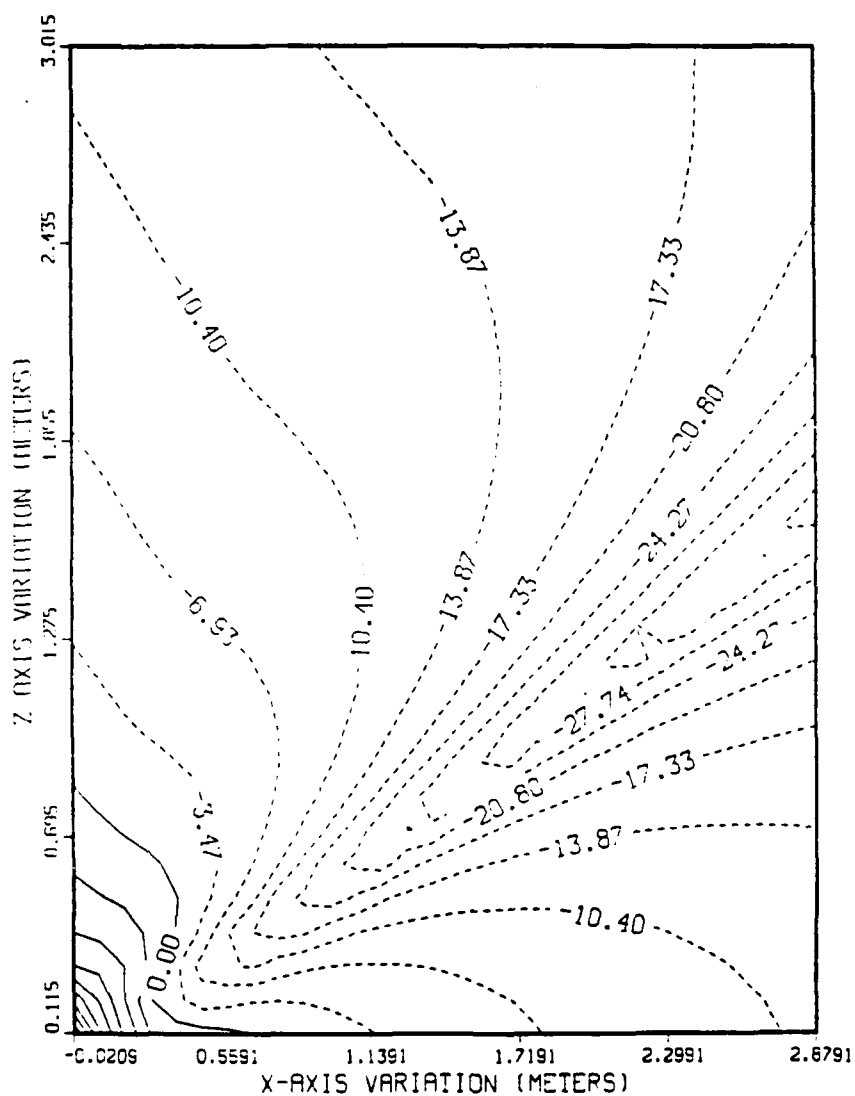


Figure 85. Total E-Field Contours  
 Monopole at Wire Grid Box Edge



# MAGNITUDE (EX PEAK) OF E-FIELD MONOPOLE 6CM AT EDGE OF WIRE GRID BOX FREQ-1GHZ-(3.75 CM FROM CENTER)

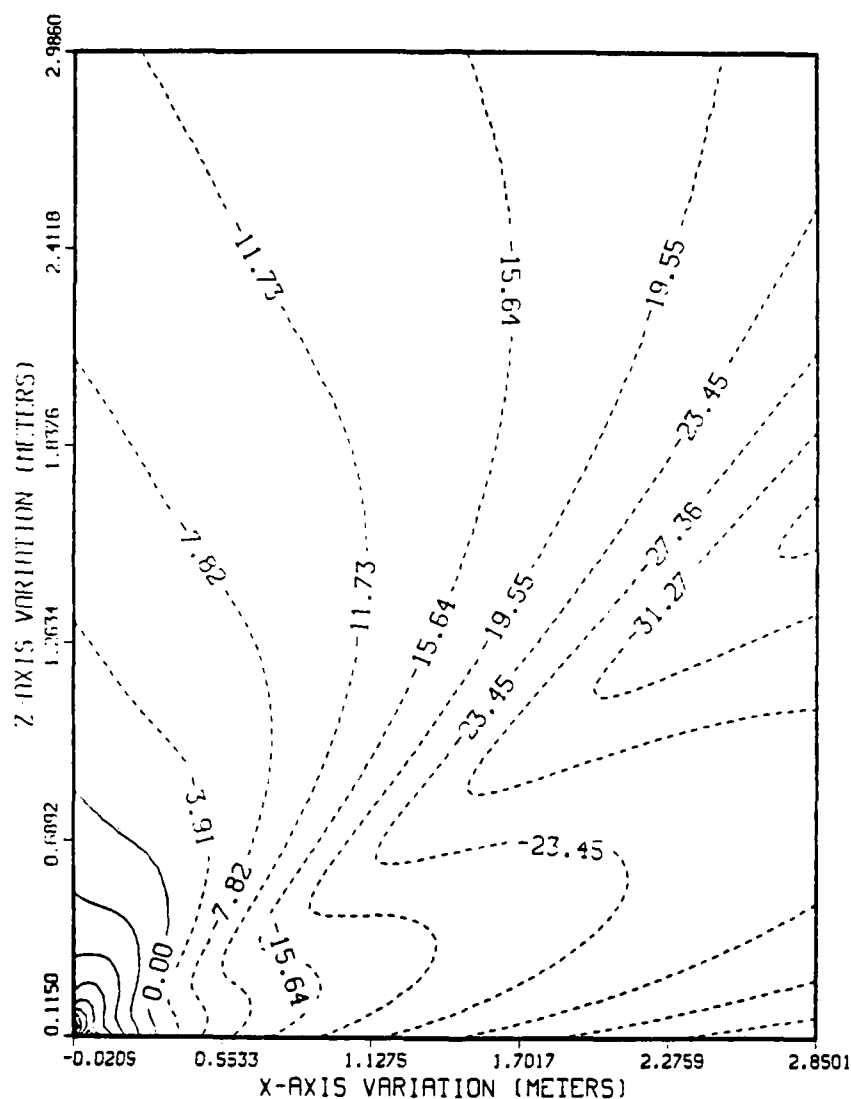


Figure 86. X-Component, E-Field Contours  
 Monopole at Wire Grid Box Edge

# PHASE OF X COMPONENT OF E-FIELD MONOPOLE 6CM AT EDGE OF WIRE GRID BOX FREQ-1GHZ-(3.75 CM FROM CENTER)

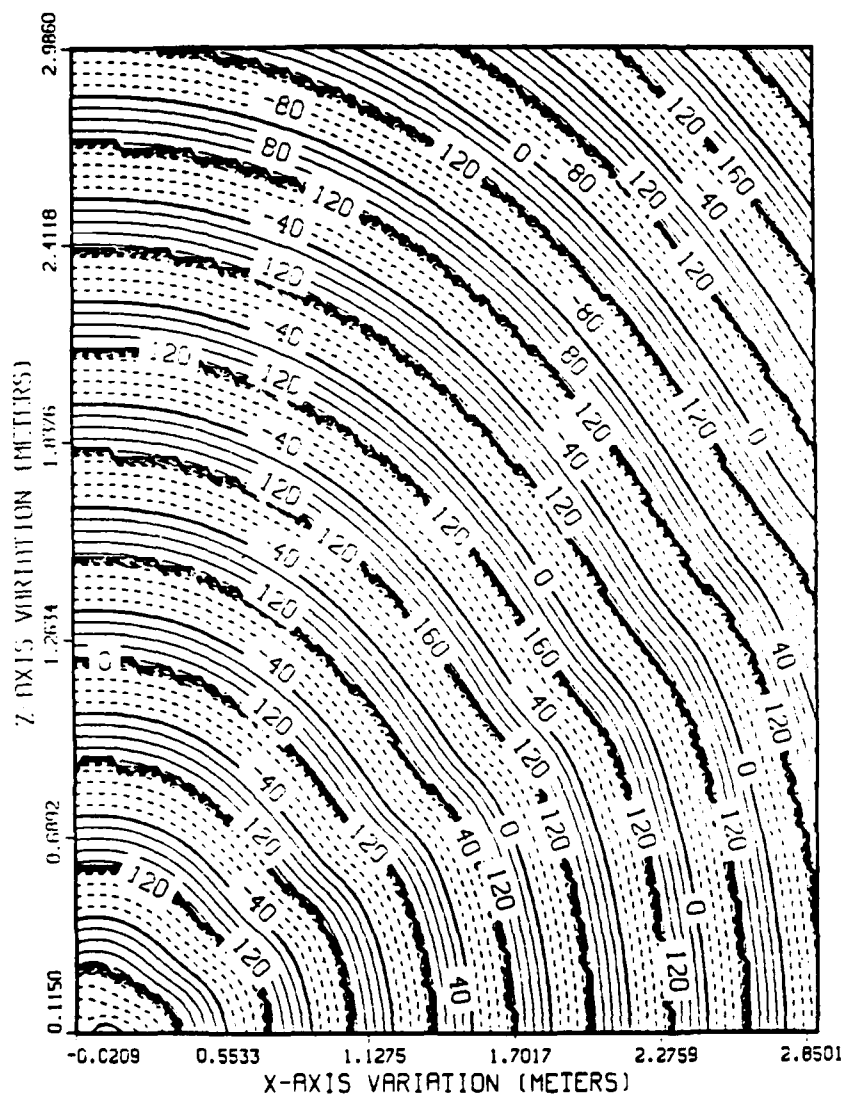


Figure 87. X-Component, E-Field Phase Contours  
 Monopole at Wire Grid Box Edge

# MAGNITUDE (EZ PEAK) OF E-FIELD MONOPOLE 6CM AT EDGE OF WIRE GRID BOX FREQ=13HZ-(3.75 CM FROM CENTER)

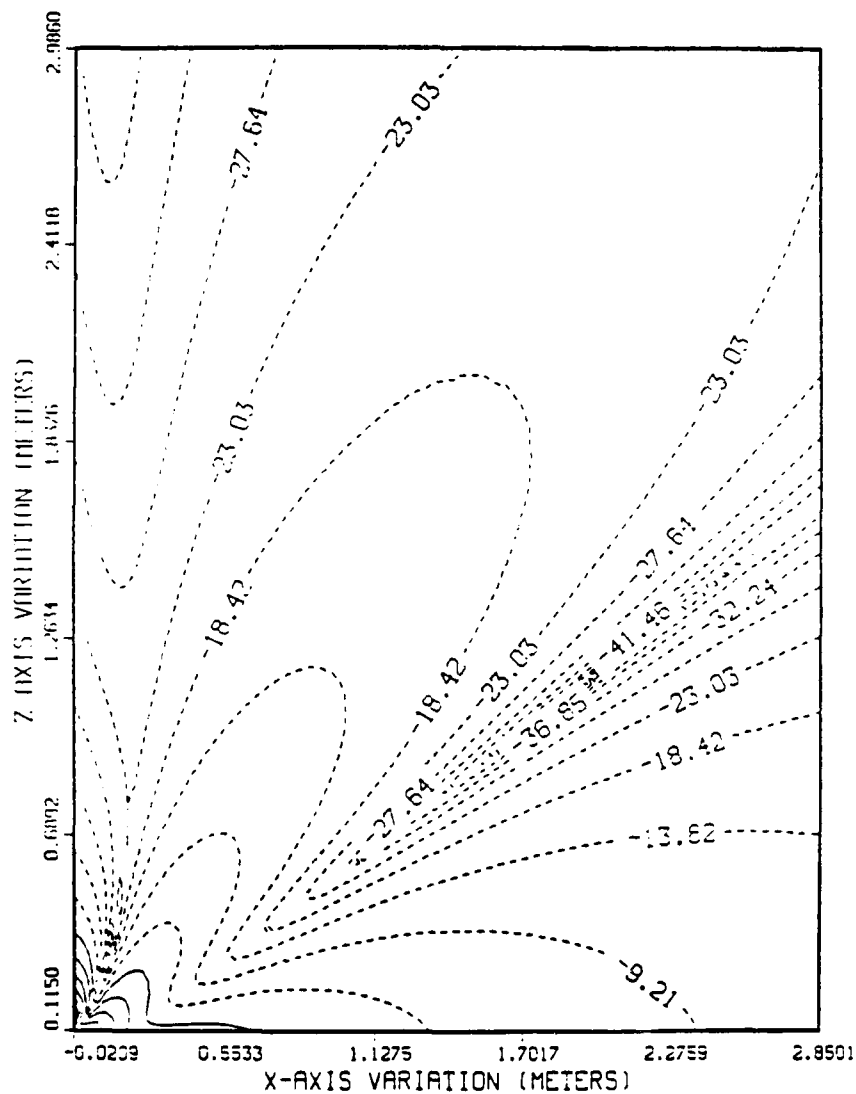


Figure 88. Z-Component, E-Field Contours  
 Monopole at Wire Grid Box Edge

# PHASE OF Z COMPONENT OF E-FIELD MONOPOLE 6CM AT EDGE OF WIRE GRID BOX FREQ-16HZ-(13.75 CM FROM CENTER)

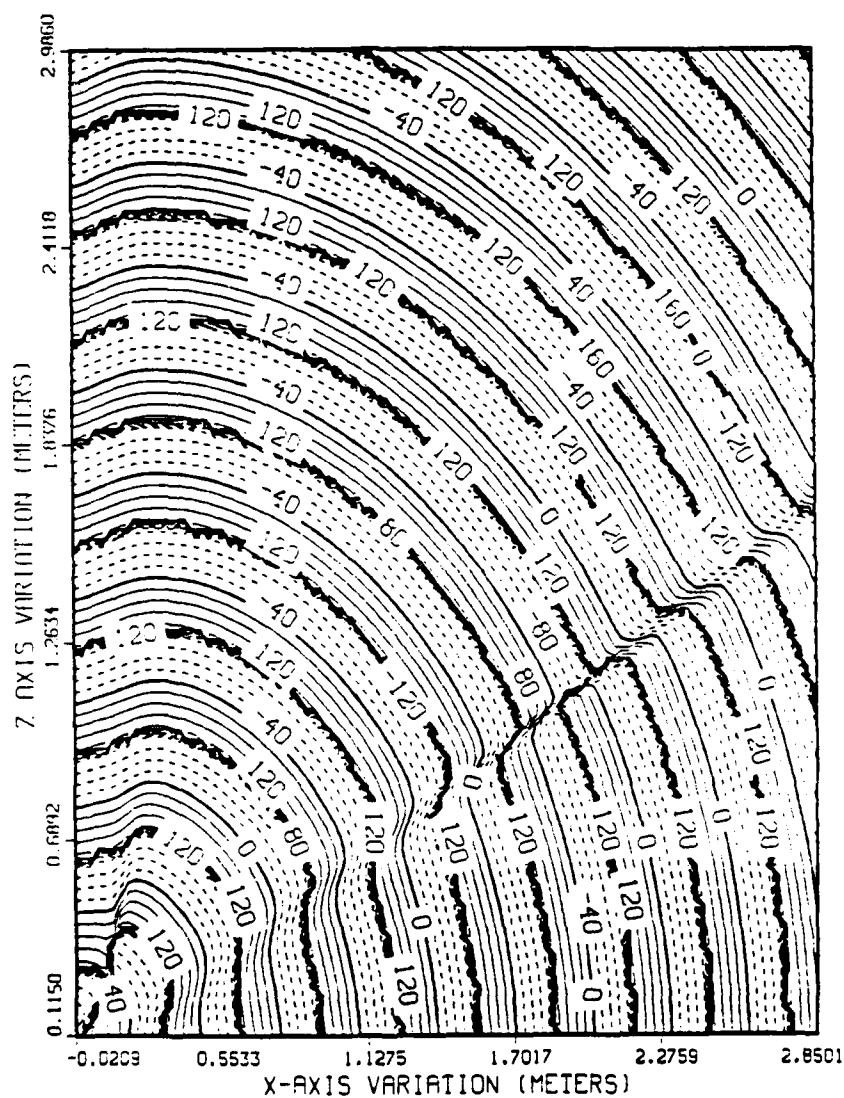
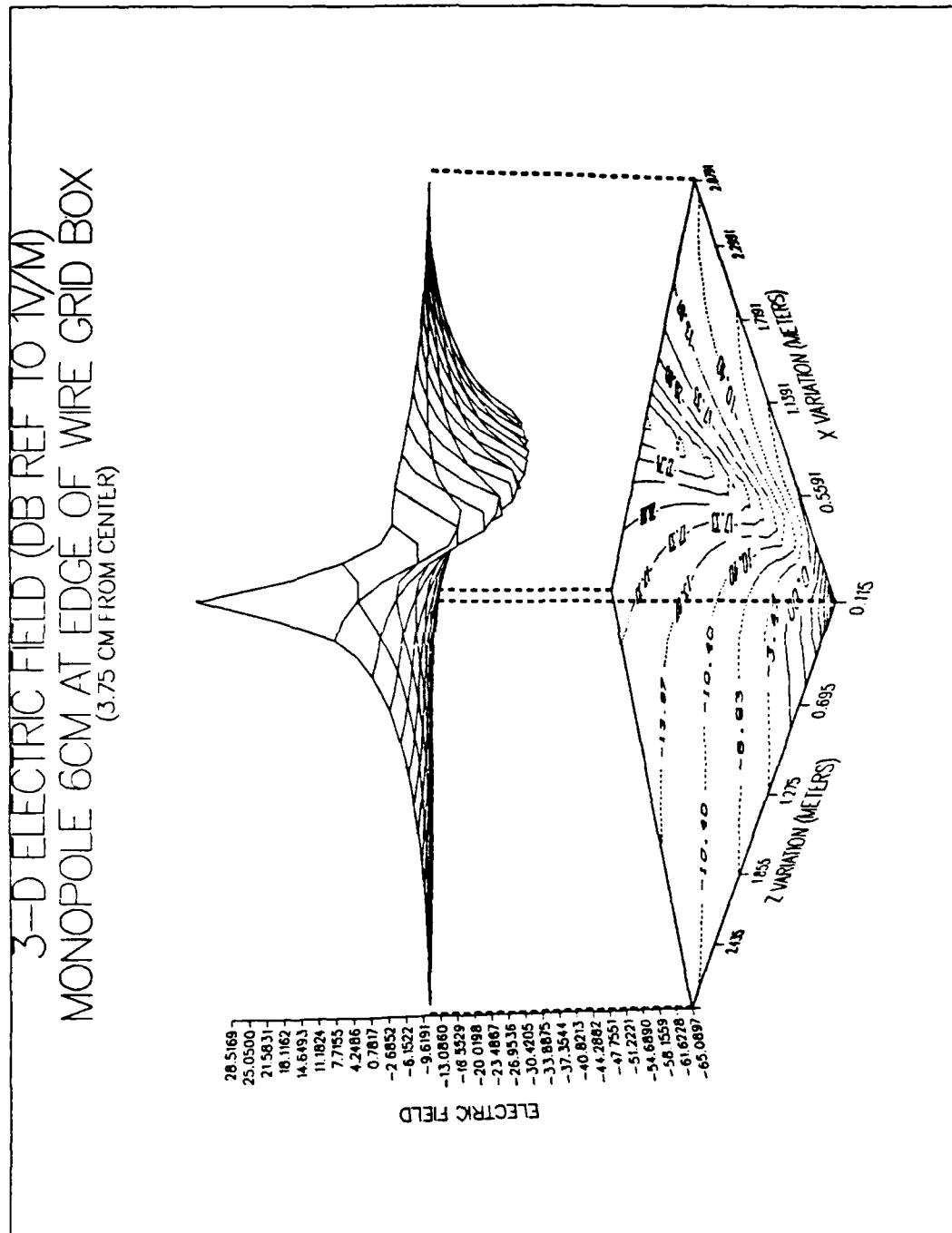


Figure 89. Z-Component, E-Field Phase Contours  
 Monopole at Wire Grid Box Edge

148



3. Monopole at Corner of Wire Grid Box vs. Monopole at Corner of Surface Patch Box

The previous two correlations between surface patch box and wire grid models continue for the corner-located monopole. Values of 1 to 1.5 dB in field strength differences, with deeper nulls, summarize the results of comparing Figures 92 to 98 with Figures 60 to 66.

CONTOUR E-FIELD (DB REF TO 1V/M)  
 MONOPOLE 6CM AT CORNER OF WIRE GRID BOX  
 FREQ-1GHZ-(5.3 CM ON DIAGONAL)

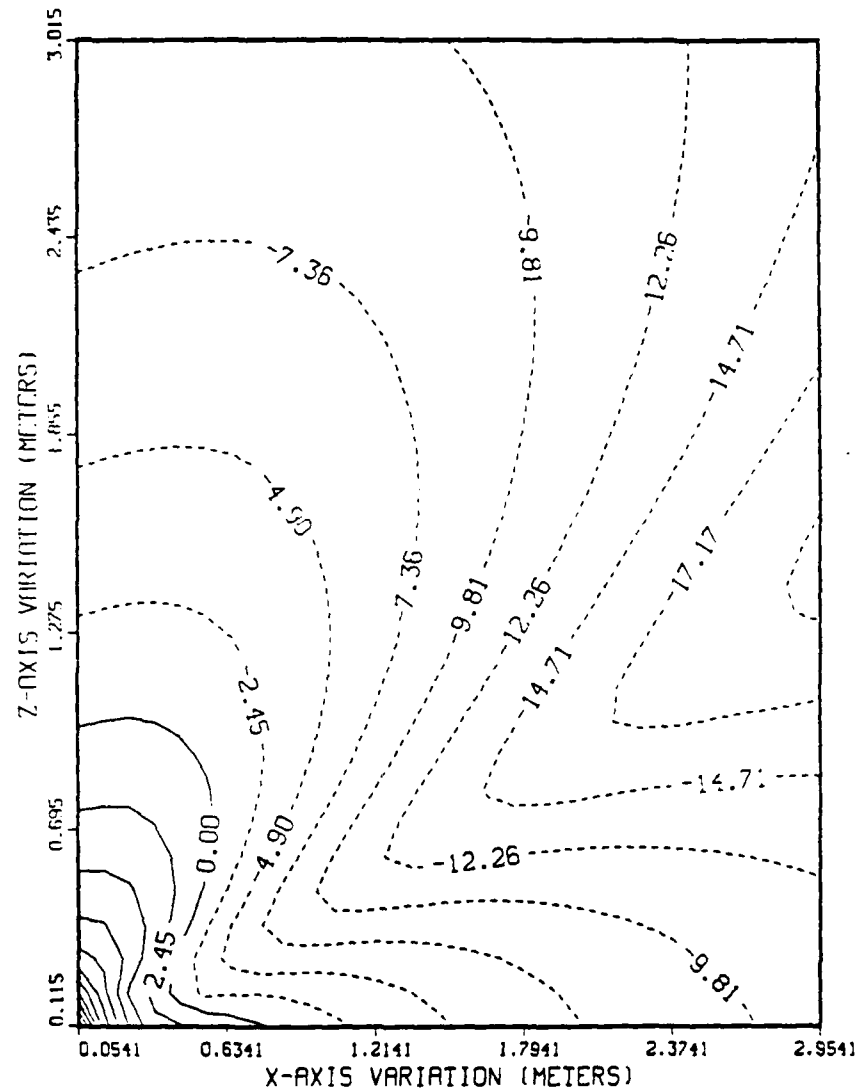


Figure 92. Total E-Field Contours  
 Monopole at Wire Grid Box Corner



# MAGNITUDE (EX PEAK) OF E-FIELD

MONOPOLE 6CM AT CORNER OF WIRE GRID BOX  
FREQ=1GHZ-(5.3CM ON DIAGONAL FROM CENTER)

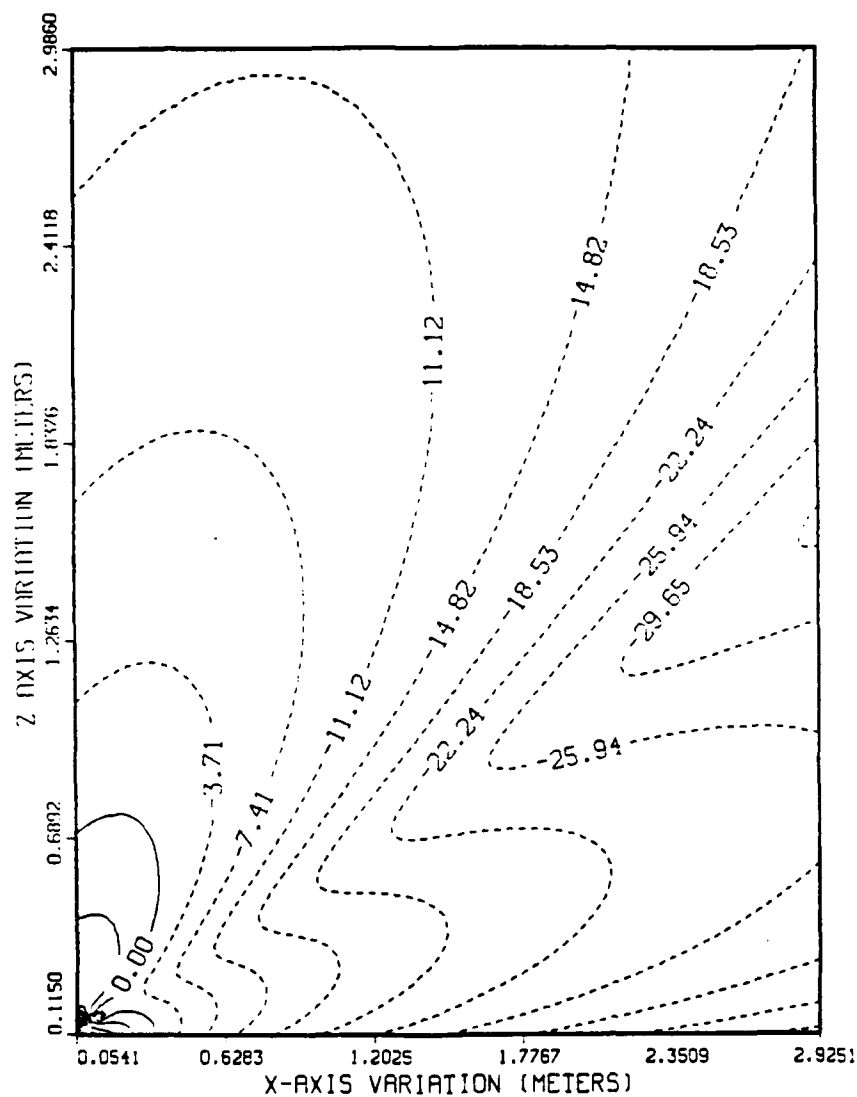


Figure 93. X-Component, E-Field Contours  
Monopole at Wire Grid Box Corner

# PHASE OF X COMPONENT OF E-FIELD

MONOPOLE 6CM AT CORNER OF WIRE GRID BOX  
FREQ-1GHZ-(5.3CM ON DIAGONAL FROM CENTER)

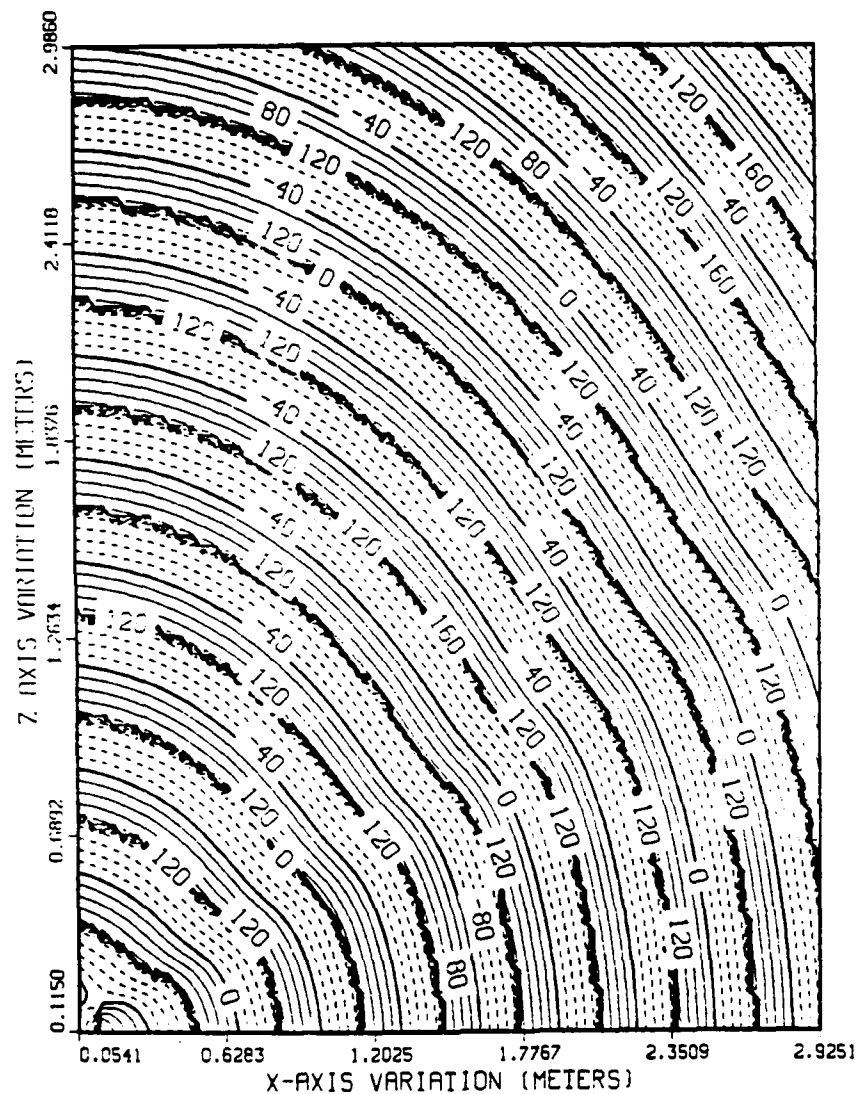


Figure 94. X-Component, E-Field Phase Contours  
Monopole at Wire Grid Box Corner

# MAGNITUDE (EZ PEAK) OF E-FIELD

MONOPOLE 6CM AT CORNER OF WIRE GRID BOX  
FREQ-1GHZ-(5.3CM ON DIAGONAL FROM CENTER)

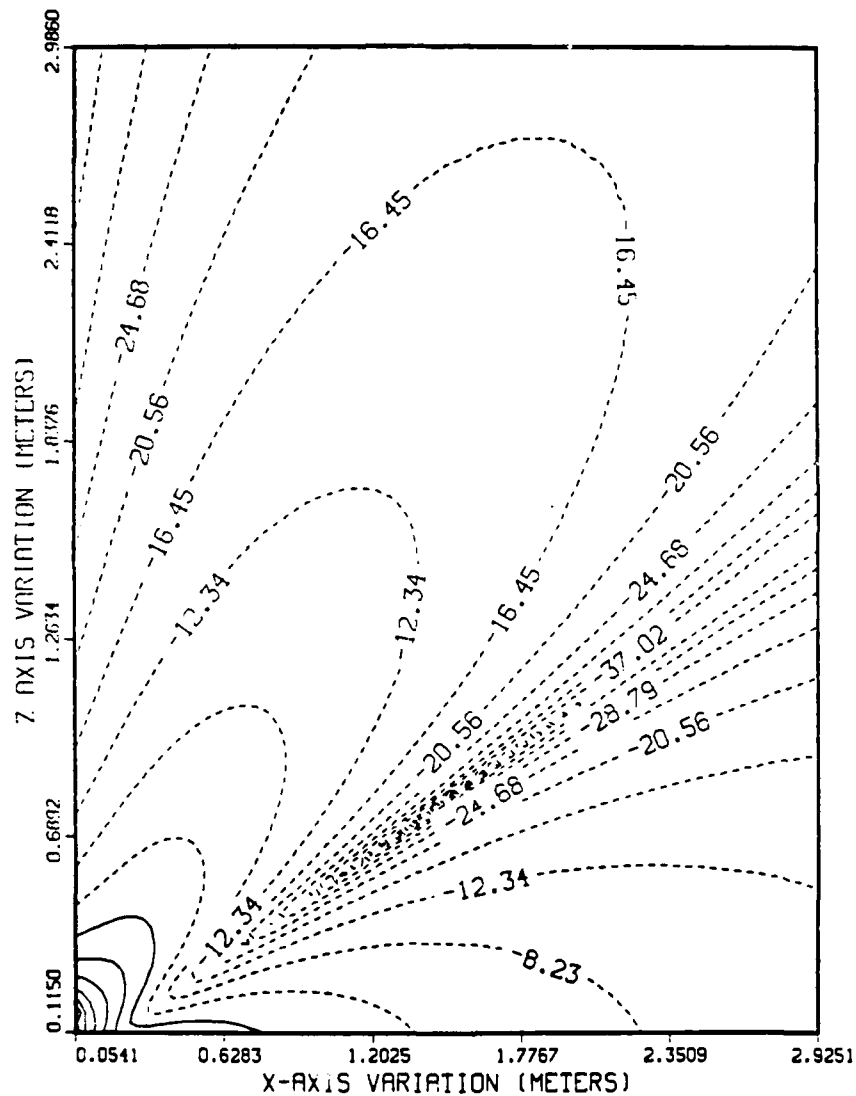


Figure 95. Z-Component, E-Field Contours  
Monopole at Wire Grid Box Corner

# PHASE OF Z COMPONENT OF E-FIELD MONOPOLE 6CM AT CORNER OF WIRE GRID BOX FREQ-1GHZ-(5.3CM ON DIAGONAL FROM CENTER)

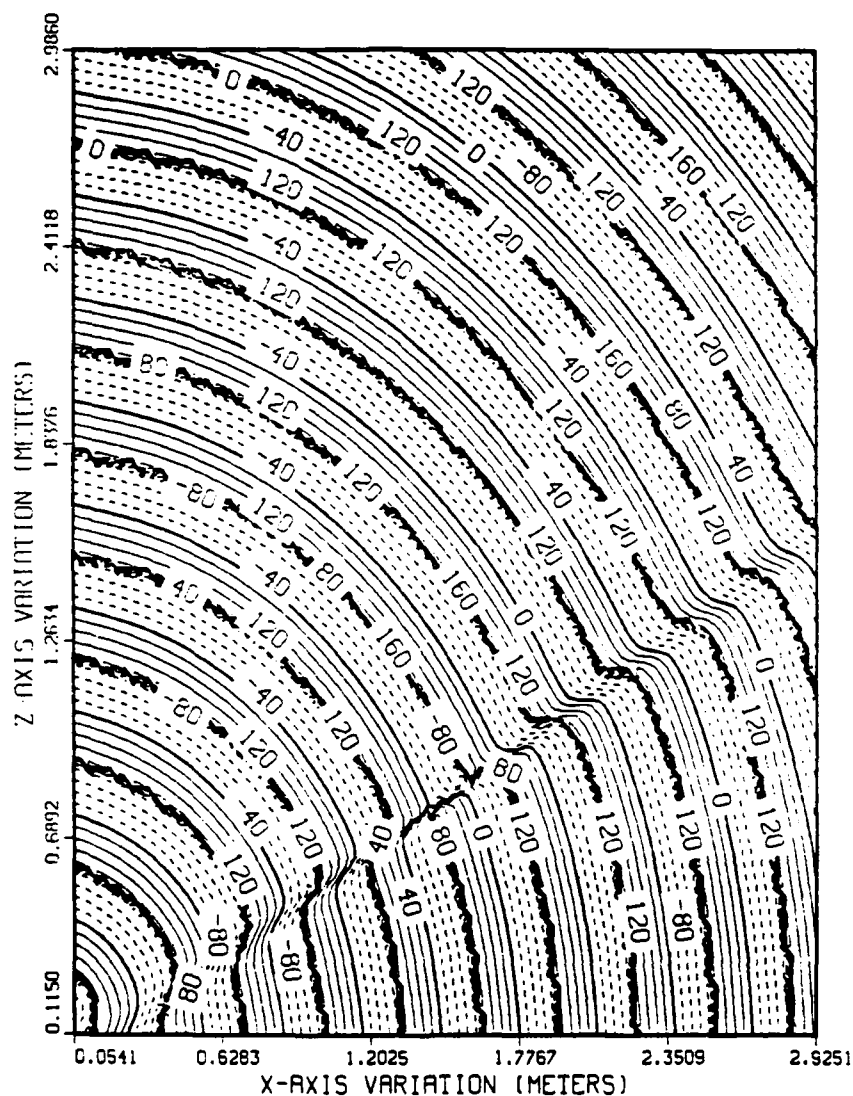


Figure 96. Z-Component, E-Field Phase Contours  
 Monopole at Wire Grid Box Corner

3-D ELECTRIC FIELD (DB REF TO 1V/M)  
MONOPOLE 6CM AT CORNER OF WIRE GRID BOX  
(5.3 CM ON DIAGONAL FROM CENTER)

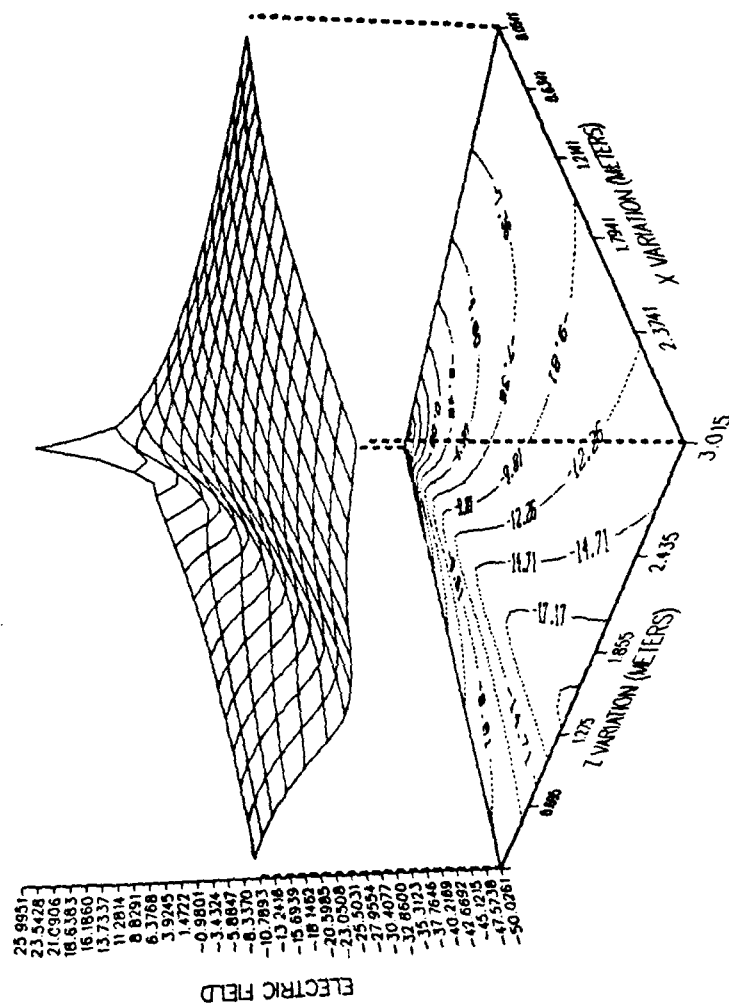


Figure 97. Total E-Field 3-D Plot, View Toward Monopole  
(Monopole at Wire Grid Box Corner)

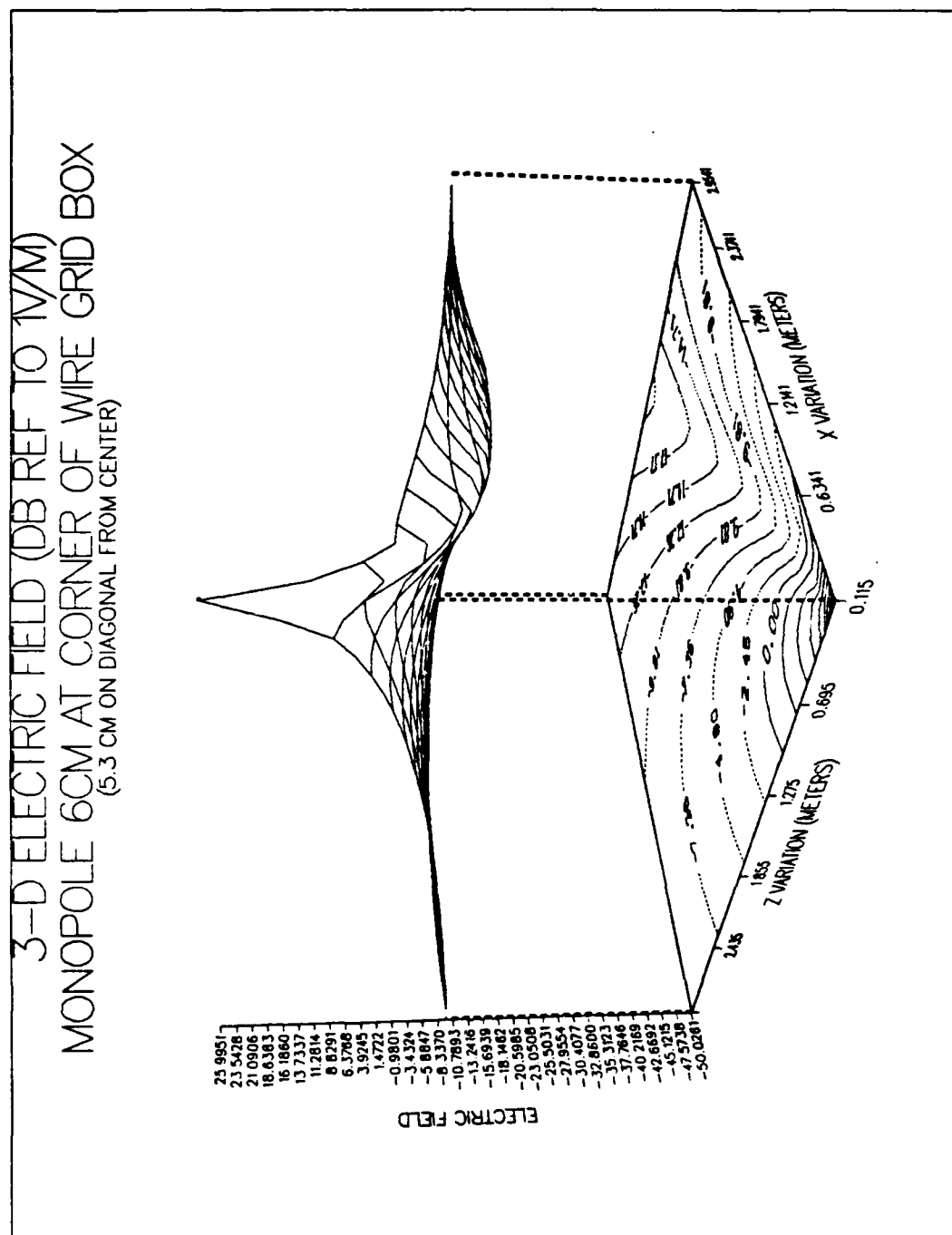


Figure 98. Total E-Field 3-D Plot, Viewed From Monopole  
(Monopole at Wire Grid Box Corner)

#### IV. CONCLUSIONS AND RECOMMENDATIONS

The goal of this investigation was to accurately predict near fields using the Numerical Electromagnetics Code (NEC) on ship-like structures. The near fields of Navy HF antennas are primary contributors to HF radiation hazards (RADHAZ). Providing reliable interference-free communications is a formidable task because of the high density of electromagnetic sources on the topside of a modern warship.

Since no validation benchmark results for near fields were available for ship antenna installations, a modeling exercise was undertaken using NEC in order to select the optimum models which would be used to calculate near fields. Box-like structures were analyzed using surface patch and wire grid modeling techniques. The simulation models consist of a  $\lambda/5$  monopole mounted on the top of a  $\lambda/3$  box at three different locations: center, edge and corner. Optimum models were selected by varying the patch density on the top surface of the box and observing the convergence of the solution for input admittance and average power gain, in order to ensure the validity of the models and improve the confidence in near field predictions. Optimum NEC models for the three different mounting geometries are:

- CENTER:  $7 \times 7 = 49$  patches on top ( $.0016\lambda^2$  patch area)
- EDGE AND CORNER:  $11 \times 11 = 121$  patches on top ( $.0009\lambda^2$  patch area)

NEC results for input admittance correlate very well with measurements. Average power gain varied between 1.80 to 2.02 (within the 10% engineering tolerance of the theoretical value). Single Precision (NPGNEC) calculations gave the same results as Double Precision (DNPGNEC).

Even though edges are not modeled in the surface patch technique [Ref. 1], this study proves that, for positions very close to an edge, good results can be obtained by careful subdividing (no special subdivision of smaller patches in the vicinity of the edge or corner was required).

Fortran algorithms were developed to produce near electric field (magnitude and phase) contours and 3-D plots using DISSPLA [Ref. 9]. The near field for the monopole on the box has the same characteristics in magnitude and phase as the monopole over a ground plane except in a region where nulls occur from box radiation and diffraction effects. The edge/corner-mounted geometries produce slightly different near electric field maps compared to center-mounted geometry.

Surface patch and wire grid models for NEC gave similar results for near fields.

Previously, generalized guidelines for near field modeling had not been developed for NEC and the use of wire grid and surface patch modeling for near field parameters was approached with caution. Guidelines developed in this study, as well as the results of the near field behavior of the



monopole antenna on the conducting box, can be used for future investigations on "ship-like" structures.

Recommendations for continuation of the present study are:

- Extend the model to larger and more complex structures which more closely approximate the ship's topside superstructure.
- Develop additional Fortran algorithms for use in near field investigations.
- Exercise a new version of the PATCH Code, "JUNCTION" [Ref. 11] in order to check the validity of the code and the computer/time cost in comparison to NEC.

The present study is an important step in the direction of modeling the effects of shipboard environments on the near field of antenna structures. It demonstrates how NEC surface patch and wire grid modeling techniques can be applied for accurate near field predictions of antennas in complex environments.

APPENDIX A  
NEC INPUT DATA FILES.

PART A: NEC INPUT DATA FILES FOR  
SURFACE PATCH MODELING

FILE: SPBOX100 DATA B1

```
CM SPBOX 5X5 PATCHES ON TOP SURFACE
CE FREQUENCY 1.00 GHZ
SM3,3,0.5,-0.5,0,0.5,-0.5,1
SC0,0,0,-0.5,1
SM3,3,0.5,-0.5,0,0.5,0,0
SC0,0,0.5,0,1
GX 0,110
SM5,5,-0.5,-0.5,1,0.5,-0.5,1
SC0,0,0.5,0.5,1
GS 0,0,0.1
GE 1
FR 0,0,0,0,1000
GN 1
WG
XQ 0
EN
```

1. Data File Surface-Patch Box Structure  
(5 x 5 patches = 25 patches on top  
surface).

FILE: SPBOX1 DATA M1

```
CM SPBOX 7X7 PATCHES ON TOP SURFACE
CE FREQUENCY 1.00 GHZ
SM3,3,0.5,-0.5,0,0.5,-0.5,1
SC0,0,0,-0.5,1
SM3,3,0.5,-0.5,0,0.5,0,0
SC0,0,0.5,0,1
GX 0,110
SM7,7,-0.5,-0.5,1,0.5,-0.5,1
SC0,0,0.5,0.5,1
GS 0,0,0.1
GE 1
FR 0,0,0,0,1000
GN 1
WG
XQ 0
EN
```

2. Data File Surface-Patch Box Structure  
(7 x 7 patches = 49 patches on top  
surface).

FILE: SPB1 DATA M1

CM SPBOX 9X9 PATCHES ON TOP SURFACE  
CE FREQUENCY 1.00 GHZ  
SM3,3,0.5,-0.5,0,0.5,-0.5,1  
SC0,0,0,-0.5,1  
SM3,3,0.5,-0.5,0,0.5,0,0  
SC0,0,0.5,0,1  
GX 0,110  
SM9,9,-0.5,-0.5,1,0.5,-0.5,1  
SC0,0,0.5,0.5,1  
GS 0,0,0.1  
GE 1  
FR 0,0,0,0,1000  
GN 1  
WG  
XQ 0  
EN

3. Data File Surface-Patch Box Structure  
(9 x 9 = 81 patches on top surface).

FILE: SPBOX11 DATA M1

CM 6 CM MONOPOLE AT CENTER OF SURFACE PATCH FREQ. 1.00 GHZ  
CM TOP SURFACE 7X7 PATCHES  
CE CALCULATION OF AVERAGE GAIN AND INPUT IMPEDANCE  
GF  
GW1,5,0,0,1,0,0,1.6,0.016  
GS 0,0,0.1  
GE 1  
EX 0,1,1,0,1,0  
RP 0,31,4,1002,0,0,3,15  
XQ 0  
EN

4. Data File 6cm Monopole at Center of  
SPBOX. Input Admittance and Average  
Power Gain Calculations

FILE: SPEDGE1 DATA M1

CM SPEDGE1 11X11 PATCHES ON TOP SURFACE (6CM AT EDGE 3.63CM FROM CENTER)  
CE FREQUENCY 1.00 GHZ  
SM3,3,0.5,-0.5,0,0.5,-0.5,1  
SC0,0,0,-0.5,1  
SM3,3,0.5,-0.5,0,0.5,0,0  
SC0,0,0.5,0,1  
GX 0,110  
SM11,11,-0.5,-0.5,1,0.5,-0.5,1  
SC0,0,0.5,0.5,1  
GS 0,0,0.1  
GE 1  
FR 0,0,0,0,1000  
GH 1  
WG  
XQ 0  
EN

5. Data File Surface-Patch Box Structure  
(11 x 11 = 121 patches on top surface).

FILE: SPEDGE11 DATA M1

CM 6 CM MONOPOLE AT EDGE 3.63CM FROM CENTER FREQUENCY 1.00 GHZ  
CM TOP SURFACE 11X11 PATCHES  
CE CALCULATION OF AVERAGE GAIN AND INPUT IMPEDANCE  
GF  
GW1,5,-0.363636,0,1,-0.363636,0,1.6,0.016  
GS 0,0,0.1  
GE 1  
EX 0,1,1,0,1,0  
RP 0,31,13,1002,0,0,3,15  
XQ 0  
EN

6. Data File 6cm Monopole at Edge (3.63cm from Center) of SPBOX. Input Admittance and Average Power Gain Calculations.

FILE: SPCNTR1 DATA M1

CM SPCNTR 11X11 PATCHES ON TOP SURFACE (6CM MONOPOLE AT CORNER 5.14 CM  
CM ON THE DIAGONAL FROM CENTER  
CE FREQUENCY 1.00 GHZ  
SM3,3,0.5,-0.5,0,0.5,-0.5,1  
SC0,0,0,-0.5,1  
SM3,3,0.5,-0.5,0,0.5,0,0  
SC0,0,0.5,0,1  
GX 0,110  
SM11,11,-0.5,-0.5,1,0.5,-0.5,1  
SC0,0,0.5,0.5,1  
GS 0,0,0.1  
GE 1  
FR 0,0,0,0,1000  
GN 1  
WG  
XQ 0  
EN

7. Data File Surface-Patch Box Structure for  
Monopole at Corner of SPBOX.

FILE: SPCNTR11 DATA M1

CM 6 CM MONOPOLE AT CORNER 5.14 CM ON THE DIAGONAL FROM CENTER  
CM TOP SURFACE 11X11 PATCHES  
CM FREQUENCY 1.00 GHZ  
CE CALCULATION OF AVERAGE GAIN AND INPUT IMPEDANCE  
GF  
GW1,5,0.363636,0.363636,1,0.363636,0.363636,1.6,0.016  
GS 0,0,0.1  
GE 1  
EX 0,1,1,0,1,0  
RP 0,31,13,1002,0,45,3,15  
XQ 0  
EN

8. Data File 6cm Monopole at Corner (5.14cm on the  
Diagonal) of SPBOX. Input Admittance and  
Average Power Gain Calculations.

PART B: NEC INPUT DATA FILES FOR  
NEAR ELECTRIC FIELD IN 2-D

FILE: SNCL DATA B1

CM SPBOX 7X7 PATCHES ON TOP SURFACE  
CE FREQUENCY 1.00 GHZ  
SM3,7,0.5,-0.5,0,0.5,-0.5,1  
SC0,0,0,-0.5,1  
SM3,3,0.5,-0.5,0,0.5,0,0  
SC0,0,0.5,0,1  
GX 0,110  
SM7,7,-0.5,-0.5,1,0.5,-0.5,1  
SC0,0,0.5,0.5,1  
GS 0,0,0.1  
GE 1  
FR 0,0,0,0,1000  
GN 1  
WG  
NX  
CM 6 CM MONOPOLE AT CENTER OF PATCH BOX  
CE NEAR E-FIELD ON X-AXIS AT 0.0166,0,0.115  
GF  
GW1,5,0,0,1,0,0,1.6,0.016  
GS 0,0,0.1  
GE 1  
EX 0,1,1,0,1,0  
PL 2,2,5,1  
NE 0,200,1,1,0.0166,0,0.115,0.01,0,0  
XQ 0  
EN

1. Data File Near Electric Field Along  
x-Axis for Monopole at Center of SPBOX.

FILE: SNCL11 DATA B1

CM SPBOX 7X7 PATCHES ON TOP SURFACE  
CE FREQUENCY 1.00 GHZ  
SM3,3,0.5,-0.5,0,0.5,-0.5,1  
SC0,0,0,-0.5,1  
SM3,3,0.5,-0.5,0,0.5,0,0  
SC0,0,0.5,0,1  
GX 0,110  
SM7,7,-0.5,-0.5,1,0.5,-0.5,1  
SC0,0,0.5,0.5,1  
GS 0,0,0.1  
GE 1  
FR 0,0,0,0,1000  
GN 1  
WG  
NX  
CM 6 CM MONOPOLE AT CENTER OF PATCH BOX  
CE NEAR E-FIELD ON Z-AXIS AT 0,0,0.175  
GF  
GW1,5,0,0,1,0,0,1.6,0.016  
GS 0,0,0.1  
GE 1  
EX 0,1,1,0,1,0  
PL 2,2,5,3  
NE 0,1,1,400,0,0,0.175,0,0,0.01  
XQ 0  
EN

2. Data File Near Electric Field Along  
z-Axis for Monopole at Center of SPBOX.

FILE: NEDGEX DATA B1

```
CM SPEDGE1 11X11 PATCHES ON TOP SURFACE (6CM AT EDGE 3.63CM FROM CENTER)
CE FREQUENCY 1.00 GHZ
SM3,3,0.5,-0.5,0,0.5,-0.5,1
SC0,0,0,-0.5,1
SM3,3,0.5,-0.5,0,0.5,0,0
SC0,0,0.5,0,1
GX 0,110
SM11,11,-0.5,-0.5,1,0.5,-0.5,1
SC0,0,0.5,0.5,1
GS 0,0,0.1
GE 1
FR 0,0,0,0,1000
GN 1
WG
NX
CM 6 CM MONOPOLE AT EDGE 3.63 CM FROM CENTER (11X11 PATCHES ON TOP)
CE NEAR E-FIELD ON X-AXIS
GF
GW 1,5,-0.363636,0,1,-0.363636,0,1.6,0.016
GS 0,0,0.1
GE 1
EX 0,1,1,0,1,0
PL 2,2,5,1
NE 0,200,1,1,-0.0197636,0,0.115,0.01,0,0
XQ 0
EN
```

3. Data File Near Electric Field Along x-Axis for Monopole at Edge of SPBOX.

FILE: NEDGEY DATA B1

```
CM SPEDGE1 11X11 PATCHES ON TOP SURFACE (6CM AT EDGE 3.63CM FROM CENTER)
CE FREQUENCY 1.00 GHZ
SM3,3,0.5,-0.5,0,0.5,-0.5,1
SC0,0,0,-0.5,1
SM3,3,0.5,-0.5,0,0.5,0,0
SC0,0,0.5,0,1
GX 0,110
SM11,11,-0.5,-0.5,1,0.5,-0.5,1
SC0,0,0.5,0.5,1
GS 0,0,0.1
GE 1
FR 0,0,0,0,1000
GN 1
WG
NX
CM 6 CM MONOPOLE AT EDGE 3.63 CM FROM CENTER (11X11 PATCHES ON TOP)
CE NEAR E-FIELD ON Y-AXIS
GF
GW 1,5,-0.363636,0,1,-0.363636,0,1.6,0.016
GS 0,0,0.1
GE 1
EX 0,1,1,0,1,0
PL 2,2,5,2
NE 0,1,200,1,-0.0363636,0.0166,0.115,0,0.01,0
XQ 0
EN
```

4. Data File Near Electric Field Along y-Axis for Monopole at Edge of SPBOX.

FILE: NEDGEZ DATA B1

CM SPEDGE1 11X11 PATCHES ON TOP SURFACE (6CM AT EDGE 3.63CM FROM CENTER)  
CE FREQUENCY 1.00 GHZ  
SM3,3,0.5,-0.5,0,0.5,-0.5,1  
SC0,0,0,-0.5,1  
SM3,3,0.5,-0.5,0,0.5,0,0  
SC0,0,0.5,0,1  
GX 0,110  
SM11,11,-0.5,-0.5,1,0.5,-0.5,1  
SC0,0,0.5,0.5,1  
GS 0,0,0.1  
GE 1  
FR 0,0,0,0,1000  
GN 1  
WG  
NX  
CM 6 CM MONOPOLE AT EDGE 3.63 CM FROM CENTER (11X11 PATCHES ON TOP)  
CE NEAR E-FIELD ON Z-AXIS  
GF  
GW 1,5,-0.363636,0,1,-0.363636,0,1.6,0.016  
GS 0,0,0.1  
GE 1  
EX 0,1,1,0,1,0  
PL 2,2,5,3  
NE 0,1,1,200,-0.0363636,0,0.175,0,0,0.01  
XQ 0  
EN

5. Data File Near Electric Field Along z-Axis for Monopole at Edge of SPBOX.

FILE: NCORNX DATA B1

CM SPCNTR 11X11 PATCHES ON TOP SURFACE (6CM MONOPOLE AT CORNER 5.14 CM  
CM ON THE DIAGONAL FROM CENTER  
CE FREQUENCY 1.00 GHZ  
SM3,3,0.5,-0.5,0,0.5,-0.5,1  
SC0,0,0,-0.5,1  
SM3,3,0.5,-0.5,0,0.5,0,0  
SC0,0,0.5,0,1  
GX 0,110  
SM11,11,-0.5,-0.5,1,0.5,-0.5,1  
SC0,0,0.5,0.5,1  
GS 0,0,0.1  
GE 1  
FR 0,0,0,0,1000  
GN 1  
WG  
NX  
CM 6 CM MONOPOLE AT CORNER 5.14 CM ON THE DIAGONAL FROM CENTER  
CM TOP SURFACE 11X11 PATCHES  
CM FREQUENCY 1.00 GHZ  
CE NEAR E-FIELD ON X-AXIS  
GF  
GW1,5,0.363636,0.363636,1,0.363636,0.363636,1.6,0.016  
GS 0,0,0.1  
GE 1  
EX 0,1,1,0,1,0  
PC 2,2,5,1  
NE 0,200,1,1,0.0529636,0.0363636,0.115,0.01,0,0  
XQ 0  
EN

6. Data File Near Electric Field Along x-Axis for Monopole at Corner of SPBOX.



FILE: NCORNY DATA B1

CM SPCNTR 11X11 PATCHES ON TOP SURFACE (6CM MONOPOLE AT CORNER 5.14 CM  
CM ON THE DIAGONAL FROM CENTER  
CE FREQUENCY 1.00 GHZ  
SM3,3,0.5,-0.5,0,0.5,-0.5,1  
SC0,0,0,-0.5,1  
SM3,3,0.5,-0.5,0,0.5,0,0  
SC0,0,0.5,0,1  
GX 0,110  
SM11,11,-0.5,-0.5,1,0.5,-0.5,1  
SC0,0,0.5,0.5,1  
GS 0,0,0.1  
GE 1  
FR 0,0,0,0,1000  
GN 1  
WG  
NX  
CM 6 CM MONOPOLE AT CORNER 5.14 CM ON THE DIAGONAL FROM CENTER  
CM TOP SURFACE 11X11 PATCHES  
CM FREQUENCY 1.00 GHZ  
CE NEAR E-FIELD ON Y-AXIS  
GF  
GW1,5,0.363636,0.363636,1,0.363636,0.363636,1.6,0.016  
GS 0,0,0.1  
GE 1  
EX 0,1,1,0,1,0  
PL 2,2,5,2  
NE 0,1,200,1,0.0363636,0.0529636,0.115,0,0.01,0  
XQ 0  
EN

7. Data File Near Electric Field Along y-Axis for  
Monopole at Corner of SPBOX.

FILE: NCORNZ DATA B1

CM SPCNTR 11X11 PATCHES ON TOP SURFACE (6CM MONOPOLE AT CORNER 5.14 CM  
CM ON THE DIAGONAL FROM CENTER  
CE FREQUENCY 1.00 GHZ  
SM3,3,0.5,-0.5,0,0.5,-0.5,1  
SC0,0,0,-0.5,1  
SM3,3,0.5,-0.5,0,0.5,0,0  
SC0,0,0.5,0,1  
GX 0,110  
SM11,11,-0.5,-0.5,1,0.5,-0.5,1  
SC0,0,0.5,0.5,1  
GS 0,0,0.1  
GE 1  
FR 0,0,0,0,1000  
GN 1  
WG  
NX  
CM 6 CM MONOPOLE AT CORNER 5.14 CM ON THE DIAGONAL FROM CENTER  
CM TOP SURFACE 11X11 PATCHES  
CM FREQUENCY 1.00 GHZ  
CE NEAR E-FIELD ON Z-AXIS  
GF  
GW1,5,0.363636,0.363636,1,0.363636,0.363636,1.6,0.016  
GS 0,0,0.1  
GE 1  
EX 0,1,1,0,1,0  
PL 2,2,5,3  
NE 0,1,1,200,0.0363636,0.0363636,0.175,0,0,0.01  
XQ 0  
EN

8. Data File Near Electric Field Along z-Axis for  
Monopole at Corner of SPBOX.

APPENDIX B  
FORTRAN PROGRAMS AND NEC INPUT DATA FILES

PART A: DESCRIPTION OF FORTRAN PROGRAMS FOR INTERFACING  
NEC OUTPUT WITH DISSPLA GRAPHICS PACKAGE

**PROGRAM I: CON1**

This Fortran program is constructed in order to generate contour plots of magnitude  $E_{\text{peak}}$  ( $E_{\text{total}}$ ) of the near electric field using NEC output in conjunction with the DISSPLA graphics package [Ref. 9]. Part of NEC's typical output which shows the calculated  $E_{\text{peak}}$ , is given in the example 1 data file, and is produced using the PL card with options 2, 2, 5, 1 and an NE card [Ref. 1]. In example 1, the 2nd column is the x-variation, with points spaced as is defined by the NE card, while the third column is the magnitude of  $E_{\text{peak}}$  ( $E_{\text{total}}$ ) which corresponds to each point in space.

The CON1 program reads the values from the 3rd column of NEC near field output, i.e., example 1 data file. It then arranges these values in an NX by NY array, for input to the subroutine CONTOR, which in turn creates the contour plots. CON1 also selects the maximum ( $E_{\text{max}}$ ) and minimum ( $E_{\text{min}}$ ) values of the electric field (3rd column of example 1 data file). Using these values in combination with the NLEVEL value (the number of levels between the contours, which in the present study is twenty), it calculates the variable FINC which is the contouring interval, which is needed by CONTOR. The values of  $E_{\text{min}}$ ,  $E_{\text{max}}$ , and FINC are displayed on the screen. The calling statement is:

CALL CONTOR (A, NX, NY, FINC)

where: A - NX by NY array containing the values to  
be contoured

NX - Number of columns in the array (in the present  
study it is 30)

NY - Number of rows in the array (in the present  
study it is 30)

The values in the array A have been arranged by CON1 as  
follows:

Diagram illustrating the arrangement of values in the array A:

The array A is represented as a grid of points. The vertical axis is labeled Z and the horizontal axis is labeled X. The array is represented as a grid of points. The top row is labeled A(1,NY), A(2,NY)..., ..., A(NX,NY). The bottom row is labeled A(1,1), A(2,1)..., ..., A(NX,1). The leftmost column is labeled A(1,NY), A(1,NY-1)..., ..., A(1,2)..., A(1,1). The rightmost column is labeled ..., A(NX,NY), ..., A(NX,1).

In the contour plots of study, the magnitude of  $E_{\text{peak}}$ , the electric field, is presented in a form of a section of a plane in 3-dimensional space composed of a (30 x 30) 900-point-window in space. The unit of magnitude used to express the electric near field in all the plots is dB with reference to one volt per meter:

$$\left[ \text{dB}(1\text{V/m}) = 20 \log_{10} \left( \frac{|E|}{1\text{V/m}} \right) \right]$$

When the magnitude of  $E_{\text{peak}}$  ( $E_{\text{total}}$ ) is plotted using NEC output in the form of example 1, the CON1 FORMAT is defined as (17x, D10.3). However, when  $E_{\text{peak}}$  of the individual components ( $E_x$  or  $E_z$ ) is plotted, the PL card with options,

2,2,4,1 is used in conjunction with an NE card [Ref. 1]. In this case, NEC output has the form of example 2. Columns in the example 2 data file are: x-variation, Ex, x-component phase, Ey, y-component phase, Ez, z-component phase. In this case, when the magnitude of individual components, x-component (Ex) or z-component (Ez), is plotted, the FORMAT in CON1 must be: (15x, D10.3) and (55x, D10.3) correspondingly.

CONTOR: This subroutine is constructed using the DISSPLA graphics package [Ref. 9] and is modified for this thesis for near electric field contours. The subroutine has comments in each step explaining its function. The variables XORIG, XSTP, XMAX, YORIG, YSTP, and YMAX, have to be defined manually by the user for each case. For each plot, the program must be compiled by the "FORTVS" command before execution. In the present study, the parameters labeled y-axis are actually the z-axis parameters.

The subroutine MYCON represents negative dB contours by dashed curves while the positive ones are solid curves. The number in parentheses of the statements, COMMON WORK and CALL BCOMON [Ref. 9], must be 5,000 for magnitude plots while for phase plots it must be 20,000 because DISSPLA needs additional workspace for smoothing the phase values.

#### PROGRAM II: CON3

This Fortran program generates contour plots of the phase of individual components (x or z components) of the

electric field from NEC output and the DISSPLA graphics package [Ref. 9]. Part of a typical NEC output is presented in the example 2 data file. This output is produced from the the PL card with options 2,2,4,1 and an NE card [Ref. 1]. The columns presented in example 2 are: x-variation, Ex, x-component phase, Ey, y-component phase, Ez, z-component phase.

The program reads the values from the 3rd and 7th columns (Phase of x and z components) and arranges them in the Array A consisting of Nx by Ny points using the FORMAT (25x, D10.3) and the FORMAT (65x, D10.3) for the phase of x and z-components correspondingly. For the case of the phase plot in the present study, the array is selected as 100 x 100 = 10,000 points. This is necessary because the near field region phase is very complicated, having abrupt variations and the DISSPLA program needs more points for the smoothing and accuracy. The number of levels between contours in the phase plots is selected to be: NLEVEL = 10 versus 20 (which was used for the magnitude plot). The number in the statement: COMMON WORK and CALL BCOMON must be 20,000, because in the case of phase plots, DISSPLA needs additional workspace for smoothing.

#### PROGRAM III: CON2

This Fortran program generates 3-D plots of magnitude  $E_{\text{peak}}$  ( $E_{\text{total}}$ ) of the near electric field. In this type of plot, a section of a plane in 3-dimensions consisting of

(30 x 30 ) 900 points is presented. Electric field values are presented as a 3rd dimension (vertical axis). The contour plot appears at the bottom of the graph (exactly the same plot as the one produced by CON1) while on the top, the electric field variation as a 3-D surface is presented. The program is the same as CON1 except that the user must input the number of levels (NLEVEL) manually from the keyboard and also has the option to select coordinates of the viewpoint: VX, VZ, and VE. CON2 uses the subroutine DMH002 of DISSPLA [Ref. 9] which is listed at the end of the program. Parameters in the statements CALL GRAF3D, CALL GRAF and CALL RLVEC3 have to be input by the user and the program has to be compiled by "FORTVS" before execution. All other information, a user may need, appears in comments in the program.

In order for DISSPLA to be automatically executed for each of the Programs I, II, or III, an EXEC file has been constructed correspondingly (CON1, 2, or 3 EXEC). The user has to input the filename of the NEC output data file (which has the form: FILENAME PLOTDATA) in the EXEC file and then typing CON1, CON2 OR CON3 in CMS, causes the execution of DISSPLA automatically. For all the programs the output is: DISSPLA METAFILE T, which can be copied to the A or B-disk and then, using the DISSPOP option, the user can select the type of output needed from a menu (Sherpa, IBM79, etc.).

FILE: DIP4      PLOTDATA B1

N809	0.242E+01	0.924E-01
N809	0.252E+01	0.935E-01
N809	0.262E+01	0.945E-01
N809	0.272E+01	0.953E-01
N809	0.282E+01	0.960E-01
N809	0.292E+01	0.965E-01
N809	0.166E-01	0.511E-02
N809	0.117E+00	0.624E-02
N809	0.217E+00	0.116E-01
N809	0.317E+00	0.168E-01
N809	0.417E+00	0.220E-01
N809	0.517E+00	0.271E-01
N809	0.617E+00	0.321E-01
N809	0.717E+00	0.369E-01
N809	0.817E+00	0.416E-01
N809	0.917E+00	0.461E-01
N809	0.102E+01	0.504E-01
N809	0.112E+01	0.545E-01
N809	0.122E+01	0.534E-01
N809	0.132E+01	0.621E-01
N809	0.142E+01	0.655E-01
N809	0.152E+01	0.688E-01
N809	0.162E+01	0.718E-01
N809	0.172E+01	0.746E-01
N809	0.182E+01	0.771E-01
N809	0.192E+01	0.795E-01
N809	0.202E+01	0.816E-01
N809	0.212E+01	0.836E-01
N809	0.222E+01	0.853E-01
N809	0.232E+01	0.869E-01
N809	0.242E+01	0.883E-01
N809	0.252E+01	0.895E-01
N809	0.262E+01	0.905E-01
N809	0.272E+01	0.914E-01
N809	0.282E+01	0.922E-01
N809	0.292E+01	0.923E-01

1. Example 1: NEC Output

```

N804 0.106E+01 0.501E-01-0.150E+03 0.000E+00 0.000E+00 0.183E-01 0.460E+02
N804 0.109E+01 0.511E-01-0.161E+03 0.000E+00 0.000E+00 0.191E-01 0.334E+02
N804 0.112E+01 0.520E-01-0.174E+03 0.000E+00 0.000E+00 0.200E-01 0.207E+02
N804 0.115E+01 0.529E-01 0.174E+03 0.000E+00 0.000E+00 0.208E-01 0.769E+01
N804 0.118E+01 0.538E-01 0.161E+03 0.000E+00 0.000E+00 0.216E-01-0.553E+01
N804 0.121E+01 0.547E-01 0.149E+03 0.000E+00 0.000E+00 0.225E-01-0.190E+02
N804 0.123E+01 0.555E-01 0.135E+03 0.000E+00 0.000E+00 0.233E-01-0.327E+02
N804 0.126E+01 0.563E-01 0.122E+03 0.000E+00 0.000E+00 0.242E-01-0.466E+02
N804 0.129E+01 0.571E-01 0.108E+03 0.000E+00 0.000E+00 0.251E-01-0.608E+02
N804 0.132E+01 0.579E-01 0.942E+02 0.000E+00 0.000E+00 0.260E-01-0.751E+02
N804 0.135E+01 0.586E-01 0.800E+02 0.000E+00 0.000E+00 0.268E-01-0.898E+02
N804 0.138E+01 0.593E-01 0.655E+02 0.000E+00 0.000E+00 0.277E-01-0.105E+03
N804 0.141E+01 0.600E-01 0.508E+02 0.000E+00 0.000E+00 0.286E-01-0.120E+03
N804 0.144E+01 0.607E-01 0.358E+02 0.000E+00 0.000E+00 0.295E-01-0.135E+03
N804 0.147E+01 0.613E-01 0.205E+02 0.000E+00 0.000E+00 0.304E-01-0.151E+03
N804 0.150E+01 0.619E-01 0.505E+01 0.000E+00 0.000E+00 0.313E-01-0.166E+03
N804 0.152E+01 0.625E-01-0.107E+02 0.000E+00 0.000E+00 0.321E-01 0.178E+03
N804 0.155E+01 0.630E-01-0.266E+02 0.000E+00 0.000E+00 0.330E-01 0.161E+03
N804 0.158E+01 0.636E-01-0.428E+02 0.000E+00 0.000E+00 0.339E-01 0.145E+03
N804 0.161E+01 0.641E-01-0.593E+02 0.000E+00 0.000E+00 0.348E-01 0.128E+03
N804 0.164E+01 0.645E-01-0.759E+02 0.000E+00 0.000E+00 0.357E-01 0.111E+03
N804 0.167E+01 0.650E-01-0.928E+02 0.000E+00 0.000E+00 0.365E-01 0.943E+02
N804 0.170E+01 0.654E-01-0.110E+03 0.000E+00 0.000E+00 0.374E-01 0.770E+02
N804 0.173E+01 0.658E-01-0.127E+03 0.000E+00 0.000E+00 0.383E-01 0.595E+02
N804 0.176E+01 0.662E-01-0.145E+03 0.000E+00 0.000E+00 0.391E-01 0.417E+02
N804 0.179E+01 0.666E-01-0.163E+03 0.000E+00 0.000E+00 0.400E-01 0.238E+02
N804 0.181E+01 0.669E-01 0.179E+03 0.000E+00 0.000E+00 0.408E-01 0.565E+01
N804 0.184E+01 0.672E-01 0.161E+03 0.000E+00 0.000E+00 0.416E-01-0.127E+02
N804 0.187E+01 0.675E-01 0.143E+03 0.000E+00 0.000E+00 0.425E-01-0.313E+02
N804 0.190E+01 0.678E-01 0.124E+03 0.000E+00 0.000E+00 0.433E-01-0.500E+02
N804 0.193E+01 0.680E-01 0.105E+03 0.000E+00 0.000E+00 0.441E-01-0.690E+02
N804 0.196E+01 0.683E-01 0.864E+02 0.000E+00 0.000E+00 0.449E-01-0.881E+02
N804 0.199E+01 0.685E-01 0.671E+02 0.000E+00 0.000E+00 0.457E-01-0.107E+03
N804 0.202E+01 0.687E-01 0.477E+02 0.000E+00 0.000E+00 0.465E-01-0.127E+03
N804 0.205E+01 0.688E-01 0.281E+02 0.000E+00 0.000E+00 0.473E-01-0.147E+03
N804 0.208E+01 0.690E-01 0.836E+01 0.000E+00 0.000E+00 0.481E-01-0.167E+03
N804 0.210E+01 0.691E-01-0.116E+02 0.000E+00 0.000E+00 0.488E-01 0.173E+03
N804 0.213E+01 0.692E-01-0.318E+02 0.000E+00 0.000E+00 0.496E-01 0.153E+03
N804 0.216E+01 0.693E-01-0.521E+02 0.000E+00 0.000E+00 0.503E-01 0.133E+03
N804 0.219E+01 0.694E-01-0.726E+02 0.000E+00 0.000E+00 0.511E-01 0.112E+03
N804 0.222E+01 0.695E-01-0.933E+02 0.000E+00 0.000E+00 0.518E-01 0.912E+02
N804 0.225E+01 0.695E-01-0.114E+03 0.000E+00 0.000E+00 0.525E-01 0.702E+02
N804 0.228E+01 0.696E-01-0.135E+03 0.000E+00 0.000E+00 0.532E-01 0.491E+02
N804 0.231E+01 0.696E-01-0.156E+03 0.000E+00 0.000E+00 0.539E-01 0.278E+02
N804 0.234E+01 0.696E-01-0.178E+03 0.000E+00 0.000E+00 0.545E-01 0.635E+01
N804 0.237E+01 0.696E-01 0.161E+03 0.000E+00 0.000E+00 0.552E-01-0.153E+02
N804 0.239E+01 0.696E-01 0.139E+03 0.000E+00 0.000E+00 0.559E-01-0.371E+02
N804 0.242E+01 0.695E-01 0.117E+03 0.000E+00 0.000E+00 0.565E-01-0.590E+02
N804 0.245E+01 0.695E-01 0.950E+02 0.000E+00 0.000E+00 0.571E-01-0.811E+02
N804 0.248E+01 0.694E-01 0.728E+02 0.000E+00 0.000E+00 0.578E-01-0.103E+03
N804 0.251E+01 0.693E-01 0.505E+02 0.000E+00 0.000E+00 0.584E-01-0.126E+03
N804 0.254E+01 0.692E-01 0.280E+02 0.000E+00 0.000E+00 0.590E-01-0.148E+03
N804 0.257E+01 0.691E-01 0.534E+01 0.000E+00 0.000E+00 0.595E-01-0.171E+03
N804 0.260E+01 0.690E-01-0.174E+02 0.000E+00 0.000E+00 0.601E-01 0.166E+03
N804 0.263E+01 0.689E-01-0.404E+02 0.000E+00 0.000E+00 0.607E-01 0.143E+03
N804 0.266E+01 0.688E-01-0.635E+02 0.000E+00 0.000E+00 0.612E-01 0.120E+03
N804 0.268E+01 0.686E-01-0.867E+02 0.000E+00 0.000E+00 0.618E-01 0.968E+02
N804 0.271E+01 0.685E-01-0.110E+03 0.000E+00 0.000E+00 0.623E-01 0.734E+02
N804 0.274E+01 0.683E-01-0.134E+03 0.000E+00 0.000E+00 0.628E-01 0.498E+02
N804 0.277E+01 0.681E-01-0.157E+03 0.000E+00 0.000E+00 0.633E-01 0.261E+02
N804 0.280E+01 0.680E-01 0.179E+03 0.000E+00 0.000E+00 0.638E-01 0.234E+01
N804 0.283E+01 0.678E-01 0.155E+03 0.000E+00 0.000E+00 0.643E-01-0.216E+02
N804 0.286E+01 0.676E-01 0.131E+03 0.000E+00 0.000E+00 0.647E-01-0.457E+02
N804 0.289E+01 0.674E-01 0.107E+03 0.000E+00 0.000E+00 0.652E-01-0.699E+02

```

## 2. Example 2: NEC Output



FILE: CON1      FORTRAN   B1

```

      REAL*8 RO
C  DEFINE THE ARRAY A(NX,NY) WHICH CONTAINS
C  THE VALUES TO BE CONTOURED. NX=NUMBER OF COLUMNS
C  AND NY=NUMBER OF ROWS OF THE ARRAY.
C
      DIMENSION A(30,30)
      EMIN=1E20
      EMAX=-1E20
      DO 50 I=1,30
        DO 40 J=1,30
          READ (12,20)RO
C  USE THIS FORMAT WHEN THE MAGNITUDE EPEAK(ETOTAL)
C  IS TO BE PLOTTED. NEC OUTPUT IN THIS CASE HAS TO
C  BE PRODUCED BY PL 2,2,5,1 AND NE CARDS.
C
          20      FORMAT (17X,D10.3)
C  USE THE FORMATS BELOW WHEN THE MAGNITUDE EPEAK
C  OF X AND Z COMPONENTS CORRESPONDINGLY IS TO BE
C  PLOTTED. NEC OUTPUT IN THESE CASES HAS TO BE
C  PRODUCED BY PL 2,2,4,1 AND NE CARDS.
C
          C20      FORMAT (15X,D10.3)
          C20      FORMAT (55X,D10.3)
          A(J,I)=20*LOG10(RO)
C  IN THIS STEP THE PROGRAM PREDICTS THE MINIMUM AND
C  AND MAXIMUM VALUES OF THE ELECTRIC FIELD.
C
          EMIN=MIN(EMIN,A(J,I))
          EMAX=MAX(EMAX,A(J,I))
        40      CONTINUE
      50      CONTINUE
      NX=30
      NY=30
C  DEFINE THE NUMBER OF LEVELS BETWEEN THE CONTOURS.
      NLEVEL=20
C  THE PROGRAM CALCULATES THE CONTOURING INTERVAL.
      FINC=(EMAX-EMIN)/(NLEVEL-1)
C  EMIN,EMAX,FINC ARE DISSPLAYED ON THE SCREEN.
      WRITE (6,*) EMIN,EMAX,FINC
C  THE FOLLOWING STATEMENT IS THE CALLING STATEMENT
C  OF THE SUBROUTINE CONTOR.
      CALL CONTOR (A,NX,NY,FINC)
      STOP
      END

```

CON00010  
 CON00020  
 CON00030  
 CON00040  
 CON00050  
 CON00060  
 CON00070  
 CON00080  
 CON00090  
 CON00100  
 CON00110  
 CON00120  
 CON00130  
 CON00140  
 CON00150  
 CON00160  
 CON00170  
 CON00180  
 CON00190  
 CON00200  
 CON00210  
 CON00220  
 CON00230  
 CON00240  
 CON00250  
 CON00260  
 CON00270  
 CON00280  
 CON00290  
 CON00300  
 CON00310  
 CON00320  
 CON00330  
 CON00340  
 CON00350  
 CON00360  
 CON00370  
 CON00380  
 CON00390  
 CON00400  
 CON00410  
 CON00420  
 CON00430  
 CON00440

3. PROGRAM I: CON1 FORTRAN. Contour plots of Magnitude for Near Electric Field.

FILE: CON1      EXEC      B1

FILEDEF 12 DISK FILENAME PLOTDATA A  
EXEC DISSPLA CON1

4. CON1 EXEC: Fortran File for Automatic Execution of DISSPLA.

FILE: CONTOR    FORTRAN    B1

```

      SUBROUTINE CONTOR(A,NX,NY,FINC)
C THIS SUBROUTINE CONTOURS AN NX BY NY ARRAY OF REGULARLY SPACED POINTS.
C
C   A : AN NX BY NY ARRAY OF REGULARLY SPACED POINTS
C   NX: NUMBER OF POINTS IN THE X-DIRECTION
C   NY: NUMBER OF POINTS IN THE Y-DIRECTION
C   FINC: CONTOUR INTERVAL
C
C   DIMENSION A(NX,NY)
C THE NUMBER IN THE PARENTHESIS OF THE FOLLOWING
C COMMAND DEFINES THE WORKSPACE IN THE DISSPLA
C GRAPHICS PACKAGE. THIS NUMBER HAS TO BE 5000 WHEN
C THE MAGNITUDE EPEAK IS TO BE PLOTTED AND 20000
C WHEN THE PHASE OF THE INDIVIDUAL COMPONENTS IS
C TO BE PLOTTED. IN THE CASE OF PHASE PLOT THE ARRAY
C IS LARGER AND DISSPLA NEEDS ADDITIONAL WORKSPACE
C FOR SMOOTHING. SAME COMMENTS CORRESPONDS TO THE
C "CALL BCOMON" STATEMENT.
C
C   COMMON WORK(5000)
C
C SET PARAMETERS FOR AXES:
C DEFINE X AXIS PARAMETERS
C
C   XORIG=0.0541
C   XSTP=0.58
C   XMAX=2.9541
C DEFINE Y AXIS PARAMETERS (CORRESPOND TO Z AXIS)
C   YORIG=0.115
C   YSTP=0.58
C   YMAX=3.015
C CALL COMPRS TO USE THE DISSPOP OPTION.
C   CALL COMPRS
C   CALL SETCLR('CYAN')
C
C SET PAGE AND PLOT SIZES, SET UP AXES FOR PLOT:
C   CALL PAGE(8.5,11.0)
C   CALL BCOMON(5000)
C   CALL AREA2D(6.0,8.0)
C
C LABEL AXES:
C   CALL XNAME('X-AXIS VARIATION (METERS)$',100)
C   CALL YNAME('Z-AXIS VARIATION (METERS)$',100)
C
C   CALL GRAF(XORIG,XSTP,XMAX,YORIG,YSTP,YMAX)
C   CALL FRAME
C
C TITLE OF THE PLOT:
C   CALL HEADIN('CONTOUR E-FIELD (DB REF TO 1V/M)$',100,2.,3)
C   CALL HEADIN('MONOPOLE 6CM AT CORNER OF WIRE GRID BOX$',100,1.,3)
C   CALL HEADIN('FREQ=1GHZ-(5.3 CM ON DIAGONAL)$',100,1.,3)
C
C MAKE CONTOURS AND DRAW:
C   CALL SETCLR('RED')
C   CALL CONMIN(3.0)
C   CALL CONANG(60.)
C   CALL CONLIN(0,'MYCON','LABELS',2,10)
C   CALL CONMAK(A,NX,NY,FINC)
C   CALL CONTUR(1,'LABELS','DRAW')
C
C END PLOT:
C   CALL ENDPL(0)
C   CALL DONEPL
C   RETURN
C   END
C
C *****
C
C   SUBROUTINE MYCON(RARRAY,IARRAY)
C   DIMENSION RARRAY(2),IARRAY(1)
C
C THIS ROUTINE MAKES NEGATIVE CONTOURS DASHED , ZERO LINES HEAVIER

```

FILE: CONTOR FORTRAN B1

C WHILE THE POSITIVE CONTOURS ARE PRESENTED BY SOLID LINES.

C

```
CALL RESET('DASH')
IF (RARAY(1) .GE. 0.) GO TO 10
CALL DASH
10 RARAY(2) = 1.
   IARAY(1) = 1
   IF (RARAY(1) .EQ. 0.) IARAY(1) = 2
   RETURN
END
```

CON00730  
CON00740  
CON00750  
CON00760  
CON00770  
CON00780  
CON00790  
CON00800  
CON00810  
CON00820

5. CONTOR FORTRAN: Subroutine Which is Used to Generate the Contour Plots.

FILE: CON3      FORTRAN   B1

C THIS PROGRAM READS THE VALUES OF THE PHASE OF EX OR EZ COMPONENT	CON00010
C FROM A NEC OUTPUT FILE (NEC OUTPUT IN THIS CASE HAS TO	CON00020
C BE PRODUCED BY A PL 2,2,4,1 AND NE CARDS.THE OUTPUT	CON00030
C IN THIS CASE IS LIKE THE ONE IN EXAMPLE 2 DATA FILE)	CON00040
C AND USING THE SUBROUTINE CONTOR FORTRAN PLOTS THE	CON00050
C VARIATION OF THE PHASE USING DISSPLA.	CON00060
C	CON00070
REAL*8 RO	CON00080
C DEFINE THE ARRAY A(NX,NY) WHICH IN THIS CASE IS COMPOSED	CON00090
C OF 100X100=10000 ELEMENTS. NX=NUMBER OF COLUMNS AND	CON00100
C NY=NUMBER OF ROWS OF THE ARRAY.	CON00110
DIMENSION A(100,100)	CON00120
EMIN=1E20	CON00130
EMAX=-1E20	CON00140
DO 50 I=1,100	CON00150
DO 40 J=1,100	CON00160
READ (12,20)RO	CON00170
C USE THIS FORMAT WHEN THE PHASE OF X COMPONENT	CON00180
C OF THE ELECTRIC FIELD IS TO BE PLOTTED	CON00190
C	CON00200
20       FORMAT (25X,D10.3)	CON00210
C USE THIS FORMAT WHEN THE PHASE OF Z COMPONENT	CON00220
C OF THE ELECTRIC IS TO BE PLOTTED	CON00230
C	CON00240
C20       FORMAT (65X,D10.3)	CON00250
A(J,I)=RO	CON00260
C IN THIS STEP THE PROGRAM PREDICTS THE MINIMUM	CON00270
C AND MAXIMUM OF THE PHASE VALUES.	CON00280
C	CON00290
EMIN=MIN(EMIN,A(J,I))	CON00300
EMAX=MAX(EMAX,A(J,I))	CON00310
40       CONTINUE	CON00320
50       CONTINUE	CON00330
NX=100	CON00340
NY=100	CON00350
C DEFINE THE NUMBER OF LEVELS BETWEEN CONTOURS	CON00360
NLEVEL=10	CON00370
C IN THIS STEP THE PROGRAM CALCULATES THE CONTOURING	CON00380
C INTERVAL	CON00390
C	CON00400
FINC=(EMAX-EMIN)/(NLEVEL-1)	CON00410
C THE VALUES OF EMIN,EMAX,FINC ARE DISPLAYED ON THE	CON00420
C SCREEN	CON00430
C	CON00440
WRITE (6,*) EMIN,EMAX,FINC	CON00450
C THE CALLING STATEMENT OF THE SUBROUTINE CONTOR FORTRAN	CON00460
CALL CONTOR (A,NX,NY,FINC)	CON00470
STOP	CON00480
END	CON00490

6. PROGRAM II: CON3 FORTRAN. Contour Plots of Phase  
for Near Electric Field.

FILE: CON3      EXEC      B1

FILEDEF 12 DISK FILENAME PLOTDATA A  
EXEC DISSPLA CON3

7. CON3 EXEC: Fortran File for Automatic Execution  
of DISSPLA.

```

C THIS PROGRAM READS THE VALUES OF THE MAGNITUDE EPEAK OF E-FIELD
C FROM NEC OUTPUT FILE AND GENERATES A PARTICULAR PLOT WHICH HAS
C THE 3-D SURFACE AT THE TOP WHILE AT THE BOTTOM THE CONTOUR
C PLOT IS PRESENTED. THE PROGRAM USES THE SUBROUTINE "DMH002" OF
C DISSPLA GRAPHICS PACKAGE WHICH IS ATTACHED HERE AT THE END.
C
      REAL*8 RO
      DIMENSION A(30,30)
      CALL COMPRS
      EMIN=1E20
      EMAX=-1E20
      DO 50 I=1,30
        DO 40 J=1,30
          READ (12,20)RO
          FORMAT (17X,D10.3)
          A(J,I)=20*LOG10(RO)
20      IN THIS STEP THE PROGRAM PREDICTS THE MAXIMUM AND MINIMUM VALUES
C OF THE MAGNITUDE OF THE ELECTRIC FIELD.
C
          EMIN=MIN(EMIN,A(J,I))
          EMAX=MAX(EMAX,A(J,I))
40      CONTINUE
50      CONTINUE
      NX=30
      NY=30
C DEFINE THE NUMBER OF LEVELS (INPUT FROM KEYBOARD)
C
      WRITE (6,70)' ENTER NLEVEL > '
      READ (5,*) NLEVEL
      NLEVEL=20
C IN THIS STEP THE PROGRAM CALCULATES THE CONTOURING INTERVAL.
      FINC=(EMAX-EMIN)/(NLEVEL-1)
C THE VALUES OF EMIN,EMAX,FINC ARE DISSPLAYED ON THE SCREEN.
      WRITE (6,*) EMIN,EMAX,FINC
C IN THIS STEP THE USER HAS TO INPUT BY THE KEYBOARD THE COORDINATES
C OF THE VIEW POINT.
C
      WRITE (6,70) ' ENTER VX,VZ,VE,> '
      READ (5,*) VX,VZ,VE
C THIS IS THE CALLING STATEMENT OF THE SUBROUTINE "DMH002"
C
      CALL DMH002 (A,NX,NY,FINC,EMIN-30,EMAX,NLEVEL,VX,VZ,VE)
      CALL DONEPL
70      FORMAT (A)
      STOP
      END
C*****
      SUBROUTINE DMH002(ZDAT,NX,NY,FINC,EMIN,EMAX,NLEVEL,VX,VZ,VE)
      DIMENSION ZDAT(30,30)
      COMMON WORK(5000)
      CALL RESET (3HALL)
      CALL PAGE (11.,8.5)
C SET AXIS PARAMETERS AND ALPHABETS
      CALL INTAXS
      CALL ZAXANG (90.)
      CALL SIMPLX
      CALL MX1ALF (5HL/CST,'#')
      CALL MX2ALF (5HSTAND,'%')
C DEFINE 3-D WORK AREA AND AXIS
      CALL AREA2D (9.5,6.5)
C DEFINE THE LABEL OF THE PLOT
      CALL HEADIN ('%3-D ELECTRIC FIELD (DB REF TO 1V/M)$',36,2.0,3)
      CALL HEADIN ('%MONOPOLE 6CM AT CORNER OF WIRE GRID BOX$',40,2.0,
13)
      CALL HEADIN ('%(5.3 CM ON DIAGONAL FROM CENTER)$',33,1.0,3)
      CALL RESET (6HHEIGHT)
C DEFINE THE LABELS FOR THE THREE AXES
      CALL X3NAME ('%X VARIATION (METERS)$',21)
      CALL Y3NAME ('%Z VARIATION (METERS)$',21)
      CALL Z3NAME ('%ELECTRIC FIELD$',15)
      CALL VOLM3D (10.,10.,8.)
C DEFINE 3-D VIEW POINT

```

CON00010  
 CON00020  
 CON00030  
 CON00040  
 CON00050  
 CON00060  
 CON00070  
 CON00080  
 CON00090  
 CON00100  
 CON00110  
 CON00120  
 CON00130  
 CON00140  
 CON00150  
 CON00160  
 CON00170  
 CON00180  
 CON00190  
 CON00200  
 CON00210  
 CON00220  
 CON00230  
 CON00240  
 CON00250  
 CON00260  
 CON00270  
 CON00280  
 CON00290  
 CON00300  
 CON00310  
 CON00320  
 CON00330  
 CON00340  
 CON00350  
 CON00360  
 CON00370  
 CON00380  
 CON00390  
 CON00400  
 CON00410  
 CON00420  
 CON00430  
 CON00440  
 CON00450  
 CON00460  
 CON00470  
 CON00480  
 CON00490  
 CON00500  
 CON00510  
 CON00520  
 CON00530  
 CON00540  
 CON00550  
 CON00560  
 CON00570  
 CON00580  
 CON00590  
 CON00600  
 CON00610  
 CON00620  
 CON00630  
 CON00640  
 CON00650  
 CON00660  
 CON00670  
 CON00680  
 CON00690  
 CON00700  
 CON00710  
 CON00720

FILE: CON2      FORTRAN B1

```

      CALL VIEW (VX,VZ,VE)
C CALL GRAF3D(XORIG,XSTEP,XMAX,YORIG,YSTEP,YMAX,EMIN,FINC,EMAX)
C
      CALL GRAF3D (0.0541,.58,2.9541,0.115,.58,3.015,EMIN,FINC,
1EMAX)
C DEFINE THE SURFACE VIA A MATRIX
      CALL BLSUR
      CALL SURMAT (ZDAT,2,30,2,30,0)
      CALL DASH
      XDEL=0.
      DO 231 I=1,3
      CALL BSHIFT (XDEL,0.)
C DRAW BEDPOST EFFECT
      CALL RESET('BASALF')
      CALL HEIGHT(.2)
      CALL COMPLX
C DEFINE A MESSAGE ON THE PLOT IF IT IS DESIRED
C CALL MESSAG('SUBROUTINE DMH002$',100,3.5,0.)
      CALL RESET('HEIGHT')
      CALL RESET('COMPLX')
C DEFINE THE 4 DASHED LINES WHICH CONNECT THE 4 CORNERS OF THE CONTOUR
C GRAPH WITH THE 3-D GRAPH.THESE 4 DASHED LINES ARE AN OPTIONAL FEATURE.
C
      CALL RLVEC3 (0.0541,0.115,ZDAT(1,1),0.0541,0.115,EMIN,0)
      CALL RLVEC3 (2.9541,0.115,ZDAT(30,1),2.9541,0.115,EMIN,0)
      CALL RLVEC3 (2.9541,3.015,ZDAT(30,30),2.9541,3.015,EMIN,0)
      CALL RLVEC3 (0.0541,3.015,ZDAT(1,30),0.0541,3.015,EMIN,0)
      XDEL=XDEL+.01
231 CONTINUE
      CALL RESET (3HDOT)
      CALL RESET (6HBSHIFT)
C ENTER GRFITI LOOP AND DEFINE 2-D PLOT
      CALL GRFITI (0.,0.,0.0,1.,0.,0.0,0.,1.,0.)
      CALL INTAXS
      CALL AREA2D (10.,10.)
C CALL GRAF (XORIG,XSTEP,XMAX,YORIG,YSTEP,YMAX)
C
      CALL GRAF (0.0541,.58,2.9541,0.115,.58,3.015)
C CONTOURING IS OPTIONAL FEATURE AND CORRESPONDS TO THE BOTTOM PLOT
C SET CONTUR PARAMETERS
      CALL BCOMON (5000)
      CALL CONMAK (ZDAT,30,30,FINC)
C
      CALL CONLIN (4,5HSOLID,6HLABELS,2,10)
      CALL CONLIN (0,'MYCON','LABELS',2,10)
      CALL CONANG (90.)
      CALL FRAME
      CALL HEIGHT (.3)
C
      CALL CONTUR (5,6HLABELS,4HDRAW)
      CALL CONTUR (1,'LABELS','DRAW')
C END GRFITI LOOP
      CALL END3GR(0)
      CALL ENDPL (0)
      RETURN
      END
C
C*****
C
      SUBROUTINE MYCON(RARRAY,IARRAY)
      DIMENSION RARRAY(2),IARRAY(1)
C
C THIS ROUTINE MAKES NEGATIVE CONTOURS DASHED AND THE ZERO LINE HEAVIER.
C THE POSITIVE CONTOURS ARE PRESENTED BY SOLID LINES
      CALL RESET('DASH')
      IF (RARRAY(1)-.GE. 0.) GO TO 10
      CALL DASH
10 RARRAY(2) = 1.
      IARRAY(1) = 1
      IF (RARRAY(1) .EQ. 0.) IARRAY(1) = 2
      RETURN
      END

```

8. PROGRAM III: CON2 FORTRAN. 3-Dimensional Plots of  
Magnitude for Near Electric Field.

FILE: CON2 EXEC B1

FILEDEF 12 DISK FILENAME PLOTDATA A  
EXEC DISSPLA CON2

9. CON2 EXEC: Fortran File for Automatic Execution of DISSPLA.

PART B: NEC INPUT DATA FOR NEAR FIELDS.  
SURFACE PATCH MODELING.

FILE: DIP4 DATA B1

CM DIPOLE L/2 ON Z AXIS.FREQUENCY 1 GHZ  
CE IN FREE SPACE. NEAR E-FIELD (30X30 POINTS)  
GW 1,5,0,0,-0.075,0,0,0.075,0.0016  
GE  
FR 0,0,0,0,1000  
EX 0,1,3,0,1,0  
PL 2,2,5,1  
NE 0,30,1,30,0.0166,0,0.115,0.1,0,0.1  
XQ 0  
EN

1. Data File Dipole  $\lambda/2$  in Free Space. Near Electric Field (for Contour Plot of Magnitude).

FILE: DIP44 DATA B1

CM DIPOLE L/2 ON Z AXIS.FREQUENCY 1 GHZ.IN FREE SPACE.  
CE NEAR E-FIELD.100X100 POINTS.  
GW 1,5,0,0,-0.075,0,0,0.075,0.0016  
GE  
FR 0,0,0,0,1000  
EX 0,1,3,0,1,0  
PL 2,2,4,1  
NE 0,100,1,100,0.0166,0,0.115,0.029,0,0.029  
XQ 0  
EN

2. Data File Dipole  $\lambda/2$  in Free Space. Near Electric Field (for Contour Plot of Phase).

FILE: MON111 DATA B1

CM MONOPOLE 6CM ON Z AXIS.FREQUENCY 1 GHZ  
CE OVER PERFECT GROUND. NEAR E-FIELD (30X30 POINTS).  
GW 1,5,0,0,0,0,0,0.06,0.0016  
GE 1  
GN 1  
FR 0,0,0,0,1000  
EX 0,1,1,0,1,0  
PL 2,2,5,1  
NE 0,30,1,30,0.0166,0,0.115,0.1,0,0.1  
XQ 0  
EN

3. Data File 6cm Monopole Over Ground Plane.  
Near Electric Field (for Contour Plot of  
Magnitude).

FILE: MONPH1 DATA B1

CM MONOPOLE 6CM ON Z AXIS.FREQUENCY 1 GHZ  
CE OVER PERFECT GROUND. NEAR E-FIELD.(100X100 POINTS).  
GW 1,5,0,0,0,0,0,0.06,0.0016  
GE 1  
GN 1  
FR 0,0,0,0,1000  
EX 0,1,1,0,1,0  
PL 2,2,4,1  
NE 0,100,1,100,0.0166,0,0.115,0.029,0,0.029  
XQ 0  
EN

4. Data File 6cm Monopole Over Ground Plane.  
Near Electric Field (for Contour Plot of  
Phase).



FILE: N1 DATA B1

```
CM SPBOX 7X7 PATCHES ON TOP SURFACE
CE FREQUENCY 1.00 GHZ
SM3,3,0.5,-0.5,0,0.5,-0.5,1
SC0,0,0,-0.5,1
SM3,3,0.5,-0.5,0,0.5,0,0
SC0,0,0.5,0,1
GX 0,110
SM7,7,-0.5,-0.5,1,0.5,-0.5,1
SC0,0,0.5,0.5,1
GS 0,0,0.1
GE 1
FR 0,0,0,0,1000
GN 1
WG
NX
CM 6 CM MONOPOLE AT CENTER OF PATCH BOX .30X30 POINTS
CE NEAR E-FIELD ON X-AXIS AT 0.0166,0,0.115(CONTOURED FIELD)
GF
GW1,5,0,0,1,0,0,1.6,0.016
GS 0,0,0.1
GE 1
EX 0,1,1,0,1,0
PL 2,2,5,1
NE 0,50,1,30,0.0166,0,0.115,0.1,0,0.1
XQ 0
EN
```

5. Data File 6cm Monopole at Center of Surface Patch Box. Near Electric Field (for Contour Plot of Magnitude).

FILE: NPH1 DATA B1

```
CM SPBOX 7X7 PATCHES ON TOP SURFACE
CE FREQUENCY 1.00 GHZ
SM3,3,0.5,-0.5,0,0.5,-0.5,1
SC0,0,0,-0.5,1
SM3,3,0.5,-0.5,0,0.5,0,0
SC0,0,0.5,0,1
GX 0,110
SM7,7,-0.5,-0.5,1,0.5,-0.5,1
SC0,0,0.5,0.5,1
GS 0,0,0.1
GE 1
FR 0,0,0,0,1000
GN 1
WG
NX
CM 6 CM MONOPOLE AT CENTER OF PATCH BOX
CE NEAR E-FIELD ON X-AXIS AT 0.0166,0,0.115.POINTS 100X100
GF
GW1,5,0,0,1,0,0,1.6,0.016
GS 0,0,0.1
GE 1
EX 0,1,1,0,1,0
PL 2,2,4,1
NE 0,100,1,100,0.0166,0,0.115,0.029,0,0.029
XQ 0
EN
```

6. Data File 6cm Monopole at Center of Surface Patch Box. Near Electric Field (for Contour Plot of Phase).

FILE: NED1 DATA B1

CM 11X11 PATCHES ON TOP SURFACE (6CM AT EDGE 3.63CM FROM CENTER)  
CE FREQUENCY 1.00 GHZ  
SM3,3,0.5,-0.5,0,0.5,-0.5,1  
SC0,0,0,-0.5,1  
SM3,3,0.5,-0.5,0,0.5,0,0  
SC0,0,0.5,0,1  
GX 0,110  
SM11,11,-0.5,-0.5,1,0.5,-0.5,1  
SC0,0,0.5,0.5,1  
GS 0,0,0.1  
GE 1  
FR 0,0,0,0,1000  
GN 1  
WG  
NX  
CM 6 CM MONOPOLE AT EDGE 3.63 CM FROM CENTER (11X11 PATCHES ON TOP)  
CE NEAR E-FIELD ON X-AXIS (CONTOURS 30X30 POINTS)  
GF  
GW 1.5,-0.363636,0,1,-0.363636,0,1.6,0.016  
GS 0,0,0.1  
GE 1  
EX 0,1,1,0,1,0  
PL 2,2,5,1  
NE 0,30,1,30,-0.0197636,0,0.115,0.1,0,0.1  
XQ 0  
EN

7. Data File 6cm Monopole at Edge of Surface Patch Box. Near Electric Field (for Contour Plot of Magnitude).

FILE: NEDPH1 DATA B1

CM 11X11 PATCHES ON TOP SURFACE (6CM AT EDGE 3.63CM FROM CENTER)  
CE FREQUENCY 1.00 GHZ  
SM3,3,0.5,-0.5,0,0.5,-0.5,1  
SC0,0,0,-0.5,1  
SM3,3,0.5,-0.5,0,0.5,0,0  
SC0,0,0.5,0,1  
GX 0,110  
SM11,11,-0.5,-0.5,1,0.5,-0.5,1  
SC0,0,0.5,0.5,1  
GS 0,0,0.1  
GE 1  
FR 0,0,0,0,1000  
GN 1  
WG  
NX  
CM 6 CM MONOPOLE AT EDGE 3.63 CM FROM CENTER (11X11 PATCHES ON TOP)  
CE NEAR E-FIELD ON X-AXIS (PHASE 100 POINTS-ONE NE CARD)  
GF  
GW 1.5,-0.363636,0,1,-0.363636,0,1.6,0.016  
GS 0,0,0.1  
GE 1  
EX 0,1,1,0,1,0  
PL 2,2,4,1  
NE 0,100,1,100,-0.0197636,0,0.115,0.029,0,0.029  
XQ 0  
EN

8. Data File 6cm Monopole at Edge of Surface Patch Box. Near Electric Field (for Contour Plot of Phase).

FILE: NC01 DATA B1

CM 11X11 PATCHES ON TOP SURFACE (6CM MONOPOLE AT CORNER 5.14 CM)  
CM ON THE DIAGONAL FROM CENTER  
CE FREQUENCY 1.00 GHZ  
SM3,3,0.5,-0.5,0,0.5,-0.5,1  
SC0,0,0,-0.5,1  
SM3,3,0.5,-0.5,0,0.5,0,0  
SC0,0,0.5,0,1  
GX 0,110  
SM11,11,-0.5,-0.5,1,0.5,-0.5,1  
SC0,0,0.5,0.5,1  
GS 0,0,0.1  
GE 1  
FR 0,0,0,0,1000  
GN 1  
WG  
NX  
CM 6 CM MONOPOLE AT CORNER 5.14 CM ON THE DIAGONAL FROM CENTER  
CM TOP SURFACE 11X11 PATCHES  
CM FREQUENCY 1.00 GHZ  
CE NEAR E-FIELD ON X-AXIS.(CONTOURS 30X30 POINTS)  
GF  
GW1,5,0.363636,0.363636,1,0.363636,0.363636,1.6,0.016  
GS 0,0,0.1  
GE 1  
EX 0,1,1,0,1,0  
PL 2,2,5,1  
NE 0,30,1,30,0.0529636,0.0363636,0.115,0.1,0,0.1  
XQ 0  
EN

9. Data File 6cm Monopole at Corner of Surface Patch Box. Near Electric Field (for Contour Plot of Magnitude).

FILE: NCCPH1 DATA B1

CM 11X11 PATCHES ON TOP SURFACE (6CM MONOPOLE AT CORNER 5.14 CM)  
CM ON THE DIAGONAL FROM CENTER  
CE FREQUENCY 1.00 GHZ  
SM3,3,0.5,-0.5,0,0.5,-0.5,1  
SC0,0,0,-0.5,1  
SM3,3,0.5,-0.5,0,0.5,0,0  
SC0,0,0.5,0,1  
GX 0,110  
SM11,11,-0.5,-0.5,1,0.5,-0.5,1  
SC0,0,0.5,0.5,1  
GS 0,0,0.1  
GE 1  
FR 0,0,0,0,1000  
GN 1  
WG  
NX  
CM 6 CM MONOPOLE AT CORNER 5.14 CM ON THE DIAGONAL FROM CENTER  
CM TOP SURFACE 11X11 PATCHES  
CM FREQUENCY 1.00 GHZ  
CE NEAR E-FIELD ON X-AXIS.(PHASE 100 POINTS-ONE NE CARD)  
GF  
GW1,5,0.363636,0.363636,1,0.363636,0.363636,1.6,0.016  
GS 0,0,0.1  
GE 1  
EX 0,1,1,0,1,0  
PL 2,2,4,1  
NE 0,100,1,100,0.0529636,0.0363636,0.115,0.029,0,0.029  
XQ 0  
EN

10. Data File 6cm Monopole at Corner of Surface Patch Box. Near Electric Field (for Contour Plot of Phase).

PART C: RADIATION PATTERNS FOR MONOPOLE  
ON THE SURFACE PATCH BOX.

FILE: SPBOXV1 DATA B1

```
CM SPBOX 7X7 PATCHES ON TOP SURFACE
CE FREQUENCY 1.00 GHZ (VERTICAL PATTERN)
SM3,3,0.5,-0.5,0,0.5,-0.5,1
SC0,0,0,-0.5,1
SM3,3,0.5,-0.5,0,0.5,0,0
SC0,0,0.5,0,1
GX 0,110
SM7,7,-0.5,-0.5,1,0.5,-0.5,1
SC0,0,0.5,0.5,1
GS 0,0,0.1
GE 1
FR 0,0,0,0,1000
GN 1
WG
NX
CM 6 CM MONOPOLE AT CENTER OF SURFACE PATCH FREQ. 1.00 GHZ
CM TOP SURFACE 7X7 PATCHES
CE RADIATION PATTERNS (VERTICAL)
GF
GW1,5,0,0,1,0,0,1.6,0.016
GS 0,0,0.1
GE
EX 0,1,1,0,1,0
PL 3,1,0,4
RP 0,181,1,1002,-90,0,1,0
XQ 0
EH
```

1. Data File 6cm Monopole at Center of Surface Patch Box. Vertical Pattern.

FILE: SPBOXH1 DATA B1

```
CM SPBOX 7X7 PATCHES ON TOP SURFACE
CE FREQUENCY 1.00 GHZ (HORIZONTAL PATTERN)
SM3,3,0.5,-0.5,0,0.5,-0.5,1
SC0,0,0,-0.5,1
SM3,3,0.5,-0.5,0,0.5,0,0
SC0,0,0.5,0,1
GX 0,110
SM7,7,-0.5,-0.5,1,0.5,-0.5,1
SC0,0,0.5,0.5,1
GS 0,0,0.1
GE 1
FR 0,0,0,0,1000
GN 1
WG
NX
CM 6 CM MONOPOLE AT CENTER OF SURFACE PATCH FREQ. 1.00 GHZ
CM TOP SURFACE 7X7 PATCHES
CE RADIATION PATTERNS (HORIZONTAL)
GF
GW1,5,0,0,1,0,0,1.6,0.016
GS 0,0,0.1
GE
EX 0,1,1,0,1,0
PL 3,2,0,4
RP 0,1,361,1002,90,0,0,1
XQ 0
EH
```

2. Data File 6cm Monopole at Center of Surface Patch Box. Horizontal Pattern.

FILE: SPEDGEV1 DATA B1

CM SPEDGE1 11X11 PATCHES ON TOP SURFACE (6CM AT EDGE 3.63CM FROM CENTER)  
CE FREQUENCY 1.00 GHZ (VERTICAL PATTERN-X AXIS CUT)  
SM3,3,0.5,-0.5,0,0.5,-0.5,1  
SC0,0,0,-0.5,1  
SM3,3,0.5,-0.5,0,0.5,0,0  
SC0,0,0.5,0,1  
GX 0,110  
SM11,11,-0.5,-0.5,1,0.5,-0.5,1  
SC0,0,0.5,0.5,1  
GS 0,0,0.1  
GE 1  
FR 0,0,0,0,1000  
GN 1  
WG  
NX  
CM 6 CM MONOPOLE AT EDGE 3.63CM FROM CENTER FREQUENCY 1.00 GHZ  
CM TOP SURFACE 11X11 PATCHES  
CE RADIATION PATTERNS (VERTICAL-X AXIS CUT)  
GF  
GW1,5,-0.363636,0,1,-0.363636,0,1.6,0.016  
GS 0,0,0.1  
GE  
EX 0,1,1,0,1,0  
PL 3,1,0,4  
RP 0,181,1,1002,-90,0,1,0  
XQ 0  
EN

3. Data File 6cm Monopole at Edge of Surface Patch Box.  
Vertical Pattern (x-Axis Cut).

FILE: SPEDGEV2 DATA B1

CM SPEDGE1 11X11 PATCHES ON TOP SURFACE (6CM AT EDGE 3.63CM FROM CENTER)  
CE FREQUENCY 1.00 GHZ (VERTICAL PATTERN-Y AXIS CUT)  
SM3,3,0.5,-0.5,0,0.5,-0.5,1  
SC0,0,0,-0.5,1  
SM3,3,0.5,-0.5,0,0.5,0,0  
SC0,0,0.5,0,1  
GX 0,110  
SM11,11,-0.5,-0.5,1,0.5,-0.5,1  
SC0,0,0.5,0.5,1  
GS 0,0,0.1  
GE 1  
FR 0,0,0,0,1000  
GN 1  
WG  
NX  
CM 6 CM MONOPOLE AT EDGE 3.63CM FROM CENTER FREQUENCY 1.00 GHZ  
CM TOP SURFACE 11X11 PATCHES  
CE RADIATION PATTERNS (VERTICAL-Y AXIS CUT)  
GF  
GW1,5,-0.363636,0,1,-0.363636,0,1.6,0.016  
GS 0,0,0.1  
GE  
EX 0,1,1,0,1,0  
PL 3,1,0,4  
RP 0,181,1,1002,-90,90,1,0  
XQ 0  
EN

4. Data File 6cm Monopole at Edge of Surface Patch Box.  
Vertical Pattern (y-Axis Cut).

FILE: SPEDGE1 DATA B1

CM SPEDGE1 11X11 PATCHES ON TOP SURFACE (6CM AT EDGE 3.63CM FROM CENTER)  
CE FREQUENCY 1.00 GHZ (HORIZONTAL PATTERN)  
SM3,3,0.5,-0.5,0,0.5,-0.5,1  
SC0,0,0,-0.5,1  
SM3,3,0.5,-0.5,0,0.5,0,0  
SC0,0,0.5,0,1  
GX 0,110  
SM11,11,-0.5,-0.5,1,0.5,-0.5,1  
SC0,0,0.5,0.5,1  
GS 0,0,0.1  
GE 1  
FR 0,0,0,0,1000  
GN 1  
WG  
NX  
CM 6 CM MONOPOLE AT EDGE 3.63CM FROM CENTER FREQUENCY 1.00 GHZ  
CM TOP SURFACE 11X11 PATCHES  
CE RADIATION PATTERNS (HORIZONTAL)  
GF  
GW1,5,-0.363636,0,1,-0.363636,0,1.6,0.016  
GS 0,0,0.1  
GE  
EX 0,1,1,0,1,0  
PL 3,2,0,4  
RP 0,1,361,1002,90,0,0,1  
XQ 0  
EH

5. Data File 6cm Monopole at Edge of Surface Patch Box.  
Horizontal Pattern.

FILE: SPCV1 DATA B1

CM SPCNTR 11X11 PATCHES ON TOP SURFACE (6CM MONOPOLE AT CORNER 5.14 CM  
CM ON THE DIAGONAL FROM CENTER  
CE FREQUENCY 1.00 GHZ. VERTICAL PATTERN (X-AXIS CUT)  
SM3,3,0.5,-0.5,0,0.5,-0.5,1  
SC0,0,0,-0.5,1  
SM3,3,0.5,-0.5,0,0.5,0,0  
SC0,0,0.5,0,1  
GX 0,110  
SM11,11,-0.5,-0.5,1,0.5,-0.5,1  
SC0,0,0.5,0.5,1  
GS 0,0,0.1  
GE 1  
FR 0,0,0,0,1000  
GN 1  
WG  
NX  
CM 6 CM MONOPOLE AT CORNER 5.14 CM ON THE DIAGONAL FROM CENTER  
CM TOP SURFACE 11X11 PATCHES  
CM FREQUENCY 1.00 GHZ  
CE RADIATION PATTERNS (VERTICAL- X AXIS CUT)  
GF  
GW1,5,0.363636,0.363636,1,0.363636,0.363636,1.6,0.016  
GS 0,0,0.1  
GE 1  
EX 0,1,1,0,1,0  
PL 3,1,0,4  
RP 0,181,1,1002,-90,0,1,0  
XQ 0  
EH

6. Data File 6cm Monopole at Corner of Surface Patch Box  
Vertical Pattern (x-Axis Cut).

FILE: SPCV2 DATA B1

CM SPCNTR 11X11 PATCHES ON TOP SURFACE (6CM MONOPOLE AT CORNER 5.14 CM  
CM ON THE DIAGONAL FROM CENTER)  
CE FREQUENCY 1.00 GHZ. VERTICAL PATTERN (45 DEGREES CUT)  
SM3,3,0.5,-0.5,0,0.5,-0.5,1  
SC0,0,0,-0.5,1  
SM3,3,0.5,-0.5,0,0.5,0,0  
SC0,0,0.5,0,1  
GX 0,110  
SM11,11,-0.5,-0.5,1,0.5,-0.5,1  
SC0,0,0.5,0.5,1  
GS 0,0,0.1  
GE 1  
FR 0,0,0,0,1000  
GN 1  
WG  
NX  
CM 6 CM MONOPOLE AT CORNER 5.14 CM ON THE DIAGONAL FROM CENTER  
CM TOP SURFACE 11X11 PATCHES  
CM FREQUENCY 1.00 GHZ  
CE RADIATION PATTERNS. VERTICAL (45 DEGREES CUT)  
GF  
GW1,5,0.363636,0.363636,1,0.363636,0.363636,1.6,0.016  
GS 0,0,0.1  
GE 1  
EX 0,1,1,0,1,0  
PL 3,1,0,4  
RP 0,181,1,1002,-90,45,1,0  
XQ 0  
EN

7. Data File 6cm Monopole at Corner of Surface Patch  
Box. Vertical Pattern (45° Cut).

FILE: SPCH1 DATA B1

CM SPCNTR 11X11 PATCHES ON TOP SURFACE (6CM MONOPOLE AT CORNER 5.14 CM  
CM ON THE DIAGONAL FROM CENTER)  
CE FREQUENCY 1.00 GHZ. HORIZONTAL PATTERN  
SM3,3,0.5,-0.5,0,0.5,-0.5,1  
SC0,0,0,-0.5,1  
SM3,3,0.5,-0.5,0,0.5,0,0  
SC0,0,0.5,0,1  
GX 0,110  
SM11,11,-0.5,-0.5,1,0.5,-0.5,1  
SC0,0,0.5,0.5,1  
GS 0,0,0.1  
GE 1  
FR 0,0,0,0,1000  
GN 1  
WG  
NX  
CM 6 CM MONOPOLE AT CORNER 5.14 CM ON THE DIAGONAL FROM CENTER  
CM TOP SURFACE 11X11 PATCHES  
CM FREQUENCY 1.00 GHZ  
CE RADIATION PATTERNS (HORIZONTAL)  
GF  
GW1,5,0.363636,0.363636,1,0.363636,0.363636,1.6,0.016  
GS 0,0,0.1  
GE 1  
EX 0,1,1,0,1,0  
PL 3,2,0,4  
RP 0,1,361,1002,90,0,0,1  
XQ 0  
EN

8. Data File 6cm Monopole at Corner of Surface Patch  
Box. Horizontal Pattern.

# APPENDIX C NEC INPUT DATA FILES

## PART A: NEC INPUT DATA FILES FOR WIRE GRID MODELING. STRUCTURE GEOMETRY

FILE: WG11 DATA B1

```
CM WIRE GRID 10 CM. LONG WITH 6CM MONOPOLE AT CENTER
CM CELLS .125 X .125 GROUND
CE DATA FILE FOR PLOTTING USING PLOTDGLP EXEC
GW 100,4,.5,-.5,1,0,-.5,1,.01
GM 1,7,0,0,0,0,0,-.125,100.100
GW 200,8,.5,-.5,1,.5,-.5,0,.01
GM 2,3,0,0,0,0,.125,0,200.201
GM 3,3,0,0,0,-.125,0,0,200.201
GW 300,4,.5,-.5,1,.5,0,1,.01
GM 4,7,0,0,0,0,0,-.125,300.303
GW 400,4,.5,-.375,1,0,-.375,1,.01
GM 5,2,0,0,0,0,.125,0,400.404
GW 500,4,.375,-.5,1,.375,0,1,.01
GM 6,2,0,0,0,-.125,0,0,500.505
GX 0,110
GW 99,8,.5,0,0,.5,0,1,.01
GM 7,3,0,0,90,0,0,0,099.099
GW 2,8,0,-.5,1,0,.5,1,.01
GW 3,8,.5,0,1,-.5,0,1,.01
GM 1,5,0.005,0,1,0.005,0,1.6,.016
GM 0.35,0,0,10,0,0,0,001.001
GE
EN
```

1. Data File Geometry of 6cm Monopole at Center  
of Wire Grid Box.

FILE: WEDG11 DATA B1

```
CM WIRE GRID 10 CM. LONG WITH 6CM MONOPOLE AT EDGE(3.75CM)
CM CELLS .125 X .125 GROUND
CE FILE FOR PLOTTING USING PLOTDGLP EXEC
GW 100,4,.5,-.5,1,0,-.5,1,.01
GM 1,7,0,0,0,0,0,-.125,100.100
GW 200,8,.5,-.5,1,.5,-.5,0,.01
GM 2,3,0,0,0,0,.125,0,200.201
GM 3,3,0,0,0,-.125,0,0,200.201
GW 300,4,.5,-.5,1,.5,0,1,.01
GM 4,7,0,0,0,0,0,-.125,300.303
GW 400,4,.5,-.375,1,0,-.375,1,.01
GM 5,2,0,0,0,0,.125,0,400.404
GW 500,4,.375,-.5,1,.375,0,1,.01
GM 6,2,0,0,0,-.125,0,0,500.505
GX 0,110
GW 99,8,.5,0,0,.5,0,1,.01
GM 7,3,0,0,90,0,0,0,099.099
GW 2,8,0,-.5,1,0,.5,1,.01
GW 3,8,.5,0,1,-.5,0,1,.01
GM 1,5,0.005,0,1,0.005,0,1.6,.016
GM 0.35,0,0,10,0,0,0,001.001
GW 0,0,0,0,0,-.375,0,0,001.001
GE
EN
```

2. Data File Geometry of 6cm Monopole at Edge  
of Wire Grid Box.



FILE: WCOG11 DATA B1

CM WIRE GRID 10 CM. LONG WITH MONOPOLE 6 CM AT CORNER(5.3CM ON DIAGONAL)  
CM CELLS .125 X .125 GROUND  
CE FILE FOR PLOTTING USING PLOTDGLP EXEC  
GW 100,4,.5,-.5,1,0,-.5,1,.01  
GM 1,7,0,0,0,0,0,-.125,100.100  
GW 200,8,.5,-.5,1,.5,-.5,0,.01  
GM 2,3,0,0,0,0,.125,0,200.201  
GM 3,3,0,0,0,-.125,0,0,200.201  
GW 300,4,.5,-.5,1,.5,0,1,.01  
GM 4,7,0,0,0,0,0,-.125,300.303  
GW 400,4,.5,-.375,1,0,-.375,1,.01  
GM 5,2,0,0,0,0,.125,0,400.404  
GW 500,4,.375,-.5,1,.375,0,1,.01  
GM 6,2,0,0,0,-.125,0,0,500.505  
GX 0,110  
GW 99,8,.5,0,0,.5,0,1,.01  
GM 7,3,0,0,90,0,0,0,099.099  
GW 2,8,0,-.5,1,0,.5,1,.01  
GW 3,8,.5,0,1,-.5,0,1,.01  
GM 1,5,0.005,0,1,0.005,0,1.6,.016  
GM 0,35,0,0,10,0,0,0,001.001  
GM 0,0,0,0,0,.375,.375,0,001.001  
GE  
EN

3. Data File Geometry of 6cm Monopole at Corner  
of Wire Grid Box.

PART B: NEC INPUT DATA FILES FOR NEAR ELECTRIC FIELDS.  
WIRE GRID MODELING

```
File: W1      DATA      B1
CM WIRE GRID 10 CM. LONG
CM CELLS .125 X .125 GROUND
CE
GM 100,4,.5,-.5,1,0,-.5,1,.01
GM 1,7,0,0,0,0,0,-.125,100.100
GM 200,8,.5,-.5,1,.5,-.5,0,.01
GM 2,3,0,0,0,0,.125,0,200.201
GM 3,3,0,0,0,-.125,0,0,200.201
GM 300,4,.5,-.5,1,.5,0,1,.01
GM 4,7,0,0,0,0,0,-.125,300.303
GM 400,4,.5,-.375,1,0,-.375,1,.01
GM 5,2,0,0,0,0,.125,0,400.404
GM 500,4,.375,-.5,1,.375,0,1,.01
GM 6,2,0,0,0,-.125,0,0,500.505
GX 0,110
GS 0,0,.1
GE 1
FR 0,0,0,0,1000
GN 1
WG
NX
CM 6 CM MONOPOLE AT CENTER OF WIRE GRID FREQ=1 GHZ
CE NEAR E-FIELD ON X-AXIS (CONTOURS 30 POINTS)
GF
GM 2,8,0,-.5,1,0,.5,1,.01
GM 3,8,.5,0,1,-.5,0,1,.01
GM 1,5,0,0,1,0,0,1.6,.016
GS 0,0,.1
GE
EX 0,1,1,0,1,0
PL 2,2,5,1
NE 0,30,1,30,0.0166,0,0.115,0.1,0,0.1
XQ 0
EN
```

1. Data File 6cm Monopole at Center of Wire Grid Box (for Contour Plot of Magnitude).

FILE: WPH1 DATA B1

```
CM WIRE GRID 10 CM. LONG
CM CELLS .125 X .125 GROUND
CE
GM 100,4,.5,-.5,1,0,-.5,1,.01
GM 1,7,0,0,0,0,0,-.125,100.100
GM 200,8,.5,-.5,1,.5,-.5,0,.01
GM 2,3,0,0,0,0,.125,0,200.201
GM 3,3,0,0,0,-.125,0,0,200.201
GM 300,4,.5,-.5,1,.5,0,1,.01
GM 4,7,0,0,0,0,0,-.125,300.303
GM 400,4,.5,-.375,1,0,-.375,1,.01
GM 5,2,0,0,0,0,.125,0,400.404
GM 500,4,.375,-.5,1,.375,0,1,.01
GM 6,2,0,0,0,-.125,0,0,500.505
GX 0,110
GS 0,0,.1
GE 1
FR 0,0,0,0,1000
GN 1
WG
NX
CM 6 CM MONOPOLE AT CENTER OF WIRE GRID FREQ=1 GHZ
CE NEAR E-FIELD ON X-AXIS (PHASE 100 POINTS)
GF
GM 2,8,0,-.5,1,0,.5,1,.01
GM 3,8,.5,0,1,-.5,0,1,.01
GM 1,5,0,0,1,0,0,1.6,.016
GS 0,0,.1
GE
EX 0,1,1,0,1,0
PL 2,2,4,1
NE 0,100,1,100,0.0166,0,0.115,0.029,0,0.029
XQ 0
EN
```

2. Data File 6cm Monopole at Center of Wire Grid (for Contour Plot of Phase).

FILE: WED1 DATA B1

```
CM WIRE GRID 10 CM. LONG
CM CELLS .125 X .125 GROUND
CE
GW 100,4,.5,-.5,1,0,-.5,1,.01
GM 1,7,0,0,0,0,0,-.125,100.100
GW 200,8,.5,-.5,1,.5,-.5,0,.01
GM 2,3,0,0,0,0,.125,0,200.201
GM 3,3,0,0,0,0,-.125,0,0,200.201
GW 300,4,.5,-.5,1,.5,0,1,.01
GM 4,7,0,0,0,0,0,-.125,300.303
GW 400,4,.5,-.375,1,0,-.375,1,.01
GM 5,2,0,0,0,0,.125,0,400.404
GW 500,4,.375,-.5,1,.375,0,1,.01
GM 6,2,0,0,0,0,-.125,0,0,500.505
GX 0,110
GS 0,0,.1
GE 1
FR 0,0,0,0,1000
GN 1
WG
NX
CM 6 CM MONOPOLE AT EDGE(3.75 CM FROM CENTER) OF WIRE GRID FREQ=1 GHZ
CE NEAR E-FIELD ON X-AXIS (CONTOURS 30 POINTS)
GF
GW 2,8,0,-.5,1,0,.5,1,.01
GW 3,8,.5,0,1,-.5,0,1,.01
GW 1,5,-.375,0,1,-.375,0,1.6,.016
GS 0,0,.1
GE
EX 0,1,1,0,1,0
PL 2,2,5,1
NE 0,30,1,30,-0.0209,0,0.115,0,1,0,0.1
XQ 0
EN
```

3. Data File 6cm Monopole at Edge of Wire Grid Box  
(for Contour Plot of Magnitude).

```
FILE: WEDPH1 DATA B1
CM WIRE GRID 10 CM. LONG
CM CELLS .125 X .125 GROUND
CE
GW 100,4,.5,-.5,1,0,-.5,1,.01
GM 1,7,0,0,0,0,0,-.125,100.100
GW 200,8,.5,-.5,1,.5,-.5,0,.01
GM 2,3,0,0,0,0,.125,0,200.201
GM 3,3,0,0,0,0,-.125,0,0,200.201
GW 300,4,.5,-.5,1,.5,0,1,.01
GM 4,7,0,0,0,0,0,-.125,300.303
GW 400,4,.5,-.375,1,0,-.375,1,.01
GM 5,2,0,0,0,0,.125,0,400.404
GW 500,4,.375,-.5,1,.375,0,1,.01
GM 6,2,0,0,0,0,-.125,0,0,500.505
GX 0,110
GS 0,0,.1
GE 1
FR 0,0,0,0,1000
GN 1
WG
NX
CM 6 CM MONOPOLE AT EDGE(3.75 CM FROM CENTER) OF WIRE GRID FREQ=1 GHZ
CE NEAR E-FIELD ON X-AXIS (PHASE 100 POINTS)
GF
GW 2,8,0,-.5,1,0,.5,1,.01
GW 3,8,.5,0,1,-.5,0,1,.01
GW 1,5,-.375,0,1,-.375,0,1.6,.016
GS 0,0,.1
GE
EX 0,1,1,0,1,0
PL 2,2,4,1
NE 0,100,1,100,-0.0209,0,0.115,0.029,0,0.029
XQ 0
EN
```

4. Data File 6cm Monopole at Edge of Wire Grid Box  
(for Contour Plot of Phase).

FILE: WCOL DATA B1

```
CM WIRE GRID 10 CM. LONG
CM CELLS .125 X .125 GROUND
CE
GW 100,4,.5,-.5,1,0,-.5,1,.01
GM 1,7,0,0,0,0,0,-.125,100.100
GW 200,8,.5,-.5,1,.5,-.5,0,.01
GM 2,3,0,0,0,0,.125,0,200.201
GM 3,3,0,0,0,-.125,0,0,200.201
GW 300,4,.5,-.5,1,.5,0,1,.01
GM 4,7,0,0,0,0,0,-.125,300.303
GW 400,4,.5,-.375,1,0,-.375,1,.01
GM 5,2,0,0,0,0,.125,0,400.404
GW 500,4,.375,-.5,1,.375,0,1,.01
GM 6,2,0,0,0,-.125,0,0,500.505
GX 0,110
GS 0,0,.1
GE 1
FR 0,0,0,0,1000
GN 1
WG
NX
CM 6 CM MONOPOLE AT CORNER(5.3CM ON DIAGONAL) OF WIRE GRID FREQ=1 GHZ
CE NEAR E-FIELD ON X-AXIS (CONTOURS 30 POINTS)
GF
GW 2,8,0,-.5,1,0,.5,1,.01
GW 3,8,.5,0,1,-.5,0,1,.01
GW 1,5,.375,.375,1,.375,.375,1.6,.016
GS 0,0,.1
GE
EX 0,1,1,0,1,0
PL 2,2,5,1
NE 0,30,1,30,0.0541,0.0375,0.115,0.1,0,0.1
XQ 0
EN
```

5. Data File 6cm Monopole at Corner of Wire Grid Box  
(for Contour Plot of Magnitude).

FILE: WCOPI1 DATA B1

```
CM WIRE GRID 10 CM. LONG
CM CELLS .125 X .125 GROUND
CE
GW 100,4,.5,-.5,1,0,-.5,1,.01
GM 1,7,0,0,0,0,0,-.125,100.100
GW 200,8,.5,-.5,1,.5,-.5,0,.01
GM 2,3,0,0,0,0,.125,0,200.201
GM 3,3,0,0,0,-.125,0,0,200.201
GW 300,4,.5,-.5,1,.5,0,1,.01
GM 4,7,0,0,0,0,0,-.125,300.303
GW 400,4,.5,-.375,1,0,-.375,1,.01
GM 5,2,0,0,0,0,.125,0,400.404
GW 500,4,.375,-.5,1,.375,0,1,.01
GM 6,2,0,0,0,-.125,0,0,500.505
GX 0,110
GS 0,0,.1
GE 1
FR 0,0,0,0,1000
GN 1
WG
NX
CM 6 CM MONOPOLE AT CORNER(5.3CM ON DIAGONAL) OF WIRE GRID FREQ=1 GHZ
CE NEAR E-FIELD ON X-AXIS (PHASE 100 POINTS)
GF
GW 2,8,0,-.5,1,0,.5,1,.01
GW 3,8,.5,0,1,-.5,0,1,.01
GW 1,5,.375,.375,1,.375,.375,1.6,.016
GS 0,0,.1
GE
EX 0,1,1,0,1,0
PL 2,2,4,1
NE 0,100,1,100,0.0541,0.0375,0.115,0.029,0,0.029
XQ 0
EN
```

6. Data File 6cm Monopole at Corner of Wire Grid Box  
(for Contour Plot of Phase).

## LIST OF REFERENCES

1. Burke, G.J. and Poggio, A.J. of Lawrence Livermore Laboratory, Naval Ocean Systems Center Technical Document 116, Numerical Electromagnetics Code (NEC), Method of Moments, January 1981.
2. Logan, J.C. and Rockway, J.W., Naval Ocean Systems Center, Technical Document 168, Calculated Electric Near Fields of Navy Shipboard HF Antennas, pp. 4-9, March 1978.
3. Chase, M. and Rockway, J.W., A Method of Detecting Significant Sources of Intermodulation Interference, IEEE Transactions of Electromagnetic Compatibility, Vol. EMC-17, No. 2, p. 47, May 1975.
4. Grich, R.J., and CDR Bruninga, R.E., USN, Electromagnetic Environment Engineering -- A Solution to the EMI Pandemic, Naval Engineers Journal, p. 203, May 1987.
5. Bhattacharya, S., A Study of the Admittance Characteristics of a Monopole Antenna Attached to a Conducting Box, Master's Thesis, University of Houston, pp. 11-13, pp. 71-73 and pp. 86-88, May 1986.
6. Bhattacharya, S., Long, S.A., Wilton, D.R., The Input Impedance of a Monopole Antenna Mounted on a Cubical Conducting Box, IEEE Transactions on Antennas and Propagation, Vol. AP-35, No. 7, pp. 756-761, July 1987.
7. Johnson, W.A., Wilton, D.R., Sharpe, R.M., Sandia National Laboratories Report SAND87-2991, Patch Code User's Manual, May 1988.
8. Molina, C.R., Numerical Electromagnetic Models of Cube-Shaped Boxes -- An Investigation for Near Field Prediction of HP Shipboard Environments, Master's Thesis, Naval Postgraduate School, Monterey, California, December 1987.
9. ISSCO Graphics Software version 9.0, DISSPLA (Display Integrated Software System and Plotting Language) User's Manual, May 1986.
10. Rockway, J.W., and Hansen, P.M., Naval Electronics Laboratory Center Report 1872, Calculated Near Fields of Navy HF Whip Antennas, pp. 27-28, 24 April 1973.
11. Wilson, D.R., and Hwu, S.W., Applied Electromagnetics Laboratory, Department of Electrical Engineering, University of Houston, Technical Document 1324, Junction Code User's Manual, August 1988.

## BIBLIOGRAPHY

Stutzman, W.L., and Thiele, G.A., Antenna Theory and Design, John Wiley and Sons, Inc., 1976.

Kraus, J.D., Antennas, McGraw-Hill Book Company, 1988.

Johnson, R.C., and Jasik, H., Antenna Engineering Handbook, McGraw-Hill Book Company, 1984.

Ramo, S., Whinnery, J.R., and Van Duzer T., Fields and Waves in Communications Electronics, John Wiley and Sons. Inc., 1984.

# INITIAL DISTRIBUTION LIST

	No. Copies
1. Defense Technical Information Center Cameron Station Alexandria, Virginia 22304-6145	2
2. Library, Code 0142 Naval Postgraduate School Monterey, California 93943-5002	2
3. Chairman, Code 62 Naval Postgraduate School Monterey, California 93943-5000	1
4. Curricular Officer, Code 32 Naval Postgraduate School Monterey, California 93943-5000	1
5. Prof. R.W. Adler, Code 62Ab Naval Postgraduate School Monterey, California 93943-5000	10
6. Prof. J.K. Breakall, Code 62Bk Naval Postgraduate School Monterey, California 93943-5000	10
7. Illinois Institute of Technology ATTN: B. Campbell 185 Admiral Cochrane Drive Annapolis, Maryland 21401	1
8. University of Mississippi Department of Electrical Engineering ATTN: A.W. Glisson University, Mississippi 38677	1
9. Naval Ocean Systems Center Code 822(T) ATTN: Mr. J. Logan 271 Catalina Boulevard San Diego, California 92152	1
10. Mr. Richard Tell 6141 W. Racel Street Las Vegas, Nevada 89131	1
11. University of Houston Electrical Engineering Department ATTN: Prof. D. Wilton 4800 Calhoun Houston, Texas 77004	1

- |   |   |
|---|---|
| 12. Hellenic Navy General Staff<br>2nd Branch, Education Department<br>Stratopedon Papagou, Holargas<br>Athens 155.61, Greece | 4 |
| 13. LT Panagiotis Elliniadis<br>G. Apostolidou 8<br>Chalkis 34100<br>Evia, Greece   | 2 |
| 14. Lawrence Livermore National<br>Laboratories<br>ATTN: Dr. V.R. Latorre, L-156<br>PO Box 808<br>Livermore, California 94550 | 1 |
| 15. Research Administration, Code 012<br>Naval Postgraduate School<br>Monterey, California 93943-5000                         | 1 |
| 16. Lawrence Livermore National<br>Laboratories<br>ATTN: Mr. G.J. Burke, L-156<br>PO Box 808<br>Livermore, California 94550   | 1 |
| 17. Naval Ocean Systems Center<br>ATTN: D. Wehner, Code 7403<br>271 Catalina Boulevard<br>San Diego, California 92152         | 1 |